

Catalytic synthesis of dimethyl carbonate and its application as a green reagent for the synthesis of aromatic carbamates

*Thesis Submitted to AcSIR
For the Award of the Degree of*

*Doctor of Philosophy
In
Chemical Sciences*



By

Nayana Tushar Nivangune

AcSIR Roll No.: 10CC14A26033

Under the guidance of

Dr. A. A. Kelkar

*Chemical Engineering and Process Development Division
CSIR-National Chemical Laboratory
Pune-411 008, India*

June 2018



सीएसआईआर - राष्ट्रीय रासायनिक प्रयोगशाला

(वैज्ञानिक तथा औद्योगिक अनुसंधान परिषद)

डॉ. होमी भाभा मार्ग, पुणे - 411 008. भारत



CSIR - NATIONAL CHEMICAL LABORATORY

(Council of Scientific & Industrial Research)

Dr. Homi Bhabha Road, Pune - 411 008. India

CERTIFICATE

This is to certify that the work incorporated in this Ph.D. thesis entitled "*Catalytic synthesis of dimethyl carbonate and its application as a green reagent for the synthesis of aromatic carbamates*" submitted by *Mrs. Nayana Tushar Nivangune* to Academy of Scientific and Innovative Research (AcSIR) in fulfillment of the requirements for the award of the Degree of **Doctor of Philosophy In Chemical Sciences**, under my supervision at *Chemical Engineering and Process Development Division, CSIR-National Chemical Laboratory Pune, India* under Academy of Scientific and Innovation Research (AcSIR), New Delhi. I further certify that this work has not been submitted to any other University or Institution in part or full for the award of any degree or diploma. Research material obtained from other sources has been duly acknowledged in the thesis.

Date: 6th June 2018

Place: Pune

Dr. A. A. Kelkar
(Supervisor)

DECLARATION

I hereby declare that the work described in the thesis entitled “**Catalytic synthesis of dimethyl carbonate and its application as a green reagent for the synthesis of aromatic carbamates**” submitted for the degree of *Doctor of Philosophy in Chemical Sciences* to the Academy of Scientific and Innovative Research (AcSIR), New Delhi, has been carried out by me at the Chemical Engineering and Process Development Division, CSIR National Chemical Laboratory, Pune-411008, India under the supervision of *Dr. A. A. Kelkar*. I further declare that the material obtained from other sources has been duly acknowledged in this thesis. The work is original and has not been submitted in part or full by me for any other degree or diploma to this or any other university.

Date: 6th June 2018

Place: Pune

Mrs. Nayana Tushar Nivangune

(Research Student)

Dedicated to My

Beloved Family.....

Acknowledgements

To my great delight I would like to express my heart-felt gratitude to Dr. A. A. Kelkar for providing me the splendid opportunity to take the first step in scientific research under his guidance. I thank him for his excellent guidance, constant encouragement, cooperation and sincere advice throughout my doctoral study. He taught me the art of writing manuscript ,how to put forth convincingly the main hypothesis and its successful demonstration, the use of the most appropriate words to convey the exact meaning, and so on. We experienced together all the ups and downs of routine work, shared the happiness of success and the depression of failure during this work.

I thank Dr. A. K. Nagia, Director, CSIR-NCL for giving me the opportunity to work in this institute and exploit all the infrastructural facilities needed for my research work. I would like to express my sincere gratitude to Dr. S. S. Joshi, Head, CEPD Division.

I thank the Council of Scientific and Industrial Research, New Delhi for the research fellowship and Academy of Scientific & Innovative Research (AcSIR) for registering me for the Ph.D. degree.

I would like to sincerely acknowledge Dr. V. V. Ranade and Dr. A. A. Kulkarni who always stood beside me whenever I needed them.

I would like to gratefully acknowledge Dr. V. H. Rane, Dr A. K. Kinage, Dr. S. K. Shingote, Dr. L. Roy and Mr. H. M. Raheja for their valuable help and co-operation during my research stay in NCL.

I wish to thank XRD, TEM, SEM, XPS, BET and NMR Central facility NCL, for characterization.

I would like to thank all my colleagues and lab mates (former and present) Dr. Muddasir Mushi, Dr. Vaishali Shende, Dr. Swapna Gade, Kunal Pardeshi, Dr. Rajendra Mane, Kamallesh, Harshad, Tushar, Avinash, Gaurav, Amol, Lakshmikant, Monica, Hanuman and suryakant for their helpful hand and cheerful attitude that had made my work very easy and enjoyable.

I would also like to thank M.Sc. project trainees Shayma, Arya, Prajakta, Atul, Varsha, Minakshi and Ramesh for their cooperation in research and personal help whenever required.

I am grateful to all my friends Dipali, Mehejabeen, Balasaheb, Pralhad, Muzammil, Priyanka, Gouri, Ajay, Priti, Sharad, Aparna, Rasika, Sharada, Suhas, Sumit, Shrikant, Sagar, Richa, Reshma, Manisha, Vipul and Unnikrishanan for their timely assistance and friendly support. I would like to thank supporting staff of CEPD division Mr. Kambale, Mr. Patne, Mr. Shinde, Mr. Vanjale, Mr. Ravi and Mr. Radha for their help.

This thesis would not have been possible without the strong faith, support and encouragement of my family. I wish to express my deep sense of gratitude to my family for their continuing understanding and sacrifice in support of my education. Their constant encouragement has made me succeed through this journey. I would like to thank my husband for being patient and supporting me during the tough writing stage of the thesis. Their support and love encouraged me to look optimistically into the future even in my stressful times. Thanks a lot for being so understanding & supportive throughout the course of this thesis period.

Date: 6th June 2018

Mrs. Nayana T. Nivangune

(Research Student)

List of Contents

Description	Page No.
Chapter Index	i
List of Figures	ix
List of Tables	xiv
List of Abbreviations	xvii
Abstract of the Thesis	xix
<hr/> <i>Chapter 1: Catalytic synthesis of Dimethyl carbonate and its application to value added products</i> <hr/>	
1.1. Introduction	2
1.2. Catalysis	3
1.2.1. Types of Catalysis	5
1.2.2. Hydrotalcites (HTs)	11
1.2.3. Hydrotalcite-like compounds	13
1.2.4. Mixed metal oxides (MMOs)	16
1.3. Green chemistry	20
1.3.1. Definition	20
1.3.2. Twelve principles of Green Chemistry	20
1.3.3. Synthetic strategy to achieve green chemistry processes	21
1.3.3.1. Catalytic processes	21
1.3.3.2. Elimination of auxiliary reagents and solvents	22
1.3.4. Dimethyl carbonate as a green reagent	23

1.4.	Dimethyl carbonate (DMC)	24
1.4.1.	Synthesis of DMC by oxidative carbonylation of methanol	27
1.4.2.	Synthesis of DMC using NO	28
1.4.3.	Synthesis of DMC by transesterification of EC with methanol	30
1.4.4.	Synthesis of DMC from urea and alcohol	31
1.4.5.	Synthesis of DMC directly from CO ₂ and methanol	33
1.4.6.	Literature on Transesterification of cyclic carbonate with methanol	36
1.5.	DMC as a methoxycarbonylating agent for aromatic carbamates	50
1.5.1.	Synthesis of carbamates by oxidative Carbonylation of Amines	51
1.5.2.	Synthesis of carbamates by the reductive carbonylation of aromatic nitro-compounds	53
1.5.3.	Synthesis of carbamates by methoxycarbonylation of aromatic amine	54
1.5.4.	Detailed literature on methoxycarbonylation of aromatic amines	55
1.6.	Aim and objectives of the thesis	64
1.7.	References	67

Chapter 2: DMC synthesis by transesterification of cyclic carbonates with methanol using heterogeneous base catalysts

Chapter 2A: Synthesis of dimethyl carbonate by transesterification of EC with methanol using MgFeCe ternary Layer double hydroxide (LDH) catalyst

2A.1.	Introduction	93
2A.2.	Materials	94
2A.3.	Catalyst preparation	95
2A.3.1.	Synthesis of Binary LDHs ($M^{2+}/M^{3+}=3:1$)	95
2A.3.2.	Synthesis of Ternary LDHs ($Mg_3:Fe_x:Ce_{1-x}$)	96

2A.3.3. Synthesis of Ternary LDHs ($Mg_3Fe_{0.85}M^{III}_{0.15}$)	97
2A.4.Characterization Methods	97
2A.4.1. X-Ray powder diffraction (XRD)	97
2A.4.2. Fourier transform-infrared spectroscopy (FT-IR)	98
2A.4.3. Transmission electron microscopy (TEM)	98
2A.4.4. N_2 sorption (BET)	98
2A.4.5. Basic properties of LDHs by Titration method	98
2A.4.6. CO_2 and NH_3 TPD	99
2A.4.7. XPS	99
2A.4.8. ICP-AES	99
2A.5. Experimental setup	100
2A.5.1. Experimental procedure for transesterification of EC with methanol	100
2A.5.2. Experimental procedure for recycle study	101
2A.5.3. Analytical methods	102
2A.6. XRD analysis of Binary LDHs	103
2A.7 Transesterification of EC with methanol	104
2A.7.1. Screening of binary LDHs for transesterification of EC with methanol	105
2A.7. Transesterification of EC with methanol using $Mg_3Fe_xCe_{1-x}$ LDHs	106
2A.8. Result and discussion	108
2A.8.1. Characterization of LDHs prepared	108
2A.8.1.1. ICP analysis: Composition of LDHs	108
2A.8.1.2. Powder X-ray Diffraction	109
2A.8.1.3. FT-IR spectroscopy	112
2A.8.1.4. Transmission Electron Microscopy	113

2A.8.1.5. Surface Area Measurements	114
2A.8.1.6. Basicity Measurement	114
2A.8.1.7. XPS analysis of the catalysts	115
2A.9. Effect of Reaction conditions	120
2A.9.1. Effect of EC: MeOH molar ratio:	121
2A.9.2. Effect of reaction temperature	122
2A.9.3. Effect of catalyst loading	123
2A.9.4. Typical reaction profile for EC to DMC	125
2A.10. Transesterification of EC and methanol using $Mg_3Fe_{0.85}M_{0.15}$	126
2A.11. Stability of the LDH-3 catalyst (leaching test)	128
2A.12. Recycle of LDH-3 catalyst	129
2A.13. Catalytic mechanism	130
2A.14. Conclusions	132
<hr/>	
<i>Chapter 2B: Synthesis of dimethyl carbonate by transesterification of cyclic carbonate (EC/PC) with methanol using Li-Al mixed metal oxide catalyst</i>	
<hr/>	
2B.1. Introduction	134
2B.2. Materials	135
2B.3. Catalyst preparation	135
2B.3.1. Synthesis of binary mixed metal oxides	136
2B.3.2. Synthesis of single-metal oxides	136
2B.4. Characterization Methods	138
2B.5. Experiment procedure for transesterification of EC/PC with methanol	138
2B.6. Result and discussion	139
2B.6.1. Characterization techniques	140

2B.6.1.1. Powder X-ray Diffraction	141
2B.6.1.2. Surface Area Measurements	143
2B.6.1.3. CO ₂ and NH ₃ TPD analysis	146
2B.6.1.3.1. CO ₂ TPD analysis of metal oxides	146
2B.6.1.3.2. NH ₃ TPD analysis of metal oxides	148
2B.7. Transesterification of EC/PC with methanol using MMOs	151
2B.8. Effect of calcination temperature	154
2B.8.1. XRD Analysis	154
2B.8.2. Surface area Analysis	155
2B.8.3. TEM analysis	156
2B.8.4. CO ₂ TPD analysis	157
2B.8.5. Effect of calcination temperature on the activity	160
2A.9. Effect of Reaction conditions	162
2A.9.1. Effect of EC: MeOH molar ratio	162
2A.9.2. Effect of reaction temperature	163
2A.9.3. Effect of catalyst loading	164
2A.9.4. Effect of reaction time	166
2B.10. Catalyst recycles study	167
2B.11. Screening of different alcohols for transesterification of EC	169
2B.12. Possible reaction mechanism	170
2B.13. DMC synthesis from PC/EC and methanol: Comparison with the literature	171
2A.14. Conclusions	173
2A.15. Overall conclusion	174
2A.16. References	177

Chapter 3: Synthesis of methyl phenyl carbamate by methoxycarbonylation of aniline with DMC using solid catalysts

Chapter 3A: Synthesis of methyl phenyl carbamate by methoxycarbonylation of aniline with DMC using Zn (Proline)₂ catalyst

3A.1. Introduction	190
3A.2. Materials	191
3A.3. Catalyst preparation	191
3A.3.1. Synthesis of M (Proline) ₂ complexes	192
3A.3.2. Synthesis of Zn (amino acid) ₂ complex	192
3A.3.3. FT-IR of M (Proline) ₂ and Zn (amino acid) ₂	193
3A.4. Experimental setup and procedure	195
3A.5. Analytical methods	195
3A.6. Quantitative analysis of reaction mixture	197
3A.6.1. External standard method	197
3A.7. Screening of catalysts for methoxycarbonylation reaction of aniline with DMC	198
3A.8. Screening of M (Proline) ₂ complexes	202
3A.9. Screening of different Zn (amino acid) ₂ complexes	203
3A.10. Effect of Reaction conditions	205
3A.10.1. Effect of catalyst loading	205
3A.10. 2. Effect of Aniline: DMC molar ratio	207
3A.10. 3. Effect of Temperature	209
3A.11. Substrate scope	212
3A.12. Stability of the Zn (Proline) ₂ (leaching test)	214

3A.13. Recycle study of Zn (Proline) ₂	215
3A.14. Proposed reaction mechanism	217
3A.15. Conclusions	218

Chapter 3B: *Synthesis of methyl phenyl carbamate by methoxycarbonylation of aniline with DMC using Ce-Zn-Zr mixed metal oxide catalyst*

3B.1. Introduction	219
3B.2. Materials	220
3B.3. Catalyst preparation (binary and ternary MMOs)	220
3B.4. Experiment procedure	221
3B.5. Analytical methods	221
3B.6. Screening of MMOs for methoxycarbonylation of aniline with DMC	222
3B.7. Effect of Zn concentration	224
3B.8. Result and discussion	226
3B.8.1. Characterization techniques of Ce ₃ Zn _x Zr ₁ MMOs	226
3B.8.1.1. XRD analysis	226
3B.8.1.2. TEM analysis	228
3B.8.1.3. Surface area and pore volume	229
3B.8.1.4. XPS analysis	230
3B.8.1.5. NH ₃ TPD analysis	239
3B.9. Effect of Reaction conditions	244
3B.9.1. Effect of catalyst loading	244
3B.9.2. Effect of Aniline: DMC molar ratio	246
3B.9.3. Effect of Temperature	248
3B.10. Stability of the Ce ₃ Zn _{0.5} Zr ₁ MMO catalyst (recycle study)	251

3B.11. Screening of aromatic amines	253
3B.12. Preliminary investigations to understand reaction pathways	255
3B.13. Conclusions	258
3B.14. Overall Conclusions	259
3B.15. Reference	261
Annexure	269
List of publications and symposia	276

List of Figures

Figure No.	Description	Page No.
Chapter 1		
1.1	Activation energy diagram	4
1.2	Steps involve in a heterogeneous catalytic reactions	9
1.3	Structure of hydrotalcite	11
1.4	Memory effect of the calcined hydrotalcite	15
1.5	Industrially important heterogeneous catalysts	17
1.6	Applications of mixed metal oxides.	17
1.7	Typical DMC reactivity pathways	23
1.8	Global consumption of DMC	25
1.9	Synthesis alternative routes of DMC	26
1.10	Block flow diagram of UBE process for gas phase synthesis of DMC	28
1.11	Various routes for MPC synthesis	51
Chapter 2		
Chapter 2A		
2A.1	Synthesis of LDHs by co-precipitation method	95
2A.2	Schematic of experimental setup	100
2A.3	A typical gas chromatograph chart showing reactants (EC and methanol), intermediate (HEMC) and products (DMC and EG).	102
2A.4	XRD patterns of all synthesized binary LDHs	104

2A.5	Effect of Ce concentration in $Mg_3Fe_xCe_{1-x}$ LDHs	108
2A.6	XRD patterns of all synthesized $Mg_3Fe_xCe_{1-x}$ LDHs	110
2A.7	FT-IR spectra of synthesized $Mg_3Fe_xCe_{1-x}$ LDHs	112
2A.8	TEM images and SAED patterns of synthesized $Mg_3Fe_xCe_{1-x}$ -	113
2A.9	Ce 3d XPS spectra of synthesized $Mg_3Fe_xCe_{1-x}$ LDHs	116
2A.10	Representative example of the deconvolution for the Ce 3d peak of LDH-6	116
2A.11	XPS O1s spectra of all synthesized $Mg_3Fe_xCe_{1-x}$ LDHs,	117
2A.12	Effect of molar ratio on EC conversion (A) and DMC selectivity (B)	121
2A.13	Effect of reaction temperature on EC conversion (A) and DMC selectivity (B)	123
2A.14	EC conversion and DMC selectivity profile at catalyst loading of 0.6-5 wt%.	124
2A.15	Typical reaction profile for EC to DMC	125
2A.16	XRD patterns of $Mg_3:Fe_{0.85}+M_{0.15}$ ternary LDHs with different M^{III} cations	126
2A.17	Catalyst leaching test	128
2A.18	Catalyst recycles study	129
2A.19	XRD patterns of fresh and used $Mg_3:Fe_{0.85}Ce_{0.15}$ (LDH-3).	130

Chapter 2B

2B.1	Synthesis of mixed metal oxides (MMOs) M^+ or $M^{2+}:Al^{3+}$ (3:1) by co-precipitation method	136
2B.2	A typical gas chromatograph chart showing reactants (PC and methanol) and products (DMC and PG).	139
2B.3	XRD patterns of hydrotalcites prepared	140
2B.4	XRD patterns of calcined (A) single metaloxides and (B) mixed metal oxides.	141
2B.5	CO_2 TPD of (A) single and (B) mixed metal oxide	147

2B.6	NH ₃ TPD of (A) single and (B) mixed metal oxide	149
2B.7	Patterns of calcined LiAl-HT at different temperatures	154
2B.8	TEM image of LiAl-HT calcined at different temperature	157
2B.9	CO ₂ -TPD of Li-Al HT calcined at different temperatures	158
2B.10	The influence of calcination temperature on the CO ₂ capture capacity	158
2B.11	A: Structure of Li-Al HT calcined at 500°C [Octahedral structure (α -LiAlO ₂)] and B: calcined at 800°C [Tetrahedral structure (β - LiAlO ₂)]	159
2B.12	Effect of reaction temperature on DMC yield (A) PC + MeOH system (B) EC+ MeOH system.	162
2B.13	Effect of Cyclic carbonate: MeOH molar ratio on DMC yield (A) PC + MeOH system (B) EC+ MeOH system	163
2B.14	Effect of catalyst concentration on conversion (A) PC + MeOH system (B) EC+ MeOH system	165
2B.15	Effect of reaction time on PC and EC conversion	166
2B.16	XRD patterns of used and fresh Li-Al 500 catalyst	168
2B.17	TEM images of (a) fresh (b) used Li-Al 500 catalyst	168
2B.18	A possible mechanism for the transesterification of ethylene carbonate with methanol catalyzed by Li-Al 500.	170

Chapter 3

Chapter 3A

3A.1	Schematic diagram of Zn (Proline) ₂ complex synthesis	191
3A.2	M (Proline) ₂ complexes	192
3A.3	FT-IR of M (Proline) ₂ complexes	193

3A.4	FT-IR of Zn (Amino acid) ₂ complexes	194
3A.5	Experimental set-up for synthesis of MPC from aniline and DMC	195
3A.6	A typical gas chromatogram for methoxycarbonylation of aniline and DMC using Zn (Proline) ₂ as catalyst	197
3A.7	Effect of catalyst loading on activity and selectivity of MPC	207
3A.8	Effect of aniline:DMC ratio on activity and selectivity of MPC	209
3A.9	Effect of reaction temperature on activity and selectivity of MPC	211
3A.10	Leaching of the catalyst	215
3A.11	XRD pattern of fresh, recycle Zn (Proline) ₂ and * ZnO phase	216
3A.12	Proposed mechanism for the Zn (Proline) ₂ complex catalyzed synthesis of MPC	218

Chapter 3B

3B.1	XRD patterns of all synthesized single, binary and ternary MMOs	226
3B.2	TEM images of A) Ce ₃ Zr ₁ B) Ce ₃ Zn _{0.25} Zr ₁ C) Ce ₃ Zn _{0.5} Zr ₁ D) Ce ₃ Zn _{0.75} Zr ₁ E) Ce ₃ Zn ₁ Zr ₁ F) Zn ₃ Zr ₁	229
3B.3	Ce 3d 3/2, 5/2 XPS spectrum of synthesized Ce ₃ Zn _x Zr ₁ MMOs	233
3B.4	O1s XPS spectrum of synthesized Ce ₃ Zn _x Zr ₁ MMOs	235
3B.5	XPS spectra of (A) Zr3d and (B) Zn 2p of all synthesized Ce ₃ Zn _x Zr ₁ MMOs	238
3B.6	NH ₃ TPD of Ce ₃ Zn _x Zr ₁ MMOs.	240
3B.7	Effect of catalyst loading on aniline conversion w.r.t reaction time	246
3B.8	Effect of Aniline: DMC molar ratio 1:5-1:20 on aniline conversion w.r.t reaction time.	248
3B.9	Effect of reaction temperature on aniline conversion w.r.t reaction time	250
3B.10	XRD patterns of Ce ₃ Zn _{0.5} Zr ₁ MMO fresh and used catalyst	252

- 3B.11 (A) TEM and SAED image of fresh $\text{Ce}_3\text{Zn}_{0.5}\text{Zr}_1$ (B) TEM and SAED image of 253
used $\text{Ce}_3\text{Zn}_{0.5}\text{Zr}_1$
- 3B.12 Schematic of methoxycarbonylation of aniline with DMC and the possible by- 255
products form during reaction
-

List of Tables

Table No.	Description	Page No.
Chapter 1		
1.1	Composition and symmetry of some natural anionic clays	12
1.2	Ionic radius of some cations, A ^o used in the synthesis of hydrotalcite like compounds	13
1.3	Some important industrial processes using metal oxide and mixed metal oxides as catalysts	18
1.4	Global DMC demand (Thousand Tons)	25
1.5	Literature survey on the synthesis of dimethyl carbonate (DMC) from cyclic carbonate and methanol	37
1.6	Literature serve on the synthesis of dimethyl carbonate from cyclic carbonate and methanol using metal oxide and mixed metal oxides	44
1.7	Literature survey on the synthesis of aromatic carbamates by methoxycarbonylation of aromatic amines with DMC	56
Chapter 2		
Chapter 2A		
2A.1	Conditions for gas chromatograph analysis	102
2A.2	Screening of binary LDHs for transesterification of EC and methanol to DMC	106
2A.3	Composition of Ce incorporated LDHs prepared based on ICP analysis	109

2A.4	Surface properties of the prepared LDHs	110
2A.5	Surface composition and relative atomic ratio for the synthesized LDHs determined from XPS measurements	118
2A.6	Effect of different metal cation $Mg_3:Fe_{0.85}:M_{0.15}$ for transesterification reaction of EC with MeOH	127

Chapter 2B

2B.1	Textural and surface acid base properties of single metal oxides	144
2B.2	Textural and surface acid base properties of mixed metal oxides	145
2B.3	Transesterification of cyclic carbonate (EC/PC) with methanol using single and mixed metal oxide catalysts	151
2B.4	Surface properties of Li-Al MMOs calcined at different temperature (300-800°C).	155
2B.5	Effect of calcination temperature on the activity	161
2B.6	Recycle study using Li-Al 500as catalyst.	
2B.7	Dialkyl carbonate synthesis by transesterification of ethylene carbonate (EC) with different alcohols using Li-Al 500 catalyst ^a	167
2B.8	DMC synthesis from PC/EC and methanol: Comparison with the literature reports	169

Chapter 3

Chapter 3A

3A.1	List of catalysts prepared	193
3A.2	Conditions for gas chromatograph analysis	196
3A.3	The effect of various catalysts on the synthesis of MPC from aniline and	200

	DMC	
3A.4	Screening of M (Proline) ₂ complexes for methoxycarbonylation of aniline with DMC	202
3A.5	Screening of various Zn (Amino acid) ₂ complexes for methoxycarbonylation of aniline and DMC.	204
3A.6	Effect of catalyst loading on methoxycarbonylation of aniline with DMC	206
3A.7	Effect of aniline:DMC molar ratio on methoxycarbonylation of aniline with DMC	208
3A.8	Effect of temperature on Methoxycarbonylation reaction of Aniline with DMC	210
3A.9	Screening of aromatic amines for methoxycarbonylation reaction with DMC	212
3A.10	Recycle study using Zn (Proline) ₂ catalyst	216
<hr/>		
Chapter 3B		
<hr/>		
3B.1	Screening of binary /ternary MMOs for synthesis of MPC from aniline and DMC	222
3B.2	Effect of Zn loading on the activity and selectivity with Ce ₃ Zr ₁ catalyst	224
3B.3	Lattice parameter (A ^o) and average crystal size of synthesized mixed metal oxides	227
3B.4	Surface area and pore volume of synthesized Ce ₃ Zn _x Zr ₁ MMOs	230
3B.5	Surface composition and relative atomic ratio of Ce3d and O1s for the Ce ₃ Zn _x Zr ₁ MMOs determined from XPS measurements.	231
3B.6	Acid properties of synthesized mixed metal oxides	239
3B.7	Effect of catalyst loading on methoxycarbonylation of aniline with DMC	245

3B.8	Effect of aniline:DMC molar ratio on methoxycarbonylation reaction of aniline with DMC	247
3B.9	Effect of temperature on methoxycarbonylation reaction of aniline with DMC	249
3B.10	Recycle study using $\text{Ce}_3\text{Zn}_{0.5}\text{Zr}_1$ ternary mixed metal oxide catalyst	251
3B.11	Screening of aromatic amines for methoxycarbonylation reaction using $\text{Ce}_3\text{Zn}_{0.5}\text{Zr}_1$	254
3B.12	Interaction of reactants/products under methoxycarbonylation conditions using $\text{Zn}(\text{Proline})_2$ catalyst	256
3B.13	Interaction of reactants/products under methoxycarbonylation conditions using $\text{Ce}_3\text{Zn}_{0.5}\text{Zr}_1$ catalyst	257

List of Abbreviations

APIs	active pharmaceutical ingredients
AC	Activated carbon
HTs	Hydrotalcites
LDHs	Layered double hydroxides
MMOs	mixed metal oxides
DFT	Density functional theory
IL	Ionic liquid
VOCs	volatile organic compounds
DMS	Dimethyl sulfide
PCO ₂	CO ₂ pressure, (MPa)
MN	methyl nitrite
DMC	Dimethyl carbonate
EC	Ethylene carbonate
TBAB	Tetrabutyl ammonium bromide
GHSV	Gas hourly space velocity
LHSV	Liquid hourly space velocity
PC	propylene carbonate
HEMC	2-hydroxy ethyl methyl carbonate
DABCO	4-diazabicyclo [2.2.2] octane
TPD	Temperature-programmed desorption
TEM	Transmission electron microscopy
TMS	Tetramethyl silane

GC-MS	Gas chromatography mass spectrometry
BET	Brunauer, Emmett and Teller
XRD	X-Ray powder diffraction
FT-IR	Fourier transform-infrared spectroscopy
MPC	Methyl N- phenyl carbamate
TON	Turnover number
TDA	Toluene diamine
MDA	Methyl diphenyl amine
MMPC	Methyl-N-methyl phenyl carbamate
XPS	X-ray photoelectron spectroscopy
NMR	Nuclear magnetic resonance spectroscopy
FID	Flame ionization detector
EG	Ethylene glycol
PTSA	methylbenzenesulfonate
TOS	Time on stream
PG	Propylene glycol
RREs	rare earth elements
SAED	selected area electron diffraction
TGA	Thermogravimetric analysis
DTA	Differential thermal analysis
g-C ₃ N ₄	Graphitic carbon nitride
PU _s	polyurethanes
NMA	N-methylaniline
NNDMA	NN-dimethyl aniline

Abstract of the thesis

Catalytic synthesis of dimethyl carbonate and its application as a green reagent for the synthesis of aromatic carbamates

Introduction

Dimethyl carbonate (DMC), is an important intermediate and is widely used in industry due to its non-toxicity, good biodegradability, and excellent solubility.¹ DMC is used as an alternative, to harmful phosgene for the synthesis of aromatic polycarbonates and isocyanates as a carbonylation reagent. It is also used in methylation reaction as a safe substitute for dimethyl sulfate, methyl halides; which are toxic and corrosive.² DMC is about 1000 times less toxic than phosgene. Moreover, because of its versatile chemical properties, DMC is used as an electrolytic solution in secondary lithium battery, as a flavoring agent in foodstuff and as a solvent in the field of paints. Owing to all these properties DMC is considered as an environmentally benign chemical and a safe reagent for many important transformations.³ Future demand for DMC is expected to grow in view of the stringent environmental regulations. Hence research work is being carried out on the development of safer routes for DMC synthesis and its utilization to value added products like aromatic carbamates by methoxycarbonylation of aromatic amines.⁴

Methyl N-phenyl carbamate (MPC) is the simplest aromatic carbamate and is widely used as intermediate in the synthesis of pesticides, insecticides, herbicides, plastics and often used as protecting groups for amine functionality.⁵ MPC is an important precursor for preparing methylene diphenyl diisocyanate (MDI) by condensation of MPC with formaldehyde, which is an important intermediate for the synthesis of polyurethanes (PUs).⁶ PUs are among the most valuable polymers produced by the chemical industry. In 2007 the global consumption of PUs as

raw material was about 12 million metric tons/year and the average annual growth rate is about 5%.

Aim of the present work was to develop an efficient and selective catalyst for the synthesis of DMC by transesterification of cyclic carbonates with methanol and synthesis of methyl-N-Phenyl Carbamate (MPC) via methoxycarbonylation of Aniline with DMC. The Thesis consists of three chapters, ***Chapter 1:*** deals with general introduction and literature available on the synthesis of DMC from cyclic carbonates and methanol and synthesis of aromatic carbamates from DMC and aromatic amines, ***Chapter 2:*** DMC synthesis by transesterification of cyclic carbonates with methanol using heterogeneous base catalysts, and ***Chapter 3:*** Synthesis of methyl phenyl carbamate by methoxy carbonylation of aniline with DMC using solid catalyst.

Chapter 1: Catalytic synthesis of Dimethyl carbonate and its application to value added products

Chapter 1 deals with general introduction to DMC and its application as a “Green Reagent” for the synthesis of value added products. Conventionally DMC was synthesized via phosgenation and presently manufactured by oxidative carbonylation of methanol; both of these routes require corrosive and poisonous gases like chlorine, COCl_2 and CO . In case of oxidative carbonylation of methanol there is a risk associated with the explosion hazard of CO/O_2 mixture. One clean and sustainable route for the synthesis of DMC is the transesterification of cyclic carbonate [ethylene carbonate (EC)/propylene carbonate (PC)] with methanol. This transesterification process was developed by Asahi Kasei Chemical, Japan and commercial plant was built by Texaco in 1987. Nowadays there are several plants based on this process in China. Transesterification process is a safe and waste less process and stoichiometric amount of ethylene

glycol is formed as a byproduct. Furthermore it implies the use of carbon dioxide as a starting material. Considerable amount of work has been carried out on the development of heterogeneous catalysts for the synthesis of DMC.⁴ From the literature it was observed that there are limited investigations on highly active and reusable catalysts for this reaction. Lower conversion of PC to DMC than EC to DMC was observed mainly due to steric factors and differences in the chemical structures of these alkylene carbonates. Thus there is a need to expand the scope of catalysts and hence work is being carried out on this important route.

DMC has a potential to provide atom efficient and safer route for the synthesis of aromatic carbamates from DMC and aromatic amines. Lot of work is being carried out on the development of catalysts for this reaction. Among all metal based catalysts; Zn and Pb metal salts have shown best catalytic activity.⁶ However, catalyst/product separation is difficult because of the homogeneous nature of these catalysts. Also, lead compounds showed high catalytic performance, but they are not environmentally friendly. Supported zinc acetate based catalysts were studied for this reaction ($\text{Zn(OAc)}_2/\text{AC}$, $\text{Zn(OAc)}_2/\alpha\text{-Al}_2\text{O}_3$ and $\text{Zn(OAc)}_2/\text{SiO}_2$)⁸ however, deactivation of Zn(OAc)_2 was observed with the formation of ZnO [reaction between methanol and Zn(OAc)_2]. Thus there is a need to develop active, selective and reusable catalyst for this important reaction.

Chapter 2: DMC synthesis by transesterification of cyclic carbonate with methanol using heterogeneous base catalysts

Chapter 2 presents work carried out on the synthesis of DMC from cyclic carbonate and methanol using heterogeneous catalysts. This chapter has been divided in two parts. Chapter 2A

deals with the synthesis of DMC using Mg-Fe-Ce ternary hydrotalcite as the catalyst, while Chapter 2B deals with DMC synthesis using Li-Al mixed metal oxide as the catalyst.

Chapter 2A: Synthesis of dimethyl carbonate by transesterification of EC with methanol using MgFeCe ternary Layer double hydroxide (LDH) catalyst.⁹

Transesterification of EC with methanol to DMC was investigated in detail using $Mg_3Fe_xCe_{1-x}$ ternary LDH as the catalyst. The LDHs were synthesized by varying Fe:Ce molar ratio in a range of 1:0–0:1. All synthesized LDHs were characterized by XRD, FT-IR, TEM, N_2 sorption, benzoic acid titration and XPS in detail and evaluated for selective synthesis of dimethyl carbonate by transesterification of ethylene carbonate with methanol.

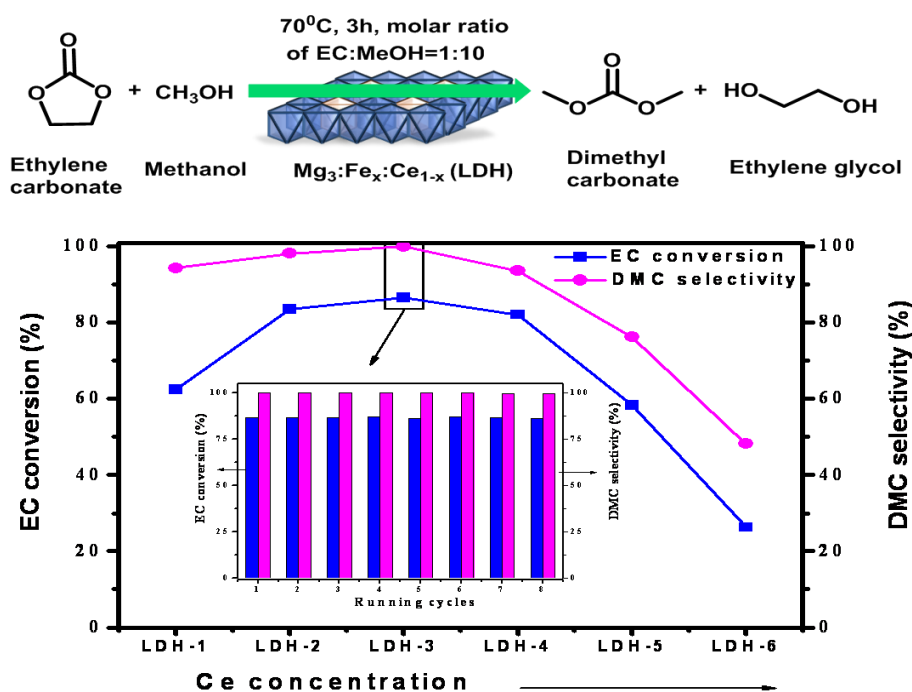


Figure 1. Schematic of transesterification of EC with methanol and Catalyst recycle study

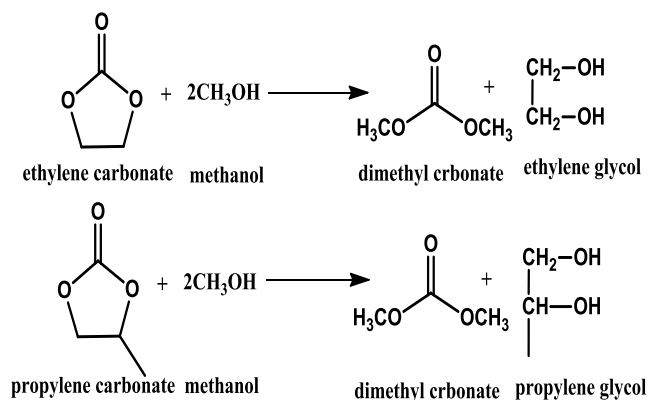
Reaction conditions: EC: 23 mmol, MeOH: 230 mmol, Catalyst: 2.5 wt% to EC, Reaction time: 3h, Temperature:70°C

Both the end members of this series Mg_3Fe_1 (LDH-1) and Mg_3Ce_1 (LDH-6) showed lower catalytic activity and selectivity to DMC. The significant increase in EC conversion and DMC selectivity was observed with appropriate concentration of Ce present in LDH structure. The activity varied in the order: LDH-6 < LDH-5 < LDH-1 < LDH-4 < LDH-2 < LDH-3. The activity trend was found to be in good agreement with structural and surface basic properties of the synthesized LDHs. Among the synthesized catalysts LDH-3 (Fe:Ce molar ratio: 0.85:0.15) showed best catalytic performance (87% EC conversion with 100% DMC selectivity) under mild reaction conditions. LDH-3 was found truly heterogeneous catalyst and was recycled seven times without loss in catalytic activity and selectivity to DMC (Fig.1). Various trivalent metals were also used to modify the LDH with composition $Mg_3Fe_{0.85}M_{0.15}$ [where $M^{3+} = La, Sm, Y$ and Cr] and the activity trend followed in order of $La \approx Ce > Sm > Y > Cr$. The best results were obtained with Ce modified Mg_3Fe_1 LDH ($Mg_3Fe_{0.85}Ce_{0.15}$) as the catalyst. The results were found to be in good agreement with the electro negativities of incorporated third metal cations [M^{3+}]. To the best of our knowledge this is the first report on the use of $Mg_3Fe_{0.85}M_{0.15}$ ternary LDH as a catalyst for this reaction.

Chapter 2B: Synthesis of dimethyl carbonate by transesterification of cyclic carbonate (EC/PC) with methanol using Li-Al mixed metal oxide catalyst DMC

synthesis by transesterification of PC/EC with Methanol was investigated using single and mixed-metal oxide (MMO) materials consisting of Li, Mg, Co, Ni, Zn, Al and/or Fe with distinct acid–base properties (Scheme 2). Binary MMOs were prepared via hydrotalcite precursors to achieve high surface area and homogeneous mixing of the resulting, typically nanosized metal oxide phases after calcination treatment. All catalysts were characterized in detail by XRD, BET,

TEM analysis and acid–base properties of the materials were determined by NH_3/CO_2 -TPD. The acid base properties of the catalysts prepared strongly influenced the activity towards DMC synthesis. Best results were observed with Li-Al 500 as the catalyst (86-75% of EC and PC conversion respectively with 100% selectivity to DMC) at 70°C for 1-3h using 2.5 wt% catalyst loading. The catalyst was highly stable and gave good performance for 5 recycle experiments with > 99% selectivity to DMC (Fig.2).



Scheme 2: Transesterification of EC/PC with methanol

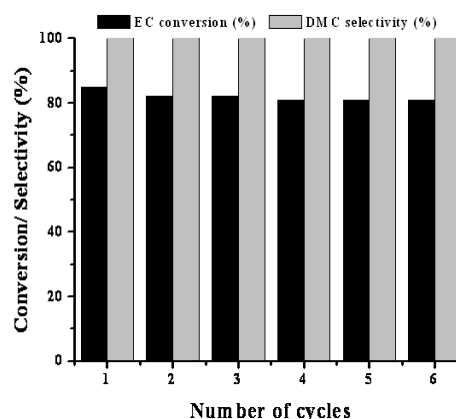


Figure 2: Catalyst recyclability test. Reaction EC:23mmol
EC: MeOH=1:10, Li-Al 500: 2.5 wt % relative to EC,
Reaction Time: 1h, Temperature: 70°C .

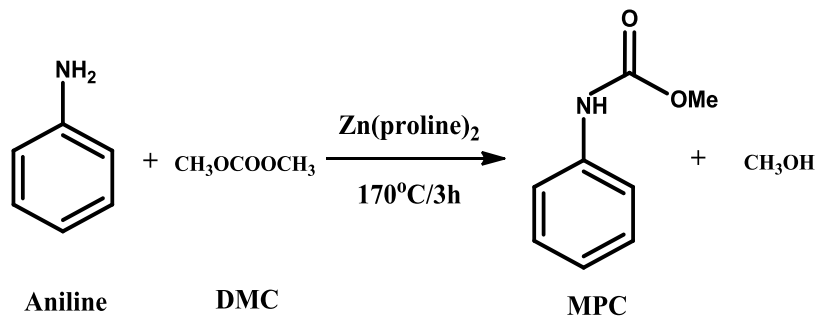
Applicability of Li-Al 500 was investigated for transesterification of EC with different alcohols including methanol, ethanol, n-propanol, n-butanol, and n-pentanol to give corresponding dialkyl carbonates as products. To the best of our knowledge, there are few reports on solid base catalysts showing high activity and selectivity to DMC for this reaction with PC as reactant at lower temperature under atmospheric pressure. Catalytic activity of Li-Al 500 was found to be superior compared to most of the reported solid catalysts under mild reaction conditions.

Chapter 3: Synthesis of methyl phenyl carbamate by methoxy carbonylation of aniline with DMC using solid catalysts

Catalytic synthesis of aromatic carbamates from aromatic amines and DMC has been investigated in chapter 3. Main aim of the work was to develop active, selective and recyclable catalyst for this reaction. Chapter 3A presents results obtained using Zn (Proline)₂ catalyst, while results obtained using Ce-Zn-Zr mixed metal oxide catalyst are presented in Chapter 3B.

Chapter 3A : Synthesis of methyl phenyl carbamate by methoxy carbonylation of aniline with DMC using Zn (Proline)₂

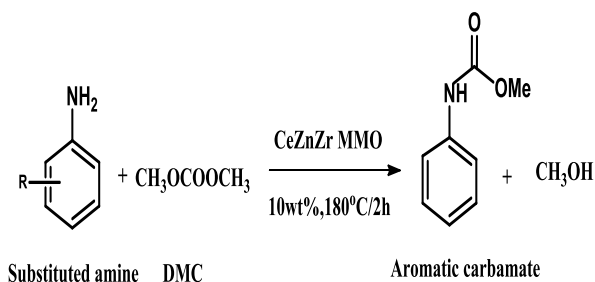
Methoxy carbonylation reaction of Aniline with DMC was carried out using M (amino acid)₂ complexes (Scheme 3). Various Zn (amino acid)₂ complexes were prepared by precipitation method. From which Zn (Proline)₂ showed the best catalytic activity towards MPC synthesis, hence detailed parametric study of reactions was carried out using Zn (Proline)₂ catalyst. Good results were observed with aniline: DMC ratio of 1:10, reaction temperature 170°C and reaction time of 3h (98.6% conversion with 97.8% selectivity to MPC in 3 h). Zn(Proline)₂ was found to be an efficient, Lewis acid catalyst for methoxycarboxylation reaction.



Scheme 3: Methoxycarbonylation of aniline with DMC

Chapter 3 B: Synthesis of methyl phenyl carbamate by methoxy carbonylation of aniline with DMC using Ce-Zn-Zr mixed metal oxide catalyst

Methoxy carbonylation reaction of aniline with DMC was carried out using binary and ternary MMOs as catalysts (Scheme 4). Various MMOs were prepared by co-precipitation method and screened for the reaction. Ternary $Ce_3Zn_{0.5}Zr_1$ MMO catalyst showed the best activity towards MPC and good results were observed with aniline: DMC ratio of 1:20 reaction temperature of $180^\circ C$ and reaction time of 2h (98.4% conversion with 98.7% selectivity to MPC). Effect of Zn concentration in Ce:Zn:Zr MMO was also studied in detail. All catalysts were characterized by various spectroscopic techniques using XRD, BET, TEM and acid properties of the materials determined by NH_3 -TPD. Zn concentration in Ce:Zn:Zr catalyst affects the activity and selectivity to MPC. Detailed parametric study was carried out using $Ce_3Zn_{0.5}Zr_1$ MMO catalyst. $Ce_3Zn_{0.5}Zr_1$ was recycled up to 6 recycle experiments with slight drop in activity. $Ce_3Zn_{0.5}Zr_1$ catalyst was found to be an efficient, stable, inexpensive and recyclable heterogeneous catalyst for methoxycarbonylation of aniline and DMC. XRD analysis of fresh catalyst and catalyst recovered after six recycle experiments showed similar pattern and did not show significant changes in the analysis (Fig.3).



Scheme 4: Methoxycarbonylation of aniline with DMC

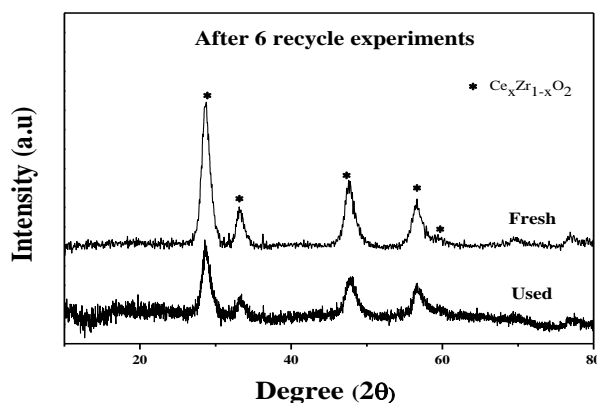


Figure 3: XRD pattern fresh and used $Ce_3Zn_{0.5}Zr_1$

References

1. Aric, F. and P. Tundo, *Dimethyl carbonate: a modern green reagent and solvent*. Russian Chemical Reviews, 2010. **79**(6): p. 479-489.
2. Tundo, P., M. Selva, and S. Memoli, *Dimethylcarbonate as a green reagent*. 2000, 87-89 ACS Publications.
3. Fiorani, G., A. Perosa, and M. Selva, *Dimethyl carbonate: a versatile reagent for a sustainable valorization of renewables*. Green Chemistry. 2018.**20**:p. 288-322.
4. Peng, W., et al., *Recent progress in phosgene-free methods for synthesis of dimethyl carbonate*. Pure and Applied Chemistry. 2011. **84**(3): p. 603-620.
5. Grego, S. and P. Tundo, *Phosgene-free carbamoylation of aniline via dimethyl carbonate*. Pure and Applied Chemistry.2012 **84**(3): p. 695-705.
6. Baba, T., et al., *Catalytic methoxycarbonylation of aromatic diamines with dimethyl carbonate to their dicarbamates using zinc acetate*. Catalysis letters, 2002. **82**(3-4): p. 193-197
7. Li, F., et al., *Condensation Reaction of Methyl N-Phenylcarbamate with Formaldehyde over H β Catalyst*. Industrial & Engineering Chemistry Research, 2014. **53**(13): p. 5406-541.
8. Zhao, X., et al., *Synthesis of MDI from dimethyl carbonate over solid catalysts*. Industrial & Engineering Chemistry Research, 2002. **41**(21): p. 5139-5144.
9. Nivangune N. et al. *MgFeCe Ternary Layered Double Hydroxide as Highly Efficient and Recyclable Heterogeneous Base Catalyst for Synthesis of Dimethyl Carbonate by Transesterification*.Catal Lett, 2017, 147,p. 2558

Chapter I

*Catalytic synthesis of Dimethyl carbonate and its
application to value added products*

1.1 Introduction

Today, we cannot expect our life without **science and technology** and most of our daily activities are influenced by technological advancements.¹ Chemical industry and Catalysis has played an important role in the day-to-day life directly or indirectly as exemplified by the manufacture of commodity chemicals, clothing, food-products, plastics, agrochemicals, pesticides and pharmaceuticals.^{2,3} While the petroleum and petrochemical industry is largely based on catalytic processes, in recent years the small volume specialty and fine chemicals are also preferred to be produced by catalytic routes. Most of the industrial chemical processes involve catalytic reactions and hence the subject of catalysis is considered as the backbone of chemical industry. Catalysis is also a key to the development of entirely new technologies or breathing new life into an otherwise, mature technology. As a result of this, the subject of catalysis has emerged, which involved catalytic process development as also the understanding of the chemistry of catalytic reactions and engineering aspects.

Over the past century industries utilizing chemistry and chemical engineering have been major contributors to worldwide economic development, however, this has led to increase in generation of toxic and hazardous wastes causing serious environmental problems. Alarmed by the increase in pollution government agencies have passed strict environmental regulation laws. This period saw the rise of environmental catalysis. This has led to many discoveries using catalysis for removal of toxic wastes, replacement of hazardous stoichiometric processes and development of environmentally compatible technologies, which generate minimum waste for conventional as well as new materials in various fields. Some of the important examples of industrial catalytic reactions are oxidation, hydrogenation, hydroformylation, carbonylation, metathesis,

hydrocyanation, alkylation, esterification and polymerization etc.⁴⁻⁶ In the early 90's the concept of environmental catalysis was conceived as 'Green Chemistry' to overcome the issue of pollution and sustainable development of chemical industry. Catalysis has played a major role in the development of Green Chemistry and at present approximately 85–90% of the products of chemical industry are made using catalytic processes.⁷

The following sections present, a brief introduction to catalysis, the background of the subject, a review of literature and specific research problems chosen along with the scope and objectives of this thesis.

1.2. Catalysis

Catalysis is a phenomenon by which chemical reactions are accelerated by small quantities of foreign substances, called catalysts. The word 'catalysis' comes from two Greek words, the prefix 'cata' meaning down and 'lysein' means 'to split or break'.⁷ The concept of catalysis was first proposed by chemist Elizabeth Fulhame and described in a 1794 book, based on her novel work in oxidation-reduction experiments.^{7a} The term catalysis was later used by Jöns Jakob Berzelius in 1835⁷ to describe reactions that are accelerated by substances that remain unchanged after the reaction. In the 1880s, Wilhelm Ostwald at Leipzig University started a systematic investigation into reactions that were catalyzed by the presence of acids and bases, and found that chemical reactions occur at finite rates and that these rates can be used to determine the strengths of acids and bases.⁸ For this work, Ostwald was awarded the 1909 Nobel Prize in Chemistry. Ostwald defined the catalyst, "Catalyst is a substance which increases the rate at which chemical reaction approaches equilibrium without becoming itself permanently involved". Catalysts work by providing an (alternative) pathway involving a different transition

state and lower activation energy.⁹ consequently, more molecular collisions have the energy needed to reach the transition state. Hence, catalysts enable reactions that would otherwise be blocked or slowed by a kinetic barrier.

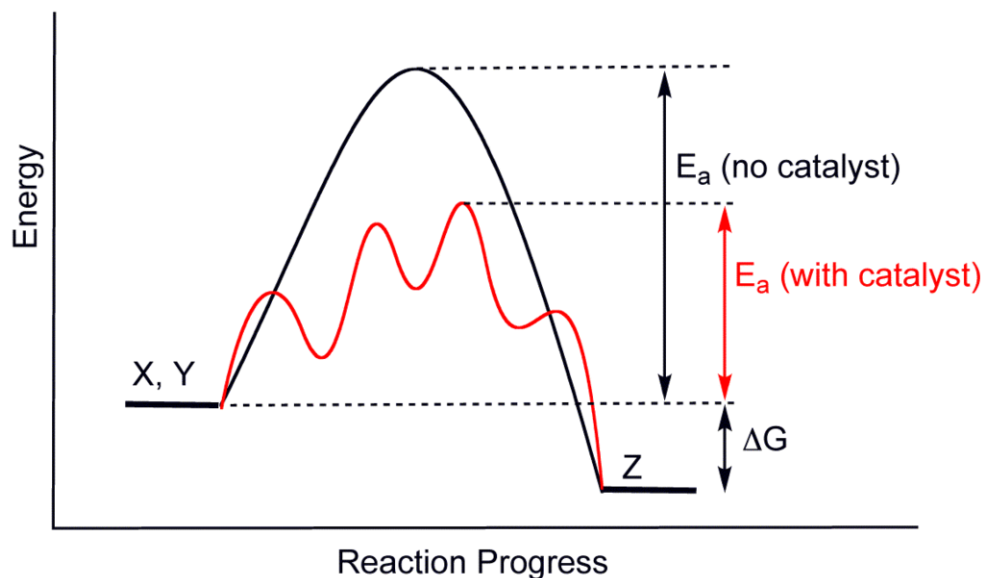


Figure 1.1: Activation energy diagram

The catalyst may increase reaction rate or selectivity, or enable the reaction at lower temperatures. This effect can be illustrated with an energy profile diagram (Fig.1.1) showing the effect of a catalyst in a hypothetical exothermic chemical reaction $X + Y$ to give Z (Scheme 1.1).⁸ The presence of the catalyst opens a different reaction pathway (shown in red) with lower activation energy. The final result and the overall thermodynamics are the same.

Catalysts generally react with one or more reactants to form intermediates that subsequently give the final reaction product, in the process regenerating the catalyst. The following is a typical reaction scheme, where C represents the catalyst, X and Y are reactants, and Z is the product of the reaction of X and Y :





Although the catalyst is consumed by reaction (1), it is subsequently regenerated in reaction (4), so it does not appear in the overall reaction equation (5):



Scheme 1.1: Mechanism of catalytic reaction

As catalyst is regenerated in a reaction, often only a small amount of the catalyst is needed to increase the rate of the reaction. Catalysts can be heterogeneous or homogeneous, depending on whether a catalyst exists in the same phase as the substrate. Biocatalysts (enzymes) are often seen as a separate group.

1.2.1. Types of Catalysis

Catalysis is generally categorized into three types. They are 1) Bio-catalysis, 2) Homogeneous catalysis 3) Heterogeneous (solid) catalysis.¹⁰ Separation of homogeneous catalyst from the reaction mixture is difficult limiting its commercial applications. In order to overcome the drawback of homogeneous catalysts various strategies are being developed to heterogenize homogeneous catalysts. The heterogenized homogeneous catalysts developed have advantage of high activity and selectivity similar to homogeneous catalyst and ease of separation like heterogeneous catalysts. This has led to Heterogenized homogeneous catalysts as separate category in the recent past.

➤ **Bio-catalysis**

Bio-catalysis is homogeneous in nature and provides regioselective and stereoselective transformations at ambient reaction conditions with almost no by-product formation.¹¹ Natural proteins (enzymes) or nucleic acids (RNAs or ribozymes and DNAs) are used to catalyse specific chemical reactions outside the living cells and the process is called as bio-catalysis.¹² Enzymes are obtained from animal tissues, plants and microbes (yeast, bacteria or fungi). Significant progress in the field of protein engineering and molecular evolution has revolutionized the world of bio-catalysis. The industrial scale syntheses of fine chemicals by using bio-catalysis include, active pharmaceutical ingredients (APIs),¹³ biofuels (e.g. lipase for the production of biodiesel from vegetable oil),^{14,15} dairy industry (e.g. protease, lipase for lactose removal, renin for cheese preparation),¹⁶ baking industry (e.g. amylase for bread softness, glucose oxidase for dough strengthening), detergent manufacturing (e.g. proteinase, lipase, amylase used to remove stains of proteins, fats, starch, respectively),¹⁷ leather industry (e.g. protease for unhairing and bating), paper industry and textile industry (e.g. amylase for removing starch from woven fabrics) etc.¹⁸

➤ **Homogeneous catalysis**

In homogeneous catalysis, the reactants, product and catalyst are present in same phase. Some examples of homogeneous catalysts are brønsted and Lewis acids, alkali and alkaline earth metal halides, ionic liquids, phase transfer catalysts, organometallic complexes and organo-catalysts etc.¹⁹ Methanol carbonylation to acetic acid²⁰ and hydroformylation of olefins²¹ represent successful applications of homogeneous catalysis on industrial scale. Homogeneous catalysts have been used in the manufacture of important bulk and fine chemicals for the polymer, pharmaceutical, paint and fertilizer industries. Important reactions carried out using homogeneous catalysis include oxidation, hydrogenation, carbonylation, hydroformylation, Heck, Suzuki and other coupling reactions, telomerization, co-polymerization and

metathesis reaction etc.²²⁻²⁴ Major advantage of homogeneous catalysis is that the catalyst is soluble in the reaction mixture, allowing a very high degree of interaction between catalyst and reactant molecules. Homogeneous catalyst is mostly discrete molecule dissolved in liquid and can activate the reactants under milder operating conditions (lower temperature and pressure conditions) compared to heterogeneous catalysts.²⁵ However, unlike with heterogeneous catalysis, the homogeneous catalyst is often irrecoverable after the reaction. Thus the main drawback of homogeneous catalysis is the separation of catalyst and products. This drawback has limited the commercial applications of homogeneous catalysis.²⁶ Thus only 15-20% of the industrial catalytic reactions involve homogeneous catalysts.

➤ **Heterogenized homogeneous catalysts**

Traditional heterogeneous catalysts (metal oxides or supported metals) exhibit lower selectivity and reactivity compared to homogeneous catalysts.²⁷ Homogeneous catalysts have high activity and selectivity, however, their separation from the reaction mixture is difficult. In order to surmount these issues, homogeneous catalyst is immobilized in to separate phase by various techniques to prepare heterogenized homogeneous catalysts. This can be achieved by immobilizing the catalyst in another liquid phase (biphasic catalysis) or by supporting the homogeneous catalyst on insoluble matrix.²⁸ Presently, biphasic catalysis and the solid supported homogeneous catalysts are widely recognized and well exploited in the academic and industrial research.²⁹ Thus “Heterogenized homogeneous catalyst” has emerged as a separate category in the recent past. The aim of this approach is to overlap the positive features of both homogeneous (selectivity and reactivity under milder reaction conditions) and heterogeneous catalyst (ease of separation of the catalyst from reaction mixture). This can be achieved through immobilization of catalysts such as metal complexes, organometallic compounds, ionic liquids on the different

solid surfaces (i.e. Al₂O₃, SiO₂, CeO₂, ZrO₂, AC, Zeolite, mesoporous material etc.) either through physisorption or chemisorption.³⁰ Covalent grafting of catalytically active species on solid surfaces is found to be most favored approach for designing heterogenized homogeneous catalysts. Catalysts can be synthesized by different methods like anchoring, tethering³¹ and encapsulation of homogeneous catalyst in inorganic matrix.³² The subject is important and has been reviewed extensively.^{25, 27, 33}

➤ **Heterogeneous catalysis**

In heterogeneous catalysis the reactant/product and catalyst are present in different phases.³⁴ Most heterogeneous catalysts are solids that act on substrates in a liquid or gaseous reaction mixture. Heterogeneous catalysts are classified depending on their uses in different forms. Various categories usually referred to are presented below:³⁵

- **Bulk catalysts**

Metals and metal alloys, Metal oxides, Mixed metal oxides, Carbides, Nitrides, Carbons, Ion exchange resins, Metal organic frameworks and Metal salts.

- **Supported catalysts**

Supported metals, supported mixed metal oxides, Surface modified oxides, Supported sulfide catalysts.

- **Coated catalysts**

Catalytically active layers of bulk or supported catalysts applied on inert structured surfaces are called as coated catalysts. Some examples of this system are monolithic honeycombs, foams and sponges, catalytic-wall reactors microstructured reactors with coated channels etc.³⁶

- **Nanomaterial based catalyst**

Heterogeneous catalysts broken up into metal nanoparticles (partial size 1-100 nm) in order to increase the surface area and active sites present on the catalyst surface which increases the rate of catalytic process. Some examples of nanocatalysts used for the important reactions are given below,

- ✓ Nano NiO catalyst supported on γ -Al₂O₃ microspheres of 3 μ m size developed by Johnson Matthey Company, for *Biomass gasification to produce high syngas* greater than 99% purity.³⁷
- ✓ Nanocatalysis of Al_{0.9}H_{0.3}PW₁₂O₄₀ nanotubes yields 96% of biodiesel from waste cooking oil as compared to 42.6% with conventional H₃PW₁₂O₄₀ catalyst.³⁸

➤ Steps involve in a heterogeneous catalytic reactions

In heterogeneous catalysis reaction takes place on the surface of catalyst and significant work has been carried out to understand mechanism of the reaction.³⁹

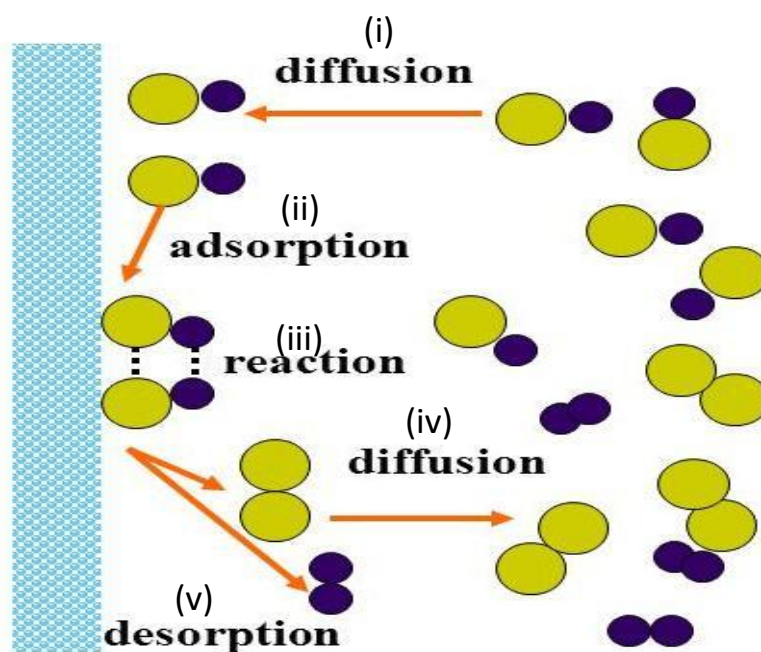


Figure 1.2: Steps involve in a heterogeneous catalytic reactions

The progress of catalytic reactions on active sites of heterogeneous surface can be resolved into five distinct steps (Fig. 1.2): (i) Diffusion of the reactants to the catalyst surface (ii) Adsorption of reactants at surface (reactant-surface interactions) (iii) Reaction on the surface (iv) Decomposition of product from the surface and (v) Diffusion of the reaction products away from the catalyst surface.^{40, 41} Industrially heterogeneous catalysts have been used for many important reactions and few examples are hydrocracking, alkylation, catalytic cracking, polymerization, ammonia synthesis, water-gas shift reaction, hydrogenation of vegetable oils, oxidation, reduction, oligomerization, esterification, hydrolysis and a variety of condensation reactions, etc.⁴²⁻⁴⁴

Main advantage of heterogeneous catalysts is very easy catalyst / product separation as compared to other catalysts. Thus most of the commercial processes use heterogeneous catalyst, which can be used in column (tubular reactor) for very long time (few months to years depending on the activity and stability).^{45,46} Consequently, the chemical industry is largely based upon heterogeneous catalysis and roughly 80-85% of all products are made using heterogeneous catalysts, and the percentage is increasing steadily.³⁵ Hydrotalcites (HTs) and HT derived mixed metal oxides (MMOs) are important class of heterogeneous catalysts used for many reactions.^{47,48} In the past few years there has been a rapid growth in publications related to the synthesis and application of HTs and derived mixed metal oxide catalysts and there are extensive review articles on this subject.⁴⁹⁻⁵¹ Since significant part of the work carried out in the present thesis is concerned with the use of HT and HT derived mixed metal oxides as catalysts, a brief introduction and applications of HT and HT derived mixed metal oxides as catalysts is given below.

1.2.2. Hydrotalcites (HTs)

In recent years hydrotalcites (HTs) have received increasing attention in the search for environmentally benign catalysts for base-catalyzed reactions.^{52,53} Replacement of the traditional homogeneous base catalysts, such as aqueous NaOH, by heterogeneous catalysts could result in the reduction of waste streams, facile separation of the catalyst, and reusability of the catalyst. The catalytic activity of HTs as well as mixed metal oxides formed by calcination of HTs have been exploited as basic catalysts in many chemical processes including Cross-aldol condensation of aldehydes and ketones, Knoevenagel condensation, Claisen–Schmidt condensation, Michael addition, Transesterification, and Alkylation at ambient temperature with high activity and selectivity.⁵⁴⁻⁵⁷

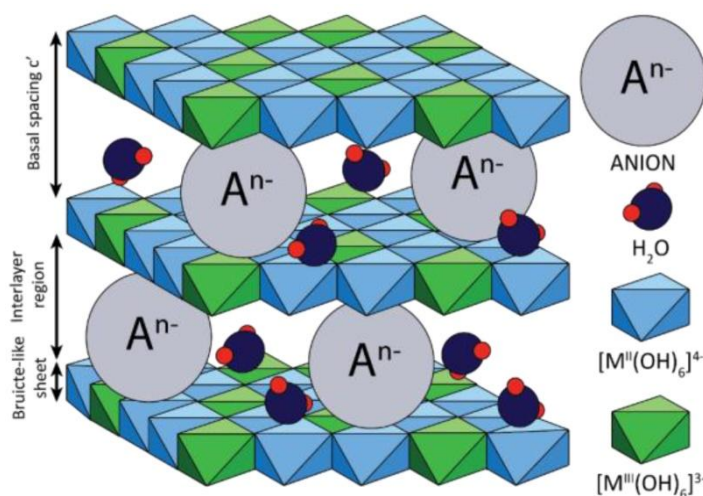


Figure 1.3: Structure of hydrotalcite

Hydrotalcite, $\text{Mg}_6\text{Al}_2(\text{OH})_{16}\text{CO}_3 \cdot 4\text{H}_2\text{O}$, is a naturally occurring anionic clay. It was first discovered in Sweden around 1842 and its name is derived from the fact that it can be easily crushed into a white powder similar to talc.⁵³ The structure of HT has been derived from brucite, $\text{Mg}(\text{OH})_2$, which exhibits layers of edge-sharing hydroxide octahedra centered by magnesium according to $\text{Mg}(\text{OH})_{6/3}$ (Fig. 1.3).

Table1.1: Composition and symmetry of some natural anionic clays.

Name	Chemical composition	Symmetry
Barbertonite	$\text{Mg}_6\text{Cr}_2(\text{OH})_{16}\text{CO}_3 \cdot 4\text{H}_2\text{O}$	Hexagonal
Desautelsite	$\text{Mg}_6\text{Mn}_2(\text{OH})_{16}\text{CO}_3 \cdot 4\text{H}_2\text{O}$	Rhombohedral
Hydrotalcite	$\text{Mg}_6\text{Al}_2(\text{OH})_{16}\text{CO}_3 \cdot 4\text{H}_2\text{O}$	Rhombohedral
Manasseite	$\text{Mg}_6\text{Al}_2(\text{OH})_{16}\text{CO}_3 \cdot 4\text{H}_2\text{O}$	Hexagonal
Pyroaurite	$\text{Mg}_6\text{Fe}_2(\text{OH})_{16}\text{CO}_3 \cdot 4.5\text{H}_2\text{O}$	Rhombohedral
Reevesite	$\text{Ni}_6\text{Fe}_2(\text{OH})_{16}\text{CO}_3 \cdot 4\text{H}_2\text{O}$	Rhombohedral
Sjögrenite	$\text{Mg}_6\text{Fe}_2(\text{OH})_{16}\text{CO}_3 \cdot 4.5\text{H}_2\text{O}$	Hexagonal
Stichtite	$\text{Mg}_6\text{Cr}_2(\text{OH})_{16}\text{CO}_3 \cdot 4\text{H}_2\text{O}$	Rhombohedral
Takovite	$\text{Ni}_6\text{Al}_2(\text{OH})_{16}\text{CO}_3 \cdot 4\text{H}_2\text{O}$	Rhombohedral

The structure of hydrotalcite has been investigated by various spectroscopic techniques like XRD, FT-IR, TEM, SEM etc.⁵³ The sheets are stacked one on top of the other and are held together by weak interactions through hydrogen bonds. Isomorphic replacement of Mg^{2+} ions by Al^{3+} results in an overall positive charge of the layers. The positive charge is compensated by the intercalation of CO_3^{2-} in the interlayer space. Also the equilibrium products of aqueous CO_3^{2-} solutions (OH^- , HCO_3^-) are present in the interlayer space as water molecules are also intercalated. The water molecules participate in hydrogen bonding to the hydroxide layers. In nature many compounds are found which have composition similar to HT i.e

$M(II)_6M(III)_2(OH)_{16}CO_3 \cdot 4H_2O$ but a different stacking sequence. The details of these compounds i.e name, composition and symmetry is listed in Table 1.1.⁵³

1.2.3. Hydrotalcite-like compounds

As stated earlier hydrotalcite is a solid compound with basic properties and has potential to replace homogeneous basic catalysts like NaOH. The molecular formula of HT is $Mg_6Al_2(OH)_{16}CO_3 \cdot 4H_2O$. In order to modify basic properties of the HT, it is possible to replace Mg with other divalent metal and Al can be replaced by other trivalent metal. With this idea various compounds have been prepared with the molecular formula $\{[M(II)_{1-x}M(III)_x(OH)_2]CO_3 \cdot (A^{n-}_{x/n}) \cdot mH_2O\}$. These materials are called as hydrotalcite like materials and have structure similar to HT. The above formula indicates that it is possible to synthesize a number of compounds with different stoichiometries; i.e with more than two metals and two anions.⁵³ Where M^{2+} represents divalent cation such as Mg^{2+} , Ca^{2+} , Zn^{2+} , etc and M^{3+} is trivalent cation such as Al^{3+} , Cr^{3+} , Fe^{3+} , Co^{3+} , etc. in the octahedral sites within the hydroxyl layers and x is equal to the ratio $M^{3+}/(M^{2+} + M^{3+})$ with a value varying in the range of 0.17-0.50. “A” is an exchangeable interlayer anion such as Cl^- , CO_3^{2-} and NO_3^- etc.

Table 1.2: Ionic radius of some cations, A° used in the synthesis of hydrotalcite like compounds

M(II)	Be	Mg	Cu	Ni	Co	Zn	Fe	Mn	Cd	Ca
	0.30	0.65	0.69	0.72	0.74	0.74	0.76	0.80	0.97	0.98
M(III)	Al	Ga	Ni	Co	Fe	Mn	Cr	V	Ti	In
	0.50	0.62	0.62	0.63	0.64	0.66	0.69	0.74	0.76	0.81

It is very important that M^{2+} and M^{3+} cations should have ionic radii not too different from 0.65 Å (characteristic of Mg^{2+}) to form a stable structure of HT like compounds.⁵³ Ionic radii of some

bivalent and trivalent cations used in the preparation of hydrotalcite like materials are listed in Table 1.2.

Acid base properties of the HTs can be tuned by using 1) various combinations of bivalent (Mg, Zn, Ni, Cu, Co) and trivalent (Al, Fe, Cr, Ni) cations and 2) by varying their molar ratios in brucite like structure. These types of materials have been widely studied and successfully used as basic catalysts for several reactions.^{53, 58} Recently incorporation of third metal cation in parent HT has attracted much more attention with the aim of modifying basicity of the catalyst.^{59, 60} Parvulescu et al.⁶¹ have prepared ternary hydrotalcite by incorporating Y^{3+} in the Mg-Al HT (Mg:Al 3:1 ratio). They observed significant improvement in the activity and selectivity for styrene epoxidation with hydrogen peroxide with ternary HT as the catalyst in acetonitrile. The electronegativity of yttrium (1.22) is lower compared to that of Al^{3+} (1.61) and results in higher basicity of the ternary HT prepared. Higher basicity of the ternary HT resulted in better epoxidation activity of this catalyst. Similar results were observed by Angelescu et al.⁶² by modifying Mg–Al HT with La and Y for cyanoethylation of ethanol.

Hydrotalcites have been used in large number of practical applications such as neutralizers (antacids), anion exchangers, polymer stabilizers, anion scavengers, catalysts and catalyst supports, adsorbents, filtration, electro active, photoactive materials and pharmaceuticals.⁶³ HTs are usually chosen over other compounds due to the versatility, simplicity, easily tailored properties and low cost of the materials. Many HT materials show unique phenomenon called “memory effect” which involves the regeneration of the layered crystalline structure from their calcined form (300-600°C), when the latter is dispersed in an aqueous solution containing suitable anion.^{53,66} Mg(Al)O exhibits a unique reconstruction ability provided that the calcination temperature is low (300-450°C) so as to avoid appearance of the spinel phase $MgAl_2O_4$ in the

calcined compound. This reconstructed material is known as “meixnerite” and behaves as Brønsted base type catalyst.^{67,68} This reconstruction is realized when calcined HTs are rehydrated in water or in flowing nitrogen saturated with water (to avoid contamination by CO_3^{2-}). The reconstructed material is more basic than the original HTs as it contains OH^- ions in the interlayer in contrast to CO_3^{2-} ions in the interlayers of the original HTs (Fig.1.4). This phenomenon of HTs allows introducing almost any kind of compensating anions that can be of use in the catalytic process.

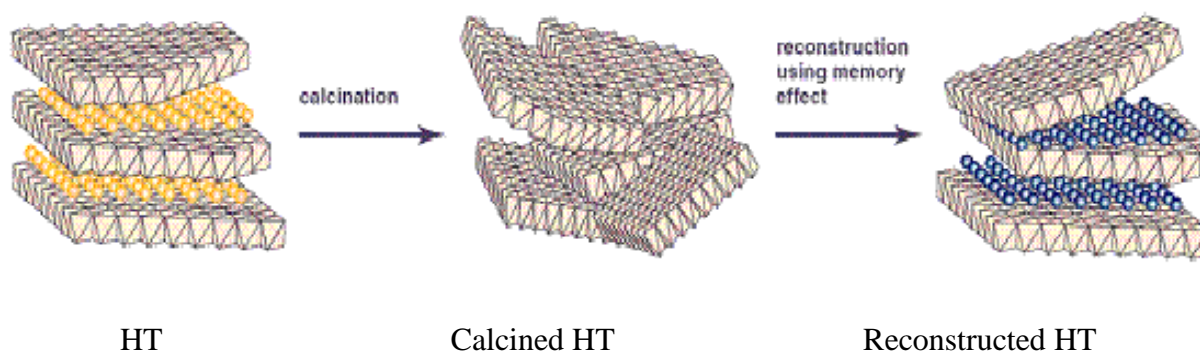


Figure 1.4: Memory effect of the calcined hydrotalcite

Hydrotalcites can be prepared by different ways: Co precipitation method, hydrothermal method, urea hydrolysis etc.⁵³ Co precipitation is the simultaneous precipitation of more than one compound from a solution.

Advantages of co precipitation method over other catalyst preparation methods are:⁵³

- It involves simple steps and is a time saving process
- The particle size and composition are easy to control
- It gives high output and recovery

Because of the advantages mentioned above the cost of HT preparation is lower for co-precipitation method. Factors that are considered important in the synthesis of HT like

compounds include the nature of the cations, their ratio, the nature of anions, pH maintained during synthesis, temperature, aging and the precipitation method.⁷⁰

The morphology of HTs is changed by thermal treatment. Thermal decomposition of HTs up to 700 °C is well-documented in the literature.⁷¹ Below 200 °C, the compounds lose the interlayer water. At 450–500 °C, the HT undergoes de-hydroxylation and decomposition of carbonate into carbon dioxide and results in the formation of corresponding metal oxides. At 660–700 °C DTA–TG analysis indicates that HT completely decomposes and FTIR analysis reveals a band of Mg–O and Al–O attributed to the spinel and periclase phase. The hydrotalcites have been used as brønsted basic catalysts for many reactions. However, metal oxides obtained after calcination of HTs are also basic in nature (Lewis basic) and have been widely used as heterogeneous basic catalysts for variety of reactions.^{72,73} The most interesting properties of the oxides obtained by calcination of HT are presented below:^{74,75}

- High surface area.
- Acid/Base properties.
- Formation of homogeneous mixtures of oxides with very small crystal size and stable to thermal treatments.

Details on the application of mixed metal oxides as catalysts (industrial and environmental importance) are discussed below.

1.2.4. Mixed metal oxides (MMOs)

Metal oxides represent one of the most important and widely employed categories of solid catalysts, either as active phases or as supports (Fig. 1.5 and 1.6). Metal oxides are utilized

both for their acid–base and redox properties and constitute the largest family of catalysts in heterogeneous catalysis.⁷⁵

Oxides containing two or more different kinds of metal cations are known as mixed metal oxides. Oxides can be binary, ternary and quaternary and so on with respect to the presence of the number of different metal cations. They can be further classified based on whether they are

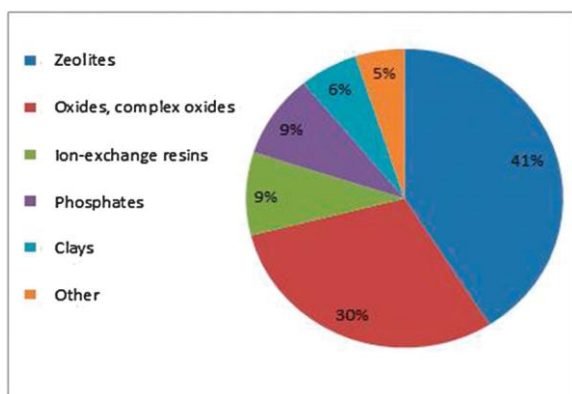


Figure 1.5: Industrially important heterogeneous catalysts.

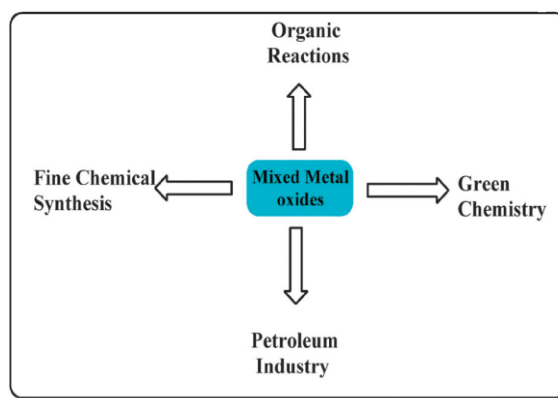


Figure 1.6: Applications of mixed metal oxides.

crystalline or amorphous. If the oxides are crystalline the crystal structure can be determined based on the oxide composition. For instance, perovskites have the general formula ABO_3 ; scheelites, ABO_4 ; spinels, AB_2O_4 ; and palmeirites, $A_3B_2O_8$.⁵⁰ The different metal cations (M_I and M_{II}) are present as $M_I^{n+}-O_x$ and $M_{II}^{n+}-O_x$ polyhedra, which are connected in various possible ways, such as corner or edge sharing, forming chains $M_I-O-M_{II}-O$, M_I-O-M_I-O or $M_{II}-O-M_{II}-O$. The arrangement of cations of a given element differs by the co-ordination and the nature of the neighbouring cations and this governs the type of bonding between the cations. Different environment of the cation that constitutes an active centre would give rise to different reactivity towards an approaching molecule. Oxide surfaces terminate by oxide O^{2-} anions, as their size is

much larger than that of M^{n+} cations. It follows that the symmetry and coordination of M^{n+} cations are lost at the surface. Moreover, the surface of an oxide may contain different types of defects and environments (kinks, steps, terraces), which play a determining role in the catalytic phenomenon.⁵⁰ This surface unsaturation is usually compensated for by a reaction with water vapour, leading to the formation of surface hydroxyls according to: $O^{2-} + H_2O \rightarrow 2OH$. OH groups are conjugated acids of lattice oxygen ions O^{2-} , which are strong bases and conjugated bases of water molecules.

Table 1.3: Some important industrial processes using metal oxide and mixed metal oxides as catalysts

Reaction	Catalyst
Steam reforming of hydrocarbons to $CO + H_2$	Ni/ Al_2O_3
Water gas shift ($CO + H_2O \rightarrow CO_2 + H_2$)	Fe oxide or mixed oxides Zn, Cu, Cr
Methane dry reforming ($CO_2 + CH_4 \rightarrow 2CO + 2H_2$)	Ni/ Al_2O_3
Methanol synthesis from $CO + CO_2 + H_2$	Cu-Zn-O/ Al_2O_3
Methanol oxidation to formaldehyde	$Fe_2(MoO_4)_3$
$SO_2 \rightarrow SO_3$ for H_2SO_4	V_2O_5
H_2S oxidation to SO_2 and H_2SO_4	Fe_2O_3/SiO_2 or $\alpha-Al_2O_3$
Metathesis	Re-O, Ru-O & W-O
Acrolein oxidation to acrylic acid	Mo-V-O
Hydrodesulphurisation of oil distillates	CoMo-O, NiMo-O, Ni-W-O/ $-Al_2O_3$
Alkanes (C_2-C_5) dehydrogenation to olefins	Cr_2O_3/Al_2O_3 or Pt/ Al_2O_3
Alkanes oxidative dehydrogenation to olefins	V based catalysts
Butane to maleic anhydride	$(VO)_2P_2O_7$
Methane oxidative coupling to ethylene	Doped rare earth oxides
Ethylene + HCl + O_2 to dichloroethane	ZnO, Cr_2O_3 , CuO
Exhaust gas elimination	Pt-Rh-Pd alloys on oxides

MMOs have been used as catalysts in various industrially important reactions such as reduction of nitroarenes, NO reduction with NH_3 , catalytic wet air oxidation of 2-chlorophenol, liquid phase catalytic oxidation of alcohols, alcohol dehydration, dehydrogenation of 2-octanol, transesterification with Na-based MMOs, destructive oxidation of $(\text{CH}_3)_2\text{S}_2$, solvent-free oxidation of primary alcohols to aldehydes using Au–Pd/TiO₂ catalysts⁷⁵ and in some other important applications which are listed in Table 1.3.⁷⁵ From Table 1.3 it is clearly observed that transition and noble group metal oxides have been frequently used as catalysts and their activity has been attributed to the outer electron configuration. Their catalytic activity may be traced to the presence of partially filled d-shells of the metal ion and to the influence of the oxide ligand field on this partially filled d-shell.⁵⁰ Mixed metal oxides are oxygen-containing combinations of two or more metallic ions in proportions that may either vary or be defined by a strict stoichiometry. Solid solutions and mixed metal oxides are classified according to their crystalline systems.

Over the past century industries utilizing chemistry and chemical engineering have been major contributors to worldwide economic development. This rapid development has led to serious environmental problems. In the early seventies concerns were raised on the alarming level of environmental pollution caused by chemical industries. Because of strict environmental regulations this period saw the rise of environmental catalysis. Also focus of the work in last several decades has been on the development of atom efficient routes with minimum waste generation. In the early 90's the concept of environmental catalysis was conceived as Green Chemistry to overcome the issue of pollution. MMOs have played an important role in the development of Green Chemistry by providing alternative to homogeneous acid and base catalysts and avoid generation of significant amount of by-product salts.

1.3. Green chemistry

1.3.1. Definition

Green chemistry has become an internationally recognized focus area of chemical science and it is defined by IUPAC as "*The invention, design and application of chemical products and processes to reduce or to eliminate the use and generation of hazardous substances*".⁷⁶

Green chemistry can also be termed as “sustainable chemistry”, since it is focused on the design of products and processes that minimize the use and generation of hazardous substances. Whereas Environmental Chemistry focuses on the effects of polluting chemicals on nature, Green Chemistry focuses on technological approaches to prevent pollution and reducing consumption of non-renewable resources. Green chemistry overlaps with all sub disciplines of chemistry but with a particular focus on chemical synthesis, process chemistry, and chemical engineering, in industrial applications.⁷⁷⁻⁷⁹ To a lesser extent, the principles of green chemistry also affects laboratory practices. The overarching goals of Green chemistry namely, more resource-efficient and inherently safer design of molecules, materials, products, and processes can be pursued in a wide range of contexts. In 1998, Paul Anastas (who then directed the green chemistry program at the US EPA) and John C. Warner (Polaroid Corporation) published a set of principles to guide the practice of Green chemistry.⁷⁷ Attempts are being made not only to quantify the greenness of a chemical process but also to factor in other variables such as chemical yield, the price of reaction components, safety in handling chemicals, hardware demands, energy profile and ease of product workup and purification. The twelve principles address a range of ways to reduce the environmental and health impacts of chemical production, and also indicate research priorities for the development of green chemistry technologies.⁸⁰

1.3.2. Twelve principles of Green Chemistry

- 1) Prevent waste formation instead of treating it.
- 2) Design atom-efficient synthetic methods.
- 3) Choose synthetic routes using non-toxic compounds where possible.
- 4) Design new products that preserve functionality while reducing toxicity.
- 5) Minimize the use of auxiliary reagents and solvents.
- 6) Design processes with minimal energy requirements.
- 7) Preferably use renewable raw materials.
- 8) Avoid unnecessary derivatization.
- 9) Replace stoichiometric reagents with catalytic cycles.
- 10) Design new products with biodegradable capabilities.
- 11) Develop real-time and on-line process analysis and monitoring methods.
- 12) Choose feedstock's and design processes that minimize the chance of accidents.

1.3.3. Synthetic strategy to achieve green chemistry processes

1.3.3.1. Catalytic processes

As suggested by the ninth principle of green chemistry, catalytic processes are preferred, when possible, because they offer several advantages compared to the stoichiometric methods including energy minimization and reduction of wastes.^{80,81} In fact, a catalyst lowers the activation energy of a process and experimental conditions should be less drastic. In addition, a heterogeneous catalyst is generally recovered and used for successive runs with economic and environmental benefits. The industrial importance of heterogeneous catalyst and their application in various fields we have discussed earlier in section 1.2.

1.3.3.2. Elimination of auxiliary reagents and solvents:

The fifth principle highlights the elimination of auxiliary substances, when possible. The auxiliary substances take part in the manipulation of a chemical reaction but they are not integral part of the molecule itself.^{80,82} Their use should be discouraged in the development of safe processes. When unavoidable, safer solvents and auxiliaries should be used. Traditional organic solvents are hazardous for the human health and environment. Both halogenated solvents (methylene chloride, chloroform, perchloroethylene, carbon tetrachloride) and aromatic hydrocarbons are carcinogens; volatile organic compounds (VOCs) represent a wide range of hydrocarbons and their derivatives are implicated in the atmospheric ozone generation.⁵¹ Unfortunately, these compounds are widely used in chemistry showing excellent solvency properties. Dimethyl carbonate (DMC) is an important intermediate and is widely used in industry and has emerged as a "Green Reagent/solvent" for synthesis of value added products.⁸³ ⁸⁴ Dimethyl carbonate (DMC) is an environmentally benign substitute for phosgene, DMS and methyl halides since it is a well-known non-toxic reagent as compared to other carboxylating or alkylating agents (phosgene and methyl halides, respectively). DMC is about 1000 times less toxic than phosgene.⁸⁵ Dimethyl carbonate does not produce inorganic salts. In fact, the leaving group, methyl carbonate, decomposes giving only methanol and CO₂ as by-products. Dimethyl carbonate is classified as a flammable liquid, smells like methanol and does not have irritating or mutagenic effects by either contact or inhalation. Therefore, it can be handled safely without the special precautions required for the poisonous and mutagenic methyl halides and DMS, and extremely toxic phosgene.⁸⁶ The details on DMC as a green reagent for the synthesis of value added products are discussed in the following section.

1.3.4. DMC as a green reagent

Reactions involving dimethyl carbonate (DMC) represent the epitome of green and environmentally sustainable transformations. DMC based processes can take advantage of the dual role of DMC as both solvent and (electrophilic) reagent to transform highly functionalized bio-based chemicals into a plethora of other molecules. The reactivity of DMC is well documented, as summarized in Fig. 1.7.⁸⁷

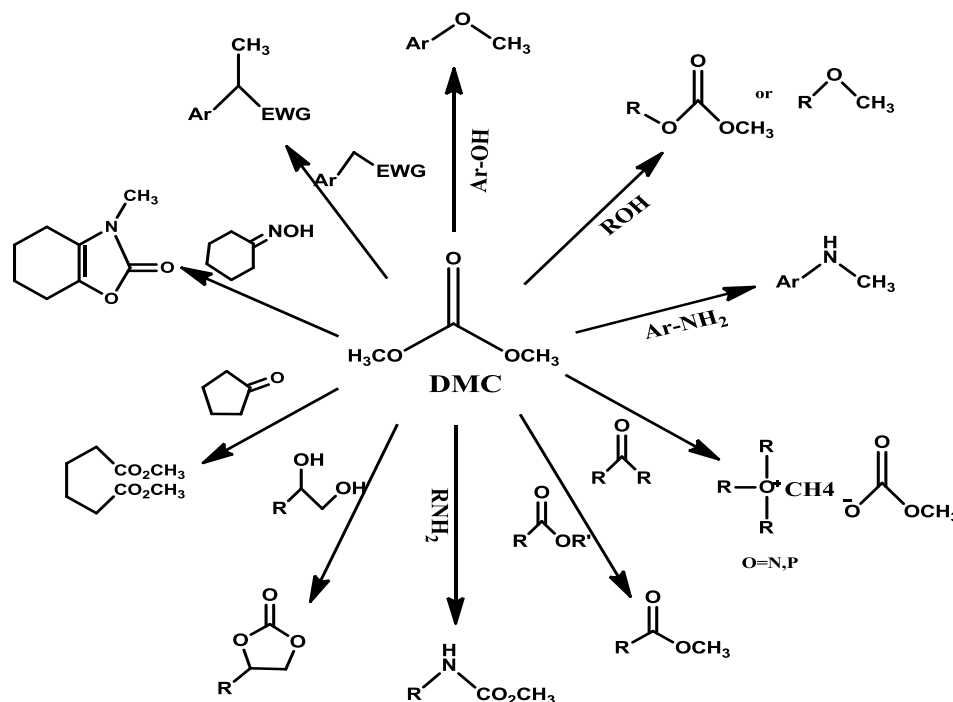


Figure 1.7: Typical DMC reactivity pathways.⁸⁷

DMC can act as a nucleophile either on the carbonyl carbon or on one of its methyl groups, and the observed chemoselectivity depends on several factors, including the nature of the nucleophile, reaction conditions and structure of the products. Some of the possible reaction pathways of DMC are listed in Fig.1.7, clockwise from the top: with phenols to yield anisoles, with alcohols to yield alkyl-methyl- or dialkyl carbonates or alkyl methyl ethers, with anilines to yield methylamines, with tertiary amines or phosphines to yield – onium methylcarbonate salts,

with esters or acids to yield methylesters, with amines and CO₂ to yield carbamates, with diols to yield cyclic carbonates, with cyclic ketones to yield diacids, with hydroxyimines to yield oxazolidinones, and with activated CH₂ groups to yield their methylated equivalents.⁸⁷

Dimethyl carbonate reacts selectively with a great variety of compounds as a methylating or carboxymethylating reagent, it requires only catalytic amount of a base and produces no waste (high atom economy). DMC can also be used to control the selectivity of the methylation and/or methoxycarbonylation reaction both on simple (amines, alcohols and thiols etc.) and more complex nucleophiles (hydrazines, sugars and aminoacids etc.). As a result, several industrial procedures already use DMC as a reagent (or a solvent) and many others are under investigation.⁸⁸ Ultimately, it must be stated that the exploitation of eco-sustainable reagents, such as DMC, is a fundamental issue for our ever-evolving society, since this will pave the way to a 'greener' future for the next generations.⁸⁹ Main aim of the present thesis was synthesis of DMC from cyclic carbonates and its application to the synthesis of aromatic carbamates. Hence a brief introduction to DMC synthesis and detailed literature report on the synthesis of DMC from cyclic carbonates and methanol and synthesis of aromatic carbamates from aromatic amines and DMC as "Green Reagent" is presented below.

1.4. Dimethyl carbonate (DMC)

Dimethyl carbonate (DMC), is an important intermediate and is widely used in industry due to its non-toxicity, good biodegradability, and excellent solubility.⁸⁹ Worldwide demand of DMC has been increasing continually because of its applications in polycarbonate industry, fuel technology, pharmaceuticals, electrochemical and catalytic reactions. According to Nexant's Chem Systems report (Fig. 1.8) 51% of DMC produced was utilized for polycarbonate

production, 24% was used as solvent, and the rest for other applications. From the Table 1.4 it can be observed that the global demand of DMC speculated in 2015 will be 3 times higher than the estimated one (2011).⁹⁰

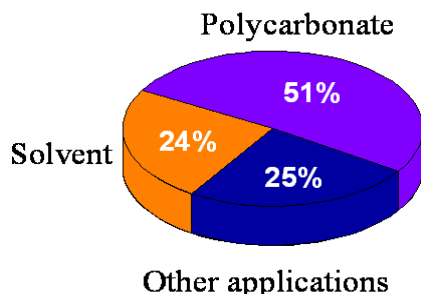


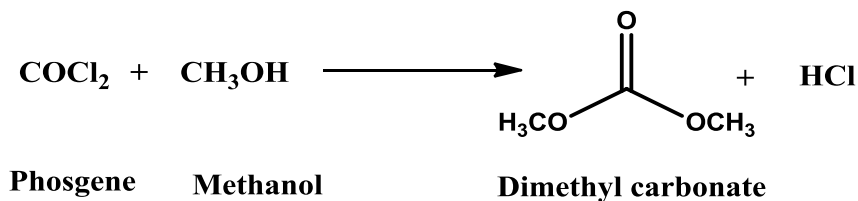
Figure 1.8: Global consumption of DMC.⁹⁰

Table 1.4: Global DMC demand (Thousand Tons)

							Average Annual	
	2002	2005	2008	2011	2014	2015	2011-2014	2015-2025
			Actual	Estimate	Forecast	Speculation	Growth rate (%)	
	2002	2005	2008	2011	2014	2015	2011-2014	2015-2025
Polycarbonate	50	112	179	218	258	516	5.8	6.5
Solvent		13	74	102	156	403	15.3	9
Other	40	43	92	109	130	452	5.9	12
Global Consumption	90	168	345	429	544	1351	8.2	8.8

The demand for DMC is expected to grow annually by 6.5% till 2025. Hence, lots of efforts have been made in order to find a sustainable route to produce DMC on a large scale.

Conventional process for synthesis of DMC based on the phosgenation of methanol was in operation till 1980.⁸⁸ In this synthesis, HCl was produced as unwanted side product (Scheme 1.2). Use of highly toxic phosgene was the major drawback of the conventional technology.



Scheme 1.2: Synthesis of DMC by phosgene and methanol

Phosgene is highly toxic in nature and also because of the formation of large excess of salts the process is not in operation. As a result several non-phosgene routes have been explored and few are used for commercial synthesis of DMC (Fig. 1.9).

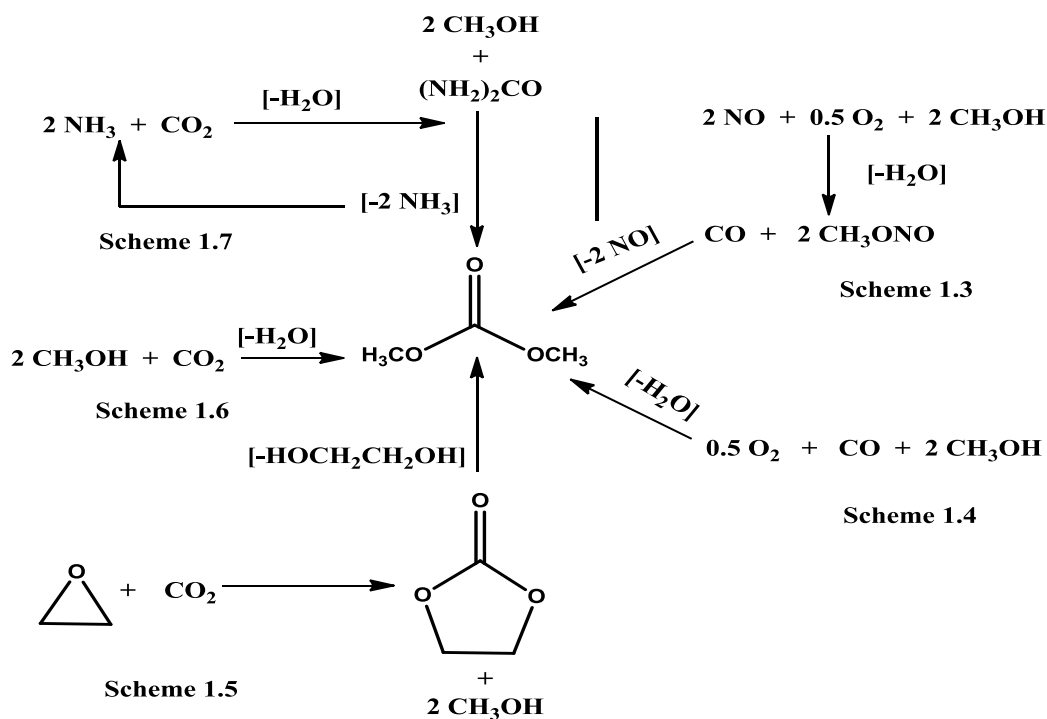


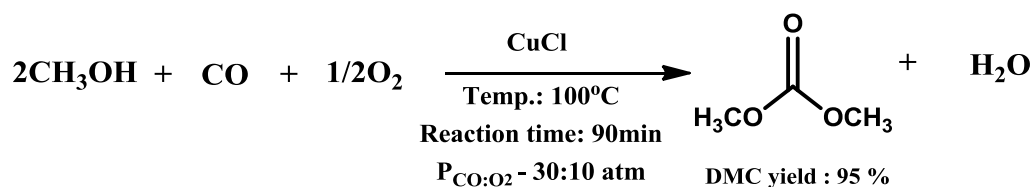
Figure 1.9: synthesis Alternative routes of DMC.

Present commercial processes involve oxidative carbonylation of methanol using copper based catalyst developed by Enichem⁹¹ (Fig. 1.9, Scheme 1.3), the methyl nitrile carbonylation process developed by Ube Industries⁹⁰ (Fig. 1.9, Scheme 1.4) and transesterification of methanol with ethylene carbonate (EC) developed by Asahi Kasei Chemical Company, Japan⁹² (Fig. 1.9, Scheme 1.5). Other alternative and safer routes being investigated for the synthesis of DMC are:

DMC synthesis directly from CO₂⁹³ (Fig. 1.9, Scheme 1.6) and Urea methanolysis⁹⁴ (Fig. 1.9, Scheme 1.7). The important literature available on the synthesis of dimethyl carbonate by non-phosgene routes are discussed below.

1.4.1. Synthesis of DMC by oxidative carbonylation of methanol

In late 1980, the Italian company Eni Chem developed a novel phosgene free route for the production of dimethyl carbonate based on oxidative carbonylation of methanol over CuCl catalyst with 95% DMC yield in 90 min reaction time at 100°C (Scheme 1.8).⁹⁵



Scheme 1.8: Oxidative carbonylation of methanol⁹⁵

From the reported literature it was observed that most of the work has been carried out with CuCl based catalysts.⁹⁶⁻⁹⁸ Though CuCl showed good activity towards DMC synthesis, it remains soluble in the reaction mixture and hence catalyst/product separation is difficult. To overcome this drawback several heterogenized CuCl based catalysts with different solid supports (silica, SBA-15, MCM-41, zeolite, activated carbon etc.) have been investigated.⁹⁹⁻¹⁰¹ Cao et al.¹⁰² reported CuCl immobilized on a diamide-modified mesoporous SBA-15 silica, which is air-stable and reusable catalyst, which showed 22% methanol conversion with 99% selectivity to DMC at 120°C in 5h reaction time. Though the heterogenized CuCl on different solid supports showed better activity (methanol conversion 7-31% and DMC selectivity 80-99%), they showed deactivation and equipment corrosion problems due to presence chlorine species in catalyst. Yuan et al.^{99,102} developed chlorine-free Cu-exchanged MCM-41 (Cu/MCM-41) however; lower

methanol conversion of 12.6% and 97.5% selectivity to DMC was observed. Though many efforts have been made to prepare chlorine free catalysts unfortunately, the activity is still far from viable for industrial application.

1.4.2. Synthesis of DMC using NO

Ube Industries developed a gas phase process for DMC synthesis from Methanol and NO over Pd based bimetallic catalyst which is a two-step process. Fig.1.10 shows a simplified schematic of the UBE process.^{103, 104} The reaction section has two reactors, one for MN (methyl nitrite) synthesis (reactor 1) and the other for DMC synthesis (reactor 2). The effluent gas from the DMC synthesis reactor is separated into the gas fractions, NO and DMC. DMC is purified by distillation from other by-products.

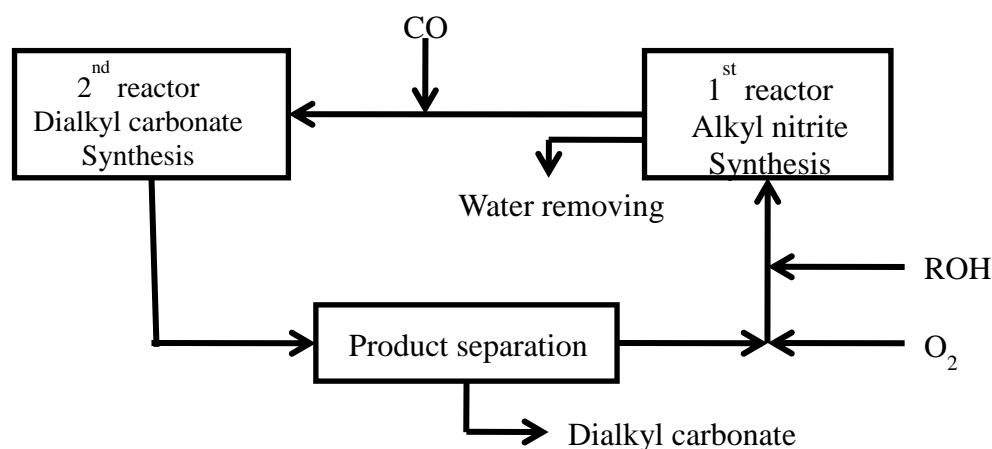
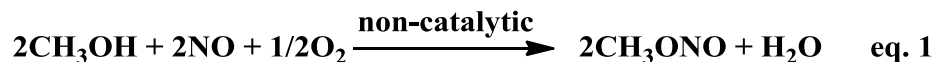
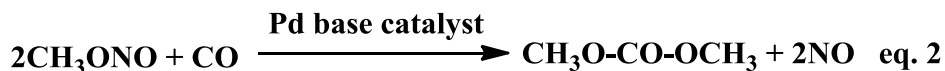


Figure 1.10: Block flow diagram of UBE process for gas phase synthesis of DMC.¹⁰³

Reactor 1: In the first reactor, methyl nitrite (MN) is non-catalytically synthesized from NO, O₂ and alcohol in the liquid phase at 60 °C with contact times ranging from 0.5 to 2 s (eq.1).



At this stage, it is necessary to remove the water formed from the reaction media in order to perform the DMC synthesis in a fully anhydrous media, so that the activity of the catalyst could be maintained with time on stream.

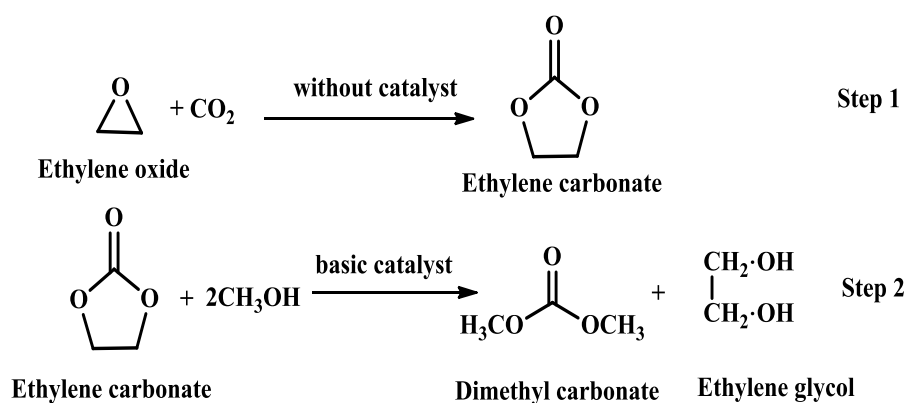


Reactor 2: The second step involves vapor phase catalytic reaction between methyl nitrite and carbon monoxide (both reactants with contents around 5–30 vol%) over an activated charcoal supported palladium chloride catalyst ($\text{Pd}^{\text{II}}\text{Cl}_2$) in a fixed-bed reactor (eq. 2). The reaction is performed in the presence of small amounts of chloride compounds diluted in an inert gas. The catalytic reaction between methyl nitrite and carbon monoxide at 100–120°C and at 0.5–1MPa formed DMC according to eq. 2. The DMC production was ranging from 200 and 600 kg [m^3 cat] h^{-1} for a contact time within the 0.5–5 s range.

Synthesis of DMC via MN carbonylation can be catalyzed by various kinds of Pd containing catalysts supported on activated carbon (AC) such as $\text{PdCl}_2\text{-CuCl}_2/\text{AC}$, $\text{PdCl}_2\text{-FeCl}_3/\text{AC}$, $\text{PdCl}_2\text{-BiCl}_3/\text{AC}$, etc.¹⁰⁵⁻¹⁰⁷ Among them, $\text{PdCl}_2\text{-CuCl}_2/\text{AC}$ catalyst performed best (6.14 mol DMC/l cat h), while CuCl_2/AC was almost inactive (0.04 mol DMC/l cat h) at 120°C, 0.4 MPa, GHSV 4000 h^{-1} .¹⁰⁴ These results suggest that Pd species are found to be active species for this reaction. Manada et al.¹⁰⁸ observed deactivation of the catalyst because of the conversion of Pd (II) species to Pd (0) in the presence of reactant CO. However, Pd (0) species could also be re-oxidized to Pd (II) species upon treatment with MN and HCl, Therefore, the catalytic performances could be maintained by adding HCl. Safety is very important in this process since MN and NO (laughing gas) are highly toxic chemicals and extreme care is required while handling MeOH, NO and oxygen in the reaction.

1.4.3. Synthesis of DMC by Transesterification of ethylene carbonate with methanol

Asahi Kasei Chemical, Japan has developed a two-step process based on transesterification of ethylene carbonate with methanol.⁹² This is one of the Green processes for DMC synthesis and was licensed to Texaco in 1987. There are several plants based on this process in China.¹⁰⁹



Scheme 1.9: DMC synthesis from transesterification of ethylene carbonate with methanol.

Transesterification of ethylene carbonate and methanol consists of two steps: the reaction of ethylene oxide with CO₂ affords ethylene carbonate in the first step (Scheme 1.9, Step 1); ethylene carbonate (EC) reacts with methanol to produce DMC and Ethylene glycol (EG) in second step (Scheme 1.9, Step 2). This process is considered as an excellent green chemical process for DMC synthesis. Asahi Kasei⁹² has commercialized this process as part of polycarbonate synthesis complex. Asahi process is one of the best processes and does not involve any toxic or hazardous chemicals, however ethylene glycol produced in stoichiometric quantities is a major problem with this process. Manufacturer having captive use of ethylene glycol can utilize this technology successfully. This process was primarily developed for the polycarbonate industry specifically for the synthesis of diphenyl carbonate (DPC) without the

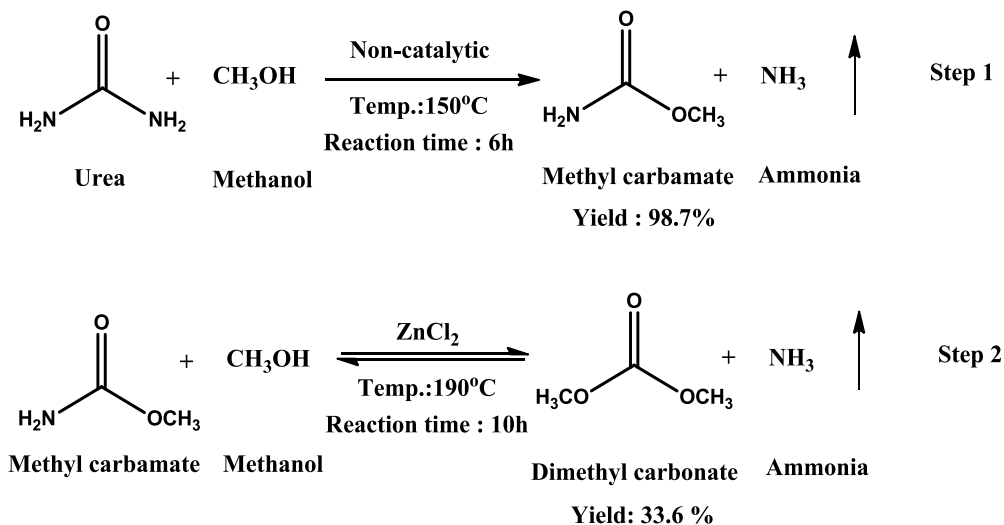
use of phosgene.¹¹⁰⁻¹¹² Catalyst preferred in this process are alkali or alkaline earth compounds [such as hydroxides, carbonates, bicarbonates, alkoxides, tertiary amines, N-containing heteroaromatics, and alkoxy metal (Sn, Ti, Zn)]^{92a} compounds as homogeneous catalysts and anion exchange resins having tertiary amino groups or quaternary ammonium groups as heterogeneous catalysts. The catalyst recycle and product separation to make process commercial feasible is major drawback of the homogeneous catalysts developed. Anion exchange resin having tertiary amino groups has been used as heterogeneous catalyst for this reaction. The reaction was carried out at 60°C with MeOH:EC molar ratio of 2 : 1 in a continuous tubular reactor with the rate of LHSV= 0.33 h⁻¹ to obtain EC conversion of 39% with 99% selectivity to DMC at steady state. Though the selectivity of DMC was observed high (99%) EC conversion was observed low (39%) in Asahi process. Intricate recycle recovery process was developed to make the process commercially feasible.^{92a}

Further work is being carried out on the development of heterogeneous solid base catalysts for ease of catalyst/product separation and as a promising alternative for homogeneous catalysts. The transesterification of propylene carbonate is also an interesting alternative for DMC synthesis and stoichiometric amount of prolylene glycol is formed as a byproduct in this reaction. In China, more than 90% of DMC is produced by transesterification of MeOH and propylene carbonate (PC).¹⁰⁹

1.4.4. DMC synthesis from urea and alcohol

Synthesis of carbonates by alcoholysis of urea was first proposed by Peter Ball¹¹³ in 1980. In this process, urea reacts with methanol to form dimethyl carbonate and ammonia. Synthesis of DMC by urea methanolysis is a two-step process. The first step is fast and produces methyl

carbamate (MC) with high selectivity even without any catalyst (Scheme 1.10 Step 1); the second step (MC to DMC) is difficult and rate-determining step (Scheme 1.10 Step 2). Hence most of the work has been carried out for find out active and selective catalyst for step 2.



Scheme 1.10: Two step DMC synthesis from urea and methanol¹¹³

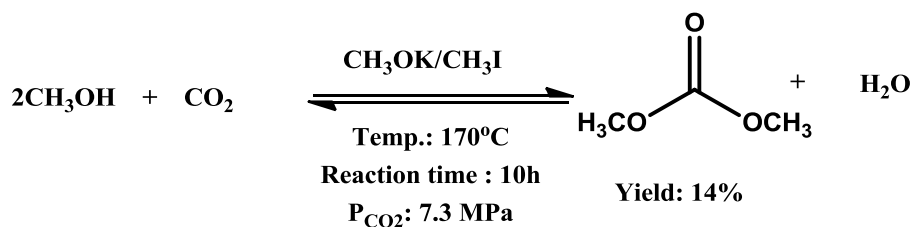
Zhao et al.¹¹⁴ have investigated the reaction of MC and methanol using various zinc compounds as a catalyst in a batch reactor. Among them, ZnCl_2 showed the highest catalytic activity and led to the DMC yield of 33.6 % under the optimal conditions (MC: 7.5 gm, MeOH: 64 gm at $190^\circ\text{C}/10\text{h}$). FT/IR spectra and XRD characterization indicated that MC is activated by Zn^{2+} through the coordination of the nitrogen atom with $\text{Zn}(\text{NH}_3)_2\text{Cl}_2$ as an intermediate in catalytic cycle after the reaction. Based on this, a possible reaction mechanism for catalyst ZnCl_2 was proposed. Though ZnCl_2 exhibited high catalytic activity in the reaction of MC and methanol, catalyst remains homogeneous in reaction mixture and difficult to separate from the reaction mixture. To overcome this various heterogenized Zn based catalyst have been explored.¹¹⁵⁻¹¹⁷ Wang et al.¹¹⁸ prepared series of zinc/iron mixed metal oxides (prepared by calcination of hydrotalcite-like compounds) as catalysts in the synthesis of DMC from MC and methanol. The MC conversion of

46.1% was obtained with 30.7% yield of DMC at the optimal reaction conditions (MC: 7.5gm, MeOH:64gm at 190°C/10h). Even though the yield is better the system suffers from low selectivity due to the formation of several by-products such as N-methyl urea (NMU) and N-methyl methyl carbamate (NNMC). Further Zhao et al.¹¹⁹ explored various lanthanum compounds as novel catalysts in the reaction of MC with methanol. Among them, La(NO₃)₃ presented the best catalytic performance with the DMC yield of 53.7 % under suitable reaction conditions (MC:7.5gm, MeOH:64gm at 180°C/8h). A possible reaction mechanism over La(NO₃)₃ was also proposed for this reaction on the basis of XRD, FT/IR and element analysis which revealed that MC is activated by La³⁺ via the coordination of the oxygen atom in carbonyl group. Though this process starts from cheap raw materials and is environmental-friendly the process suffers from major drawback: 1) Ammonia produced in the first step can restrict the formation of the DMC. 2) Low selectivity of DMC due to formation of side products (NMU and NNMC) and DMC decomposition under reaction conditions in the presence of catalyst leads to lower DMC yield. Further work is necessary to develop strategy for efficient removal of by-product ammonia and product DMC to shift the equilibrium towards right side and improve the overall yield of the reaction.

1.4.5. Synthesis of DMC directly from CO₂ and methanol

Synthesis of DMC from CO₂ and methanol provides atom efficient and Green route with only water as the by-product. Major advantage of this route is that CO₂ is nontoxic, non-corrosive, non-flammable and is abundant.¹²⁰ Also CO₂ is a Green-house gas and there is urgent need for utilization of the same for synthesis of value added chemicals. Thus reaction of CO₂ and methanol provides greener route for the synthesis of DMC.¹²⁰ So far, several studies have been

carried out on the development of various catalyst systems for the direct synthesis of DMC from CO₂ and methanol.



Scheme 1.11: Synthesis of DMC from CO₂ and methanol¹²¹

Shan et al.¹²¹ carried out synthesis of DMC from Methanol and CO₂ in the presence of CH₃OK and CH₃I under optimized reaction conditions (170°C/10h /CO₂ pressure 7.3Mpa) with DMC yield of 14% (Scheme 1.11). CH₃OK/CH₃I exhibits better efficiency however separation and recyclability of the catalysts is difficult due to its homogeneous nature. Further many efforts have been made for the synthesis of heterogeneous catalysts for this reaction. Catalyst studied are mainly metal oxides, based on Ce, Zr, Si, Co and Cu and the reactions were carried out in a temperature range of 120-180 °C and yield of DMC obtained was very poor (0.5-7%).¹²²⁻¹²⁵ Water produced during the reaction deactivates the catalyst and thus many efforts have been made in recent years to search for effective dehydrating agents under reaction conditions. Nitriles including acetonitrile, benzonitrile and 2-cyanopyridine etc.¹²⁶⁻¹²⁸ were found to be the most efficient dehydrating agents for organic carbonate synthesis and to improve the methanol conversion. Recently, 2-cyanopyridine was successfully used as dehydrating agent by Honda et al.¹²⁷ reaching high DMC yield of around 94% with 96% selectivity in the presence of CeO₂, at 120 °C for 12h under 5MPa CO₂ pressure. Major challenge in this process is the development of water tolerant heterogeneous catalyst with high and stable activity. If such a catalyst is developed, this will be the best and most economic route for DMC synthesis. Significant work is being carried out on this route by leading companies showing its importance. Major problems of

this route are thermodynamic equilibrium, moisture sensitivity of the catalyst and kinetic inertness of CO₂.

Thus in conclusion, many efforts have been made for the development of phosgene-free route for DMC synthesis. Present commercial processes involve oxidative carbonylation of methanol using copper based catalyst developed by Enichem, the methylnitrile carbonylation process developed by Ube Industries and transesterification of methanol with ethylene carbonate developed by Asahi Kasei. However, the Enichem process is hazardous in nature because of explosion risk associated with the use of CO/O₂ mixture and difficulties in the separation of pure DMC from DMC-water-methanol azeotropic mixture. Similarly Ube process uses toxic NO in stoichiometric quantity and hence is environmentally unacceptable. Asahi process is environmentally benign and does not involve any toxic chemical; however, stoichiometric production of ethylene glycol is major drawback of this process. Asahi process is used by polycarbonate manufacturers having captive usage of ethylene glycol formed as the by-product. Also, significant amount of work is being carried out to develop other alternative and safer routes for the synthesis of DMC. DMC synthesis directly from CO₂ suffers from thermodynamic equilibrium and kinetic inertness of CO₂. Also water form during the process deactivates the catalyst. DMC synthesis from urea and methanol is also being looked as a promising route. However, Ammonia produced in the first step can restrict the formation of the DMC and lower selectivity to DMC due to formation of side products (NMU and NMMC). Because of all these drawbacks the catalytic activity as well as yield of DMC is low. Significant work needs to be carried out to improve stability of the catalyst and also improve yield of DMC for further developments.

The Transesterification process commercialized by Asahi is Green process and implies the use of carbon dioxide as a starting material. Ethylene glycol or Propylene glycol obtained as co-products can be converted to EC and PC respectively by reaction with Urea.¹²⁹ It is by far the most mature commercial process for the synthesis of dimethyl carbonate. However, catalyst used is homogeneous metal alkoxide or ion exchange resin containing tetramethyl ammonium chloride and carbonate functionality and intricate separation process is necessary to make this process commercially feasible.⁹² Also stability of the ion exchange resin is important for long life of the catalyst. To overcome this issue significant work is being carried out on the development of improved heterogeneous catalyst for transesterification of EC or PC with methanol to DMC. The detailed literature review on transesterification process is given below.

1.4.6. Literature on Transesterification of cyclic carbonate with methanol

There are several patents^{110-112,130} as well as publications¹⁴⁹⁻¹⁶³ in recent times on the synthesis of DMC by transesterification of cyclic carbonate with methanol, leading to the development of new and improved catalysts for this important reaction. The reaction has been investigated in detail using both homogeneous as well as heterogeneous catalysts. Homogeneous catalysts investigated include soluble metal salts like carbonates, bicarbonates, alkali and alkaline earth metal alkoxides, tin complexes and ionic liquids etc.^{35-38,131} Though the activity is high with homogeneous catalysts, separation and reuse of the catalyst is a major problem. Consequently, heterogeneous basic catalysts such as composite basic anion-exchange resins, metal oxides and mixed metal oxides, hydrotalcites, supported ILs, smectite and graphitic carbon nitride, have gained much more interest recently and the details are discussed in Table 1.5.³⁹⁻⁴²

Table 1.5: Literature survey on the synthesis of dimethyl carbonate (DMC) from cyclic carbonate and methanol

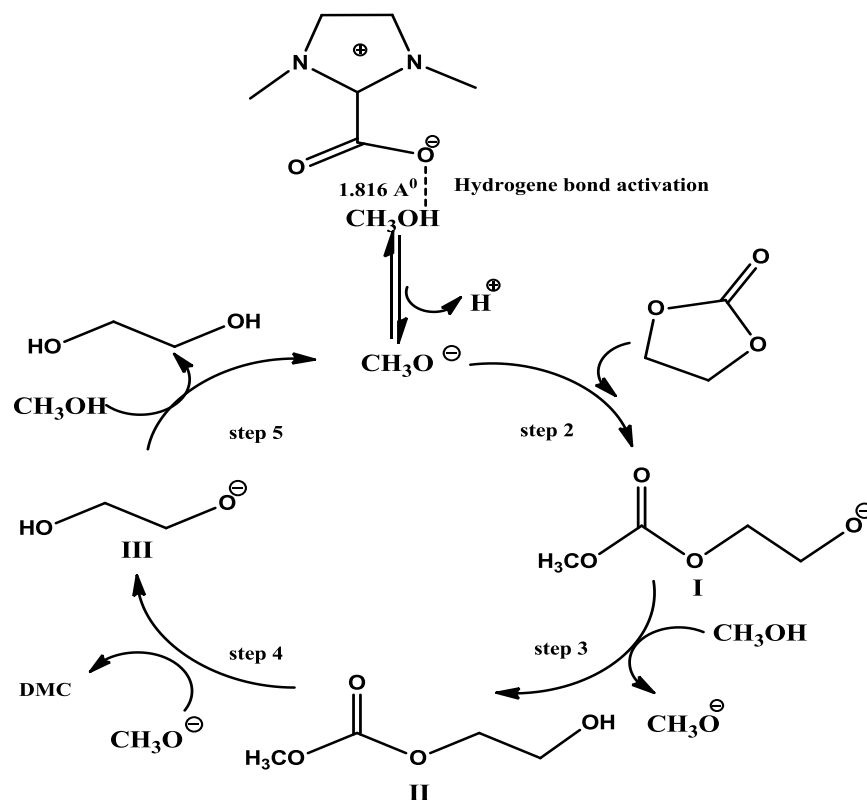
Entry	Catalyst	Reaction conditions			Results		Remarks	Ref.
		Reactants EC/PC [*] :MeOH mol/mol	Temp °C	Time h	EC/PC [*] Conv. (%)	DMC Yield (%)		
1	NaOCH ₃	1:4	60	0.5	67	66.5	Na containing homogeneous salts studied in this system.	132
2	KOH LiOH NaOH	1:4	25	1	42 61 56	40 61 55	Activity follows in order LiOH>NaOH> KOH > K ₂ CO ₃ under the same reaction conditions. The rate constant was estimated to be 0.02538 (dm ³ /mol) ^{0.21} /min at 298 K using NaOH as catalyst.	133
3	poly-4-vinyl pyridine (PVP)	1:8	140	4	96	82	PVP was found to be highly efficient homogeneous recyclable catalyst. The catalyst was recycled by distillation for three times with slight drop in activity (~10%)	134

4	1,3-dimethyl-imidazolium-2-carboxylate (DMIC)	1:10	110	0.8	81	79	The DMIC salt used in this study represented an easily synthesized, cheap and environmentally benign catalyst. The reaction mechanism was also proposed according to experimental and DFT studies (details are given below).	135
5	DABCO-based basic ionic liquids [C ₄ DABCO]OH	1:15	70	6	90	81	Various DABCO-based basic ILs were screened and good results were obtained with [C ₄ DABCO] OH. A possible reaction mechanism was also discussed, reaction initiates with activation of methanol on nitrogen of [C ₄ DABCO]OH.	131
6	BMIImCl	1:8 (MW power 100W)	140	0.25	59	57	[1- <i>n</i> -butyl-3-methyl imidazolium chloride (BMIImCl)] Microwave activation led to high yield of DMC in just 15 minutes.	136
7	QS-MCM-41	1:8 P _{CO₂} = 1.17 MPa.	180	4	78	76	Quaternary ammonium salt immobilized on mesoporous MCM-41(QS-MCM-41) was used as heterogeneous catalyst. However it was observed that catalyst requires high temperature and CO ₂ pressure to achieve 76% DMC yield.	137
8	[SmIm]OH On MCF	1:10	65	5	85	82.4	1-(triethoxysilyl)propyl-3-methylimidazolium hydroxide [SmIm] OH was grafted on the mesocellular silica foams (MCF) to obtain [SmIm]OH on MCF catalyst. The catalytic activity is attributed to its 3D mesoporosity with ultra-large	138

							pore size of MCF.	
9	K-TS-1	1:4	reflux	3	68	57	Potassium present in the silanol group (Si-O-K) in the vicinity of titanium is responsible for the activity.	139
10	Amberlyst A-21	1:8	110	5	36	31	The kinetics for reaction was studied and the rate expression was found to exhibit first order dependence and the energy of activation was found to be 85.8kJmol ⁻¹ .	140
11	S-Mg-1	1:7.5	150	2	73	66	Smectite modified with MgO(S-MgO) results in high surface area 339m ² /g. Catalyst was found to be active up to two cycles with slight decreases in the catalytic activity (66-65%)	141
12	MgO/g-C ₃ N ₄ (MgO on Graphitic carbon nitride)	1:8 P _{CO2} =0.6MPa	140	4	81	70	The incorporation of MgO has effectively enhanced the overall basicity of g-C ₃ N ₄ . Reaction was carried out at higher temperature in presence of CO ₂ . CO ₂ used to avoid decomposition of EC.	142
13	Mesostructured graphitic carbon nitride (CN-MCF)	1:10 1:10* P _{CO2} :0.6MPa	160 160*	6 6*	78 16*	78 13.2*	Activity of catalyst is attributed to its high surface area and N-containing species, Activity of PC observed low than EC due to the existence of the +I effect and steric hindrance derived from the side methyl group of PC.	143
14	Na ₂ WO ₄ .2H ₂ O	1:10 1:10(3.4MPa)	50	5	83	83	Activity was very high with Na ₂ WO ₄ as catalyst and 83% DMC yield obtained at RT. Catalyst was observed less active	144

		CO ₂)*	150*	4*	54*	49.6*	in the case of PC as compared to EC.	
15	Fe–Zn double metal cyanide (DMC)	1:10	180	8*	84*	85*	The Fe–Zn DMC catalyst is reusable up to 5 recycle experiments, with little loss in activity. The Lewis-acidic sites of catalyst (Zn ²⁺ cations) are the possible active sites for this reaction.	145
16	Mg/Al HT 2.5:1	1/4	reflux	3	54	40	Mg-Al hydrotalcite basic catalyst having large amount of OH ⁻ sites showed the good activity.	146
17	Mg/Al HT 5:1	1:10 1:10*	80 130*	4 4*	82 72 *	80.8 69*	Effect of Mg-Al ratio of hydrotalcite on activity was studied for this reaction. The hydrotalcite with Mg/Al= 5 showed best activity.	147
18	NiAl-SiO ₃	1:10	90	3	NA	58	According to author reaction is more selectively catalyzed towards the desired product due to the higher basic sites (due to Ni) and lower acidity due to interlayer silicate anion of the NiAl-SiO ₃ HT material.	148

From Table 1.5 it was clearly observed that transesterification of cyclic carbonates with alcohols to generate DMC follows a nucleophilic substitution mechanism. The reaction is mainly catalyzed by basic compounds and the strength of basicity plays a crucial role in their activity. Soluble alkali-metal bases including KOH, LiOH and NaOH provided a good catalytic activity. Among them sodium alkoxide (DMC yield 66.5%) was considered as the most promising catalyst for industrial application because of its low price and excellent performance.¹³³ However, considering corrosivity of sodium alkoxide, Jagtap et al.¹³⁴ applied poly(4-vinylpyridine) as a novel, homogeneous base catalyst and it could be separated from the reaction system by distillation or phase separation and showed little loss of activity after three recycles (Table 1.5, Entry 3). Recently, ILs have also been utilized as catalysts for DMC synthesis via transesterification. It is noteworthy that the activity of the IL catalysts depended on the bulkiness of the cation as well as the nucleophilicity of the anion (Table 1.5, Entries 4-6).^{131,135,136} Zhang et al.¹³⁵ studied the effect of cations and anions of ionic liquids (ILs) on catalytic activity for the synthesis of dimethyl carbonate (DMC) and demonstrated that an easily prepared carboxylic functionalized dimidazolium salt (DMIC) exhibited higher activity and 79% yield of DMC was obtained under the metal-free and halogen-free conditions (Table 1.5, Entry 4). The reaction mechanism was also proposed according to experimental and DFT studies (Scheme 1.12). As shown in Scheme 1.12 first, CH₃OH was activated by DMIC through strong hydrogen bonding and more easily formed CH₃O⁻ (Scheme 1.12, Step 1). Based on the DFT study the hydrogen bond length was found to be 1.816 Å. Then, the CH₃O⁻ attacked the carbonyl carbon of EC and intermediate (I) was produced simultaneously (Scheme 1.12, Step 2).



Scheme 1.12: Proposed reaction mechanism for DMC synthesis by Zhang et al. on DMIC-IL.¹³⁵

Subsequently, intermediate (II) (HEMC), which was a monoester product, was generated while the proton of CH_3OH was captured by the intermediate (I) (Scheme 1.12, Step 3). Further nucleophilic substitution of intermediate (II) by CH_3O^- produced DMC and ethylene glycol anion (intermediate III) (Scheme 1.12, step 4). Finally, EG was generated by proton transfer between intermediate (III) and CH_3OH (Scheme 1.12, step 5). Particularly, step 4 was proposed to be more difficult than step 2. Therefore it was reasonable that less active catalysts like ILs especially with larger steric hindrance could give more monoester products, and low temperature also easily led to formation of HEMC. Yang et al.¹³¹ ascribed the decrease of activity and selectivity to increase in alkyl chain length and reduction of hydrophilicity as well as solubility

for DABCO-derived basic ILs (Table 1.5, Entry 5). In order to simplify the catalyst separation, immobilization of IL has also been attempted, and is discussed below.

Immobilization of ILs onto supports can simplify the separation process, retaining catalytic properties. Commercial silica and MCM-41 (Table 1.5, Entries 7-8) were utilized to immobilize ILs by impregnation, and heterogenized catalysts were found to be easily recovered and reused or allowed to continuously perform in a fixed bed reactor with slight drop in activity.¹³⁷

To date, a variety of heterogeneous catalysts, such as basic anion-exchange resins,¹³⁹⁻¹⁴¹ graphitic carbon nitride¹⁴²⁻¹⁴³ and Fe–Zn double metal cyanide DMC¹⁴⁵ (Table 1.5, Entries 10-15) have been developed for DMC synthesis via transesterification. As a typical solid-base catalyst, hydrotalcite-type materials (HTs) were also investigated for DMC synthesis (Table 1.5, Entries 17-19) however very small amount of work has been carried out with the same. Bajaj et al.¹⁴⁷ reported that the catalyst activity was influenced by Mg–Al ratio and Mg–Al HT with molar ratio of 5:1 showed maximum basicity and activity towards DMC. Unfortunately, significant decrease in activity was observed after fourth recycle due to structural changes in catalyst indicating lower stability of the catalyst. According to Watanabe et al.¹⁴⁶ basicity (–OH sites) of HT plays an important role in this transesterification reaction. Mg–Al HT with excess amount of –OH anions was found to be an effective catalyst for DMC synthesis. The main function of the solid base is to abstract H⁺ from alcohol molecules to form alkoxy species; therefore, the strength of base dominates the rate of reaction, while the amount of basic sites determines the reaction rate. Additionally, well-developed porosity and high surface area usually offer more exposed active sites and enhance their accessibility to reactants. Thus, many efforts have been carried out to find out heterogeneous catalysts having high surface area and more active sites present on the catalyst surface.

Basic metal oxides (MMOs) are one of the important classes of solid catalysts having tunable acid base property, large surface area, low cost and simple preparation process. There are various types of the MMOs studied for this reaction and the details are given in Table 1.6.

Table 1.6: Literature serve on the synthesis of dimethyl carbonate from cyclic carbonate and methanol using metal oxide and mixed metal oxides.

Entry	Catalyst	Reaction conditions			Results		Remarks	Ref.
		Reactants EC/PC*:MeOH mol/mol	Temp. °C	Time h	EC/PC* Conv. (%)	DMC Yield (%)		
1	MgO	25:200	150	4	82	59.8	MgO was active catalyst among all metal oxides screened. Reaction done at high temperature which leads to DMC decomposition. CO ₂ use to decrease the rate of DMC decomposition.	149
		CO ₂ : 8MPa	150	4	66*	66*		
2	CaO	1:4*	50*	0.5*	47*	45*	CaO a strong base showed good activity for PC at lower temperature.	150

3	CaO-ZrO ₂	1:6*	150*	2*	-	55*	Ca ²⁺ was uniformly doped into the lattice of ZrO ₂ to form CaO-ZrO ₂ MMO and showed strong base properties measured by CO ₂ -TPD .	151
4	CaO-ZnO	10:100*	25* for LHSV of 2 h ⁻¹	4*	-	87*	The catalyst was found to retain its activity up to 60 h and thereafter, a slight decrease in the activity was observed. This was due to deactivation of CaO to Ca(OH) ₂ which leaches out in to the product stream.	152
5	Na-Al ₂ O ₃	1:4	70	6	NA	65	The activity was influence by the presence of monovalent cation (NH ₄ ⁺ , Na ⁺) in aluminates.	153
6	Meso-CeO ₂	1:10 1:10*	140 140*	2 2*	76.3 18 *	73.24 16.3*	Activity of catalyst towards PC observed was low than EC due to the steric hindrance in PC. High reaction temperature was necessary to facilitate the reaction.	154
7	Na-CeO ₂ / K-CeO ₂	1:5	65	4	NA	64	To improve the base strength, metal oxides with strong basicity such as Na and K oxides were introduced in to mesoporous ceria.	155
8	Au/CeO ₂	10:100*	140*	6*	63*	55*	The influence of the amount of gold on the catalytic activity of Au/CeO ₂ catalyst was studied. It was observed that beyond a certain gold loading the selectivity towards DMC decreases due	156

							to the decomposition of PC.	
9	Ce _{0.8} La _{0.2}	10:100*	170*	6*	74*	74*	Activity of synthesized catalysts increases with an increase in lanthanum content in the catalysts. Ce _{0.2} La _{0.8} catalyst showed highest activity having large amount of acid base sites.	157
10	Ce-Cu	1:10*	160*	4*	65*	61*	Ce-Cu catalyst having highest amount of basic sites was found to be most effective. Catalyst was recycled upto 3 recycle experiments with slight drop in activity.	158
11	Zn-Y	30:240	65	2	70	69	Effect of calcination temperature was studied in detail. Zn ₃ -Y calcined at 400 ⁰ C showed best activity having maximum amount of basic sites. The catalyst can be reused without significant loss in activity even after six runs.	159
12	Mg/La MMO	1:10 1:10*	130 150*	2 2*	73 69*	71 64*	Mg/La MMOs with varying Mg/La molar ratios were synthesized and screened for this reaction. MMO with a ratio of 1:3 gave best activity.	160
13	Cu-Zn-Al 300	10:100*	160*	4*	70.6*	65.8*	Prepared CuZnAl MMO calcined at 300 ⁰ C posses more amount of both acid and base sites, which are responsible for better activity towards PC transesterification reaction.	161

14	Mg-Al-La oxide	1:10 1:10*	80 100*	4 4*	89 35*	87.2 31*	Catalytic activities of ternary oxides derived from rare-earth modified hydrotalcites were studied. These catalysts were reusable, with little loss in catalytic activity/selectivity.	162
15	Ca(OCH ₃) ₂	1.07 kmol/m ³ : 21.4kmol/m ³ N ₂ =0.69 MPa	20*	5*	86*	85*	Methanol pretreated CaO [Ca(OCH ₃) ₂] significantly enhances catalytic activity and reduces induction time.	163

Wang et al.^{149,150} observed good activity for reaction of PC and methanol at low temperatures with CaO compared to MgO. The observed result was attributed to higher base strength of CaO and larger number of basic sites (Table 1.6, Entries 1-2). Wang et al.¹⁵¹ investigated incorporation of Ca²⁺ into ZrO₂ (prepared by co-precipitation method) as the catalyst for DMC synthesis. The presence of Ca²⁺ and Zr⁴⁺ in homogeneous CaO–ZrO₂ solid solution increased the basicity of lattice oxygen on the surface and led to good activity with this catalyst. Deng et al.¹⁵⁹ found that the generation of large amount of medium basic sites ($7.2 < H < 9.8$ as determined by Hammett indicator method) in ZnO–Y₂O₃ was responsible for the good catalytic activity. Amount of basic sites depended on the elemental composition and calcination temperature. Kumar et al.¹⁶¹ synthesized Cu-Zn-Al (CZA) ternary MMO from hydrotalcite precursor calcined at different temperatures. They observed that total basicity and acidity of MMOs decreased with an increase in the calcination temperature. CZA calcined at 300°C showed highest amount of total basic and acid sites. Higher basic strength observed was due to the coordination of surface O²⁻. PC conversion of 70% with 94% DMC selectivity was observed at EC: methanol molar ratio of 1:10, 160°C for 4h. Detailed investigations showed that the surface acid and base functionalities play major role during synthesis of DMC by transesterification of cyclic carbonate and methanol.

Rare-earth element modification of Mg–Al hydrotalcites (Table 1.6, Entry 14) resulted in the enhancement of DMC yield, and a linear correlation between PC conversion or TON and surface density of basic sites was reported by Srinivas's group.¹⁶² Recently Chaudhari et al.¹⁶³ studied the effect of pretreated CaO with methanol (Table 1.6, Entry 15). They observed significant difference in CO₂ TPD of fresh CaO, PC pretreated CaO and methanol pretreated CaO. They observed that the amount of weak basic sites (at 380°C) on CaO decreased after methanol pretreatment, whereas the amount of strong basic sites (at 426 and 768 °C) increased significantly

compared to pure CaO. Therefore, they concluded that there is a strong correlation between strong basic sites and catalytic activity. The activity increased significantly with reduction in induction period for the methanol pretreated CaO catalyst.

Significant work is being carried out on the development of improved catalysts for the synthesis of DMC from EC/PC and methanol. Simple inorganic, organic bases and ionic liquids (ILs) were found to be active catalysts for DMC synthesis; still applications are limited because of difficulties in catalyst-product separation due to its homogeneous nature. Further Immobilization of the IL on different supports has been explored but high cost of catalyst has limited their application. Considerable amount of work has been carried out on the development of heterogeneous catalysts for the synthesis of DMC. Heterogeneous catalysts based on mixed metal oxides, smectite, anion-exchange resin, Na-dawsonite, mesoporous graphitic carbon nitride and Binary hydrotalcites (i.e. LDHs) etc. have been studied for transesterification reaction. Among all heterogeneous catalysts investigated mixed metal oxides were found to be active catalysts for this reaction, however, they require either high reaction temperature (100–160 °C) or high catalyst loading (10–25 wt%). The catalyst was recycled four to five times, but catalyst activation at high temperature was required in most of the cases during each recycle experiment. This potentially may cause problem in continuous or large scale operation. In this context it is still challenging task to develop heterogeneous catalysts exhibiting high catalyst activity and high stability for the synthesis of DMC from EC and methanol under mild reaction conditions. Activity of all the catalysts screened for PC and methanol to DMC reaction was found to be lower compared to that observed for the reaction of EC and methanol to DMC. The lower conversion of PC observed was mainly due to steric factors and differences in the chemical structures of EC and PC and required high reaction temperature and time. Thus there is a need to

develop highly active, selective and recyclable catalyst for this important reaction and hence lot of work is being carried out in this direction.

1.5. Dimethyl carbonate as a methoxycarbonylating agent for aromatic carbamates

As discussed earlier (Section 1.3.4.) DMC has emerged as a ‘Green Reagent’ for the synthesis of various chemicals and methoxycarbonylation of aromatic amines provides phosgene free route for the synthesis of aromatic carbamates.¹⁶⁴

Aromatic carbamates are important intermediates in drug synthesis,^{165,166} agrochemicals,¹⁶⁷ and polyurethane (PU) based polymers.¹⁶⁸⁻¹⁷⁰ Carbamates present stable form of isocyanates and can be easily converted in to isocyanates at high temperatures (170°C) in the presence of a suitable catalyst.¹⁷¹ Polyurethanes are manufactured by combining diols and diisocyanates. Polyurethanes are among the most valuable polymers produced by the chemical industry. In 2007 the global consumption of polyurethane as raw material was about 12 million metric tons/year and the average annual growth rate is about 5%.^{171a} Aromatic diisocyanates currently account for more than 90% of the global production of diisocyanates, mainly toluene diisocyanate (TDI) and methylene diphenyldiisocyanate (MDI).^{172,173} N-methyl phenyl carbamate (MPC) is also an important precursor for preparing methylene diphenyldiisocyanate (MDI) by condensation of MPC with formaldehyde.^{174, 175} Conventionally aromatic carbamates are manufactured exclusively by phosgene technology (Fig.1.11, Scheme 1.13).^{175,176} This method poses great concerns for both environmental and safety problems because of the toxicity and corrosion properties of phosgene itself. So efforts have been made for the preparation of organic carbamates using non-phosgene reagents.

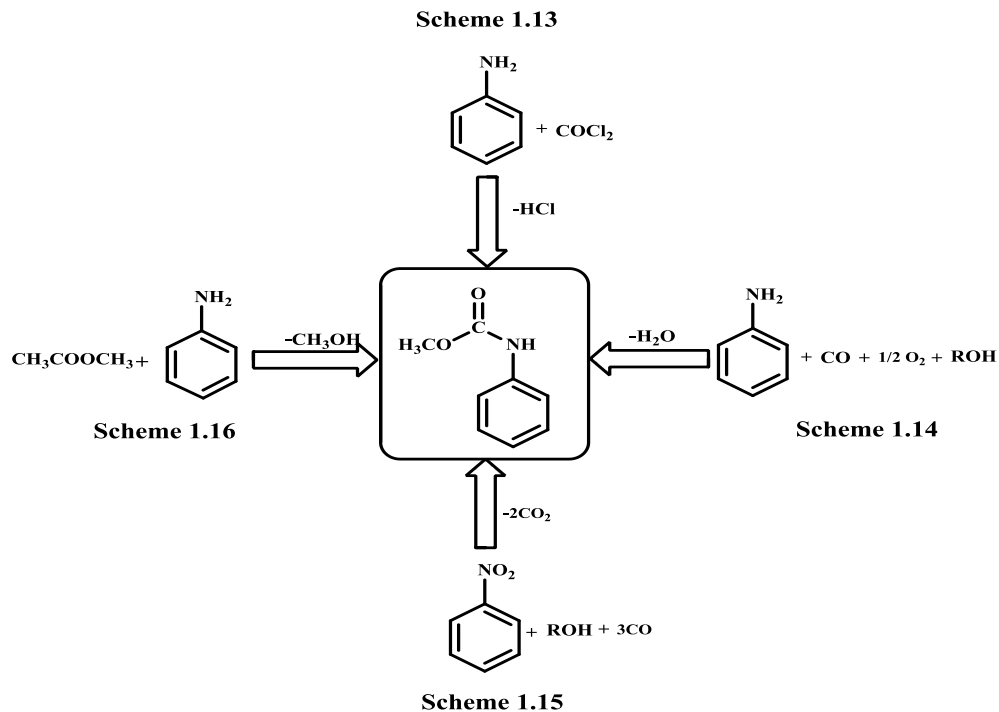


Figure 1.11: Various routes for MPC synthesis

Therefore, less-expensive and benign alternatives to the current process have been explored by many academic and industrial researchers over the last decades. Currently, the studies on phosgene-free synthesis of organic carbamate is mainly focused on oxidative carbonylation of aromatic amines (Fig. 1.11, Scheme 1.14)¹⁷⁷ reductive carbonylation of nitro derivatives (Fig.1.11, Scheme 1.15)¹⁷⁰ and methoxycarbonylation of amines using DMC as a reagent (Fig. 1.11, Scheme 1.16).¹⁷⁸ Important literature available on the synthesis of aromatic carbamates by non-phosgene routes is presented below.

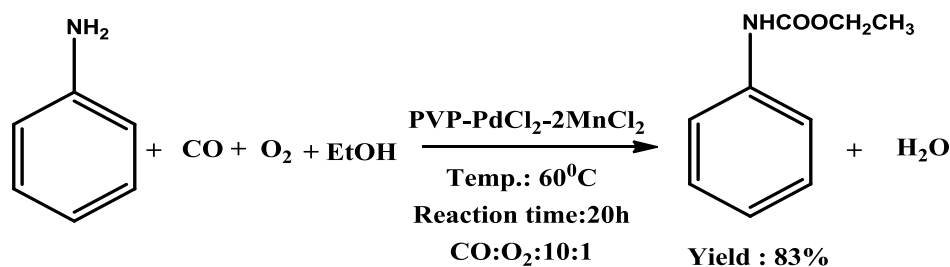
1.5.1. Synthesis of carbamates by Oxidative carbonylation of aromatic amines

Oxidative carbonylation of aromatic amine to carbamate is reported to be effectively carried out using variety of Nobel metal catalyst such as Pd, Pt, Rh, Ir and Ru etc. in the presence

of promoters or reoxidants such as iodide compounds or P-benzoquinone etc., under high pressure of CO:O₂ (3 - 10 MPa) and high reaction temperature (100-220°C).⁸²

Fukuoka et al.¹⁷⁹ have reported the use of supported transition metal catalysts (2% Pd, 5% Pt, 5% Rh, 5% Ru, 5% Ir on Carbon) for oxidative carbonylation of aniline. They found that the activity of the catalyst decreased in the order Pd>Rh>Ru>Pt>Ir. They have screened several halogen containing promoters and the activity was found to decrease in the order: I>Br>Cl. The best result was observed with Pd/C using NaI as a promoter (95% conversion of aniline with 93% yield of methyl phenyl carbamate (MPC) at 160°C in 2 h).

Liao et al.¹⁸⁰ have reported an efficient synthesis of carbamate, using polymer-supported palladium manganese bimetallic catalyst showing 83% yield to corresponding carbamate (Scheme 1.17).



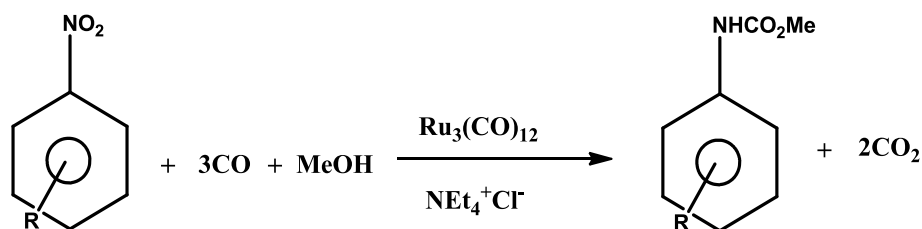
Scheme 1.17: Efficient synthesis of carbamate, using polymer-supported palladium manganese bimetallic catalyst¹⁸⁰

Shi et al.¹⁸¹ have reported carbonylation of amines with variety of alcohols using palladium and ionic liquid. Results showed that BMImBF₄ ionic liquid + Pd(phen)Cl₂ is an effective catalytic system to give 99% conversion of aniline and 98% selectivity to methyl phenyl carbamate at 175°C/1h. Recently, Saliu and co-workers¹⁷⁷ have reported synthesis of methyl-N-phenyl carbamate by using Co(salen) complex catalyst. Catalysts were active and 82% aniline conversion and 87% MPC selectivity was obtained at 100°C in 12h reaction time. Though only

water is formed as the by-product, toxicity of CO and explosion hazards associated with the use of CO/O₂ mixture has limited commercial application of this process.

1.5.2. Synthesis of carbamates by the reductive carbonylation of aromatic nitro-compounds

The reductive carbonylation of aromatic nitro-compounds to the corresponding carbamates is an interesting approach towards synthesis of carbamates (Scheme 1.18). The carbonylation reaction of nitro-aromatics is an exothermic reaction and is catalyzed by palladium, ruthenium, and to a lesser extent by rhodium. Furthermore, platinum, iridium, and iron have also been reported to be active for this reaction.¹⁸²⁻¹⁸⁴ Cenini et al.¹⁸² studied reductive carbonylation of nitrobenzene to give PhNHCOOMe in the presence of Ru₃(CO)₁₂ catalyst. Reaction was carried out in toluene-methanol mixture in the presence of chelating ligand such as diphenyl phosphinomethane (DPPM) and 88% conversion of nitrobenzene and 81% selectivity to carbamate was obtained at 170°C in 3 h reaction time (Scheme 1.18)



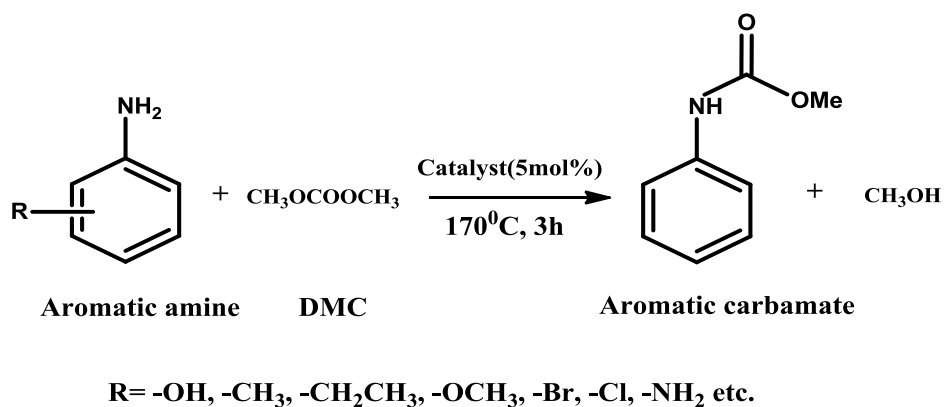
Scheme 1.18: Reductive carbonylation of nitrobenzene to give carbamate

Izumi et al.¹⁸³ observed 84% aniline conversion with 97% selectivity to carbamate under the optimized reaction conditions with PdCl₂-heteropoly anion (as a modifier) catalyst system [PdCl₂/modifier/solvent(DME)/MeOH/Ph-NO₂ = 1/0.5/400/200/100 (molar ratio), 150°C, 3h].

Karpinska et al.¹⁸⁵ studied reductive carbonylation of 1,3-dinitrobenzene, 1,4-dinitrobenzene and 2,4-dinitrotoluene to respective dicarbamates in the presence of PdCl₂/Fe/I₂/Py catalyst system and complete conversion of dinitrobenzene to the corresponding dicarbamates was achieved with selectivity of 87, 68, and 55% respectively at 180°C for 2h. In this process only one-third of CO could be used efficiently with the formation of two moles of CO₂ as by-product. Overall selectivity of the reaction based on CO is very low, the separation of CO from CO₂ would increase the operation cost. Additionally, the presence of co-catalysts gives rise to the corrosion problems and makes recovery of the catalyst difficult and hence the process is not investigated in detail for further applications.

1.5.3. Synthesis of carbamates by methoxycarbonylation of aromatic amine

The aromatic carbamates can also be synthesized from amines and dimethyl carbonate using homogeneous and heterogenous catalysts (Scheme 1.19).¹⁸⁶



Scheme 1.19: Synthesis of aromatic carbamates from various substituted amines and DMC¹⁸⁷

Aromatic carbamate synthesis by methoxycarbonylation of aromatic amines using DMC as a greener reagent has emerged as promising alternative route. In this reaction methanol is formed

as the by-product, which can be converted back to DMC by oxidative carbonylation of methanol with CO.¹⁸⁸ Thus, the route based on DMC has a potential to provide atom efficient and safer route for the synthesis of carbamates from DMC and amines.

Several efforts have been made towards the development of environmentally friendly routes using non-toxic reagents for the preparation of carbamate such as, reductive carbonylation of nitro aromatics and oxidative carbonylation of amines. However, synthesis of carbamate by reductive carbonylation of nitro compounds suffers from a lack of economic viability as it utilizes only one-third of CO and there exists difficulty in separation of CO from CO₂ formed as the by-product. In oxidative carbonylation process, although CO can be utilized effectively, the toxicity of CO and explosion hazards associated with the use of CO/O₂ gas mixture has limited the progress of this route. Also, these two processes required severe reaction conditions such as high temperature and pressure, and a noble metal catalyst such as Pd or Ru for the carbonylation reactions. Aromatic carbamate by methoxycarbonylation with DMC is safer route and hence is being investigated in detail. Because of multifunctional nature of DMC achieving high selectivity to carbamate product is challenging and development of active and selective catalyst is important. The detailed literature survey on the methoxycarbonylation of aromatic amines with DMC is discussed below.

1.5.4. Detailed literature on methoxycarbonylation of aromatic amine

There are several patents^{186,187,189-191} as well as publications on the synthesis of aromatic carbamate from methoxycarbonylation of aromatic amine and DMC. The details are presented in Table 1.7.

Table 1.7: Literature survey on the synthesis of aromatic carbamates by methoxycarbonylation of aromatic amines with DMC

Entry	Catalyst	Substrate	Reaction conditions			Results		Remarks	Ref.
			Reactants Aniline:DMC mmol/mmol	Temp (°C)	Time (h)	Aniline Conv. (%)	MPC Yield (%)		
1	$Zn_4O(OOCNEt_2)_6$	Aniline	1:5	170	2	99	98	Anhydrous Zn-N,N-diethylcarbamate complex used as catalyst showed good activity for methoxycarbonylation of both aniline and 4-4 Dimethylenedianiline (MDA)	172
		MDA				99	62		
2	$Zn_4O(OAc)_6$	Aniline	1:25	180	2	99	96	Zn acetate showed good activity for aniline, TDA and MDA however catalyst remains homogeneous in reaction mixture.	192
		TDA	1:25	190	4	99	97		
		MDA	1:25	180	2	99	97		
3	$Pb(OAc)_2 \cdot xH_2O$	Aniline	1:5	160	1	94.7	92	Pd acetate and Zn acetate showed good activity to MPC however it remains homogeneous in reaction mixture.	193
	$Zn(OAc)_2 \cdot 2H_2O$					93.7	91		

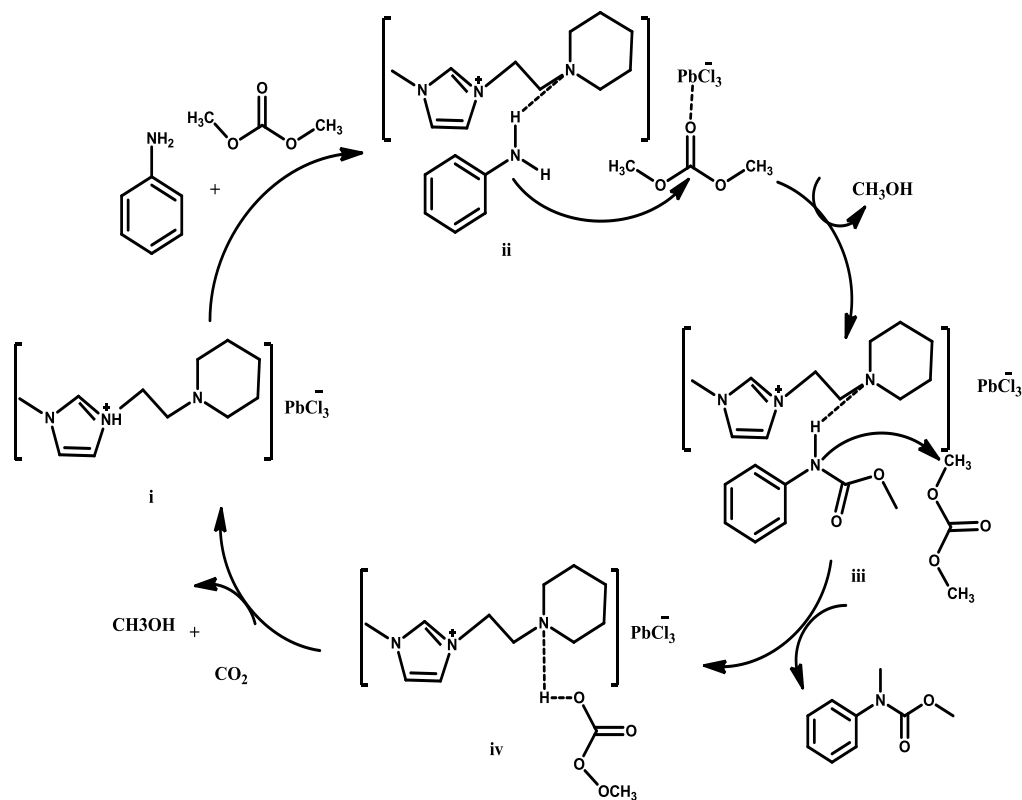
4	Pb(OAc) ₂ .xH ₂ O	TDA	1:20	170	4	100	97.7	Methanol (by-product) deactivates catalyst however catalyst can be regenerated by treatment of acetic acid.	194
5	Zn(OAc) ₂ /AC	Aniline	1:7	150	8	-	78	Zn(OAc) ₂ heterogenized on different solid support i.e γ -Al ₂ O ₃ , AC, ZSM-5, SiO ₂ and MgO. It was observed that activity was significantly affected by support. Activity decreased from AC > α -Al ₂ O ₃ > ZSM-5 > SiO ₂ > MgO.	169
6	Zn(OAc) ₂ /Al ₂ O ₃	TDA	1:20	150	7	-	53.3	With increase in reaction temperature decrease in TDC yield was observed due to the formation of by-products i.e N methyl TDA and polyurea.	170
7	Zn(OAc) ₂ .H ₂ O	Aniline	1:20	130	1	68	68	It was observed that the induction period was shortened by pretreatment of the Zn(OAc) ₂ with DMC	195
		MDA	1:20	130	2	47	41		
	DMC pretreated Zn(OAc) ₂ .H ₂ O	Aniline	1:20	130	1	80	80		
		MDA	1:20	130	2	100	92		
8	Yb(OTf) ₃	Aniline	1:5	80	8	-	96	Catalyst remains soluble in reaction mixture, however catalyst can be recover by adding few	196

								ml of CH ₂ Cl ₂ (by precipitation)	
9	K ₂ CO ₃	Aniline	1:3	180	22	-	41	Mechanism of the reaction has been investigated in terms of Pearson's Hard-Soft Acid-Base (HSAB) theory.	197
10	ZnO-TiO ₂	Aniline	1:20	180	7	96	66.9	Lewis acid sites favor MPC synthesis.	190
11	ZrO ₂ /SiO ₂	Aniline	1:20	170	7	98	79	Decreases in MPC yield was observed with increase in temperature due to the formation of byproducts i.e NMA and DPU (due to decarboxylation and condensation of MPC).	198
12	AlSBA-15	Aniline	1:10	100	3	99	70	The acid sites inside the mesoporous cavities of AlSBA-15 are more accessible due to a larger pore size leading to a high conversion of substrate and Lewis acidity of aluminium leads to the formation of MPC.	199
13	[PEmim]PbCl ₃ -IL	Aniline	1:5	160	4	87	8 (MPC) 72 (MMPC)	Acid-base sites of [PEmim]PbCl ₃ are important for this reaction. [PEmim]PbCl ₃ increases the electrophilicity of DMC and the nucleophilicity of aniline by its acid and base sites.	200

14	[ZnCO ₃] ₂ - [Zn(OH) ₂] ₃	Aniline	1:10	160	5	96	94	Activity of catalyst decreased after two recycle experiments	178
15	L-Proline-TBAB	Aniline	1:5	RT	3	-	94	L-proline is insoluble in DMC and the presence of a phase transfer catalyst TBAB can improve the solubility of L-proline. This may be the possible reason for the enhanced reaction rates and activity at room temperature.	201
16	Iron – chrome catalyst TZC-3/1	Aniline	2:1	150	3	Trace amount	-	TZC-3/1 was found to be the most active catalyst in case of aliphatic amines (n-hexylamine) whereas in case of aniline no conversion was observed.	202

From the literature survey it was observed that both homogeneous and heterogeneous catalysts have been investigated for the synthesis of aromatic carbamates, mainly methyl phenyl carbamate (MPC). Homogeneous catalysts studied include: $\text{Zn(OAc)}_2 \cdot 2\text{H}_2\text{O}$, $\text{Pb(OAc)}_2 \cdot x\text{H}_2\text{O}$, K_2CO_3 , Yb(OTf)_3 and bifunctional IL{[PEmim]PbCl₃-IL} etc. Ono et al.¹⁹³ synthesized MPC using metal salts like $\text{Zn(OAc)}_2 \cdot 2\text{H}_2\text{O}$, $\text{Pb(OAc)}_2 \cdot x\text{H}_2\text{O}$ as catalysts and obtained 91-92% yield of MPC at aniline: DMC ratio 1:5 in 2h at 160°C. $\text{Zn(OAc)}_2 \cdot 2\text{H}_2\text{O}$ was also found to be active for reaction with other aromatic amines like toluene diamine (TDA) and methyl diphenyl amine (MDA) and showed 96-97% yield of corresponding carbamates at a substrate: DMC mole ratio of 1:25 at 180°C in 2h reaction time. Li et al.¹⁹⁵ investigated the effect of pretreatment of Zn(OAc)_2 with DMC for methoxycarbonylation of aniline. It was observed that the pretreated Zn(OAc)_2 showed good activity (80% yield at 160°C/1h) as compared to Zn(OAc)_2 (68% yield at 160°C/1h) (Table 1.8; Entry 7). It was observed that the induction period was shortened by pretreatment of Zn(OAc)_2 with DMC. According to Geo et al.²⁰⁰ acid–base bi-functional ionic liquid, 1-(2-(1'-piperidiny)ethyl)-3-methyl imidazoliumtrichlorolead ([PEmim]PbCl₃), is an efficient catalyst for the reaction of aniline and DMC to methyl-N-methyl-N-phenylcarbamate (MMPC 72% and MPC 8% yield). The high reactivity of [PEmim][PbCl₃] is attributed to its ability to activate both aniline and DMC by the acidic and basic sites cooperatively. Density functional theory (DFT) calculations were carried out to understand structure and electronic properties of [PEmim]PbCl₃, complex of [PEmim]PbCl₃ and aniline, and complex of [PEmim]PbCl₃ and DMC. The calculations showed that [PEmim]PbCl₃ can increase the electrophilicity of DMC and the nucleophilicity of aniline by its acid and base sites respectively. Based on these results reaction mechanism was proposed (Scheme 1.20). Steps involved in reaction mechanism are as follows (Scheme 1.20): (i) [PEmim]PbCl₃ has both acidic and basic

sites. The acidic site of Pb^{2+} interacts with DMC to form $\text{Pb}^{2+}\text{OC}(\text{OCH}_3)_2$ species. In the meanwhile, the basic site of piperidinyl group activates aniline through the formation of hydrogen bond ($\text{N}-\text{H} \cdots \text{N}$) (ii). The activated aniline undergoes the nucleophilic attack on the carbonyl group of $\text{Pb}^{2+}\text{OC}(\text{OCH}_3)_2$ species to form methyl-N-phenyl carbamate species (iii). Methyl-N-phenyl carbamate species undergoes the nucleophilic attack on the methyl group of another molecular DMC to give methyl-N-methyl-N-phenylcarbamate and the species (iv). $[\text{PEmim}]\text{PbCl}_3$ (i) is recycled from species (iv) with the release of methanol and carbon dioxide.²⁰⁰



Scheme 1.20: A proposed reaction mechanism for the formation of Methyl-N-methyl phenyl carbamate using $[\text{PEmim}]\text{PbCl}_3$ ²⁰⁰

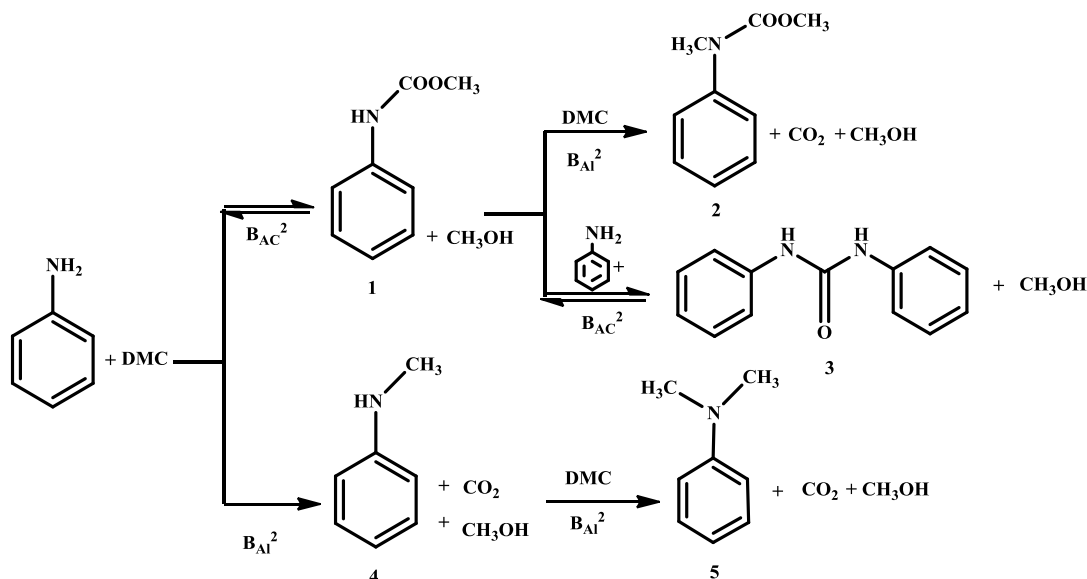
Jain et al.²⁰¹ studied reaction of amines and dimethyl carbonate (DMC) in the presence of catalytic amounts of L-proline and tetrabutylammonium bromide (TBAB) to obtain methyl carbamates in good yields under mild reaction conditions (94% yield/ 3h/ RT). According to authors, L-proline is insoluble in DMC and the presence of a phase transfer catalyst TBAB improves the solubility of L-proline resulting in enhanced reaction rates. Good activity of catalyst was observed at room temperature, which is contradictory to literature reports. According to Margetić and co-workers²⁰³ aromatic amines such as aniline did not react with dimethyl carbonate at room temperature.

Thus $\text{Zn}(\text{OAc})_2 \cdot 2\text{H}_2\text{O}$ and $\text{Pb}(\text{OAc})_2 \cdot x\text{H}_2\text{O}$ were found to give best catalytic performance for the synthesis of aromatic carbamates (yield of carbamates \Rightarrow 95%). However, catalyst/product separation is difficult because of the homogeneous nature of these catalysts and lead compound suffers from environmental problem. To overcome this problem Zhang et al.¹⁶⁹ have immobilized $\text{Zn}(\text{OAc})_2 \cdot 2\text{H}_2\text{O}$ on different solid supports like $\gamma\text{-Al}_2\text{O}_3$, activated Carbon (AC), ZSM-5, SiO_2 and MgO to prepare heterogenized homogeneous catalysts. It was observed that activity was significantly affected by different supports and activity decreased in the order: $\text{AC} > \alpha\text{-Al}_2\text{O}_3 > \text{ZSM-5} > \text{SiO}_2 > \text{MgO}$. Among these Zn/AC showed good activity (87% MPC yield), however deactivation of immobilized $\text{Zn}(\text{OAc})_2$ to ZnO was observed during recycle of the catalyst [due to reaction between methanol and $\text{Zn}(\text{OAc})_2$].

Several other heterogeneous catalysts (Al-SBA-15, Al-MCM-41 and Zn, Ti, Zr, Si, Ce based mixed metal oxides etc.) have been investigated for the reaction of aromatic amines and DMC.^{190,198,199,178} Zhao et al.¹⁹⁸ studied $\text{ZrO}_2/\text{SiO}_2$ MMO catalyst for the reaction and 98.6% aniline conversion with 79.8% MPC yield was obtained at 170°C in 7h with DMC: Aniline mole

ratio of 20 and catalyst loading of 20 wt%. However, the catalyst was deactivated after the reaction and could not be recycled.

DMC can be act both as a methylating and methoxycarbonylating agent. Tundo and co-workers have made significant contributions to the use of DMC as reagent for various transformations.^{85, 86,89,178,197} According to Tundo¹⁷⁸ two different pathways (alkylation/ acylation) can be promoted in parallel. Scheme 1.21 shows the mechanism of carbamoylation of aniline via DMC chemistry. As depicted in Scheme 1.21, besides methyl *N*-phenylcarbamate **1**, several by-products are formed by the reaction of aniline with DMC, i.e., *N*-methyl aniline **4** and *N,N*-dimethyl aniline **5**. Furthermore, the methyl phenyl carbamate **1**, once formed, can react further either with DMC to give the methyl *N*-phenylcarbamate **2** or with aniline to form the diphenylurea **3**. It is noteworthy that the reactions leading to the formation of carbamate **1** and urea **3** are equilibrium reactions (B_{Ac2} mechanism), meanwhile the reactions leading to the methyl derivatives **2**, **4**, and **5** are not equilibrium reactions (B_{Al2} mechanism).



Scheme 1.21: Synthesis of the methyl *N*-phenylcarbamate **1** by reaction of aniline with DMC.

The synthetic pathways.¹⁷⁸

The selectivity between methylation (alkylation) and carbamoylation (acylation) depends on a large number of factors besides the catalyst such as the nature of the nucleophilic species, reaction temperature, and even the substrate-to-DMC ratio.^{85,86,89} Therefore, the key point in this process is the choice of catalyst and optimization of reaction parameters which can give high selectivity to N carbamate products. The synthesis of carbamate from aromatic amine and dimethyl carbonate (DMC) in the presence of homogeneous, supported heterogeneous, and heterogeneous catalysts have been investigated in detail. Mostly the works have been carried out using Zn based homogeneous and heterogeneous catalysts.

Among all metal based catalysts; homogeneous Zn and Pb metal salts showed best catalytic activity. However, catalyst/product separation is difficult because of the homogeneous nature of these catalysts. Also, lead compounds showed high catalytic performance, but they are not environmentally friendly. Supported zinc acetate based catalysts were studied for this reaction ($\text{Zn(OAc)}_2/\text{AC}$, $\text{Zn(OAc)}_2/\alpha\text{-Al}_2\text{O}_3$ and $\text{Zn(OAc)}_2/\text{SiO}_2$) however, deactivation of Zn(OAc)_2 was observed with the formation of ZnO. Therefore, by taking into account the economic importance of carbamates as isocyanate precursors, it is necessary to develop active catalysts which give high yield, low amounts of by-products and are easily recycled.

1.6. Aim and Objectives of the thesis

Utilization of safer reagents and renewable feed stocks is essential for the sustainable development of society. Much attention has been devoted to applying green catalytic processes to convert renewable feed stocks to commodity chemicals and clean fuels. Recently dimethyl carbonate (DMC) has emerged as “Green Reagent” and substitute for toxic phosgene, dimethyl sulphate and organic halides in carbonylation and N-methylation reactions. Conventionally

dimethyl carbonate is produced by phosgenation or oxidative carbonylation route however, both the routes have disadvantages. DMC is produced by various non-phosgene routes including oxidative carbonylation of methanol (Enichem process), the methylnitrilecarbonylation process developed by Ube Industries and transesterification of methanol with ethylene carbonate (EC) developed by Asahi Kasei Chemical, Japan. Asahi process is environmentally safe process and several plants are based on this route and focus of the work is on the development of efficient catalysts for this route. DMC has emerged as “Green Reagent” because of its non-toxic properties and multifunctionality. With the availability of DMC from non-phosgene route focus of the work has been on the development of new routes for the synthesis of specialty chemicals utilizing DMC. Synthesis of aromatic amines by methoxycarbonylation of aromatic amines with DMC is one such important example. Significant amount of work is being carried out on the development of homogeneous as well as heterogeneous catalysts for these reactions. Based on the brief literature reports presented in this chapter, present study was focused on the development of heterogeneous catalysts for selective synthesis of these products. With these objectives following specific problems were chosen for the work.

- ❖ DMC synthesis by Transesterification of cyclic carbonate with methanol
 - ✓ Synthesis and characterization of hydrotalcites and hydrotalcite derived MMOs catalyst based on Mg, Li, Al, Fe, Ce, La, Sm and other transition metals.
 - ✓ Transesterification of EC/ PC with methanol
 - ✓ Optimization of reaction conditions to achieve high selectivity to DMC
 - ✓ Recycle/recovery of the catalyst.

- ❖ Synthesis of aromatic carbamates by methoxycarbonylation of aromatic amines with DMC
 - ✓ Synthesis and characterization of heterogeneous catalysts based on Zn, Ce, Zr, Co and other transition metals.
 - ✓ Methoxycarbonylation of aniline as a model substrate.
 - ✓ Optimization of reaction conditions to achieve high selectivity to carbamate derivatives
 - ✓ Recycle/recovery of the catalyst.

1.7. References

1. Cajas, F., *Public understanding of science: Using technology to enhance school science in everyday life*. International Journal of Science Education, 1999.**21**(7): p. 765-773.
2. Chandler, A.D., *Shaping the industrial century: the remarkable story of the evolution of the modern chemical and pharmaceutical industries*. Vol.46. 2009: Harvard University Press.
3. Vennestram, P.N.R., et al., *NextGeneration Catalysis for Renewables: Combining Enzymatic with Inorganic Heterogeneous Catalysis for Bulk Chemical Production*. ChemCatChem, 2010.**2** (3): p. 249-258.
4. Franke, R., D. Selent, and A. Börner, *Applied hydroformylation*. Chemical reviews, 2012.**112** (11): p. 5675-5732.
5. Auer, E., et al., *Carbons as supports for industrial precious metal catalysts*. Applied Catalysis A: General, 1998.**173** (2): p. 259-271.
6. Bartholomew, C.H. and R.J. Farrauto, *Fundamentals of industrial catalytic processes*: John Wiley & Sons.
7. Chorkendorff, I. and J.W. Niemantsverdriet, *Concepts of modern catalysis and kinetics*: 2017. John Wiley & Sons. 7a) Laidler, K. J.; Cornish-Bowden, A., Elizabeth Fulhame and the discovery of catalysis: 100 years before Buchner. *Cornish-Bowden (1997) pp 1997*, 123-126.
8. Somorjai, G.A. and Y. Li, *Introduction to surface chemistry and catalysis*: 2010. John Wiley & Sons.
9. Masel, R.I., *Chemical kinetics and catalysis*. 2001: Wiley-Interscience New York.

10. Mizuno, N. and M. Misono, *Heterogeneous catalysis*. Chemical reviews, 1998. **98**(1): p. 199-218.
11. Bommarius, A.S. and B.R. Riebel, *Introduction to biocatalysis*. Biocatalysis, 2004: p. 1-18.
12. Schmid, A., et al., *Industrial biocatalysis today and tomorrow*. nature, 2001. **409**(6817): p. 258.
13. Tao, J. and J.-H. Xu, *Biocatalysis in development of green pharmaceutical processes*. Current opinion in chemical biology, 2009.**13**(1): p. 43-50.
14. Jemli, S., et al., *Biocatalysts: application and engineering for industrial purposes*. Critical reviews in biotechnology, 2016.**36** (2): p. 246-258.
15. Hubenova, Y. and M. Mitov, *Extracellular electron transfer in yeast-based biofuel cells: A review*. Bioelectrochemistry, 2015.**106**: p. 177-185.
16. Gopinath, S.C.B., et al., *Strategies to characterize fungal lipases for applications in medicine and dairy industry*. BioMed research international.**2013**.
17. Tao, J.A., G.-Q. Lin, and A. Liese, *Biocatalysis for the pharmaceutical industry: discovery, development, and manufacturing*. 2009: John Wiley & Sons.
18. Choi, J.-M., S.-S. Han, and H.-S. Kim, *Industrial applications of enzyme biocatalysis: current status and future aspects*. Biotechnology advances, 2015.**33**(7): p. 1443-1454.
19. Cornils, B., et al., *Applied Homogeneous Catalysis with Organometallic Compounds: A Comprehensive Handbook in Four Volumes*. 2018.Vol. 4: John Wiley & Sons.
20. Paulik, F.E. and J.F. Roth, *Novel catalysts for the low-pressure carbonylation of methanol to acetic acid*. Chemical Communications (London), 1968(24): p. 1578a-1578a.

21. Breit, B. and W. Seiche, *Hydrogen bonding as a construction element for bidentate donor ligands in homogeneous catalysis: regioselective hydroformylation of terminal alkenes*. Journal of the American Chemical Society, 2003.**125**(22): p. 6608-6609.
22. Zhang, C., et al., *Palladium Imidazol-2-ylidene Complexes as Catalysts for Facile and Efficient Suzuki Cross-Coupling Reactions of Aryl Chlorides with Arylboronic Acids*. The Journal of Organic Chemistry, 1999.**64**(11): p. 3804-3805.
23. Stevens, P.D., et al., *Recycling of homogeneous Pd catalysts using superparamagnetic nanoparticles as novel soluble supports for Suzuki, Heck, and Sonogashira cross-coupling reactions*. Chemical Communications, 2005(35): p. 4435-4437.
24. Hagen, H., J. Boersma, and G. van Koten, *Homogeneous vanadium-based catalysts for the Ziegler Natta polymerization of olefins*. Chemical Society Reviews, 2002.**31**(6): p. 357-364.
25. Cole-Hamilton, D.J., *Homogeneous catalysis--new approaches to catalyst separation, recovery, and recycling*. Science, 2003.**299**(5613): p. 1702-1706.
26. Cornils, B. and W.A. Herrmann, *Concepts in homogeneous catalysis: the industrial view*. Journal of Catalysis, 2003.**216**(1-2): p. 23-31.
27. Bailar Jr, J.C., *Heterogenizing homogeneous catalysts*. Catalysis Reviews Science and Engineering, 1974.**10**(1): p. 17-36.
28. Petrucci, M.G.L. and A.K. Kakkar, *Heterogenizing homogeneous catalysis*. Advanced Materials, 1996.**8**(3): p. 251-253.
29. Barbaro, P. and F. Liguori, *Heterogenized homogeneous catalysts for fine chemicals production: materials and processes*. 2010, Vol. 33: Springer Science & Business Media.

30. Westerhaus, F.A., et al., *Heterogenized cobalt oxide catalysts for nitroarene reduction by pyrolysis of molecularly defined complexes*. *Nature Chemistry*, 2013, **5**(6): p. 537-543.
31. Dooos, B.M.L., I.F.J. Vankelecom, and P.A. Jacobs, *Aspects of immobilisation of catalysts on polymeric supports*. *Advanced synthesis & catalysis*, 2006.**348**(13): p. 1413-1446.
32. He, J., et al., *Designing a capsule catalyst and its application for direct synthesis of middle isoparaffins*. *Langmuir*, 2005.**21**(5): p. 1699-1702.
33. Augustine, R., et al., *A new technique for anchoring homogeneous catalysts*. *Chemical Communications*, 1999(13): p. 1257-1258.
34. George, S.M., *Introduction: heterogeneous catalysis*. *Chemical reviews*, 1995. **95**(3): p. 475-476.
35. Deutschmann, O., et al., *Heterogeneous catalysis and solid catalysts*. *Ullmann's Encyclopedia of Industrial Chemistry*, 2009.
36. Krabetz, R., et al., *Preparation of coated catalysts*. 1981, *U.S. Patent No. 4,305,843*.
37. Li, J., et al., *Development of nano-NiO/Al₂O₃ catalyst to be used for tar removal in biomass gasification*. *Environmental science & technology*, 2008.**42**(16): p. 6224-6229.
38. Wang, J., et al., *Aluminumdodecatungstophosphate (Al_{0.9}H_{0.3}PW₁₂O₄₀) nanotube as a solid acid catalyst one-pot production of biodiesel from waste cooking oil*. *BioResources*, 2009.**4**(4): p. 1477-1486.
39. Goodman, D.W., *Model studies in catalysis using surface science probes*. *Chemical reviews*, 1995. **95**(3): p. 523-536.
40. Ertl, G., *Reactions at surfaces: from atoms to complexity (Nobel Lecture)*. *Angewandte Chemie International Edition*, 2008.**47**(19): p. 3524-3535.

41. Paulis, M., et al., *Influence of the surface adsorption desorption processes on the ignition curves of volatile organic compounds (VOCs) complete oxidation over supported catalysts*. Applied Catalysis B: Environmental, 2000.**26**(1): p. 37-46.
42. Fechete, I., Y. Wang, and J.C. Vdrine, *The past, present and future of heterogeneous catalysis*. Catalysis Today, 2012.**189**(1): p. 2-27.
43. Tanabe, K. and W.F. Hderich, *Industrial application of solid acid base catalysts*. Applied Catalysis A: General, 1999.**181**(2): p. 399-434.
44. Boreskov, G.K., *Heterogeneous catalysis*. 2003: Nova Publishers.
45. Hlderich, W.F. and G. Heitmann, *Synthesis of intermediate and fine chemicals on heterogeneous catalysts with respect to environmental protection*. Catalysis Today, 1997.**38**(2): p. 227-233.
46. Elnashaie, S.S.E.H., *Modelling, simulation and optimization of industrial fixed bed catalytic reactors*. Vol. 7. 1994: CRC Press.
47. Chmielarz, L., et al., *Influence of Cu, Co and Ni cations incorporated in brucite-type layers on thermal behaviour of hydrotalcites and reducibility of the derived mixed oxide systems*. Thermochemica Acta, 2002.**395**(1-2): p. 225-236.
48. Chmielarz, L., et al., *Catalytic activity of Co-Mg-Al, Cu-Mg-Al and Cu-Co-Mg-Al mixed oxides derived from hydrotalcites in SCR of NO with ammonia*. Applied Catalysis B: Environmental, 2002.**35**(3): p. 195-210.
49. Katz, L. and R. Ward, *Structure relations in mixed metal oxides*. Inorganic Chemistry, 1964.**3**(2): p. 205-211.

50. Gawande, M.B., R.K. Pandey, and R.V. Jayaram, *Role of mixed metal oxides in catalysis science versatile applications in organic synthesis*. Catalysis Science & Technology, 2012. **2**(6): p. 1113-1125.
51. Rao, C.N.R., *Transition-metal oxides*, in *Solid state chemistry*. 1974.
52. Miyata, S., *Hydrotalcites in relation to composition*. Clays Clay Miner, 1980. **28**(1): p. 50-56.
53. Cavani, F., F. Trifira, and A. Vaccari, *Hydrotalcite-type anionic clays: Preparation, properties and applications*. Catalysis Today, 1991. **11**(2): p. 173-301.
54. Cantrell, D.G., et al., *Structure-reactivity correlations in MgAl hydrotalcite catalysts for biodiesel synthesis*. Applied Catalysis A: General, 2005. **287**(2): p. 183-190.
55. Climent, M.J., et al., *Base catalysis for fine chemicals production: Claisen-Schmidt condensation on zeolites and hydrotalcites for the production of chalcones and flavanones of pharmaceutical interest*. Journal of Catalysis, 1995. **151**(1): p. 60-66.
56. Sels, B.F., D.E. De Vos, and P.A. Jacobs, *Hydrotalcite-like anionic clays in catalytic organic reactions*. Catalysis Reviews, 2001. **43**(4): p. 443-488.
57. Rao, K.K., et al., *Activation of MgAl hydrotalcite catalysts for aldol condensation reactions*. Journal of Catalysis, 1998. **173**(1): p. 115-121.
58. Mills, S.J., et al., *Nomenclature of the hydrotalcite supergroup: natural layered double hydroxides*. Mineralogical Magazine, 2012. **76**(5): p. 1289-1336.
59. Chen, Y., et al., *Structure and photoluminescence of MgAlEu ternary hydrotalcite-like layered double hydroxides*. Journal of Solid State Chemistry, 2012. **183**(9): p. 2222-2226.

60. Velu, S. and C.S. Swamy, *Synthesis and physicochemical properties of a new copper-manganese-aluminium ternary hydrotalcite-like compound*. Journal of materials science letters, 1996. **15**(19): p. 1674-1677.
61. Pavel, O.D., et al., *The activity of yttrium-modified Mg, Al hydrotalcites in the epoxidation of styrene with hydrogen peroxide*. Applied Catalysis A: General, 2011.**403**(1-2): p. 83-90.
62. Pavel, O.D., et al., *HYDROTALCITE-LIKE COMPOUNDS, SOLID-BASE CATALYSTS FOR CYANOETHYLATION REACTION*. 2005.
63. Othman, M.R., Z. Helwani, and W.J.N. Fernando, *Synthetic hydrotalcites from different routes and their application as catalysts and gas adsorbents: a review*. Applied Organometallic Chemistry, 2009.**23**(9): p. 335-346.
64. Ding, S.-N., et al., *Glucose oxidase immobilized in alginate/layered double hydroxides hybrid membrane and its biosensing application*. Analytical Sciences, 2009.**25**(12): p. 1421-1425.
65. Barik, S., et al., *Nano-MgAl-layered double hydroxide application to cotton for enhancing mechanical, UV protection and flame retardancy at low cytotoxicity level*. Cellulose, 2017.**24**(2): p. 1107-1120.
66. Palomares, A.E., et al., *Using the memory effect of hydrotalcites for improving the catalytic reduction of nitrates in water*. Journal of Catalysis, 2004.**221**(1): p. 62-66.
67. Debecker, D.P., E.M. Gaigneaux, and G. Busca, *Exploring, tuning, and exploiting the basicity of hydrotalcites for applications in heterogeneous catalysis*. Chemistry-A European Journal, 2009.**15**(16): p. 3920-3935.

68. Alvarez, M.G., et al., *Tunable basic and textural properties of hydrotalcite derived materials for transesterification of glycerol*. Applied Clay Science, 2012. **58**: p. 16-24.
69. Rocha, J., et al., *Reconstruction of layered double hydroxides from calcined precursors: a powder XRD and ^{27}Al MAS NMR study*. Journal of Materials Chemistry, 1999. **9**(10): p. 2499-2503.
70. Zhao, Y., et al., *Preparation of layered double-hydroxide nanomaterials with a uniform crystallite size using a new method involving separate nucleation and aging steps*. Chemistry of Materials, 2002. **14**(10): p. 4286-4291.
71. Orthman, J., H.Y. Zhu, and G.Q. Lu, *Use of anion clay hydrotalcite to remove coloured organics from aqueous solutions*. Separation and Purification Technology, 2003. **31**(1): p. 53-59.
72. Corma, A., et al., *Lewis and Bronsted basic active sites on solid catalysts and their role in the synthesis of monoglycerides*. Journal of Catalysis, 2005. **234**(2): p. 340-347.
73. Liu, Y., et al., *Transesterification of poultry fat with methanol using MgAl hydrotalcite derived catalysts*. Applied Catalysis A: General, 2007. **331**: p. 138-148.
74. Shen, J., et al., *Synthesis and surface acid/base properties of magnesium-aluminum mixed oxides obtained from hydrotalcites*. Langmuir, 1994. **10**(10): p. 3902-3908.
75. Vadrine, J.C., *Heterogeneous Catalysis on Metal Oxides*. Catalysts, 2017. **7**(11): p. 341.
76. Matlack, A., *Introduction to green chemistry*: CRC Press.
77. Anastas, P.T., L.G. Heine, and T.C. Williamson, *Green chemical syntheses and processes: introduction*. 2000, ACS Publications.
78. Dunn, P.J., A. Wells, and M.T. Williams, *Green chemistry in the pharmaceutical industry*: 2010. John Wiley & Sons.

79. Clark, J.H. and D.J. Macquarrie, *Handbook of green chemistry and technology*. 2008: John Wiley & Sons.
80. Van Arnum, S.D., *An approach towards teaching green chemistry fundamentals*. Journal of chemical education, 2005.**82**(11): p. 1689.
81. Sheldon, R.A., I. Arends, and U. Hanefeld, *Green chemistry and catalysis*. 2007: John Wiley & Sons.
82. Poliakoff, M. and P. Licence, *Sustainable technology: green chemistry*. nature, 2007. **450**(7171): p. 810.
83. Jimnez-Gonzalez, C.n., D.J.C. Constable, and C.S. Ponder, *Evaluating the Greenness of chemical processes and products in the pharmaceutical industry a green metrics primer*. Chemical Society Reviews, 2012.**41**(4): p. 1485-1498.
84. Sheldon, R.A., *Green solvents for sustainable organic synthesis: state of the art*. Green Chemistry, 2005.**7**(5): p. 267-278.
85. Aric, F. and P. Tundo, *Dimethyl carbonate: a modern green reagent and solvent*. Russian Chemical Reviews, 2010.**79**(6): p. 479-489.
86. Tundo, P., M. Selva, and S. Memoli, *Dimethyl carbonate as a green reagent*. 2000, 87-89 ACS Publications.
87. Fiorani, G., A. Perosa, and M. Selva, *Dimethyl carbonate: a versatile reagent for a sustainable valorization of renewables*. Green Chemistry. 2018.**20**: p. 288-322.
88. Peng, W., et al., *Recent progress in phosgene-free methods for synthesis of dimethyl carbonate*. Pure and Applied Chemistry, 2011.**84**(3): p. 603-620.
89. Tundo, P. and M. Selva, *The chemistry of dimethyl carbonate*. Accounts of chemical research, 2002.**35**(9): p. 706-716.

90. Nexant's ChemSystems report 2012S12, Dimethyl Carbonate 1A00101.0012.4120
91. Pacheco, M.A. and C.L. Marshall, *Review of dimethyl carbonate (DMC) manufacture and its characteristics as a fuel additive*. Energy & Fuels, 1997.**11**(1): p. 2-29.
92. Fukuoka, S., et al., *Green and sustainable chemistry in practice: development and industrialization of a novel process for polycarbonate production from CO₂ without using phosgene*. Polymer journal, 2007.**39**(2): p. 91. (92a) Fukuoka, S.; Kawamura, M.; Komiya, K.; Tojo, M.; Hachiya, H.; Hasegawa, K.; Aminaka, M.; Okamoto, H.; Fukawa, I.; Konno, S., A novel non-phosgene polycarbonate production process using by-product CO₂ as starting material. *Green Chemistry* **2003**, 5, (5), 497-507.
93. Choi, J.-C., et al., *Selective and high yield synthesis of dimethyl carbonate directly from carbon dioxide and methanol*. Green Chemistry, 2002.**4**(3): p. 230-234.
94. Wang, M., et al., *Synthesis of dimethyl carbonate from urea and methanol over solid base catalysts*. Catalysis Communications, 2006.**7**(1): p. 6-10.
95. Romano, U., et al., *Method for the preparation of esters of carbonic acid*. 1980, US Patent 4,218,391,.
96. Han, M.S., et al., *Synthesis of dimethyl carbonate by vapor phase oxidative carbonylation of methanol over Cu-based catalysts*. Journal of Molecular Catalysis A: Chemical, 2001. **170**(1-2): p. 225-234.
97. Dong, W.-S., et al., *Ionic liquid as an efficient promoting medium for synthesis of dimethyl carbonate by oxidative carbonylation of methanol*. Applied Catalysis A: General, 2008.**334**(1-2): p. 100-105.

98. Yang, P., et al., *Mesoporous bimetallic PdCl₂-CuCl₂ catalysts for dimethyl carbonate synthesis by vapor phase oxidative carbonylation of methanol*. *Applied Catalysis A: General*, 2003.**241**(1-2): p. 363-373.
99. Yuan, Y., W. Cao, and W. Weng, *CuCl₂ immobilized on amino-functionalized MCM-41 and MCM-48 and their catalytic performance toward the vapor-phase oxy-carbonylation of methanol to dimethylcarbonate*. *Journal of Catalysis*, 2004.**228**(2): p. 311-320.
100. Cao, Y., et al., *CuCl catalyst heterogenized on diamide immobilized SBA-15 for efficient oxidative carbonylation of methanol to dimethylcarbonate*. *Chemical Communications*, 2003(7): p. 908-909.
101. Ren, J., et al., *Oxidative carbonylation of methanol to dimethyl carbonate over CuCl/SiO₂TiO₂ catalysts prepared by microwave heating: The effect of support composition*. *Applied Catalysis A: General*, 2009.**366**(1): p. 93-101.
102. Cao, W., H. Zhang, and Y. Yuan, *CuCl₂ Immobilized on Amino-Functionalized MCM-41 and MCM-48 as Efficient Heterogeneous Catalysts for Dimethyl Carbonate Synthesis by Vapor-Phase Oxidative Carbonylation of Methanol*. *Catalysis letters*, 2003. **91**(3-4): p. 243-246.
103. Keller, N., G. Rebmann, and V. Keller, *Catalysts, mechanisms and industrial processes for the dimethylcarbonate synthesis*. *Journal of Molecular Catalysis A: Chemical*, 2010.**317**(1-2): p. 1-18.
104. Yamamoto, Y., *Vapor phase carbonylation reactions using methyl nitrite over Pd catalysts*. *Catalysis Surveys from Asia*, 2010.**14**(3-4): p. 103-110.
105. Punnoose, A., et al., *Characterization of CuCl₂/PdCl₂/activated carbon catalysts for the synthesis of diethyl carbonate*. *Energy & Fuels*, 2002.**16**(1): p. 182-188.

106. Wang, S.-P., et al., *Effects of potassium promoter on the performance of PdCl₂CuCl₂/AC catalysts for the synthesis of dimethyl carbonate from CO and methyl nitrite*. Chinese Chemical Letters, 2015.**26**(11): p. 1359-1363.
107. Xiong, H., et al., *CuCl/phen/NMI in homogeneous carbonylation for synthesis of diethyl carbonate: Highly active catalyst and corrosion inhibitor*. Industrial & Engineering Chemistry Research, 2009.**48**(24): p. 10845-10849.
108. Mauri, M.M., U. Romano, and F. Rivetti, *Dimethyl carbonate: a new building block for organic chemicals production*. ChemInform, 1985.**16**(42).
109. Huang, S., et al., *Recent advances in dialkyl carbonates synthesis and applications*. Chemical Society Reviews, 2015.**44**(10): p. 3079-3116.
110. Romano, U. and U. Melis, *Process for the preparation of dialkylcarbonates*. 1977, US Patent 4,062,884.
111. Duranleau, R.G., E.C.Y. Nieh, and J.F. Knifton, *Process for production of ethylene glycol and dimethyl carbonate*. 1987, US Patent 4,691,041.
112. Tojo, M. and K. Oonishi, *Process for continuously producing dialkyl carbonate and diol*. 2002, US Patent 6,479,689.
113. Ball, P., H. Fllmann, and W. Heitz, *Carbonates and polycarbonates from urea and alcohol*. Angewandte Chemie International Edition in English, 1980.**19**(9): p. 718-720.
114. Zhao, W., et al., *Synthesis of dimethyl carbonate from methyl carbamate and methanol with zinc compounds as catalysts*. Industrial & Engineering Chemistry Research, 2008.**47**(16): p. 5913-5917.
115. Wang, M., et al., *Synthesis of dimethyl carbonate from urea and methanol over ZnO*. Industrial & Engineering Chemistry Research, 2005.**44**(19): p. 7596-7599.

116. Wu, X., et al., *Dimethyl carbonate synthesis over ZnOCaO bi-functional catalysts*. Catalysis Communications, 2014.**46**: p. 46-50.
117. Zhang, C., et al., *Selective synthesis of dimethyl carbonate from urea and methanol over Fe₂O₃/HMCM-49*. Catalysis Science & Technology, 2012.**2**(2): p. 305-309.
118. Wang, D., et al., *Zn/Fe mixed oxide: Heterogeneous catalyst for the synthesis of dimethyl carbonate from methyl carbamate and methanol*. Catalysis Communications, 2010,**11**(5): p. 430-433.
119. Wang, D., et al., *Synthesis of dimethyl carbonate from methyl carbamate and methanol over lanthanum compounds*. Fuel Processing Technology, 2010.**91**(9): p. 1081-1086.
120. Santos, B.A.V., et al., *Review for the direct synthesis of dimethyl carbonate*. ChemBioEng Reviews, 2014.**1**(5): p. 214-229.
121. Cai, Q., et al., *Synthesis of dimethyl carbonate from methanol and carbon dioxide using potassium methoxide as catalyst under mild conditions*. Catalysis letters, 2005. **103**(3-4): p. 225-228.
122. Yoshida, Y., et al., *Direct synthesis of organic carbonates from the reaction of CO₂ with methanol and ethanol over CeO₂ catalysts*. Catalysis Today, 2006.**115**(1-4): p. 95-101.
123. La, K.W., et al., *Effect of acid base properties of H₃PW₁₂O₄₀/CeO₂ catalysts on the direct synthesis of dimethyl carbonate from methanol and carbon dioxide: A TPD study of H₃PW₁₂O₄₀/CeO₂ catalysts*. Journal of Molecular Catalysis A: Chemical, 2007. **269**(1-2): p. 41-45.
124. Wang, X.J., et al., *Direct synthesis of dimethyl carbonate from carbon dioxide and methanol using supported copper (Ni, V, O) catalyst with photo-assistance*. Journal of Molecular Catalysis A: Chemical, 2007. **278**(1-2): p. 92-96.

125. Wu, X.L., et al., *Direct synthesis of dimethyl carbonate (DMC) using Cu-Ni/VSO as catalyst*. Journal of Molecular Catalysis A: Chemical, 2006. **249**(1-2): p. 93-97.
126. Honda, M., et al., *Catalytic CO₂ conversion to organic carbonates with alcohols in combination with dehydration system*. Catalysis Science & Technology, 2014. **4**(9): p. 2830-2845.
127. Honda, M., et al., *Ceria-catalyzed conversion of carbon dioxide into dimethyl carbonate with 2-cyanopyridine*. ChemSusChem, 2013. **6**(8): p. 1341-1344.
128. Honda, M., et al., *Tandem Carboxylation-Hydration Reaction System from Methanol, CO₂ and Benzonitrile to Dimethyl Carbonate and Benzamide Catalyzed by CeO₂*. ChemCatChem, 2011. **3**(2): p. 365-370.
129. Bhanage, B.M., et al., *Transesterification of urea and ethylene glycol to ethylene carbonate as an important step for urea based dimethyl carbonate synthesis*. Green Chemistry, 2003. **5**(4): p. 429-432.
130. Krimm, H., H.-J. Buysch, and H. Rudolph, *Process for the preparation of dialkyl carbonates*. 1981, US Patent 4,307,032.
131. Yang, Z.-Z., et al., *Dimethyl carbonate synthesis catalyzed by DABCO-derived basic ionic liquids via transesterification of ethylene carbonate with methanol*. Tetrahedron Letters, 2010. **51**(21): p. 2931-2934.
132. Frevel, L.K. and J.A. Gilpin, *Carbonate synthesis from alkylene carbonates*. 1972, US Patent 3,642,858.
133. Han, M.S., et al., *Kinetics of dimethyl carbonate synthesis from ethylene carbonate and methanol using alkali-metal compounds as catalysts*. Reaction Kinetics and Catalysis Letters, 2001. **73**(1): p. 33-38.

134. Jagtap, S.R., M.D. Bhor, and B.M. Bhanage, *Synthesis of dimethyl carbonate via transesterification of ethylene carbonate with methanol using poly-4-vinyl pyridine as a novel base catalyst*. *Catalysis Communications*, 2008.**9**(9): p. 1928-1931.
135. Wang, J.-Q., et al., *Synthesis of dimethyl carbonate catalyzed by carboxylic functionalized imidazolium salt via transesterification reaction*. *Catalysis Science & Technology*, 2012.**2**(3): p. 600-605.
136. Dharman, M.M., et al., *Significant influence of microwave dielectric heating on ionic liquid catalyzed transesterification of ethylene carbonate with methanol*. *Journal of Molecular Catalysis A: Chemical*, 2009. **303**(1-2): p. 96-101.
137. Kim, D.-W., et al., *Production of dimethyl carbonate from ethylene carbonate and methanol using immobilized ionic liquids on MCM-41*. *Catalysis Today*, 2011.**164**(1): p. 556-560.
138. Xu, J., et al., *Ionic liquid immobilized on mesocellular silica foam as an efficient heterogeneous catalyst for the synthesis of dimethyl carbonate via transesterification*. *Applied Catalysis A: General*, 2013.**464**: p. 357-363.
139. Tatsumi, T., Y. Watanabe, and K.A. Koyano, *Synthesis of dimethyl carbonate from ethylene carbonate and methanol using TS-1 as solid base catalyst*. *Chemical Communications*, 1996(19): p. 2281-2282.
140. Dhuri, S.M. and V.V. Mahajani, *Studies in transesterification of ethylene carbonate to dimethyl carbonate over Amberlyst 21 catalyst*. *Journal of Chemical Technology and Biotechnology*, 2006.**81**(1): p. 62-69.
141. Bhanage, B.M., et al., *Synthesis of dimethyl carbonate and glycols from carbon dioxide, epoxides and methanol using heterogeneous Mg containing smectite catalysts: effect of*

- reaction variables on activity and selectivity performance. Green Chemistry, 2003.5(1): p. 71-75.*
142. Xu, J., et al., *Simple preparation of MgO/g-C₃N₄ catalyst and its application for catalytic synthesis of dimethyl carbonate via transesterification. Catalysis Communications, 2017.95: p. 72-76.*
143. Xu, J., et al., *Mesostructured graphitic carbon nitride as a new base catalyst for the efficient synthesis of dimethyl carbonate by transesterification. Catalysis Science & Technology, 2013.3(12): p. 3192-3199.*
144. Sankar, M., et al., *Transesterification of cyclic carbonates with methanol at ambient conditions over tungstate-based solid catalysts. Applied Catalysis A: General, 2006.312: p. 108-114.*
145. Srivastava, R., D. Srinivas, and P. Ratnasamy, *FeZn double-metal cyanide complexes as novel, solid transesterification catalysts. Journal of Catalysis, 2006.241(1): p. 34-44.*
146. Watanabe, Y. and T. Tatsumi, *Hydrotalcite-type materials as catalysts for the synthesis of dimethyl carbonate from ethylene carbonate and methanol. Microporous and mesoporous materials, 1998.22(1-3): p. 399-407.*
147. Murugan, C. and H.C. Bajaj, *Transesterification of propylene carbonate with methanol using Mg-Al-CO₃ hydrotalcite as solid base catalyst.*
148. Gandara-Loe, J.s., et al., *Layered double hydroxides as base catalysts for the synthesis of dimethyl carbonate. Catalysis Today, 2017.296: p. 254-261.*
149. Wei, T., et al., *Effect of base strength and basicity on catalytic behavior of solid bases for synthesis of dimethyl carbonate from propylene carbonate and methanol. Fuel Processing Technology, 2003.83(1-3): p. 175-182.*

150. Wei, T., et al., *Synthesis of dimethyl carbonate by transesterification over CaO/carbon composites*. *Green Chemistry*, 2003.**5**(3): p. 343-346.
151. Wang, H., et al., *Influence of preparation methods on the structure and performance of CaOZrO₂ catalyst for the synthesis of dimethyl carbonate via transesterification*. *Journal of Molecular Catalysis A: Chemical*, 2006. **258**(1-2): p. 308-312.
152. Sankar, M., S. Satav, and P. Manikandan, *Transesterification of cyclic carbonates to dimethyl carbonate using solid oxide catalyst at ambient conditions: environmentally benign synthesis*. *ChemSusChem*, 2010.**3**(5): p. 575-578.
153. Stoica, G., S.n. Abell, *Na-dawsonite derived aluminates for DMC production by transesterification of ethylene carbonate*. *Applied Catalysis A: General*, 2009.**365**(2): p. 252-260.
154. Xu, J., et al., *Efficient synthesis of dimethyl carbonate via transesterification of ethylene carbonate over a new mesoporous ceria catalyst*. *Applied Catalysis A: General*, 2014.**484**: p. 1-7.
155. Li, T.-T., et al., *In situ generation of superbasic sites on mesoporous ceria and their application in transesterification*. *Journal of Molecular Catalysis A: Chemical*, 2012.**352**: p. 38-44.
156. Jurez, R., A. Corma, and H. Garc, *Gold nanoparticles promote the catalytic activity of ceria for the transalkylation of propylene carbonate to dimethyl carbonate*. *Green Chemistry*, 2009.**11**(7): p. 949-952.
157. Kumar, P., V.C. Srivastava, and I.M. Mishra, *Synthesis and characterization of CeLa oxides for the formation of dimethyl carbonate by transesterification of propylene carbonate*. *Catalysis Communications*, 2015.**60**: p. 27-31.

158. Kumar, P., V.C. Srivastava, and I.M. Mishra, *Dimethyl carbonate synthesis by transesterification of propylene carbonate with methanol: Comparative assessment of Ce-M (M= Co, Fe, Cu and Zn) catalysts*. *Renewable Energy*, 2016.**88**: p. 457-464.
159. Wang, L., et al., *Efficient synthesis of dimethyl carbonate via transesterification of ethylene carbonate with methanol over binary zinc-yttrium oxides*. *Catalysis Communications*, 2011.**16**(1): p. 45-49.
160. Murugan, C. and H.C. Bajaj, *Mg/La mixed oxide as catalyst for the synthesis of dimethyl carbonate from cyclic carbonates and methanol*. *Indian journal of chemistry*, 2013.**52A**(4) 459-466
161. Kumar, P., V.C. Srivastava, and I.M. Mishra, *Dimethyl carbonate synthesis from propylene carbonate with methanol using CuZnAl catalyst*. *Energy & Fuels*, 2015.**29**(4): p. 2664-2675.
162. Unnikrishnan, P. and D. Srinivas, *Highly active and reusable ternary oxide catalyst for dialkyl carbonates synthesis*. *Journal of Molecular Catalysis A: Chemical*, 2015.**398**: p. 42-49.
163. Raghunath, V., *Intriguing Catalyst (CaO) Pretreatment Effects and Mechanistic Insights during Propylene Carbonate Transesterification with Methanol*. *ACS Sustainable Chemistry & Engineering*, 2017.**5**(6), 4718-4729.
164. Chaturvedi, D., *Recent developments on the carbamation of amines*. *Current Organic Chemistry*, 2011.**15**(10): p. 1593-1624.
165. Ray, S. and D. Chaturvedi, *Application of organic carbamates in drug design. Part 1: Anti-cancer agents-recent reports*. *Drugs Fut*, 2004.**29**(4): p. 343-357.

166. Asaka, T., A. Manaka, and H. Sugiyama, *Recent developments in macrolide antimicrobial research*. *Current topics in medicinal chemistry*, 2003.**3**(9): p. 961-989.
167. Ma, J., et al., *Differential responses of eight cyanobacterial and green algal species, to carbamate insecticides*. *Ecotoxicology and Environmental safety*, 2006.**63**(2): p. 268-274.
168. Wills, A.J., Y. Krishnan-Ghosh, and S. Balasubramanian, *Synthesis of a polymer-supported oxazolidine aldehyde for asymmetric chemistry*. *The Journal of Organic Chemistry*, 2002.**67**(19): p. 6646-6652.
169. Zhao, X., et al., *Synthesis of MDI from dimethyl carbonate over solid catalysts*. *Industrial & Engineering Chemistry Research*, 2002.**41**(21): p. 5139-5144.
170. Tafesh, A.M. and J. Weiguny, *A review of the selective catalytic reduction of aromatic nitro compounds into aromatic amines, isocyanates, carbamates, and ureas using CO*. *Chemical reviews*, 1996. **96**(6): p. 2035-2052.
171. Latourette, H.K. and O.H. Johnson, *Preparation of aromatic isocyanates*. 1959, US Patent 2,908,703. (171a) Vetter, Jeroen. "A safer route to MDI—An assessment of a phosgene free manufacturing process." *Rijksuniversiteit, Groningen, The Netherlands* 2010.
172. Dreier, T., et al., *Zinc cluster compounds and their use as catalysts in the reaction of amines with dialkyl carbonates*, 2016.US Patent App. 14/890,053,.
173. Baba, T., et al., *Catalytic methoxycarbonylation of aromatic diamines with dimethyl carbonate to their dicarbamates using zinc acetate*. *Catalysis letters*, 2002. **82**(3-4): p. 193-197.

174. Li, F., et al., *Condensation Reaction of Methyl N-Phenylcarbamate with Formaldehyde over H β Catalyst*. *Industrial & Engineering Chemistry Research*, 2014.**53**(13): p. 5406-5412.
175. Yanji, W., Z. Xinqiang, and L. Fang, *Study of clean synthesis process for methylene diphenyl diisocyanateâ€¦.Catalytic Synthesis and Condensation of Methyl Pheneyl Carbamate*.*Acta Petrolei Sinica Petroleum Processing Section*, 1999.**15**(6): p. 9-14.
176. Keller, H.-J. and T. Braxmeier, *Isocyanates Part 3.7 Synthesis of carbamates by DMAP-catalyzed reaction of amines with di-tert-butylidicarbonate and alcohols*. *Tetrahedron Letters*, 1996.**37**(33): p. 5861-5864.
177. Saliu, F., B. Putomatti, and B. Rindone, *Nitrogen-containing organobases as promoters in the cobalt (II) Schiff base catalyzed oxidative carbonylation of amines*. *Tetrahedron Letters*, 2012.**53**(28): p. 3590-3593.
178. Grego, S. and P. Tundo, *Phosgene-free carbamoylation of aniline via dimethyl carbonate*. *Pure and Applied Chemistry*.2012 **84**(3): p. 695-705.
179. Fukuoka, S., M. Chono, and M. Kohno, *A novel catalytic synthesis of carbamates by oxydative alkoxy carbonylation of amines in the presence of palladium and iodide*. *Journal of the Chemical Society, Chemical Communications*, 1984(6): p. 399-400.
180. Wan, B., S. Liao, and D. Yu, *Polymer-supported palladiummanganese bimetallic catalyst for the oxidative carbonylation of amines to carbamate esters*. *Applied Catalysis A: General*, 1999.**183**(1): p. 81-84.
181. Shi, F., J. Peng, and Y. Deng, *Highly efficient ionic liquid-mediated palladium complex catalyst system for the oxidative carbonylation of amines*. *Journal of Catalysis*, 2003.**219**(2): p. 372-375.

182. Cenini, S., et al., *Effects of neutral ligands in the reductive carbonylation of nitrobenzene catalysed by Ru₃(CO)₁₂ and Rh₆(CO)₁₆*. Journal of molecular catalysis, 1988.**49**(1): p. 59-69.
183. Izumi, Y., et al., *Reductive carbonylation of nitrobenzene catalyzed by heteropolyanion-modified palladium*. Journal of molecular catalysis, 1992.**72**(1): p. 37-46.
184. Valli, V.L.K. and H. Alper, *Reductive carbonylation of mono-and dinitroarenes catalyzed by montmorillonitebipyridinylpalladium (II) acetate and ruthenium carbonyl*. Journal of the American Chemical Society, 1993.**115**(9): p. 3778-3779.
185. Karpińska, M., J. Skupińska, and P. Baran, *Carbonylation of aromatic dinitro compounds with carbon monoxide to respective dicarbamates in the presence of the PdCl₂/Fe/I₂/Py catalytic system*. Journal of Molecular Catalysis A: Chemical, 2009. **303**(1-2): p. 43-51.
186. Daughenbaugh, R.J., *Production of carboxylic acid amides and carbamates using cobalt catalysts*. 1981, US Patent 4,258,200.
187. Romano, U. and R. Tesei, *Process for the preparation of aromatic carbonates*. 1977, US Patent 4,045,464.
188. King, S.T., *Reaction mechanism of oxidative carbonylation of methanol to dimethyl carbonate in CuY zeolite*. Journal of Catalysis, 1996.**161**(2): p. 530-538.
189. Gurgiolo, A.E., *Preparation of carbamates from aromatic amines and organic carbonates*. 1981, US Patent 4,268,683.
190. Mark, V., *Process for the preparation of aromatic carbonates*. 1985, US Patent 4,554,110.
191. Brill, W., *Preparation of carbamates*. 1973, US Patent 3,763,217.

192. Reixach, E., et al., *Alkoxy carbonylation of Industrially Relevant Anilines Using $Zn_4O(O_2CCH_3)_6$ as Catalyst*. Industrial & Engineering Chemistry Research, 2012.**51**(50): p. 16165-16170.
193. Fu, Z.-H. and Y. Ono, *Synthesis of methyl N-phenyl carbamate by methoxycarbonylation of aniline with dimethyl carbonate using Pb compounds as catalysts*. Journal of molecular catalysis, 1994.**91**(3): p. 399-405.
194. Wang, S., et al., *Investigations of catalytic activity, deactivation, and regeneration of Pb(OAc)₂ for methoxycarbonylation of 2, 4-toluene diamine with dimethyl carbonate*. Industrial & Engineering Chemistry Research, 2007.**46**(21): p. 6858-6864.
195. Li, F., et al., *The Induction Period and Novel Active Species in Zn(OAc)₂ Catalyzed Synthesis of Aromatic Carbamates*. Catalysis letters, 2017.**147**(6): p. 1478-1484.
196. Curini, M., et al., *Carbamate synthesis from amines and dimethyl carbonate under ytterbium triflate catalysis*. Tetrahedron Letters, 2002.**43**(28): p. 4895-4897.
197. Tundo, P., et al., *Direct synthesis of N-methylurethanes from primary amines with dimethyl carbonate*. Pure and Applied Chemistry, 2005.**77**(10): p. 1719-1725.
198. Li, F., et al., *Synthesis of methyl N-phenyl carbamate from aniline and dimethyl carbonate over supported zirconia catalyst*. Industrial & Engineering Chemistry Research, 2006.**45**(14): p. 4892-4897.
199. Lucas, N., et al., *Non-phosgene route for the synthesis of methyl phenyl carbamate using ordered ALSBA-15 catalyst*. Journal of Molecular Catalysis A: Chemical, 2008. **295**(1-2): p. 29-33.

200. Zhang, L., et al., *Experimental and theoretical investigation of reaction of aniline with dimethyl carbonate catalyzed by acidbase bifunctional ionic liquids*. *Catalysis Today*, 2010.**158**(3-4): p. 279-285.
201. Kumar, S. and S.L. Jain, *L-prolinTBAB-catalyzed phosgene free synthesis of methyl carbamates from amines and dimethyl carbonate*. *New Journal of Chemistry*, 2013.**37**(9): p. 2935-2938.
202. Litwinowicz, M. and J. Kijeski, *Carbamoylation of primary, secondary and aromatic amines by dimethyl carbonate in a flow system over solid catalysts*. *Sustainable Chemical Processes*, 2015.**3**(1): p. 1.
203. Margetić, Davor, et al. *Reactions of dimethyl carbonate with aliphatic amines under high pressure*. *Synthetic communications*, 2011.**41.15**:p. 2283-2289.

Chapter 2

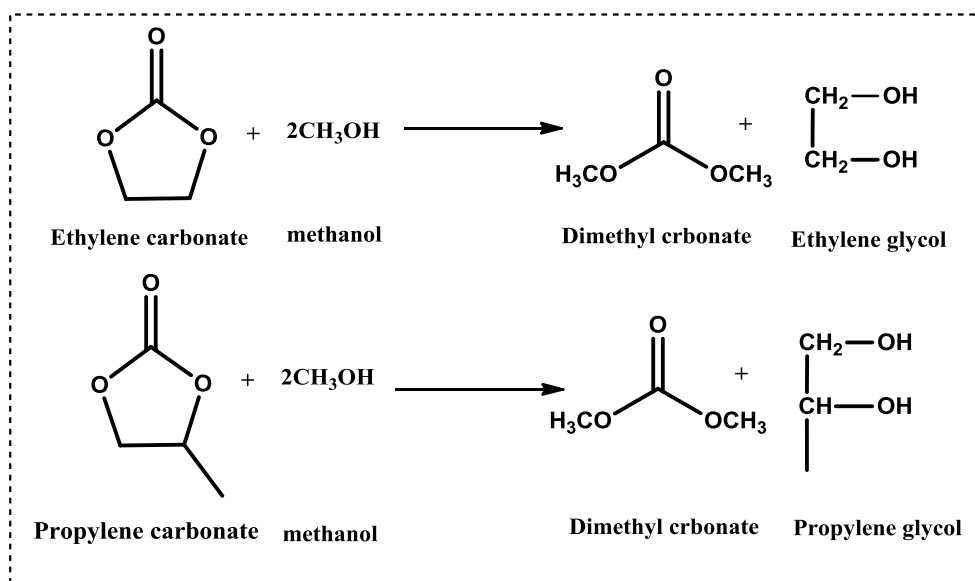
DMC synthesis by transesterification of cyclic carbonates with methanol using heterogeneous base catalysts

Introduction

Dimethyl carbonate (DMC) has emerged as a “Green Reagent” because of its non-toxic nature and multifunctionality. DMC is used as a safe replacement for toxic phosgene in carbonylation and for dimethyl sulphate and methyl halides in methylation reactions.¹ In addition, DMC has potential applications as an electrolyte in lithium batteries as a polar aprotic solvent and as an octane booster in gasoline to meet oxygenate specifications.² With the availability of DMC based on non-phosgene routes; lot of work is being carried out on the synthesis of various chemicals using DMC as a Green Reagent.^{1a} DMC is being synthesized using various non-phosgene routes as discussed in Chapter 1 (Section 1.4.).³⁻⁶ Landmark development has been the synthesis of DMC by transesterification of cyclic carbonate [ethylene carbonate (EC)/propylene carbonate (PC)] with methanol commercialized by Asahi Kasei Corporation.⁷ This is a safe and atom efficient process and ethylene glycol is formed as the by-product. Ethylene glycol is an important chemical and also can be converted back to ethylene carbonate by reaction with urea.⁸ Various homogeneous as well as heterogeneous catalysts have been investigated for this reaction.⁹⁻¹² Among all heterogeneous catalysts investigated mixed metal oxides were found to be active catalysts for this reaction, however, they require either high reaction temperature (100–160 °C) or high catalyst loading (10–25wt%).¹³⁻²⁰ This potentially may cause a problem in continuous or large scale operation. In this context it is still a challenging task to develop heterogeneous catalysts exhibiting high catalyst activity and high stability for the synthesis of DMC from EC and methanol under mild reaction conditions.

In this chapter we have synthesized dimethyl carbonate by transesterification of cyclic carbonate (EC/PC) with methanol using various heterogeneous base catalysts (Scheme 2.1). All catalysts

were synthesized by reported procedures and further characterized in detail by XRD, FT-IR, BET, TPD, TEM and XPS analysis. Further this chapter is divided into two parts (A) Synthesis of dimethyl carbonate by transesterification of EC with methanol using MgFeCe ternary Layered double hydroxide (LDH) as a catalyst (B) Synthesis of dimethyl carbonate by transesterification of cyclic carbonate (EC/PC) with methanol using Li-Al mixed metal oxide as a catalyst.



Scheme 2.1: Synthesis of dimethyl carbonate from transesterification of ethylene (EC) / propylene carbonate (PC) with methanol.

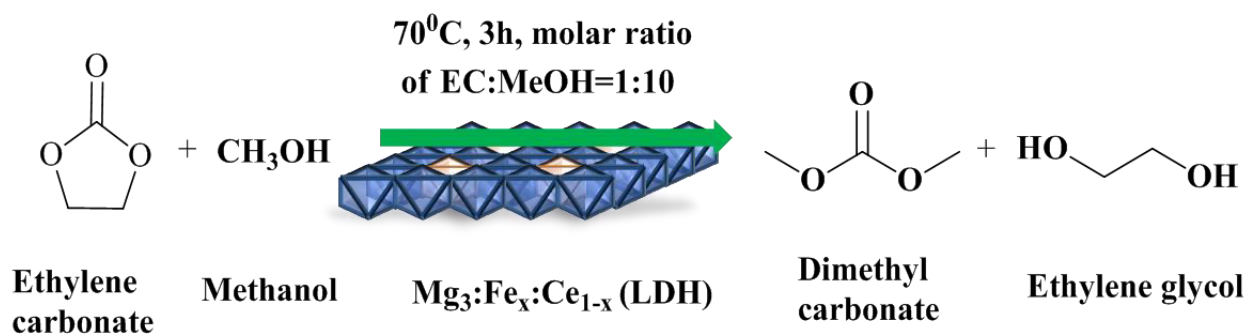
Chapter 2A

Synthesis of dimethyl carbonate by transesterification of EC with methanol using MgFeCe ternary Layered double hydroxide (LDH) catalyst

2A.1. Introduction

Hydrotalcites (HTs) or Layered double hydroxides (LDHs) constitute a class of layered compounds complementary to classic clays and have been widely investigated as solid base catalysts for several transformations.²¹ As mentioned earlier there are limited reports on the use of hydrotalcites as catalysts for transesterification of EC and methanol to DMC.²² It is well known that basicity of LDH can be tuned by proper choice of M^{2+} and M^{3+} metal cations or by varying the molar ratio of M^{2+}/M^{3+} .²³ Recently incorporation of third metal cation in parent LDH has attracted much more attention with the aim of modifying basicity of the catalyst (as discussed in section 1.2.2.1.). Pavel et al.²⁴ have prepared ternary hydrotalcite by incorporating Y^{3+} in the Mg-Al LDH (Mg:Al 3:1 ratio) and they observed significant improvement in the activity and selectivity for styrene epoxidation with hydrogen peroxide as oxidant and ternary LDH as the catalyst in acetonitrile. The electronegativity of yttrium (1.22) is lower compared to that of Al^{3+} (1.61) and results in higher basicity of the ternary LDH prepared. Higher basicity of the ternary LDH resulted in better epoxidation activity of this catalyst. Similar results were observed by Angelescu et al.^{24a} by modifying Mg–Al LDH with La and Y for cyanoethylation of ethanol.

In this work Efforts have been made, to tailor basic properties of LDHs by incorporating additional trivalent metal [M^{3+}] in the LDH. A series of $Mg_3Fe_xCe_{1-x}$ LDHs were synthesized by varying molar ratio of Fe:Ce (keeping Mg:Fe+Ce mole ratio of 3:1 constant) and characterized in detail by various spectroscopic techniques. Influence of Ce and its concentration on the properties and catalytic activity of Mg:Fe layered double hydroxide ($Mg_3Fe_xCe_{1-x}$) for DMC synthesis (Scheme 2A.1) was investigated in detail.



Scheme 2A.1: Schematic diagram of synthesis of dimethyl carbonate from ethylene carbonate and methanol over $Mg_3Fe_xCe_{1-x}$ LDHs.

2A.2. Materials

Ethylene carbonate (99%), benzoic acid (99.5%), $Ce(NO_3)_3 \cdot 6H_2O$, $Sm(NO_3)_3 \cdot 6H_2O$ (99%), $La(NO_3)_3 \cdot 6H_2O$ (99%) were purchased from Sigma-Aldrich Co. Chemical reagents including Ethylene glycol (99%), DMC (99.5%), $Mg(NO_3)_2 \cdot 6H_2O$ (99.5%), $Zn(NO_3)_2 \cdot 6H_2O$ (99.5%), $Al(NO_3)_2 \cdot 9H_2O$ (99.5%), $Co(NO_3)_2 \cdot 6H_2O$ (99.8%), $Ni(NO_3)_2 \cdot 6H_2O$ (99%), $Mg(NO_3)_2 \cdot 6H_2O$, NaOH (99.5%), Na_2CO_3 (99.5%), phenolphthalein, bromothymol blue, were obtained from Loba Chemical Co., India. KBR IR grade (99.8%), IPA (99.5%), methanol (99.8%), $Fe(NO_3)_3 \cdot 9H_2O$ (98%), toluene (99.8%) were purchased from Merck India.

2A.3. Catalyst preparation

Binary and ternary LDHs were synthesized as per the literature reports.^{21,25} The detailed synthesis procedures are given bellow.

2A.3.1. Synthesis of Binary LDHs ($M^{2+}/M^{3+}=3:1$)

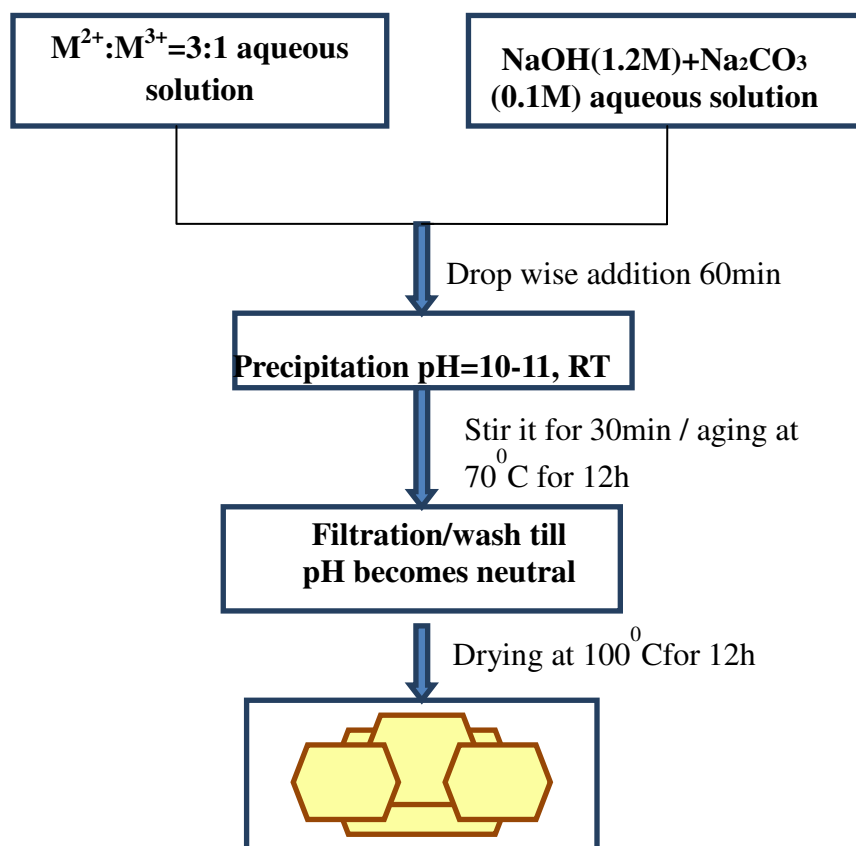


Figure 2A .1: Synthesis of LDHs by co-precipitation method

Binary LDHs M^{2+}/M^{3+} were synthesized by co-precipitation method²¹ by keeping M^{2+}/M^{3+} ratio 3:1, where $M^{2+} = \text{Mg, Co, Ni or Zn}$ and $M^{3+} = \text{Al, Fe or Ce}$. Aqueous solutions A and B were prepared in 100 ml de-ionized water. Solution A contains M^{2+} nitrate (60 mmol) and M^{3+} nitrate (20mmol). Solution B was prepared by dissolving NaOH (1.2M) and Na_2CO_3 (0.1M) in deionized water. Solutions A and B were simultaneously added drop wise in 100 ml de-ionized

water with vigorous stirring at room temperature. During addition, pH of the solution was maintained at 10-11 by addition of appropriate amount of solution B. The formed suspension was continuously stirred for 30 min and aged at 70°C for 12 h. Finally the solid formed was separated by filtration and washed thoroughly with de-ionized water until pH of the water wash was 7. Resultant solid was then dried at 100°C for 12 h. Various LDHs were prepared using different metal precursors and were labeled as Mg₃-Al₁, Mg₃-Fe₁ (LDH-1), Co₃-Al₁, Ni₃-Al₁, Zn₃-Al₁ and Mg₃-Ce₁ (LDH-6) depending on the metals used.

2A.3.2. Synthesis of Ternary LDHs (Mg₃Fe_xCe_{1-x})

A series of ternary Mg₃Fe_xCe_{1-x} LDHs were synthesized by co-precipitation method, where x was varied between 0.95-0.55. The Mg:Fe+Ce molar ratio was kept constant at 3:1; while Fe:Ce molar ratio was varied (0.95:0.05 to 0.55:0.45). In a typical procedure solution A was prepared by dissolving desired amount of Mg(NO₃)₂·6H₂O, Fe(NO₃)₃·9H₂O and Ce(NO₃)₃·6H₂O in deionized water and solution B was prepared by dissolving NaOH (1.2M) and Na₂CO₃ (0.1M) in deionized water. Solutions A and B were added simultaneously while pH of the resultant solution was maintained at 10–11 with constant stirring at room temperature. The formed suspension was continuously stirred for 30 min and aged at 70°C for 12 h. Then the precipitate was filtered, washed several times with deionized water till filtrate became neutral. Finally, the synthesized ternary LDHs were dried at 100°C for 12 h in air. LDHs prepared with different Mg₃Fe_xCe_{1-x} molar ratios, 3:0.95:0.05, 3:0.85:0.15, 3:0.75:0.25 and 3:0.55:0.45 were named as, LDH-2, LDH-3, LDH-4 and LDH-5 respectively.

2A.3.3. Synthesis of Ternary LDHs ($\text{Mg}_3\text{Fe}_{0.85}\text{M}^{3+}_{0.15}$) with other trivalent metals

Other ternary LDHs were prepared by using M^{3+} other than Ce (Where $\text{M}^{3+} = \text{La}, \text{Sm}, \text{Y}$ and Cr). Same procedure was used by preparing “solution A” with appropriate amounts of $\text{Mg}(\text{NO}_3)_2 \cdot 6\text{H}_2\text{O}$, $\text{Fe}(\text{NO}_3)_3 \cdot 9\text{H}_2\text{O}$ and nitrate of M^{3+} metal to be used instead of $\text{Ce}(\text{NO}_3)_3 \cdot 6\text{H}_2\text{O}$. LDHs prepared with different M^{3+} ($\text{M}^{3+} = \text{La}, \text{Sm}, \text{Y}$ and Cr) were named as $\text{Mg}_3\text{Fe}_{0.85}\text{La}_{0.15}$, $\text{Mg}_3\text{Fe}_{0.85}\text{Sm}_{0.15}$, $\text{Mg}_3\text{Fe}_{0.85}\text{Y}_{0.15}$ and $\text{Mg}_3\text{Fe}_{0.85}\text{Cr}_{0.15}$ respectively.

2A.4. Characterization Methods

The catalysts were characterized by a number of physicochemical and spectroscopic techniques including X-Ray powder diffraction (XRD),^{26,27} Fourier transform-infrared spectroscopy (FT-IR),²⁸ N_2 sorption (BET),³¹⁻³³ Basicity calculation by titration,^{29,34-36} CO_2 and NH_3 Temperature programmed desorption (TPD),³⁷ Elemental analysis by inductively coupled plasma-atomic emission spectroscopy (ICP-AES),^{40,41} Transmission electron microscopy (TEM)^{38,39} and X-ray photoelectron spectroscopy (XPS).^{42,43} Each technique is unique by itself and provides important information on the structural and textural features, metal leaching and basicity of the catalyst materials. Details on characterization method of each technique is given below.

2A.4.1. X-Ray powder diffraction (XRD)

XRD patterns of all samples were recorded on a P Analytical PXRD system (Model X-Pert PRO-1712), using Ni filtered $\text{Cu K}\alpha$ radiation ($\lambda = 0.154 \text{ nm}$) as an X-ray source (current

intensity, 30 mA; voltage, 40 kV) and an X-accelerator detector. The samples were scanned in a 2θ range of 10° – 80° .

2A.4.2. Fourier transform-infrared spectroscopy (FT-IR)

FT-IR spectra were recorded on a Shimadzu 8201 spectrophotometer in 400 – 4000 cm^{-1} region. The samples were diluted prior to measurement with KBr in a 2/98 mixture ratio.

2A.4.3. Transmission electron microscopy (TEM)

TEM analysis was performed on a Jeol Model JEM 1200 electron microscope operated at an accelerating voltage of 120 kV. A small amount of specimen was prepared by ultrasonically suspending the powder sample (2mg) in IPA (5ml), and drops of the suspension were deposited on a carbon coated copper grid dried at room temperature before analysis.

2A.4.4. N₂ sorption (BET)

The N₂ adsorption–desorption isotherms at $-196\text{ }^{\circ}\text{C}$ were obtained using a Thermo surfer BET instrument and the surface areas were deduced using the BET equation. Before analysis, the samples were out gassed at $100\text{ }^{\circ}\text{C}$ for 6 h.

2A.4.5. Basic properties of LDHs by Titration method

LDHs will decompose during heating in CO₂ TPD analysis. Hence the weak and strong basic sites of LDH samples were measured by titration method. For this purpose 0.15 g of vacuum dried solid sample was suspended in 2 mL of indicator solution and titration was carried out using 0.01 M benzoic acid solution in toluene. Indicator solution for the determination of

weak basic sites ($pK_a = 7.1$) contained 0.01 g of bromothymol blue in 100 mL toluene. The amount of strong basic sites ($pK_a = 9.3$) were determined in the presence of an indicator solution containing 0.01 g of Phenolphthalein in 100 mL toluene.

Note: Basic sites of LDHs were determined by titration method however basic sites of mixed metal oxides (MMOs, Chapter 2B) were estimated by CO_2 TPD. Details of TPD method are given below.

2A.4.6. CO_2 and NH_3 TPD

Acid-base properties of the materials were estimated by temperature-programmed desorption (TPD) of adsorbed CO_2 and NH_3 using TPDRO 1100 (Thermo Fisher Scientific) instrument and the procedure was as follows. A sample (200 mg) was pre treated for 2 h at $200^\circ C$ in He, cooled to $50^\circ C$, saturated with a gas containing the probe molecule (4.5% CO_2 or 5% NH_3 in He) and flushed afterward with He for 20 min. TPD measurements were performed at a heating rate of $10^\circ C/min$ under He flow ($20 mL min^{-1}$) temperature was ramped to $800^\circ C$ and held at this temperature for 15 min. The total amount of each type of basic and acid sites was determined by integration of the deconvoluted peaks from the TPD curves. Deconvolution of TPD data was carried out by using Origin-6 software.

2A.4.7. XPS

XPS spectra were recorded on a VG Microtech Multilab ESCA3000 spectrometer equipped with non-monochromatised Mg- $K\alpha$ radiations ($h\nu = 1253.6 eV$). All the binding energies were standardized according to carbon ($C 1s = 284.8 eV$) and the peak fitting was carried out using the XPSPEAK-41 software.

2A.4.8. ICP-AES

The composition of metal ions was analyzed by inductively coupled plasma-Atomic emission spectrometry (ICP-AES) (Optima 2000DVICP-AES, Perkin Elmer, USA). Samples were prepared by dissolving 2mg of sample in 5 mL of nitric acid and diluted to 50 mL with distilled water for analysis.

2A.5. Experimental setup

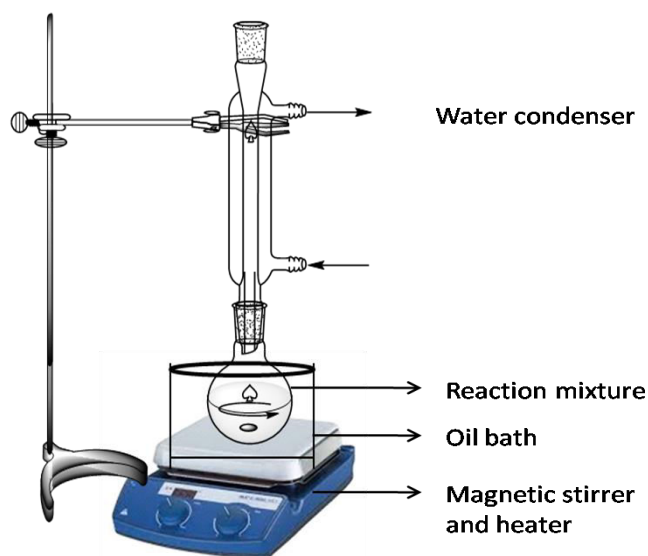


Figure 2A.2: Schematic of experimental setup.

2A.5.1. Experimental procedure for transesterification of EC with methanol

The schematic of experimental setup is presented in Fig. 2A.2. The reactions were carried out in a 50 ml round bottom (RB) flask equipped with a reflux condenser under vigorous stirring. Typically, the RB was charged with 23 mmol of EC, 230 mmol of methanol and 2.5 wt% of catalyst (relative to EC). The reaction was carried out at 70°C oil bath temperature for 1-3h reaction time under vigorous stirring. In some experiments internal temperature of the reaction

mixture were examined by thermocouple and it was observed that temperature of the reaction mixture remains near boiling point of methanol $\sim 63^{\circ}\text{C}$ throughout the reaction. After completion of the reaction, the RB was cooled to room temperature; the solid catalyst was separated from the solution by filtration. Sample was analyzed by gas chromatography to monitor the progress of the reaction.

2A.5.2. Experimental procedure for recycle study

Transesterification of EC and DMC was carried out as per the procedure described earlier (Section 2A.5.1.). The reaction mixture was cooled to room temperature. The catalyst from the reaction mixture was recovered by centrifugation, washed with methanol, and then dried overnight at 100°C for 12 h in air. The recovered catalyst was used to perform a new reaction of transesterification by charging EC and methanol to the glass reactor.

2A.5.3. Analytical methods

The analysis of reaction samples was carried out with the help of gas chromatograph (Agilent 6890N) equipped with FID detector and an innowax capillary column (30 m length \times 0.53 mm ID \times $\sim 1\mu\text{m}$ film thickness). Formation of DMC and EG as products was confirmed by GC-MS analysis with Agilent GC-MS (Agilent 6890N (GC) 5973 (MSD)) equipped with HP-5 capillary column. The standard GC analysis conditions used for the analysis of reactants and products of reaction are given in Table 2A.1.

Table 2A.1: Conditions for gas chromatograph analysis

Inlet	Temperature: 250°C		
	Pressure : 10psi		
Split ratio: 50:1			
Oven	Ramp °C	Temp. °C	Hold time (min)
		40	2
	30	220	9
	Total Run time 15 min		
Flame ionization Detector	Temperature: 250°C		
Hydrogene: 40ml/min			
Zero air: 400ml/min			

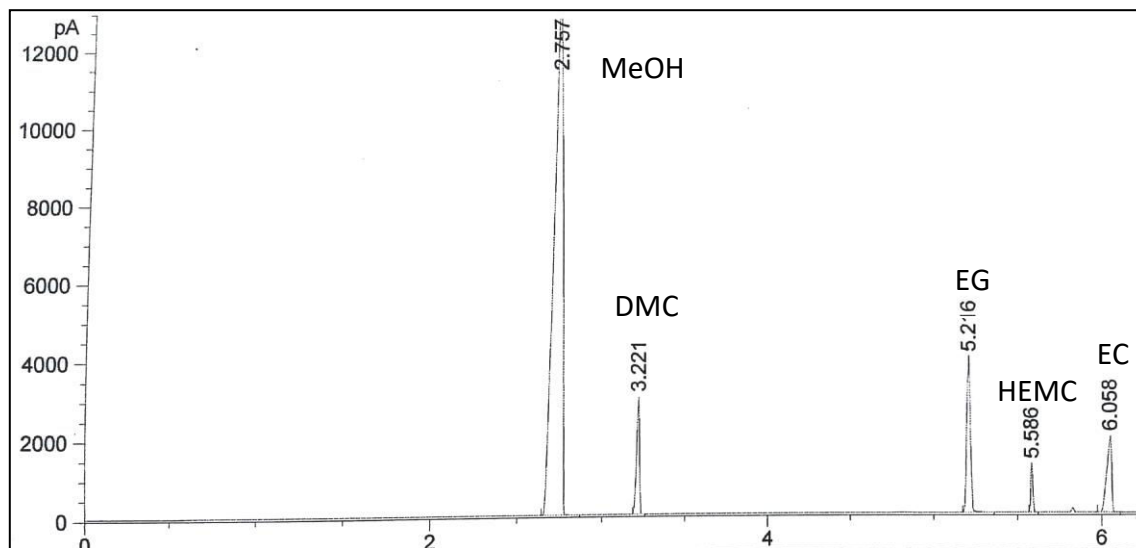


Figure 2A.3: A typical gas chromatograph chart showing reactants (EC and methanol), intermediate (HEMC) and products (DMC and EG). Methanol, DMC, EG, HEMC and EC (Retention times of peaks at 2.75, 3.22, 5.21 and 5.586, 6.05 minute)

Atypical gas chromatogram obtained for transesterification reaction of EC with methanol using the analytical conditions given in Table 2A.1 is presented in Fig. 2A.3. The distinct separation of all the reactants and products was obtained.

2A.5.3.1. Quantitative analysis of reaction mixture: External standard method

Quantitative analysis of the reaction mixture was carried out by using external standard method. In this method known quantities of reactants and products were dissolved in appropriate solvent (methanol or DMC) in 25 ml volumetric flask to make total volume 25 ml. Weight of each component was noted. Four such, samples with different concentration of reactants (EC) and products (DMC and EG) were prepared. The quantities were chosen such that they covered maximum and minimum amount for each component. Analysis of these samples was done on GC and calibration curve was generated and amount/area i.e. response factor was calculated. In this analysis method the reaction sample to be analyzed and standard samples prepared are different and hence this method is called as external standard method. The EC conversion and product selectivity were calculated by using the following equations:

$$\text{EC conversion (\%)} = \frac{\text{Initial moles of the EC} - \text{Final moles of EC}}{\text{Initial moles of the EC}} \times 100 \quad (1)$$

$$\text{DMC selectivity (\%)} = \frac{\text{Moles of the DMC formed}}{\text{Moles of the EC consumed}} \times 100 \quad (2)$$

2A.6. XRD analysis of Binary LDHs

XRD analysis of all the LDHs prepared was carried out to confirm the formation of LDH material (Fig. 2A.4).

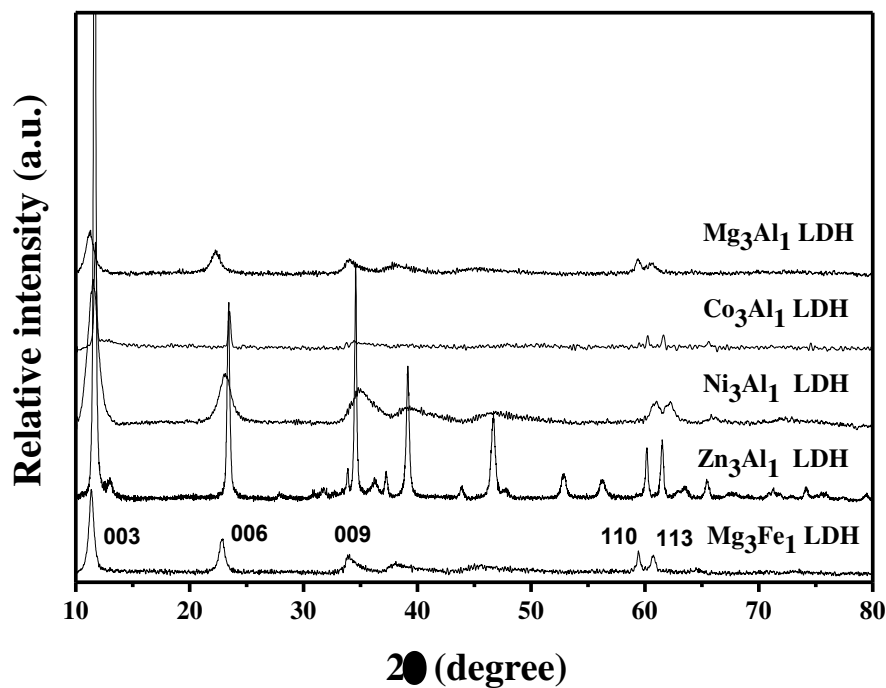
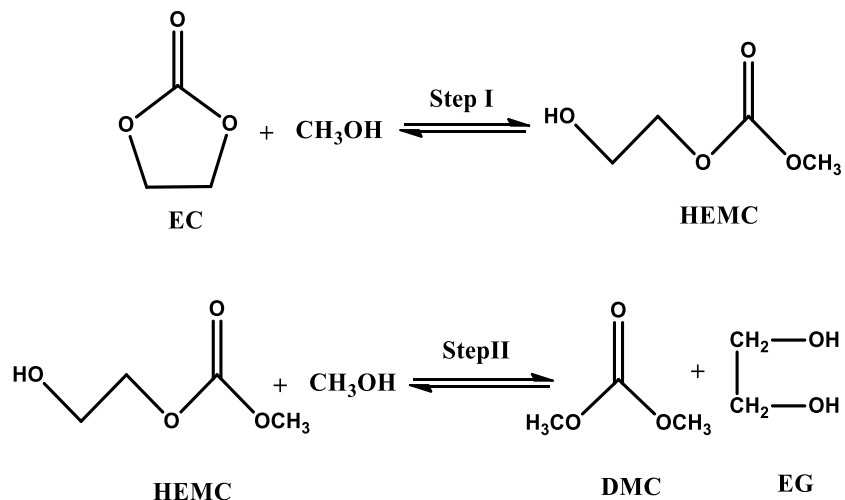


Figure 2A.4: XRD patterns of all synthesized binary LDHs

From Fig.2A.4 it was clearly observed that all LDHs have symmetrical reflections for (003), (006), (110), (113) planes. A sharp peak at (003) plane indicated the formation of a highly crystalline material.^{44, 45} The reflections were indexed to a hexagonal lattice with an R3m rhombohedral symmetry. All diffraction peaks have characteristics of a well crystalline single hydrotalcite-like phase as previously reported (LDH: JCPDS file no. 38-487).⁴⁵

2A.7. Transesterification of EC with methanol to DMC

The catalytic transesterification of ethylene carbonate with methanol involves two equilibrium steps as shown in the Scheme 2A.2.²²



Scheme 2A.2:The transesterification of EC with MeOH

In the first step, reaction of EC and methanol leads to the formation of 2-hydroxy ethyl methyl carbonate (HEMC) as the product. The amount of HEMC formed from EC and MeOH (Scheme 2A.2 step I) is dependent on the type of catalyst employed and reaction conditions used in the process (temperature, EC:MeOH ratio and catalyst loading). The formation of HEMC as an intermediate was confirmed by GC-MS analysis. The reaction of HEMC with another molecule of methanol leads to the formation of DMC and EG as products (Scheme 2A.2 step II). Both the reactions are equilibrium and hence the selectivity pattern will be strongly dependent on the reaction conditions employed.

2A.7.1 Screening of LDHs for transesterification of EC with methanol

All the LDHs prepared were screened for transesterification of EC and methanol and the results are presented below (Table 2A.2).

Table 2A.2: Screening of binary LDHs for transesterification of EC and methanol to DMC.

Entry	Catalyst	Conversion	Selectivity	
		EC (%)	DMC (%)	
1	Mg _{2.5} -Al ₁	54	87	Reported
2	Mg ₅ -Al ₁	82.9	98.6	Reported
3	Mg ₃ -Al ₁	59	93	This work
4	Mg ₃ -Fe ₁ (LDH-1)	62	93	This work
5	Zn ₃ -Al ₁	26	92	This work
6	Co ₃ -Al ₁	12	90	This work
7	Ni ₃ -Al ₁	9	91	This work

Reaction conditions: EC: 23mmol, MeOH: 230mmol, M²⁺/ M³⁺ LDHs catalyst: 2.5 wt% relative to EC, reaction time: 3 h, temperature: 70 °C.

From the results presented in Table 2A.2 it was clearly observed that the Mg₃-Fe₁ (62% EC conversion and 93% DMC selectivity) and Mg-Al LDHs (59% EC conversion and 93% DMC selectivity) gave good catalytic activity as compared to other binary LDHs screened (Table 2A.2, Entry 5-7). This may be due to the basic property of M²⁺ cation where Mg²⁺ is an alkali earth metal have high basicity as compared to other transition metal cations (Zn, Co and Ni). Activity decreased in order Mg₃-Fe₁ > Mg₃-Al₁ > Zn₃-Al₁ > Co₃-Al₁ > Ni₃-Al₁ with EC conversion in a range of 9-59%. Significant amount of work was done by Bajaj and Watanabe et al.^{22a} using Mg-Al LDH as catalyst for same reaction system (Table 2A.2, Entry 1-2). Results obtained with

Mg_3Fe_1 are comparable to those reported for $\text{Mg}_{2.5}\text{Al}_1$ by Bajaj et al.²² and hence Mg_3Fe_1 LDH was selected for further study.

2A.7.2. Transesterification of EC with methanol using $\text{Mg}_3\text{Fe}_x\text{Ce}_{1-x}$ LDHs

The activity of Mg_3Fe_1 was good, however, EC conversion of 62% was observed at 70°C in 3 h reaction time. In order to improve activity of the catalyst, the effect of third metal cation on activity of Mg_3Fe_1 LDH was studied. Ceria (1.01 Å) has lower electronegativity compared to Fe (0.65 Å) and incorporation of Ce in the Mg-Fe LDH could result in increase in the basicity of $\text{Mg}_3\text{Fe}_x\text{Ce}_{1-x}$ LDHs and better activity towards DMC synthesis. With this idea in mind a series of $\text{Mg}_3\text{Fe}_x\text{Ce}_{1-x}$ LDHs were synthesized by varying molar ratio of Fe:Ce (keeping Mg:Fe+Ce mole ratio of 3:1 constant). Synthesized Ce promoted $\text{Mg}_3\text{Fe}_x\text{Ce}_{1-x}$ LDHs were investigated for the transesterification reaction and the results are presented in Fig. 2A.5. From the results, activity trend was in the order of LDH-1 < LDH-2 < LDH-3 > LDH-4 > LDH-5 > LDH-6. Catalyst activity increased with increase in Ce concentration up to a level (0 < 0.05 < 0.15) and decreased with further increase in Ce concentration (0.25 > 0.55 > 1). Among all synthesized catalysts LDH-3 showed highest EC conversion (87%) and DMC selectivity (100%). Results were found to be optimum and marginally better as compared to MgAl LDH catalyst reported in the literature (Table 2A.2, Entries 1-2). It should be noted that both binary systems LDH-1 ($\text{Mg}_3\text{:Fe}_1$) and LDH-6 ($\text{Mg}_3\text{:Ce}_1$) were found to be less active (EC conversion 62 and 26% with DMC selectivity 93 and 48% respectively) as compared to LDH-3. Lower selectivity was observed due to the formation of intermediate (HEMC, Scheme 2A.2), which was confirmed with GC-MS analysis. Thus the activity observed was strongly dependent on the Ce concentration in the synthesized LDHs. In order to get more insight on the performance of various LDHs prepared,

all $Mg_3Fe_xCe_{1-x}$ LDHs prepared were characterized in detail and the results obtained are discussed below.

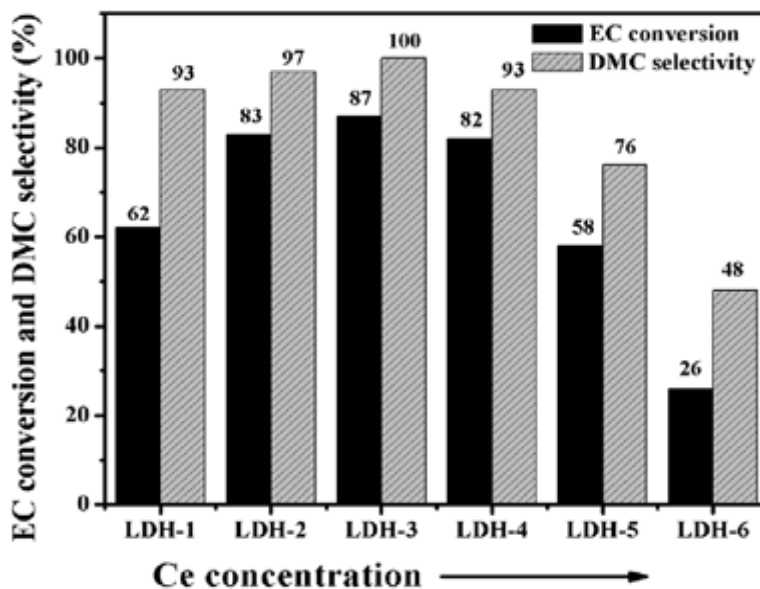


Figure 2A.5: Effect of Ce concentration in $Mg_3Fe_xCe_{1-x}$ LDHs towards the transesterification reaction.

Reaction conditions: EC: 23mmol, MeOH: 230mmol, EC: MeOH molar ratio: 1:10, $Mg_3Fe_xCe_{1-x}$ LDHs catalyst: 2.5 wt% relative to EC, reaction time: 3 h, temperature: 70°C

2A.8. Result and discussion

2A.8.1. Characterization of LDHs prepared

2A.8.1.1. ICP analysis: Composition of LDHs

Elemental chemical compositions of $Mg_3Fe_xCe_{1-x}$ LDHs were determined with the help of ICP-AES method (Table 2A.3). Metal composition in all “neat” LDH samples obtained by ICP - analysis (measured), was found to be in good agreement with the estimated values (theoretical).

Table 2A.3.Composition of Ce incorporated LDHs prepared based on ICP analysis.

Sample	ICP analysis	
	Theoretical	Measured
LDH-1	Mg ₃ Fe ₁	2.98:1
LDH-2	Mg ₃ Fe _{0.95} Ce _{0.05}	3:0.92:0.04
LDH-3	Mg ₃ Fe _{0.85} Ce _{0.15}	2.97:0.83:0.13
LDH-4	Mg ₃ Fe _{0.75} Ce _{0.25}	2.9:0.73:0.23
LDH-5	Mg ₃ Fe _{0.55} Ce _{0.45}	3:0.53:0.44
LDH-6	Mg ₃ Ce ₁	3:0.97

2A.8.1.2. Powder X-ray Diffraction analysis of LDHs

The XRD patterns of all synthesized Mg₃Fe_xCe_{1-x} LDHs with different Fe:Ce molar ratios (mole ratio of Mg:Fe+Ce = 3:1) are shown in Fig. 2A.6. LDH-1 to LDH-3 showed typical features of highly crystalline LDH materials with R3m rhombohedral space group symmetry.^{46, 47} No other phase was detected in these samples indicating that cerium species are successfully incorporated into LDHs. Nevertheless, with increase in Ce concentration for LDH-4 to LDH-6; decrease in crystallinity (better ordering of brucite sheets) which is directly proportional to the peak intensity and sharpness of (003) and (006) planes; was observed.

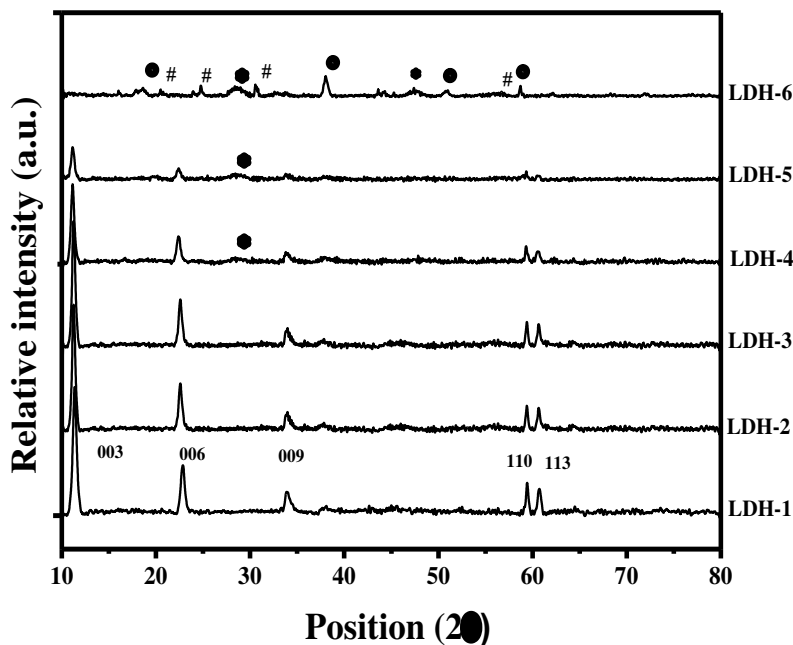


Figure 2A.6: XRD patterns of all synthesized $Mg_3Fe_xCe_{1-x}$ LDHs (LDH-1 to LDH-6).

Where # : $Ce_2(CO_3)_2(OH)_2 \cdot H_2O$, O: $Mg(OH)_2$, *: $Ce(OH)_4$

Table 2A.4: Surface properties of the prepared LDHs

Sample	Lattice parameters (\AA^0)				Surface area (m^2/g)	Pore volume (cm^3/g)	Pore diameter (nm)	Basic sites ($\times 10^{-4}$ mole/g)	
	d(003)	d(110)	a	c				Weak basic sites	Strong basic sites
LDH-1	7.78	1.566	3.112	23.34	67	0.51	16.8	1.8	1
LDH-2	7.85	1.564	3.128	23.55	128	0.8	23	2.4	1.2
LDH-3	7.88	1.572	3.144	23.64	136	0.81	24.3	2.8	1.3
LDH-4	7.92	1.576	3.152	23.76	134	0.78	22.7	3.0	1.0
LDH-5	7.93	1.577	3.154	23.79	133	0.76	21.6	3.5	0.8
LDH-6	nd	nd	nd	nd	129	0.73	20.2	4.5	0.5

nd = not detected

$a=2d_{110}$

$c=3d_{003}$

This is due to the substitution of Fe (0.65 Å) by larger ionic radii of Ce (1.01 Å), which inhibits the intercalation of Ce in LDH structure and also leads to significant distortion in the layers.^{48,49}

At higher Ce concentration (LDH-6, Fe:Ce = 0:1) the layered structure collapsed completely and formation of phases like Mg(OH)₂ (PCPDF-86-0441), Ce(OH)₄ and Ce₂(CO₃)₂·(OH)₂·H₂O (PCPDF-46-0369) was observed.^{50,51} The lower electro negativities of rare earth elements (REEs), could favor formation of these species at the initial stage of precipitation.⁵² The lattice parameters 'a' and 'c' were calculated from XRD analysis (formulae given at the end of Table 2A.4) and are summarized in Table 2A.4.

Parameter 'a' ($a = 2d_{110}$) depends mainly on the average radius of the metal cation. Increase in Parameter 'a' observed may be due to the isomorphous substitution of Fe by Ce having larger ionic radius.⁵³ Thus more Ce insertion leads to an increase in average radius of cations in the layers and this leads to increase in 'a' parameter.

Parameter 'c' ($c = 3d_{003}$) depends on the thickness of octahedral sheets, the anion size and their orientation within the interlayer space and the electrostatic attraction between different layers.⁵⁴ Lower polarizing ability of the Ce results in weak electrostatic interaction between the layers and interlayer anions and leads to increase in the layer spacing resulting in increase of the 'c' parameter value. Thus increase in values of parameters 'a' and 'c' with increase in Ce concentration (Table 2A.4, LDH-1 << LDH-5) may be attributed to larger ionic radii and lower polarizing ability of Ce.^{53, 54}

2A.8.1.3. FT-IR analysis of LDHs

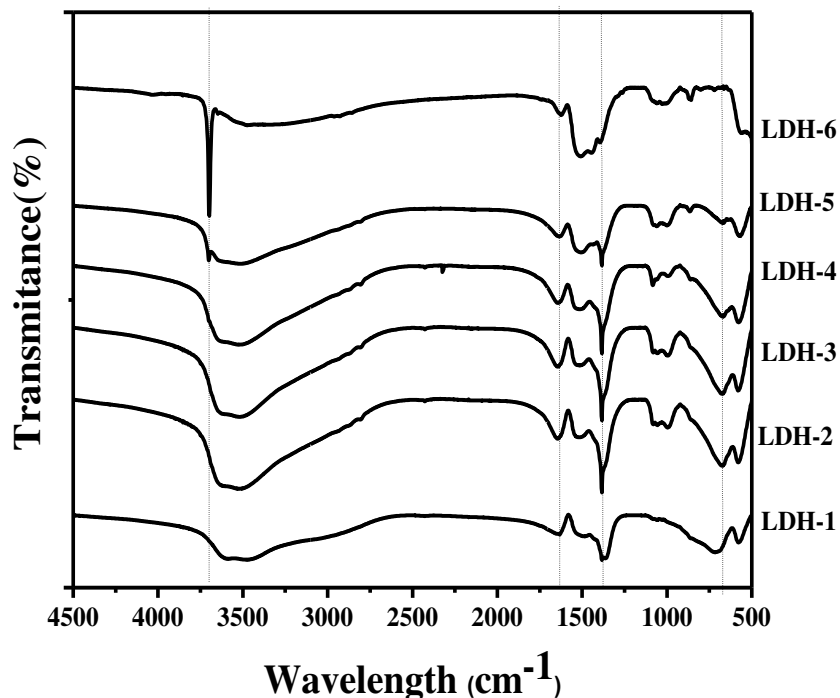


Figure 2A.7: FT-IR spectra of synthesized $\text{Mg}_3\text{Fe}_x\text{Ce}_{1-x}$ LDHs.

The FT-IR spectral information can be used to determine the actual bonding type in the expected compounds and to confirm the substitution of Ce in the brucite layer. FT-IR spectra of all LDH samples (Fig. 2A.7) showed broad band centered around 3500 cm^{-1} due to the stretching mode of hydroxyl groups present in the brucite-like layers and from the interlayer water molecules of the hydroxide structure. The band at 3681 cm^{-1} was observed in LDH-4 << LDH-6; which is characteristic of non-hydrogen bound -OH group.⁵⁵ A weaker band at 1630 cm^{-1} is owing to the bending mode of water molecules. IR absorption bands at 1510 cm^{-1} , 1382 cm^{-1} (ν_3), 852 cm^{-1} (ν_2), and 1056 cm^{-1} (ν_1) are attributed to the carbonate anion environment.^{21,56,57} The bands recorded in the low-frequency region of the spectrum ($<700\text{ cm}^{-1}$) are assigned to the translational mode of M-O-H and M-OH-M vibrations. Significant difference in these bands was observed with

an increase in Ce concentration of synthesized LDHs. The FT-IR spectra of the LDH-1 to LDH-3 showed the typical bands of the hydrotalcite-like compounds.⁵⁶ In case of LDH-4 to LDH-6 a new band was observed at 3681 cm^{-1} , which corresponds to non bonded $-\text{OH}$ group vibrations for $\text{M}(\text{OH})_x$.

2A.8.1.4. Transmission Electron Microscopy (TEM) analysis of LHDs

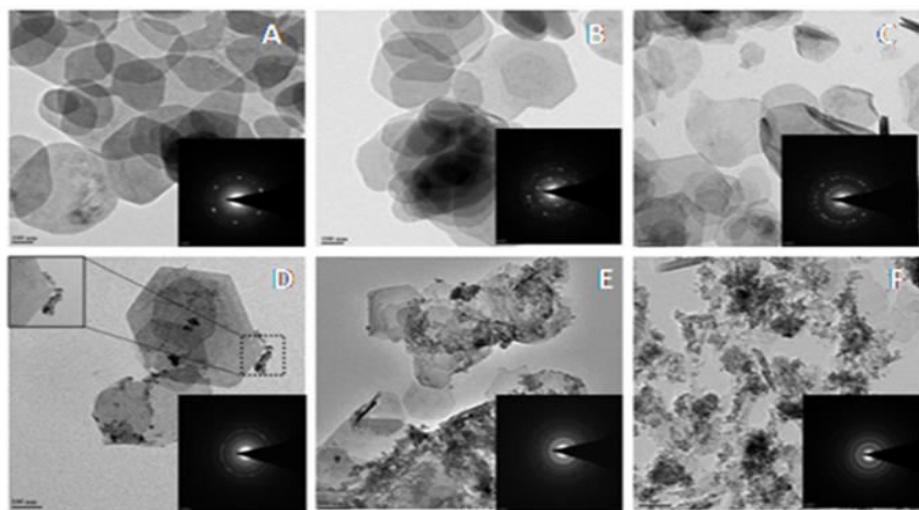


Figure 2A.8: TEM images and SAED patterns of synthesized $\text{Mg}_3\text{Fe}_x\text{Ce}_{1-x}$ LDHs (A) LDH-1, (B) LDH-2, (C) LDH-3, (D) LDH-4, (E) LDH-5 and (F) LDH-6

The influence of Ce concentration on the crystal shape and size was clearly observed from the morphology of all synthesized materials (Fig.2A.8). The TEM images (Fig.2A.8A–C) showed that the LDHs (LDH-1 to LDH-3) are composed of crystallites with the typical plate like morphology and often hexagonal shaped.^{21,53} However, in LDH-4 and LDH-5 (Fig.2A.8D, E) particles of irregular shape with agglomerated small particles [mostly of $\text{Ce}(\text{OH})_4$] on the surface and edges of crystallites were observed. In case of LDH-6 (Fig. 2A.8F) the layered structure was absent with significant increase in agglomerated particles. The crystalline nature of the

individual materials (LDH-1 to LDH-6) was further checked by selected area electron diffraction (SAED) patterns shown in the Fig.2A.8 (A–F). LDH-1 to LDH-3 samples showed good crystalline nature which decreased with increase in Ce concentration (LDH-4 to LDH-6).⁵⁸

2A.8.1.5. Surface Area Measurements of LDHs

BET surface areas and textural properties of catalysts were determined by nitrogen adsorption–desorption isotherms and the values obtained are summarized in Table 2A.4. The BET surface area, pore volume and pore size increased with increase in Ce concentration from LDH-1 to LDH-3. LDH-3 showed nearly two times more surface area ($136 \text{ m}^2/\text{g}$) than parent LDH-1 ($67 \text{ m}^2/\text{g}$). With further increase in Ce content from LDH-4 to LDH-6; slight decrease in surface area and pore volume was observed. This may be due to (1) distortion in layer structure because of incorporation of excess amount of Ce, (2) deposition of the agglomerated particles formed during precipitation conditions or their incorporation into the pore system of LDH.⁵⁹

2A.8.1.6. Basicity Measurement of LDHs

The nature of the active species present on the surface is important for establishing the properties of the catalyst. Consequently, basic properties of the catalysts were determined by benzoic acid titration of the basic sites in the presence of pH indicators based on the literature report^{35,36} and the results are presented in Table 2A.4. The strong basic sites correspond to –OH sites present in brucite like structure and weak basic sites correspond to carbonate species and simple metal bonded –OH group $[\text{M}(\text{OH})_x]$ present in synthesized materials.⁶⁰ From the Table 2A.4 it can be clearly observed that the weak basic sites increased consistently with increase in Ce concentration LDH-1 to LDH-6. However strong basic sites increased with

increase in Ce concentration from LDH-1 to LDH-3 and decreased with further increase in Ce concentration for LDH-4 to LDH-6. Parent LDH-1 has less number of strong and weak basic sites than Ce incorporated LDHs (LDH-2 and LDH-3). The increase in basic properties and also the increase in surface area for Ce incorporated LDHs (LDH-2 and LDH-3) can be correlated to exchange of Fe with Ce having lower electronegativity.⁶¹

2A.8.1.7. XPS analysis of LDHs

The XPS analysis of all catalysts was carried out to understand the surface species present and their oxidation state. XPS analysis confirmed the presence of Mg, Fe, Ce and O in the catalysts as expected. However, the nature of peaks for Ce and O changed with change in Ce content of the catalyst (LDH-2 to LDH-5). In order to understand the effect of Ce concentration on surface active sites ($-OH$); detailed analysis of Ce 3d and O1s was carried out for LDHs synthesized. XPS spectrum indicated presence of Ce^{3+} and Ce^{4+} (Fig. 2A.9) in all the samples and also O1s showed two different peaks for all these samples. In order to gain more insight; deconvolution of Ce3d and O1s peaks was carried out with the help of XPSPEAK-41 software. Since the data is exhaustive representative analysis for Ce3d is presented in Fig. 2A.10 and data for O1s is presented in Fig. 2A.11. Fig. 2A.9 shows the XPS spectra of Ce 3d for the synthesized LDHs (LDH-2 to LDH-5) and the peaks corresponding to Ce^{3+} and Ce^{4+} are marked with dotted line. XPS spectra of the Ce 3d core level can be resolved into 10 groups; the five main 3d_{5/2} peaks are denoted as v_o (881.7 eV), v (882.9 eV), v' (885.7 eV), v'' (889.0 eV), and v''' (897.6 eV), and the five peaks corresponding to 3d_{3/2} are assigned as u_o (899.1 eV), u (901.2 eV), u' (903.0 eV), u'' (907.7 eV), and u''' (916.8 eV), respectively.⁶² Relative percentage of cerium species was

calculated from the area ratio of $Ce^{3+}/(Ce^{4+} + Ce^{3+}) \times 100$, and $Ce^{4+}/(Ce^{4+} + Ce^{3+}) \times 100$ where $Ce^{3+} = v_0 + v' + u_0 + u'$ and $Ce^{4+} = v + v'' + v''' + u + u'' + u'''$ and the results are presented in Table 2A.5.

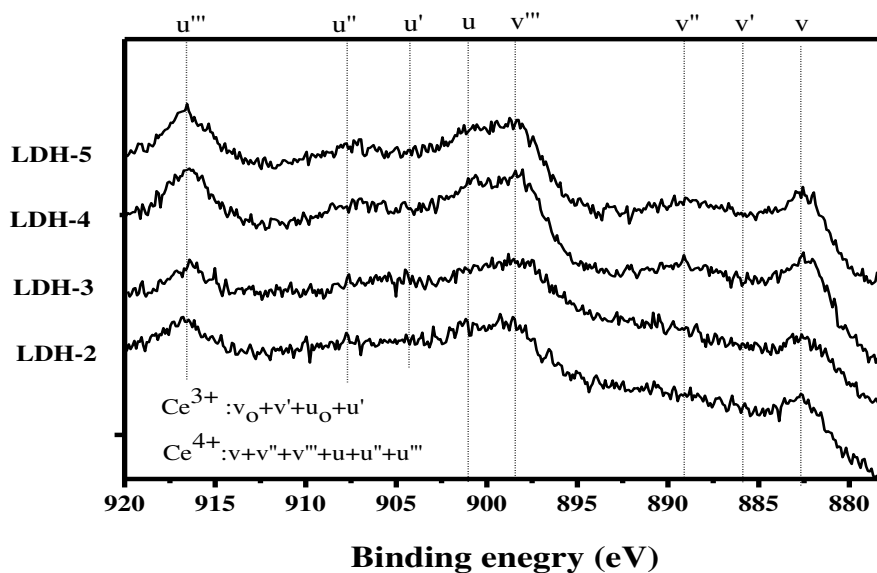


Figure 2A.9: Ce 3d XPS spectra of synthesized $Mg_3Fe_xCe_{1-x}LDHs$ (Ce^{3+} and Ce^{4+} contributions are highlighted with dotted line).

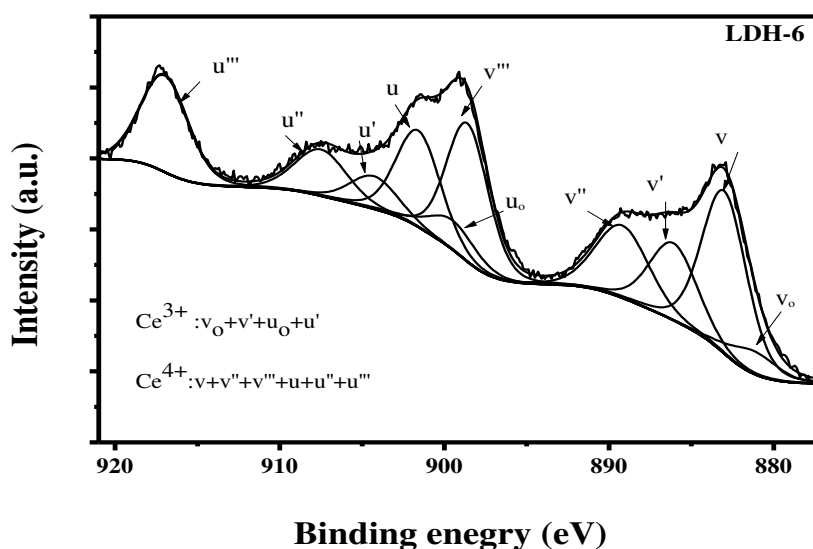


Figure 2A.10: Representative example of the deconvolution for the Ce 3d peak of LDH-6.

The peaks attributed to O 1s are observed at 530.6 and 532.3 eV (Fig.2A.11). The first one, with a very low intensity is characteristic of O^{2-} (attributed to carbonate species) designated as “ O_{β} ”, whereas the high intensity second peak corresponds to the oxygen species in hydroxide form ($-OH$) designated as “ O_{α} ” (Fig. 2A.11).⁶³ The quantitative analysis of the Ce 3d and O1s XPS peaks for the samples is summarized in Table 2A.5 and includes percentage concentrations of the Ce^{4+} , Ce^{3+} , O_{α} and O_{β} species present on the material surface.

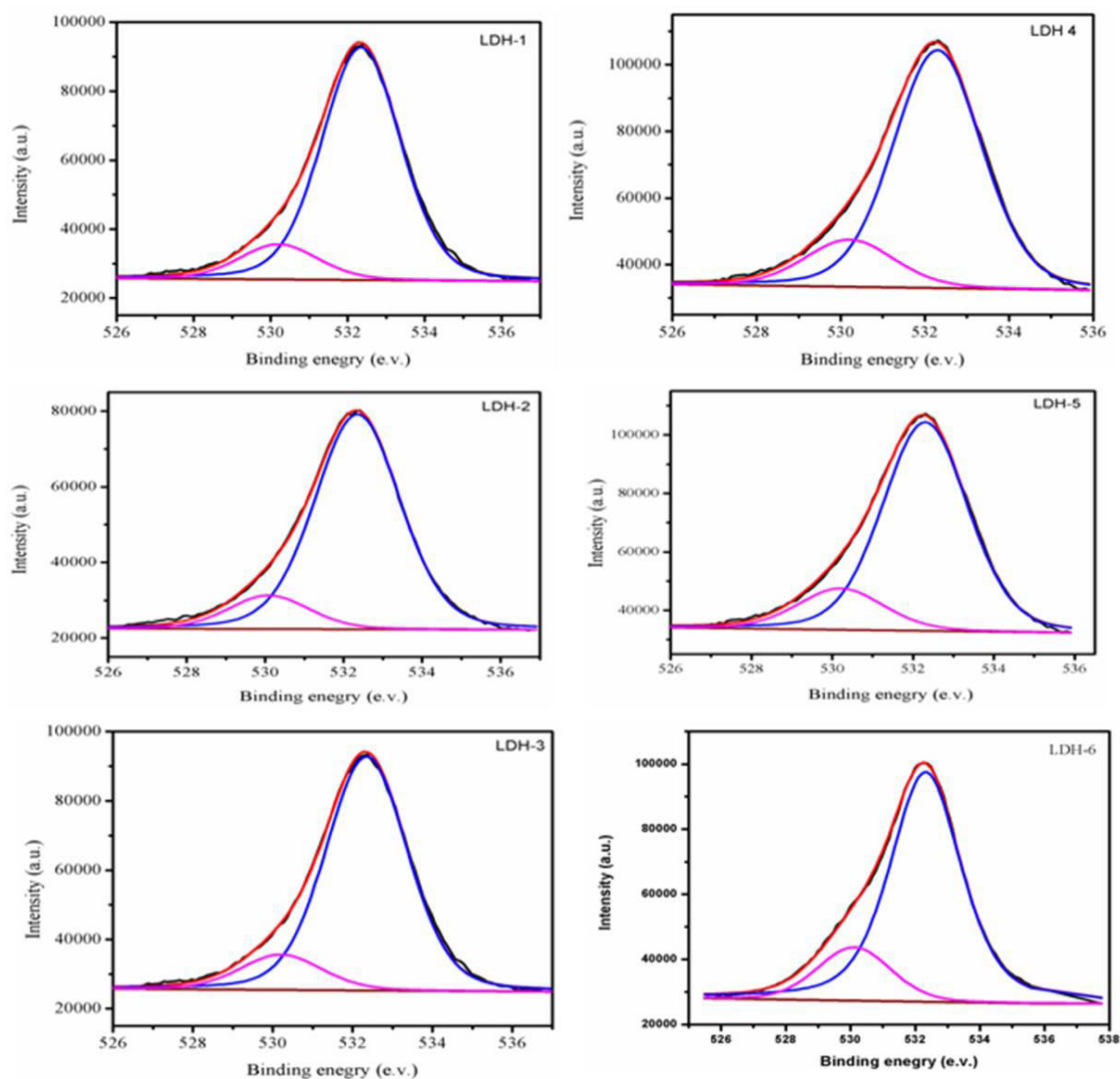


Figure 2A.11: XPS O1s spectra of all synthesized $Mg_3Fe_xCe_{1-x}$ LDHs, peaks correspond to oxygen bonded carbon species (O_{β}) is 530.6 eV and oxygen in hydroxide form is 532.3 eV (O_{α}).

Table 2A.5. Surface composition and relative atomic ratio for the synthesized LDHs determined from XPS measurements

Sample	%				Ce ³⁺ : Ce ⁴⁺	O _α : O _β
	Ce ³⁺	Ce ⁴⁺	O _α	O _β		
LDH-1	nd	nd	78.3	21.6	nd	3.6
LDH-2	49.5	50.4	86.9	13	0.98	6.6
LDH-3	47.2	52.7	87.2	12.7	0.9	6.8
LDH-4	39.7	60.2	85.2	14.3	0.7	5.9
LDH-5	33.2	66.7	84.7	15.3	0.5	5.5
LDH-6	30.9	69.1	81.6	18.4	0.4	4.4

nd : not detected

From the Table 2A.5 it was clearly observed that the gradual increase in Ce⁴⁺ concentration has taken place from LDH-4 to LDH-6 (60.2–69.1%) with increase in Ce concentration. This indicates that increase in Ce concentration has led to increase in Ce⁴⁺ present on the surface in the form of Ce(OH)₄. The amount of Ce in LDH structure also affects the concentration of surface O_α and O_β (Table 2A.5). Parent compound (LDH-1) has surface O_α concentration of 78.3% and increased with Ce loading for materials having LDH structure intact (86.9% for LDH-2 and 87.2% for LDH-3). Further increase in ceria concentration (LDH-4 to LDH-6) led to marginal drop in the concentration of surface O_α (85.2–81.6%) with rise in O_β (14.3–18.4%). Probably with increase in Ce concentration (LDH-4 to LDH-6) the distortion in the layer structure occurred; which led to marginal decrease in surface O_α group and relatively O_β species

are exposed to the sample surface. This also supports the formation of $\text{Ce}(\text{OH})_4$ with increase in ceria loading (LDH-4 – LDH-6)

The detailed characterization results demonstrate that the structural, textural and chemical properties of the LDHs can be fine-tuned by doping with appropriate amount of another trivalent metal such as Ce. XRD, FT-IR and TEM analysis (Fig.2A.6-2A.8) clearly showed that LDH-1 to LDH-3 formed well defined LDH structure with high crystallinity (better ordering of brucite sheets). No other phase was detected, implying that Ce was well incorporated in the prepared LDHs. Among which LDH-3 showed high surface area and pore volume with high amount of strong basic sites present on LDH surface (Table 2A.4). Further with increase in Ce concentration (LDH-4 to LDH-6) distortion in layered structure was observed from XRD, TEM and XPS analysis. This may be due to the isomorphic substitution of Fe by Ce having larger ionic radii. In case of LDH-4 and LDH-5 precipitation of $\text{Ce}(\text{OH})_4$ on surface was clearly observed and confirmed by XRD, TEM and FT-IR analysis. LDH structure was totally absent for LDH-6 (Fe:Ce = 0:1) and mixed hydroxide, carbonate phases were observed. These observations are found to be consistent with surface area, pore volume and strong basic site densities (hydroxyl groups present in the brucite-like structure) of LDHs, which marginally decreased from LDH-4 to LDH-6. Distortion in LDH structure resulted in the decrease in surface area, pore volume and structure bonded –OH groups (strong basic sites). According to literature reports, the structure bonded –OH group are strong basic in nature than simple metal bonded –OH groups ($\text{Mg}(\text{OH})_2$ or $\text{Ce}(\text{OH})_4$).^{60,61} The decrease in the intensity of FT-IR band at 3500 cm^{-1} (–OH) for LDH-4 to LDH-6 (Fig.2A.7); also supports this observation. Characterization of the catalysts indicated that layered structure was intact till LDH-3 and LDH-3 was found to be material with higher surface area, pore volume and higher amount of strong basic sites.

The observed activity trend (Fig. 2A.5) was found to be in good agreement with physicochemical properties of synthesized LDHs. Thus, EC conversion was lower with LDH-1 (62%) and increased with Ce concentration [LDH-2 (83%)<LDH-3(87%)]. Best results were obtained with LDH-3 ($\text{Mg}_3\text{Fe}_{0.85}\text{Ce}_{0.15}$) having highest amount of strong base sites ($1.3 \times 10^{-4} \text{ mol/g}$) present on LDH surface with high surface area ($136 \text{ m}^2/\text{g}$) and pore volume ($0.81 \text{ cm}^3/\text{g}$) as compared to other LDHs. With further increase in Ce concentration (LDH-4–LDH-6) strong basic sites, surface area and pore volume decreased (Table 2A.4) and could be attributed to the formation and deposition of $\text{Ce}(\text{OH})_4$ phase and distorted nature of layered structure of LDHs; which reduced the catalyst activity. This is in accordance with the results obtained by Kannan et al.⁶⁴ for hydroxylation of phenol using CoNiAl ternary LDH as catalyst. They concluded that strong basic sites (hydroxyl groups) play an important role in catalytic activity and the appropriate geometry and concentration of both the metal cations in a well ordered two dimensional lattice could be responsible for the activity observed. The most active catalyst (LDH-3) was taken for further study. The effect of reaction conditions on the activity and selectivity was studied in detail.

2A.9. Effect of Reaction conditions

The effect of EC: MeOH molar ratio, reaction temperature and catalyst loading was investigated in detail for transesterification of EC and methanol using LDH-3 as the catalyst. All the experiments in this study were carried out with sampling in a time range of 1-5 h. Conversion/selectivity Vs time profiles were obtained under various reaction conditions and the results are presented below.

2A.9.1. Effect of EC:MeOH molar ratio

The effect of EC/CH₃OH molar ratio (1:5 to 1:20) on the transesterification reaction was investigated using LDH-3 catalyst and the results are presented in Fig. 2A.12.

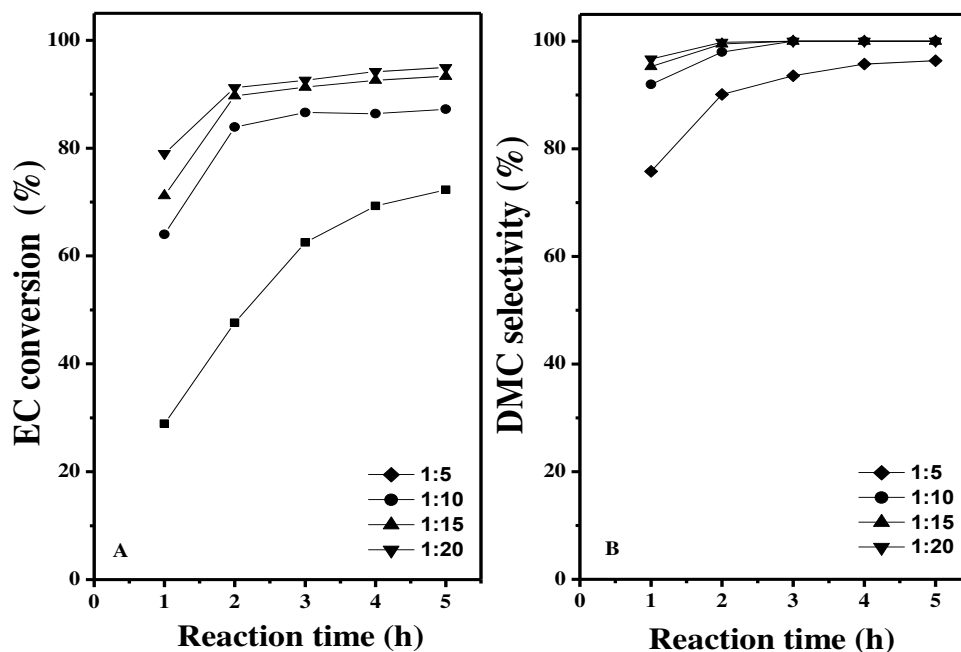


Figure 2A.12: Effect of molar ratio on EC conversion (A) and DMC selectivity (B)

Reaction conditions: EC: 23 mmol, EC: MeOH: 1:5-1:20, Catalyst (LDH-3): 2.5 wt % relative to EC, Reaction time: 1-5 h, Temperature: 70°C.

From Fig. 2A.12 it was clearly observed that the EC/CH₃OH molar ratio had a significant impact on the transesterification reaction. Transesterification of EC and methanol ($\text{EC} + \text{MeOH} \rightleftharpoons \text{DMC} + \text{EG}$) is an equilibrium controlled reaction and hence excess methanol is required to shift the equilibrium towards right and achieve high selectivity to DMC as the product. Activity was low at a EC: methanol molar ratio of 1:5 and only 28.9% conversion of EC was observed in 1 h. Conversion increased gradually and reached to 72% in 5 h. Selectivity to DMC was very high

(>90%) except at 1 h reaction time. In this case additional peak was observed in GC. GC-MS analysis indicated this peak to be intermediate product HEMC (2-hydroxy ethyl methyl carbonate) formed by the reaction of one molecule of methanol with EC (Scheme 2A.2 step I). As the reaction progressed this intermediate was converted to DMC by reaction with another molecule of methanol. EC conversion increased significantly with increase in EC: methanol ratio up to EC: methanol ratio of 1:10 and was not significantly affected with further increase in the ratio. Selectivity to DMC was very high at higher EC: methanol molar ratio. This is expected, since at high methanol concentration equilibrium is shifted towards right resulting in very high conversion of EC and high selectivity to DMC. From Fig.2A.12 it was observed that EC conversion increased with increase in reaction time till 3 h and was not significantly affected with further increase in reaction time. Best results (94.9% conversion of EC with 100% selectivity to DMC) were obtained at EC: methanol molar ratio of 1:20. Results clearly indicate influence of EC: methanol molar ratio on EC conversion and DMC selectivity.

2A.9.2. Effect of reaction temperature

The effect of reaction temperature on the activity and selectivity was investigated in a temperature range of 30-70°C and the results are presented in Fig. 2A.13. From Fig 2A.13 it was observed that EC conversion as well as selectivity to DMC increased significantly with increase in the temperature. Thus at 30°C EC conversion of 18% with 43% selectivity to DMC was observed. EC conversion and DMC selectivity increased with increase in temperature and 51% conversion of EC with 66% selectivity to DMC was observed at 50°C. Low selectivity to DMC was because of the formation of HEMC as major product (Scheme 2A.2 step I).

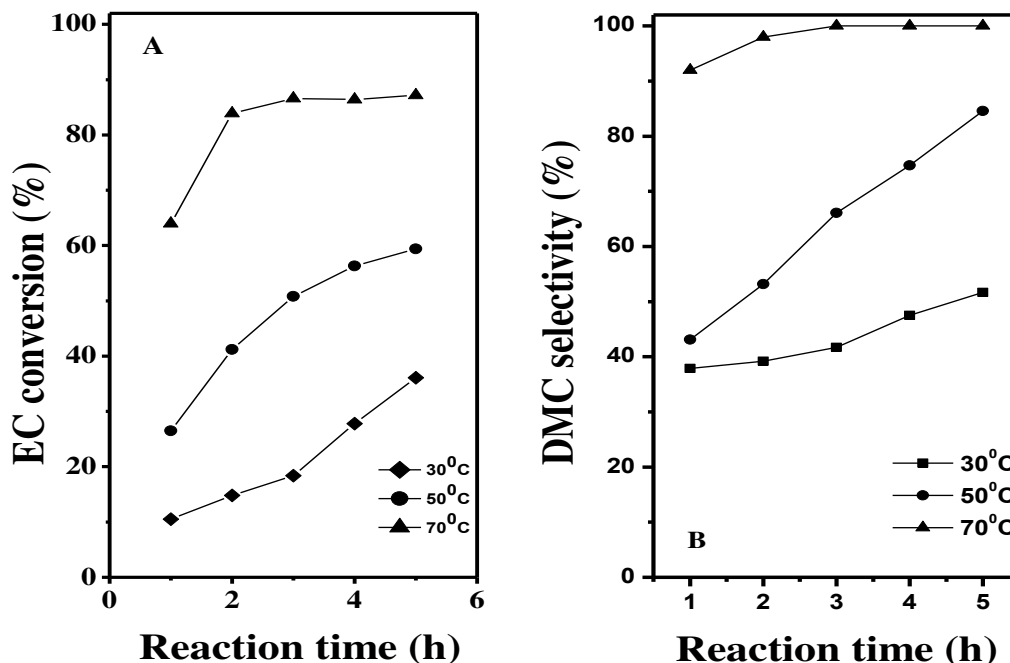


Figure 2A.13: Effect of reaction temperature on EC conversion (A) and DMC selectivity (B)

Reaction conditions: EC: 23 mmol, MeOH: 230 mmol, Catalyst (LDH-3): 2.5 wt % relative to EC, Reaction time: 1-5 h, Temperature: 30-70°C.

Results indicate that higher temperature as well as higher EC: methanol mole ratio is necessary for the conversion of intermediate HEMC to DMC. Wang et al.¹⁰ also have observed similar results in the transesterification of EC and methanol using carboxylic functionalized imidazolium salt as the catalyst. Good results (87% EC conversion and 100% DMC selectivity) were obtained at 70°C and hence further work was carried out at this temperature.

2A.9.3. Effect of catalyst loading

The effect of catalyst loading was investigated in a range of 0.6 to 5 wt.% with respect to EC and the results are presented in Figure 2A.14. Activity was low at a catalyst loading of 0.6 wt% and 72% conversion of EC with 93% selectivity to DMC was observed. Activity and

selectivity to DMC increased with catalyst loading and 87% conversion of EC with 100% selectivity to DMC was observed at a catalyst loading of 2.5 wt%. The improved performance observed with increase in catalyst loading can be attributed to increase in basic sites available for the reaction. Further increase in catalyst loading (2.5–5 wt%) had marginal effect on EC conversion (87–89%) showing high selectivity to DMC (100%). Catalyst loading of 2.5 wt% was taken as optimum for this reaction and used for further study.

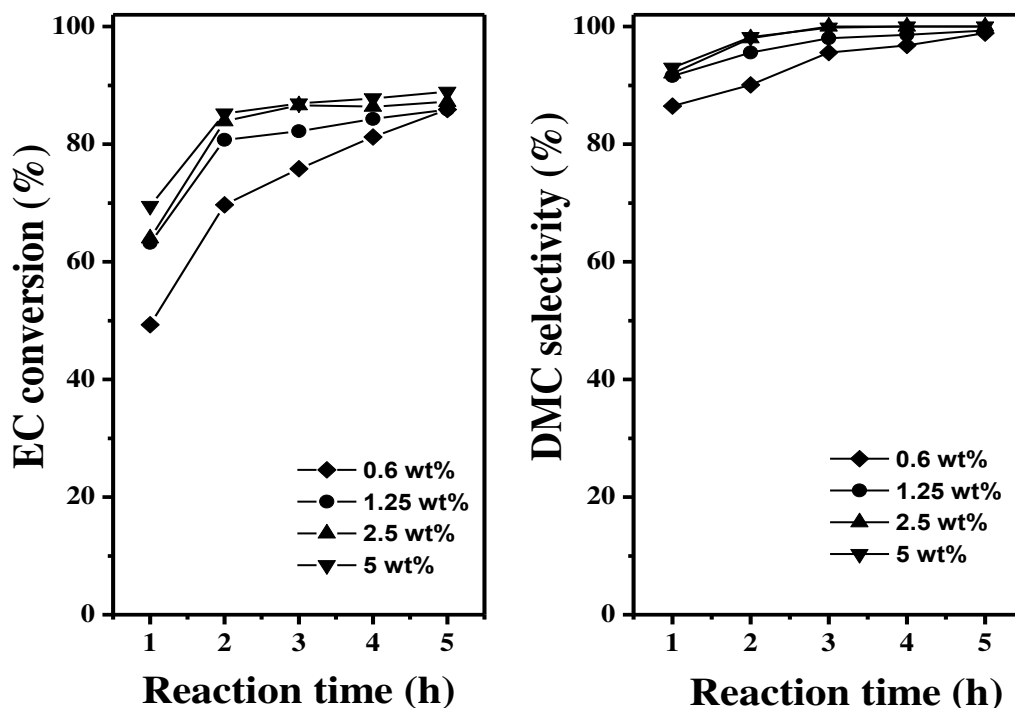


Figure 2A.14: EC conversion and DMC selectivity profile at catalyst loading of 0.6-5 wt%.

Reaction conditions: EC: 23 mmol, MeOH: 230 mmol, Catalyst (LDH-3): 0.6-5 wt % relative to EC, Reaction time: 1-5 h, Temperature: 70°C.

2A.9.4. Typical reaction profile for EC to DMC

From the optimization of reaction conditions it was observed that the best results (87% EC conversion with 100% selectivity to DMC) were obtained with catalyst loading of 2.5 wt%, reaction temperature 70 °C and EC /CH₃OH molar ratio 1:10 i.e. Finally typical conversion/selectivity vs time plot under optimized reaction conditions using LDH-3 catalyst is presented in Fig. 2A.15.

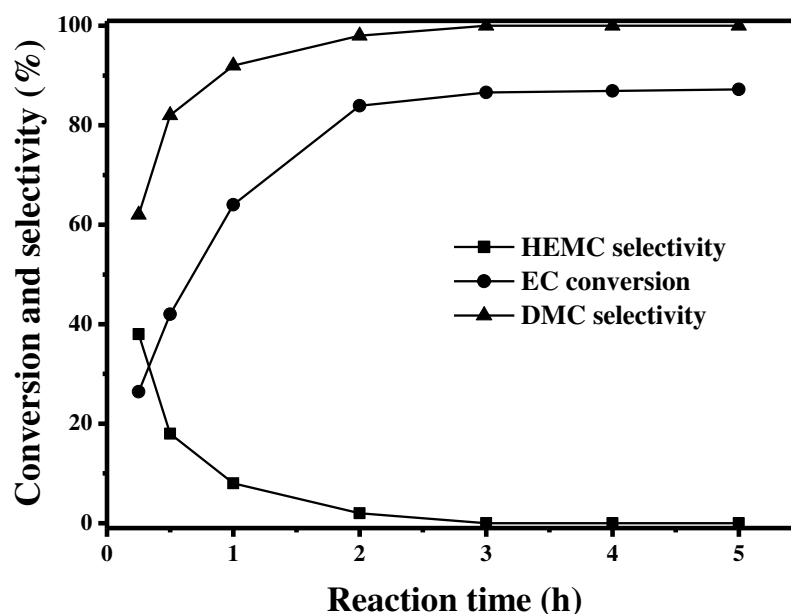


Figure 2A.15: Typical reaction profile for EC to DMC

Reaction conditions: EC: 23mmol, MeOH: 230mmol, EC: MeOH molar ratio: 1:10, Catalyst (LDH-3): 2.5 wt% relative to EC, Reaction time: 3 h, Temperature: 70°C

EC conversion and DMC selectivity increased, while HEMC selectivity decreased with increase in reaction time. Thus at 30 minute 43 % EC conversion with 82% selectivity to DMC and 18% selectivity to HEMC (intermediate product) was observed. EC conversion as well as DMC selectivity increased as the reaction progressed and 87% EC conversion with 100% selectivity to

DMC was observed at 3 h reaction time. Further prolonging the reaction time had no positive effect on EC conversion indicating that the reaction has reached the equilibrium.¹⁵ Lower selectivity of DMC observed at intermediate time intervals is due to the formation of HEMC as intermediate product. Overall mass balance of the reaction was very good throughout the course of the reaction and no other product was detected by GC analysis.

2A.10. Transesterification of EC and methanol using $\text{Mg}_3\text{Fe}_{0.85}\text{M}_{0.15}$ LDHs

After optimization of reaction conditions with $\text{Mg}_3\text{Fe}_{0.85}\text{Ce}_{0.15}$ (LDH-3) it was decided to investigate the effect of incorporation of other trivalent metals $\text{Mg}_3\text{Fe}_{0.85}\text{M}_{0.15}$ (instead of Ce) on the performance of the catalyst. For this purpose LDHs were prepared by varying M^{3+} [where $\text{M}^{3+} = \text{La, Sm, Y and Cr}$] by keeping the molar ratio of $\text{Mg}:\text{Fe}:\text{M}^{3+}$ constant at 3:0.85:0.15 LDHs.

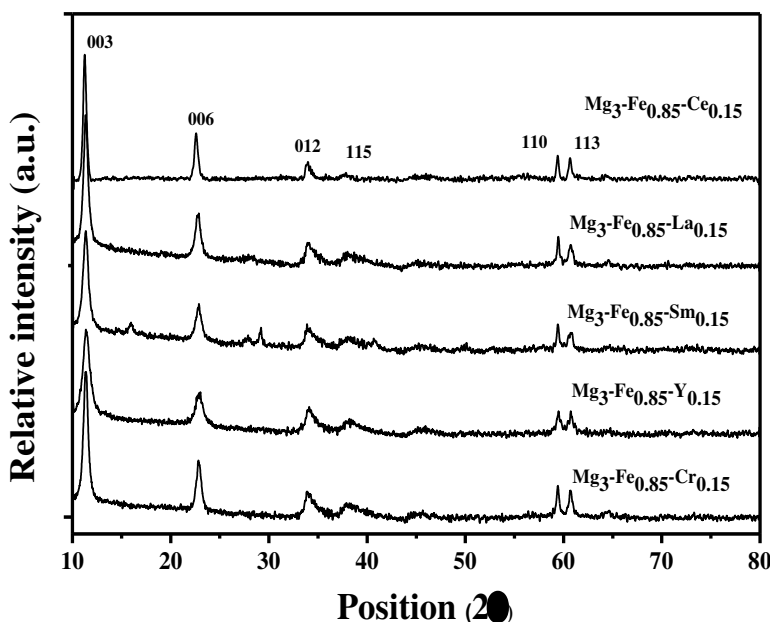


Figure 2A.16: XRD patterns of $\text{Mg}_3\text{Fe}_{0.85}\text{M}_{0.15}$ ternary LDHs with different M^{III} cations.

All synthesized $Mg_3:Fe_{0.85}+M_{0.15}$ LDHs showed typical X-ray diffractions pattern of LDHs materials Fig.2A.16.^{44,45} LDHs prepared were screened for transesterification of EC and methanol and the results are presented in Table 2A.6.

Table 2A.6: Effect of different metal cation $Mg_3:Fe_{0.85}:M_{0.15}$ for transesterification reaction of EC with MeOH

Catalyst	EC conversion (%)	DMC selectivity (%)
$Mg_3:Fe_1$	62	94
$Mg_3:Fe_{0.85}:La_{0.15}$	85	99
$Mg_3:Fe_{0.85}:Ce_{0.15}$	87	100
$Mg_3:Fe_{0.85}:Sm_{0.15}$	81	95
$Mg_3:Fe_{0.85}:Y_{0.15}$	67	82
$Mg_3:Fe_{0.85}:Cr_{0.15}$	56	78

Reaction conditions: EC: 23mmol, MeOH: 230mmol, EC: MeOH molar ratio: 1:10,

$Mg_3:Fe_{0.85}+M_{0.15}$ LDHs catalyst: 2.5 wt% relative to EC, Reaction time: 3 h, Temperature: 70°C

All the LDHs screened were active for the synthesis of DMC. EC conversion as well as selectivity to DMC was significantly affected by the trivalent metal used. Activity and selectivity followed in the order of $La \approx Ce > Sm > Y > Cr$. Among all LDHs $Mg_3Fe_{0.85}Ce_{0.15}$ (LDH-3) showed best activity and selectivity for this reaction. The results were found to be consistent with the electro negativities of the metal cations ($1.1 \approx 1.12 < 1.17 < 1.22 < 1.66$ respectively). Incorporation of third cation which has low electro negativity results in the increase in basic

property of LDH and leads to better activity.^{52,53} The difference in the electro negativities of La and Ce is very small and expectedly the catalyst activities observed were comparable. Thus Ce incorporated $Mg_3:Fe_1$ LDH was found to be best catalyst for transesterification reaction.

2A.11. Stability of the LDH-3 catalyst (leaching test)

Leaching of the LDH-3 into the reaction mixture was studied during the course of the reaction. Reaction was carried out under selected reaction conditions (EC: MeOH 1:10, 70°C for 30 min). After 30 min reaction was stopped and catalyst was separated by filtration of hot reaction mixture (~50°C). The filtered reaction mixture was charged to the glass reactor and the reaction was continued for next 1-3h under same reaction conditions. The results are shown in the Fig. 2A.17.

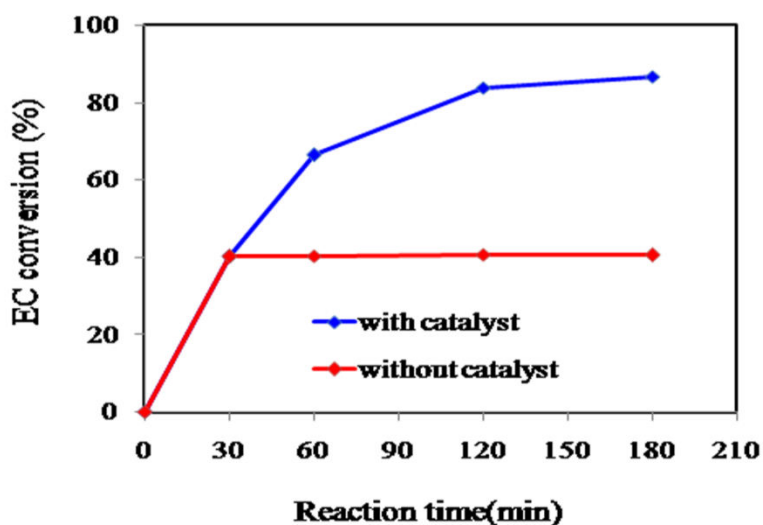


Figure 2A.17: Catalyst leaching test by hot filtration of reaction mixture for the transesterification of ethylene carbonate with methanol.

Reaction conditions: EC: 23mmol, MeOH: 230mmol, EC: MeOH molar ratio: 1:10, Catalyst (LDH-3): 2.5 wt% relative to EC, Reaction time: 0.5-3h, Temperature: 70°C

It was found that in the absence of the catalyst, there was no further increase in the EC conversion, which indicated that there was no leaching and transesterification is purely a heterogeneously catalyzed reaction.

2A.12. Recycle of LDH-3 catalyst

After confirming that the catalyst did not leach out during reaction, stability of the catalyst was investigated. For this purpose the reaction was carried out as usual and the catalyst was separated and dried at 70°C and used for next experiment by adding EC and methanol in required quantities.

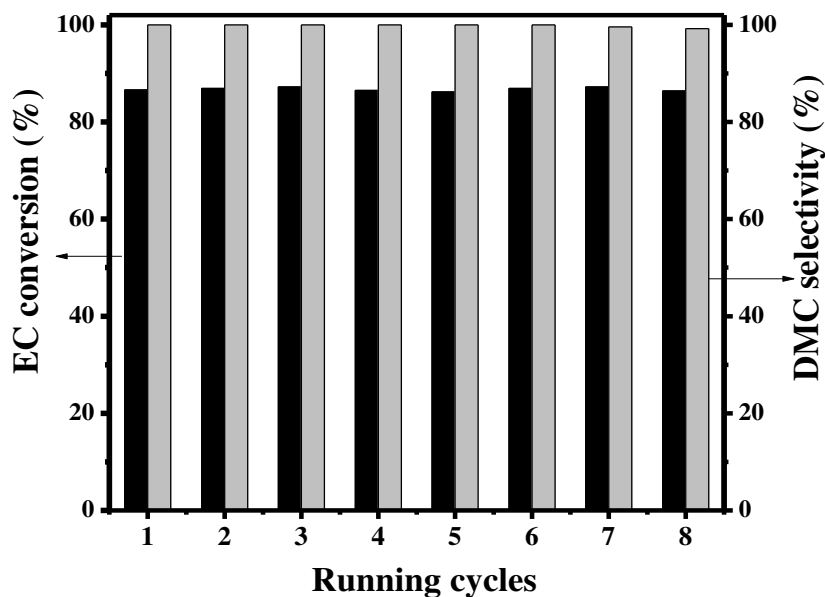


Figure 2A.18: Catalyst recycles study,

Reaction conditions: EC: 23mmol, MeOH: 230mmol, EC: MeOH molar ratio: 1:10, Catalyst (LDH-3): 2.5 wt% relative to EC, Reaction time: 3 h, Temperature: 70°C

Catalyst was recycled seven times using the same procedure (Section 2A.5.2.) and the results are presented in Fig. 2A.18. It was observed that the catalyst retained its original activity and high

selectivity to DMC for seven recycle experiments indicating excellent stability. At the end of the 7 recycle experiments the XRD analysis of the used catalyst was carried out (Fig. 2A.19). No change in the XRD pattern was observed for used catalyst, indicating high stability of the catalyst (LDH-3) towards transesterification reaction.

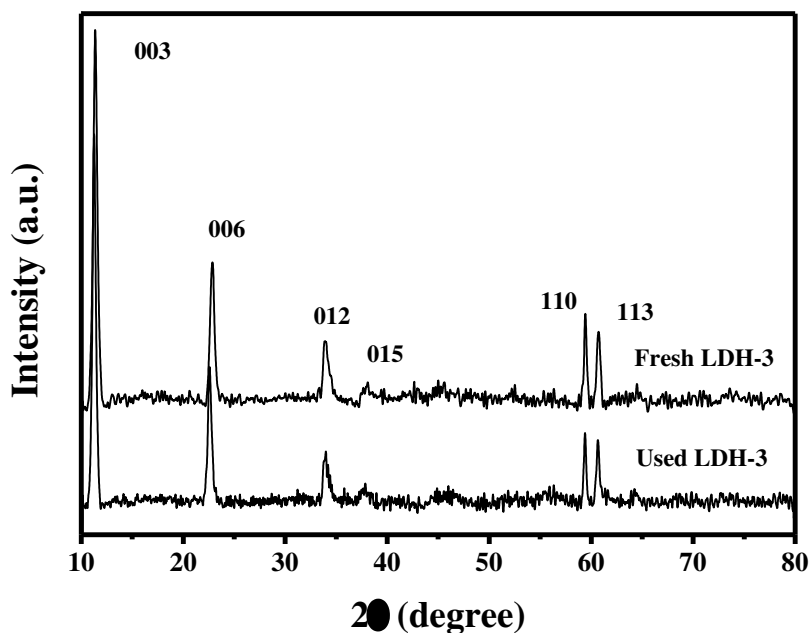
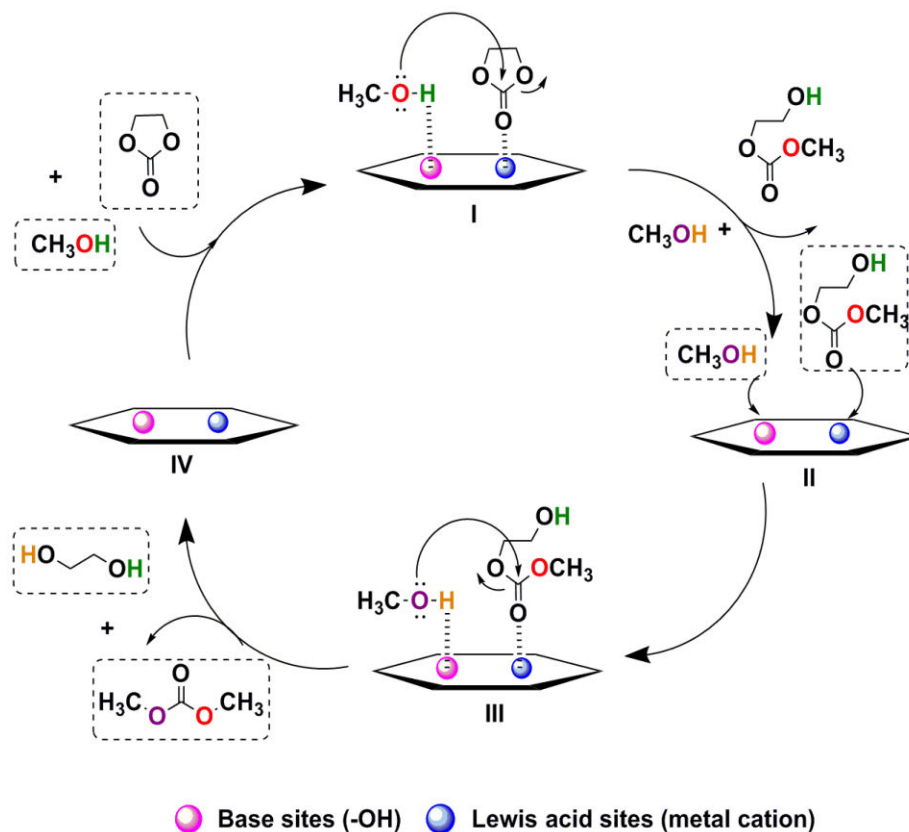


Figure 2.19A: XRD patterns of fresh and used $Mg_3:Fe_{0.85}Ce_{0.15}$ (LDH-3).

2A.13. Catalytic mechanism

Mechanism of the transesterification of EC with methanol has been discussed in several reports.^{9,14,20} Hydroxy groups (strong basic sites) present on LDH surface play an important role in transesterification reaction which was studied by many researchers using various spectroscopic techniques. According to Roeffaers et al.⁶⁵ transesterification of 5-carboxyfluorescein with 1-butanol over [Li–Al] layered double hydroxide catalyst occurs on the basal planes of the outer crystal surface whereas the hydrolysis reaction takes place on the crystal edges. Additionally, Greenwell et al.⁶⁶ have proposed that surface bonded –

OH anion may directly participate in the catalytic reaction and act more than the simple metal hydroxyl group based on density functional theory (DFT) calculations.



Scheme 2A.3: A possible mechanism for the transesterification of ethylene carbonate with methanol catalyzed by LDH-3

In the present work, significant improvement in EC conversion was observed with the incorporation of Ce in the $\text{Mg}_3\text{-Fe}_1$ LDH (LDH-3). Detailed characterization of the catalyst indicated the presence of more amount of active sites (-OH group) on LDH surface with high surface area compared to parent $\text{Mg}_3\text{-Fe}_1$ LDH (LDH-1). Taking into account the literature reports and results observed in the present work a probable mechanism has been proposed (Scheme 2A.3); where the -OH species and metal cations

present above the LDH surface act as strong base and Lewis acid sites respectively. The reaction begins with the abstraction of proton from methanol on -OH sites of LDH to generate methoxy anion. Activation of carbonyl carbon of EC on Lewis acid sites of LDHs generates relatively charged carbonyl carbon (Scheme 2A.3, Step I). Generated methoxy anion attacks on the activated carbonyl carbon of EC to form HEMC as the intermediate product (Scheme 2A.3, Step II). In next step (Scheme 2A.3, Step III) another methanol molecule interacts in similar fashion to form DMC and EG as the final products and the catalyst is regenerated back (Scheme 2A.3, Step IV). The formation of HEMC as an intermediate product was observed at low EC: CH₃OH ratios (Fig. 2A.12) and at low reaction temperature (Fig. 2A.13) leading to poor selectivity to the target DMC.

2A.14. Conclusions

Transesterification of EC with methanol to DMC was investigated in detail using Mg₃Fe_xCe_{1-x} ternary LDH as the catalyst. The LDHs were synthesized by varying Fe:Ce molar ratio in a range of 1:0 to 0:1. Both the end members of this series Mg₃Fe₁ (LDH-1) and Mg₃Ce₁ (LDH-6) showed lower catalytic activity and selectivity to DMC. The significant increase in EC conversion and DMC selectivity was observed with appropriate concentration of Ce present in LDH structure. The activity varied in the order LDH-6 < LDH-5 < LDH-1 < LDH-4 < LDH-2 < LDH-3. Among the synthesized catalysts LDH-3 (Fe:Ce molar ratio: 0.85:0.15) showed best catalytic performance (87% EC conversion with 100% DMC selectivity) under mild reaction conditions. LDH-3 was found to be truly heterogeneous catalyst and was recycled seven times without loss in catalytic activity and high selectivity to DMC. The activity trend was found to be in good

agreement with structural and surface basic properties of the synthesized LDHs. Various trivalent metals were also used to modify the LDH with composition $Mg_3Fe_{0.85}M_{0.15}$ [where $M^{3+} = La, Sm, Y$ and Cr] and the activity trend followed in order of $La \approx Ce > Sm > Y > Cr$. The best results were obtained with Ce modified $Mg_3:Fe_1$ LDH ($Mg_3Fe_{0.85}Ce_{0.15}$) as the catalyst. The results were found to be in good agreement with the electronegativities of incorporated third metal cations [M^{3+}]. To the best of our knowledge this is the first report on the use of $Mg_3Fe_{0.85}Ce_{0.15}$ ternary LDH as a catalyst for this reaction.

Chapter 2B

Synthesis of dimethyl carbonate by transesterification of cyclic carbonate (EC/PC) with methanol using Li-Al mixed metal oxide catalyst.

2B.1. Introduction

Mixed metal oxide (MMO) is class of heterogeneous catalysts mostly utilized both for their acid–base and redox properties for industrial important reactions.⁶⁷ MMOs can be binary, ternary and quaternary depending on the presence of different metal cations. The acid base properties of mixed metal oxides can be modified by proper combination of different metal cations. From the literature report (Chapter 1 section 1.4.6.) it was observed that most of the work on the synthesis of DMC from EC/PC and methanol has been carried out with mixed metal oxide catalysts.⁶⁸⁻⁷² Reported catalysts showed less activity with PC as a reactant compared to that with EC as a reactant. Lower activity observed with PC as a reactant was attributed mainly to differences in the chemical structures of these alkylene carbonates (steric factor).⁶⁹⁻⁷¹ Mixed metal oxides showed moderate activity for PC to DMC (18-72% PC conversion and 90-98% DMC selectivity) and required high reaction temperature (120-160°C).⁶⁸⁻⁷² Activity of MMOs was attributed to the amount and proper balance of acidic and basic sites.^{15,69}

To gain more insight into the role of acidic and basic sites in the reaction, we have investigated the catalytic performance of single and mixed-metal oxide materials consisting of Li, Mg, Co, Ni, Zn and Al. Binary mixed metal oxides were prepared by calcination of hydrotalcite precursors to obtain nanosized metal oxide phases with high surface area and homogeneous mixing. All catalysts were characterized in detail by XRD, BET, TEM and NH₃-/CO₂-TPD

analysis and were screened for transesterification of EC/PC with methanol. Optimization of reaction conditions was carried out for transesterification of EC/PC and methanol with LiAlO_2 MMO and various dialkyl carbonates were prepared by transesterification of EC with different alcohols including methanol, ethanol, n-propanol, n-butanol, and n-pentanol. Very good results were obtained with PC and methanol at 70°C with LiAlO_2 as the catalyst. To the best of our knowledge, LiAlO_2 is one of the few catalysts with high activity and selectivity for DMC synthesis at 70°C with PC and methanol as reactants.

2B.2. Materials

Ethylene carbonate (99%), $\text{Li}(\text{NO}_3)_2 \cdot 3\text{H}_2\text{O}$ (99%) were purchased from Sigma-Aldrich Co., USA. Chemical reagents including Ethylene glycol (99%), DMC (99.5%), $\text{Zn}(\text{NO}_3)_2 \cdot 6\text{H}_2\text{O}$ (99.5%), $\text{Al}(\text{NO}_3)_3 \cdot 9\text{H}_2\text{O}$ (99.5%), $\text{Co}(\text{NO}_3)_2 \cdot 6\text{H}_2\text{O}$ (99.8%), $\text{Ni}(\text{NO}_3)_2 \cdot 6\text{H}_2\text{O}$ (99%), $\text{Mg}(\text{NO}_3)_2 \cdot 6\text{H}_2\text{O}$, NaOH (99.5%), Na_2CO_3 (99.5%), Propylene carbonate (99.8%) were obtained from Loba Chemical Co., India.

2B.3. Catalyst preparation

Binary mixed metal oxide and Single metal oxide catalysts were synthesized by co-precipitation method²¹⁻²⁵ followed by calcination at $500^\circ\text{C}/2\text{h}$ in air. The detailed catalyst synthesis procedures are given below.

2B.3.1. Synthesis of binary mixed metal oxides

Mixed-metal oxides (MMOs) with the general formula M^+ or $\text{M}^{2+}/\text{Al}^{3+}$ containing Li^+ as a monovalent cation, Mg^{2+} , Co^{2+} , Ni^{2+} or Zn^{2+} as bivalent cations and Al^{3+} as a trivalent cation with constant molar ratio of M^+ or $\text{M}^{2+}:\text{Al}^{3+} = 3:1$ were synthesized by co-precipitation method. Thus

various MMOs $\text{Li}^+\text{-Al}^{3+}$, $\text{Mg}^{2+}\text{-Al}^{3+}$, $\text{Co}^{2+}\text{-Al}^{3+}$, $\text{Ni}^{2+}\text{-Al}^{3+}$ and $\text{Zn}^{2+}\text{-Al}^{3+}$ were synthesized (Fig. 2B.1) and the procedure is presented below.

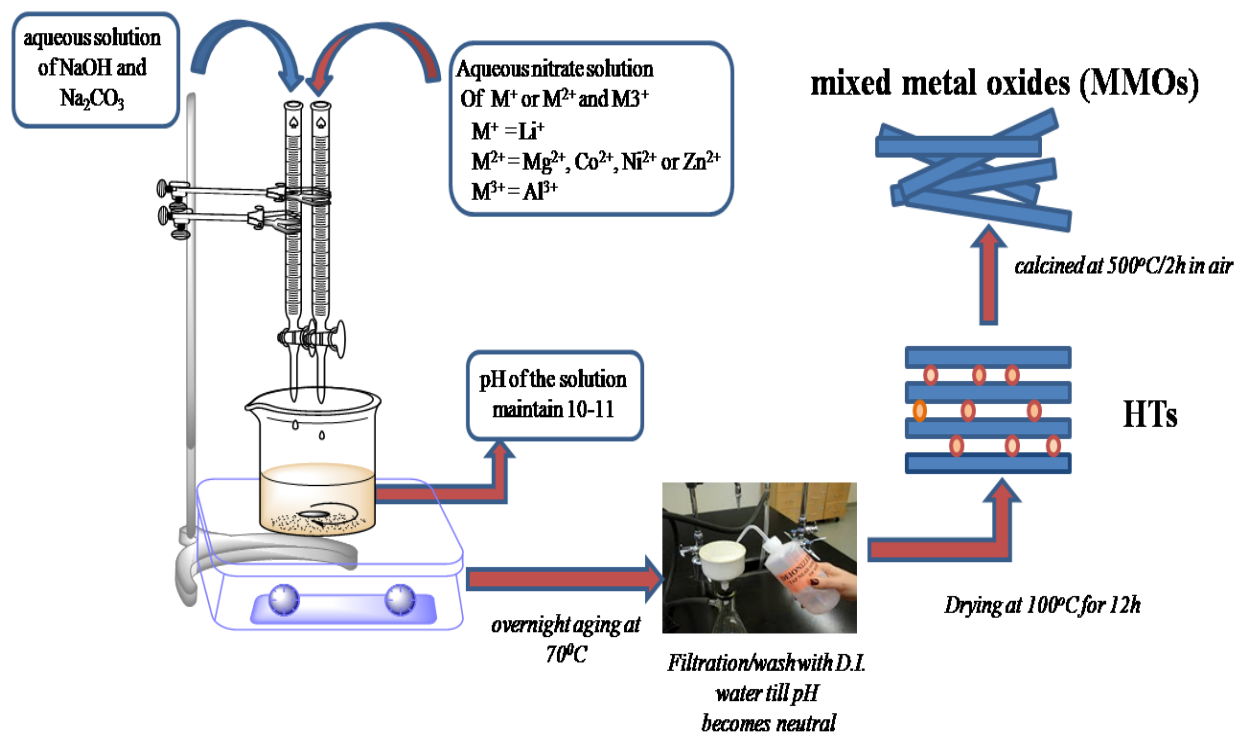


Figure 2B.1: Synthesis of mixed metal oxides (MMOs) M^+ or $\text{M}^{2+}:\text{Al}^{3+}$ (3:1) by co-precipitation method.

An aqueous nitrate solution (100 mL) of an appropriate amount of the monovalent or bivalent (60mmol) cation and trivalent cation (20mmol) was added drop wise into a beaker containing 100 mL of deionized water under vigorous stirring at room temperature. The pH of the solution was kept constant at 10-11 by adding a second aqueous solution of NaOH and Na_2CO_3 (2 M). The resulting precipitate was left for aging in the reaction mixture at 70°C for 15 h. Then the precipitate was filtered, washed several times with deionized water till filtrate became neutral. Finally, the synthesized hydrothermal precursors were dried at 100°C for 12 h in air. Activation of dried solid was carried out at $500^\circ\text{C}/2\text{h}$. Synthesized hydrothermal precursors were denoted as $\text{Li}_3\text{Al}_1\text{-HT}$, $\text{Mg}_3\text{Al}_1\text{-HT}$, $\text{Co}_3\text{Al}_1\text{-HT}$, $\text{Ni}_3\text{Al}_1\text{-HT}$ and $\text{Zn}_3\text{Al}_1\text{-HT}$ respectively. Mixed-metal

oxides after calcination of the corresponding materials with hydrotalcite structures were denoted as Li-Al 500, Mg-Al 500, Co-Al 500, Ni-Al 500 and Zn-Al 500 respectively. The activation of $\text{Li}_3\text{Al}_1\text{-HT}$ was carried out at different temperatures at $300^\circ\text{C}/2\text{h}$, $500^\circ\text{C}/2\text{h}$, $700^\circ\text{C}/2\text{h}$, $800^\circ\text{C}/2\text{h}$ and activated samples were labeled as Li-Al300, Li-Al500, Li-Al700 and Li-Al800 respectively.

2B.3.2. Synthesis of single-metal oxides

The synthesis of single-metal oxides (MgO , Co_2O_3 , NiO , ZnO , Al_2O_3 and Fe_2O_3) was carried out by following the same protocol by using aqueous solution of the respective nitrate precursor. An aqueous nitrate solution (100 mL) of an appropriate amount of the metal precursor [$\text{Mg}(\text{NO}_3)_2 \cdot 6\text{H}_2\text{O}$ or $\text{Co}(\text{NO}_3)_2 \cdot 6\text{H}_2\text{O}$ or $\text{Ni}(\text{NO}_3)_2 \cdot 6\text{H}_2\text{O}$ or $\text{Zn}(\text{NO}_3)_2 \cdot 6\text{H}_2\text{O}$ or $\text{Al}(\text{NO}_3)_3 \cdot 9\text{H}_2\text{O}$] was added drop wise into a beaker containing 100 mL of deionized water under vigorous stirring at room temperature. The pH of the solution was kept constant at 10-11 by adding a second aqueous solution of NaOH and Na_2CO_3 (2 M). The resulting precipitate was left to age in the reaction mixture at 70°C for 15 h. Then the precipitate was filtered, washed several times with deionized water till filtrate became neutral and finally, dried at 100°C for 12 h in air. Activation of dried solid was carried out at $500^\circ\text{C}/2\text{h}$ and denoted as MgO , Co_3O_4 , NiO , ZnO and Al_2O_3 respectively.

2B.4. Characterization Methods

Catalysts were characterized in detail by various techniques like X ray diffraction (XRD), BET surface area measurement by N_2 sorption and CO_2 - NH_3 TPD and TEM. The details of characterization methods are given in chapter 2A Section 2A.4.

2B.5. Experiment procedure for transesterification of EC/PC with methanol

The transesterification of cyclic carbonate (EC/PC) with methanol over MMOs was performed in a 50 ml jacketed glass reactor equipped with magnetic stirrer and reflux condenser. Typically, the reactor was charged with 23 mmol of cyclic carbonate (EC/PC), methanol 230 mmol and 2.5wt% of catalyst (relative to EC/PC). The reaction was carried out at 70°C for 1-3h reaction time under vigorous stirring. After completion of the reaction, the glass reactor was cooled to room temperature; the solid catalyst was separated from the solution by filtration. Sample was analyzed by gas chromatography to monitor the progress of the reaction. The gas chromatograph (Agilent 6890N) was equipped with an FID detector and innowax capillary column (30 m length \times 0.53 mm ID \times ~1 μ m film thickness). Formation of products was confirmed by GC-MS (Agilent 6890N (GC) 5973 (MSD)) equipped with HP-5 capillary column. The cyclic carbonate conversion and product selectivity were calculated by using the following equations:

$$\text{Conversion(\%)} = \frac{\text{cyclic carbonate initial (mmol)} - \text{cyclic carbonate final (mmol)}}{\text{cyclic carbonate initial (mmol)}} \times 100 \quad (1)$$

$$\text{Selectivity (\%)} = \frac{\text{DMC formed (mmol)}}{\text{cyclic carbonate consumed (mmol)}} \times 100 \quad (2)$$

$$\text{Yield (\%)} = \frac{\text{DMC formed (mmol)}}{\text{cyclic carbonate initial (mmol)}} \times 100 \quad (3)$$

Typical GC analysis for the reaction of EC and methanol is presented in Fig. 2A.2 and discussed in the earlier section. Similarly Fig. 2B.2 represents a typical gas chromatograph chart obtained for transesterification reaction of PC with methanol. The reaction proceeded smoothly with Li-Al 500 as the catalyst and formation of products was confirmed by GC and GC-MS analysis. The

distinct separation of all the reactants and products was obtained. (Methanol, DMC, PG and PC peaks appear at 2.71, 3.20, 5.09 and 5.73 minute retention time respectively).

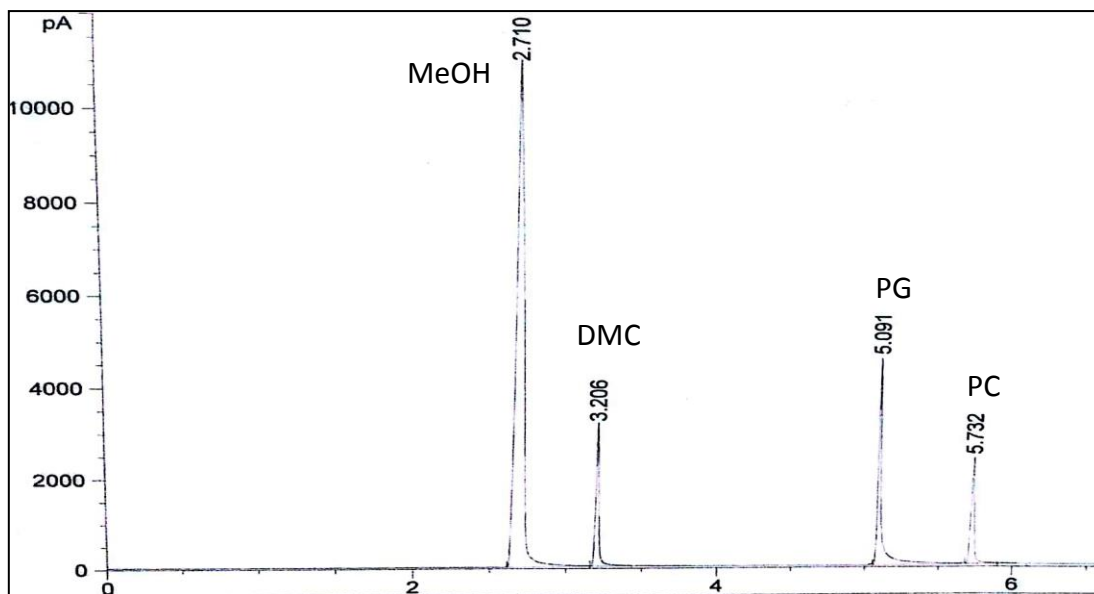


Figure 2B.2: A typical gas chromatograph chart showing reactants (PC and methanol) and products (DMC and PG).

2B.6. Result and discussion

2B.6.1. Characterization of MMOs

All synthesized binary and single MMOs were characterized in detail by using various spectroscopic techniques and screened for transesterification of EC/PC with methanol and the results obtained are presented below.

2B.6.1.1. Powder X-ray Diffraction

All the synthesized hydrotalcites (precursors for MMOs), MMOs obtained on calcinations of hydrotalcites (binary MMOs) and single metal oxides were characterized in detail by XRD (Fig. 2B.3 and 4).

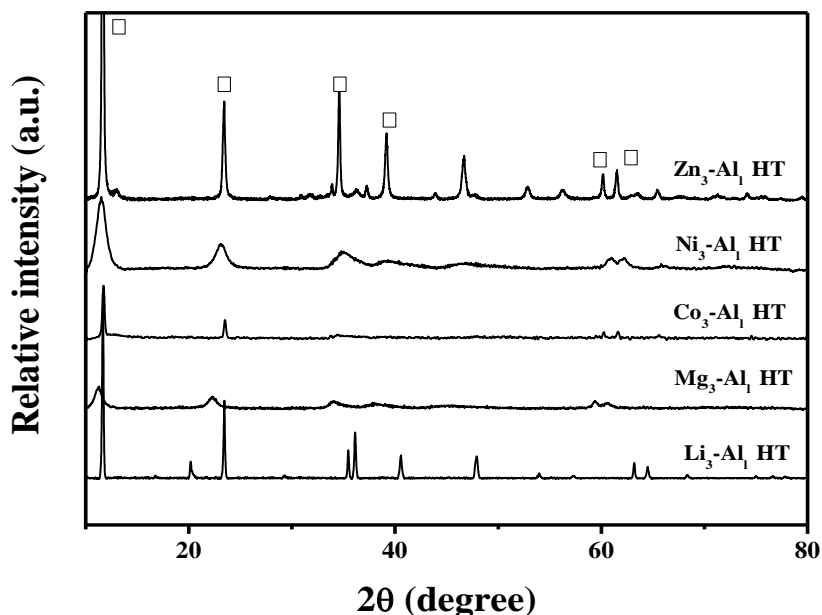
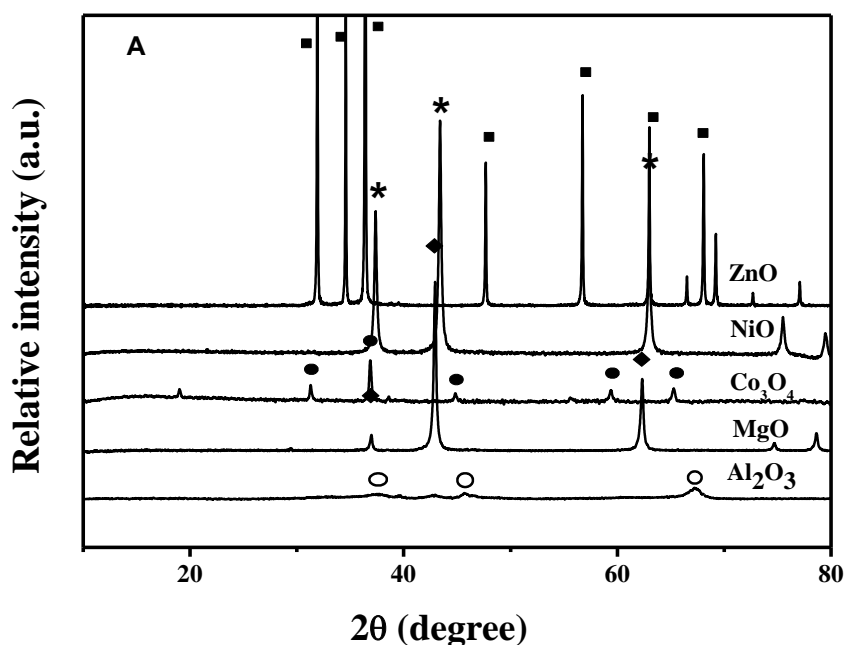


Figure 2B.3: XRD patterns of hydrotalcites prepared □ characteristic peaks for hydrotalcite (HT) As-synthesized $\text{Mg}_3\text{Al}_1\text{-HT}$, $\text{Co}_3\text{Al}_1\text{-HT}$, $\text{Ni}_3\text{Al}_1\text{-HT}$ and $\text{Zn}_3\text{Al}_1\text{-HT}$ materials showed reflection peaks which are characteristic to hydrotalcite materials as indicated in JCPDS file No. 14-0191 [sharp intense reflections of (003), (006) planes in the angle region ($2\theta < 25^\circ$), broad reflections of (012), (015) and (018) planes in the middle angle region ($2\theta = 30\text{-}50^\circ$) and sharp reflections of (110) and (113) planes in the high angle region ($2\theta = 55\text{-}65^\circ$)].⁴⁴⁻⁴⁵ The XRD pattern of as-synthesized $\text{Li}_3\text{Al}_1\text{-HT}$ is notably different from the other hydrotalcite materials and displays sharp characteristic reflections corresponding to HT material and confirmed from JCPDS file No. 42-0729 [reflection plane (002), (101) and (004) in the angle region ($2\theta < 25^\circ$), (006), (008), and (303) planes in the angle region ($2\theta = 30 - 65^\circ$)] and no other crystalline phases were detected.⁷³⁻⁷⁴

The XRD analysis for single metal oxides is presented in Fig. 2A.4A. The XRD pattern of MgO clearly showed the cubic periclase phase ($2\theta = 36.7, 42.8, 62.1^\circ$, JCPDS: 45-0946). NiO showed characteristic peaks of cubic phase ($2\theta = 37.2, 43.4, 62.6, 75.6, 75.6, 79.5^\circ$ JCPDS: 78-0643). Similarly Cobalt oxide showed formation of cubic Co_3O_4 phase ($2\theta = 19, 31.3, 36.9, 44.7, 59.4, 65.3, 65.3^\circ$ JCPDS: 74-1656). ZnO was well characterized by the hexagonal wurtzite phase with characteristic peaks at $31.7, 34.2, \text{ and } 36.1^\circ$ (JCPDS: 80-0075). Al_2O_3 showed low crystallinity with characteristic peaks of amorphous Al_2O_3 phase ($2\theta = 37.0, 45.6 \text{ and } 67.1^\circ$, JCPDS: 29-0063).

XRD analysis of Hydrotalcite-derived mixed metal oxides and Single metal oxides



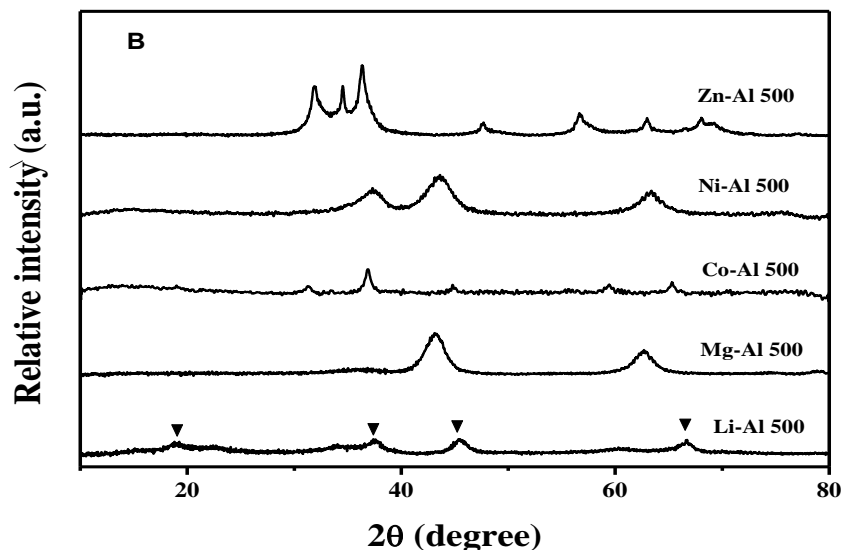


Figure 2B.4: XRD patterns of calcined (A) single metaloxides and (B) mixed metal oxides. The symbols indicate the following crystal phases: ■ hexagonal wurtzite phase of ZnO, ◆ cubic periclase phase of MgO, * cubic phase of NiO, ● cubic Co_3O_4 phase and ▼ hexagonal crystalline phase of $\alpha\text{-LiAlO}_2$.

After calcination at $500^\circ\text{C}/2\text{h}$, the hydrotalcite structure (Fig.2B.4A) was destroyed with the formation of metal oxide and mixed metal oxide phases as shown in Fig.2.23B. For Mg-Al 500, the cubic periclase phase of MgO was well recognized. Zn-Al 500 revealed the presence of hexagonal ZnO phase. Similarly Ni-Al 500 and Co-Al 500 mixed metal oxides confirmed the presence of NiO and Co_3O_4 phases respectively. In all the Al-containing materials, the phase for aluminium oxide was not detected, implying well incorporation and thus high dispersion of these metal ions in the oxide structures.^{75,76} The XRD pattern of Li-Al 500 reveals the reflections of hexagonal phase of crystalline $\alpha\text{-LiAlO}_2$ which is a single phase structure consistent with that reported in JCPDS: 44-0224. Li-Al 500 displays the sharp characteristic reflections corresponding to (003), (101), (104) and (110) planes of the crystalline $\alpha\text{-LiAlO}_2$ structure.⁷⁷ This is in contrast to the results of other Al- containing materials; which mainly showed the

reflections of dominant metal oxides i.e.(MgO,Co₃O₄, NiO and ZnO) and peaks corresponding to mixed metal oxide phase could not be identified. These results are in good agreement with the work done by Rosseinsky et al.⁷⁵ XRD analysis of calcined Mg₃Al₁, Co₃Al₁ and Ni₃Al HTs showed the presence of oxides of bivalent cations (Mg²⁺,Co²⁺andNi²⁺) as the major crystalline phase, however corresponding MMO phase was not observed in their work.⁷⁵

From the XRD analysis (Fig. 2B.3) it was clearly observed that as synthesized material showed characteristic peaks of hydrotalcite (HT) phase. Calcination of hydrotalcites at 500°C/2h destroyed HT structure and resulted in the formation of oxide phases (Fig.2B.4). All calcined M²⁺:M³⁺ MMO showed presence of major single metal oxide phase (MgO, Co₃O₄, NiO and ZnO) except Li-Al 500 where α -LiAlO₂ phase was observed.

Textural and acid base properties of all metal oxides prepared were investigated and the details are presented in Tables 2B.1 and 2B.2.

2B.6.1.2. Surface Area Measurements

Specific surface areas of the single metal oxides are presented in Table 2B.1. The surface area of single-metal oxides decreased in order Al₂O₃> MgO> NiO> Co₃O₄> ZnO. The highest surface area was observed for Al₂O₃ (210 m²/g), while lowest surface area was observed for ZnO (32m²/g). In case of mixed-metal oxides (Table 2B.2), the M²⁺:M³⁺ ratio used is 3:1 and hence the major contributions to the surface area will come from the bivalent metal ions. Surface area of mixed metal oxides decreased in the order Li-Al 500> Mg-Al 500> Co-Al 500> Ni-Al 500> Zn-Al 500. Highest surface (156 m²/g) was observed with Li-Al 500. The variation in surface observed is as expected and in accordance with the literature reports.⁷⁵⁻⁷⁶

Table 2B.1: Textural and surface acid base properties of single metal oxides

Entry	Catalyst	Crystalline phase	BET surface area m ² /g	CO ₂ uptake* (μmol /g)		NH ₃ uptake* (μmol /g)	
1	MgO	periclase	162	129	Weak: 0 Medium:103 Strong: 26	27	Weak: 0 Medium:0 Strong: 27
2	Al ₂ O ₃	amorphos-Al ₂ O ₃	210	34	Weak: 0 Medium:34 Strong: 0	139	Weak: 43 Medium:57 Strong: 39
3	Co ₃ O ₄	cubic	59	51	Weak: 0 Medium: 38 Strong: 13	104	Weak: 34 Medium:51 Strong: 19
4	ZnO	wurtzite	32	64	Weak: 0 Medium:36 Strong: 28	38	Weak: 9 Medium:29 Strong: 0
5	NiO	cubic	47	0	Weak: 0 Medium:0 Strong: 0	117	Weak: 7 Medium:78 Strong: 32

* Total amount of acid and base sites, Weak: 100-250°C, Medium: 250-450°C and Strong:>450°C

Table 2B.2: Textural and surface acid base properties of mixed metal oxides

Entry	Catalyst	Crystalline phase	BET surface area m ² /g	CO ₂ uptake*		NH ₃ uptake*	
				(μmol /g)	(μmol /g)	(μmol /g)	(μmol /g)
1	Zn-Al 500	ZnO (wurtzite)	62	191	Weak: 86 Medium:82 Strong: 23	98	Weak: 36 Medium:37 Strong:25
2	Ni-Al 500	NiO	87	21	Weak : 12 Medium:0 Strong: 9	113	Weak:29 Medium:62 Strong:22
3	Co-Al 500	Co ₃ O ₄ cubic	92	139	Weak : 72 Medium:31 Strong: 36	114	Weak: 51 Medium:43 Strong:20
4	Mg-Al 500	MgO (periclase)	139	192	Weak:47 Medium:76 Strong: 69	121	Weak:16 Medium:48 Strong:57
5	Li-Al 500	α-LiAlO ₂	156	274	Weak: 59 Medium:133 Strong: 82	177	Weak:43 Medium:61 Strong:73

*Total amount of acid and base sites, Weak 100-250°C, Medium 250-450°C and Strong >450°C

2B.6.1.3. CO₂ and NH₃ TPD analysis

The strength and the total amount of basic and acidic sites of the single and mixed-metal oxides were estimated by CO₂ and NH₃ TPD analysis respectively. The amount of desorbed gases, corresponding to the amount of basic and acidic sites, is reflected in the peak area, where the desorption peak temperature indicates the strength of acidic or basic sites. Fig. 2B.5 and 6 present the desorption profiles of CO₂ and NH₃ from the thermally treated catalysts (in air at 500°C). The total amount of each type of basic and acid sites were determined by integration of the deconvoluted peaks from the TPD curves using origin (6.1) software and the quantified results are summarized in Table 2B.1 and Table 2B.2. TPD (CO₂ and NH₃) analysis was performed up to 800°C, in order to estimate basic and acidic sites with different strengths present on the catalysts.

2B.6.1.3.1. CO₂ TPD analysis of metal oxides

Desorption peaks were observed at different temperatures for different metal oxides (Fig. 2B.5). The strength of the basic sites can be assigned to temperature ranges of 100-250°C, 250-450°C and >450°C corresponding to the presence of active sites, such as surface OH⁻ groups (weak Brønsted basicity), Mⁿ⁺- O²⁻ (medium-strength Lewis basicity), and low-coordinated O²⁻ (strong Lewis basicity) respectively.⁷³

From CO₂ TPD analysis it was observed that in case of single metal oxides, MgO showed highest basicity with CO₂ desorption peaks with maximum at 376°C (Fig. 2B.5A) showing the presence of higher amount of basic sites (129 μmol /g). This was mainly due to medium strength basic sites (103 μmol /g). All other metal oxides (ZnO, Co₃O₄ and Al₂O₃) exhibited very low CO₂ desorption peak, indicating there is less amount of basic sites present on the surface (64, 51 and

34 $\mu\text{mol/g}$ respectively) and mostly moderately basic sites (Table 2B.1, Entry 2-4). However, no basic sites were observed for NiO. Basicity of metal oxides prepared decreased in the order $\text{MgO} > \text{ZnO} > \text{Co}_3\text{O}_4 > \text{Al}_2\text{O}_3$.

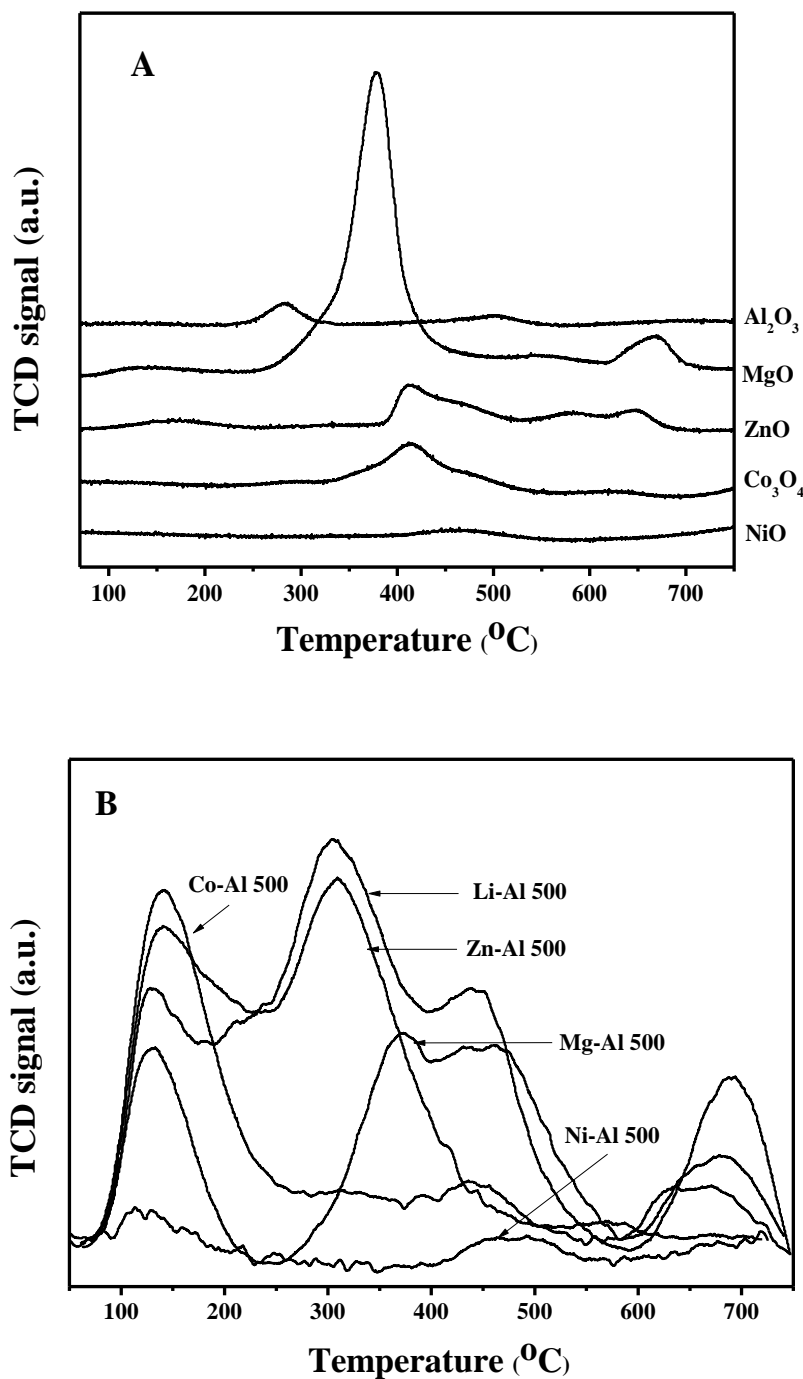


Figure 2B.5: CO₂ TPD of (A) single and (B) mixed metal oxide

Binary MMOs (Fig.2B.5B) exhibited CO₂ desorption peaks over a wide range of temperature indicating the presence of basic sites with different base strengths. The base strength distribution of the MMOs varied depending on the M²⁺ or M⁺ transition metal cation (Zn, Co, Ni, Mg and Li) used in combination with Al³⁺ cation (M⁺/M²⁺:Al mole ratio:3:1). The basicity decreased in the order: Li-Al 500 > Mg-Al 500 > Zn-Al 500 > Co-Al 500 > Ni-Al 500 and the basicity values obtained are given in Table 2B.2. Lowest basicity (21 μmol /g) was observed for Ni-Al 500. From all synthesized MMOs Li-Al 500, showed maximum amount of basic sites (274 μmol /g) with 59, 133 and 82 μmol/g of weak, medium and strong-strength basic sites respectively. Increase in basicity observed for Li-Al 500 was mainly due to (1) The addition of Li⁺ improves the partial negative charge of oxygen ions in Al₂O₃ due to the lower ionization potential of Li compared with Al, which leads to the presence of weak and moderate basic sites on Al₂O₃ surface.⁷⁷ (2) The strong basic sites originate from [O²⁻] which is resulted from the substitution of Al³⁺ by Li⁺ in the Al₂O₃ lattice.⁷⁷ The results obtained are found to be in accordance with those obtained by Shumaker et al.⁷³ They observed that Li-Al MMO possesses higher amount of medium and strong Lewis base sites compared to Mg-Al, Mg-Fe and MgO metal oxides and showed best activity for synthesis of biodiesel by Transesterification of soybean oil with methanol.⁷³

2B.6.1.3.2. NH₃ TPD analysis of metal oxides

Acid properties of the synthesized metal oxides were also studied using NH₃ TPD analysis and the results are presented in Fig. 2B.6 A and B. Quantity of NH₃ desorbed from the weak (<250°C), moderate (250-450°C) and strong (>450°C) acidic sites are shown in Tables 2B.1-2. From the Table 2B.1 it was clearly observed that single metal oxides (Fig. 2B.6A) Co₃O₄, NiO and Al₂O₃ possessed acid sites (104, 117 and 139 μmol/g respectively) over a wide temperature range of 100-600°C with major contribution from medium acid sites. NiO showed maximum

acid sites at 430°C (78 $\mu\text{mol/g}$) mainly due to presence of medium strength of acid sites. MgO and ZnO possessed fewer acid sites (27 $\mu\text{mol/g}$ (Strong acid sites) and 52 $\mu\text{mol/g}$ (mostly medium acidic sites)) respectively. Significant difference was observed in the NH_3 TPD profiles of binary MMOs (Fig.2B.6B) showing different strength of acid sites.

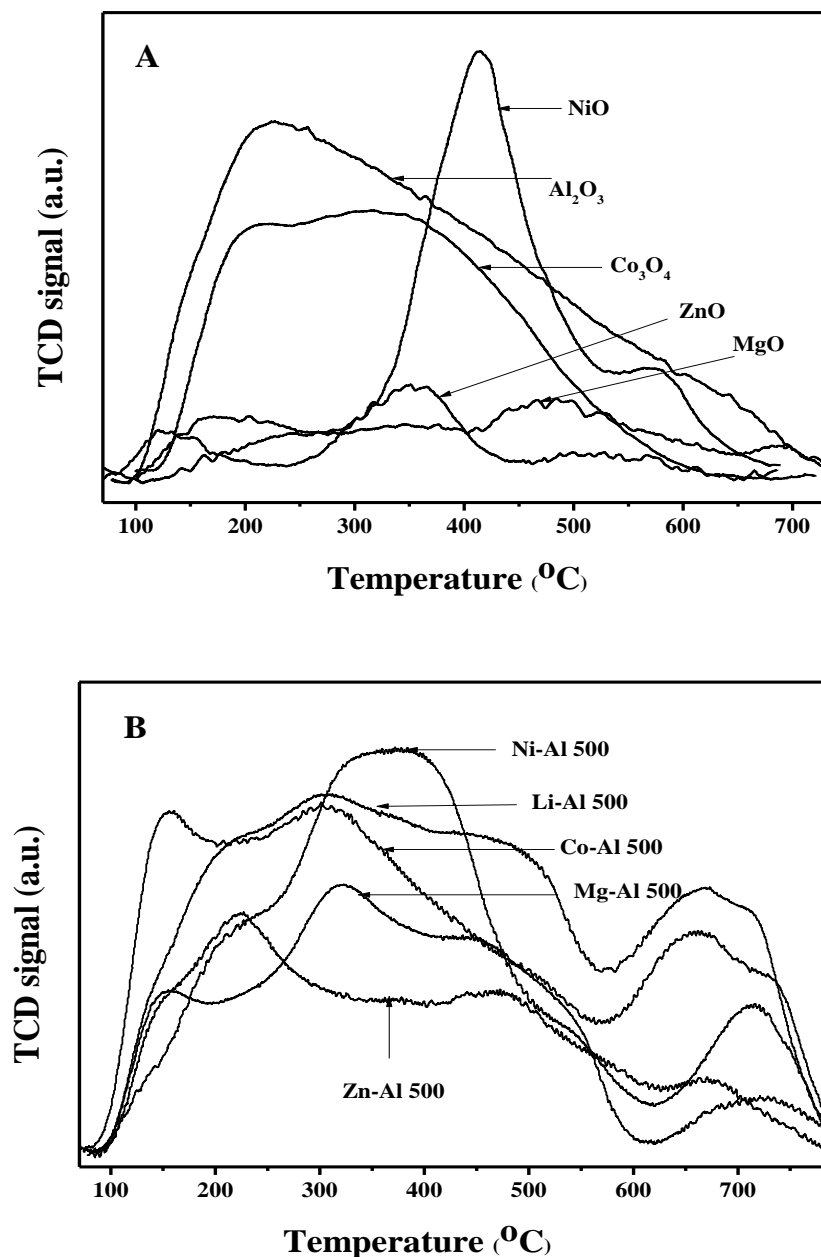


Figure 2B.6: NH_3 TPD of (A) single and (B) mixed metal oxide

In general the contribution of moderate acidic was high for MMOs prepared, followed by weak acidic sites and strong acidic sites. However, for MMOs with basic metals like Mg and Li the contribution of strong acidic sites was marginally higher followed by medium acidic sites. Total acid sites decreased in following order: Li-Al 500 > Mg-Al 500 > Co-Al 500 > Ni-Al 500 > Zn-Al 500 (177, 121, 114, 113, 98 $\mu\text{mol/g}$ respectively). Similar enhanced acidity and basicity by incorporation of foreign metal ions into the metal oxide structure has been reported by Urakawa et al.⁷⁶ Thus total amount of acidic sites of MgO and ZnO were improved by incorporation of Al^{3+} and Fe^{3+} cations (i.e., Mg-Al, Mg-Fe, Zn-Al and Zn-Fe) in the mixed metal oxide.

From the CO_2 and NH_3 TPD, it was clearly observed that the acid base properties of single metal oxides varied based on the property of the metal. Thus MgO was basic in nature and had maximum base sites mostly medium strength base sites. All other single metal oxides had less basic sites and mostly medium basic strength. Total amount of acid sites in MgO were low (27 $\mu\text{mol/g}$) and strongly acidic Al_2O_3 , NiO and Co_3O_4 exhibited acidic sites in a range of 104-139 $\mu\text{mol/g}$ with medium strength acid sites in more quantity. The amount of acid, base sites and their distribution varied significantly with the incorporation of trivalent metal (Al^{3+}) in the mixed metal oxides. All mixed metal oxides (except Ni-Al 500) exhibited weak, moderate and strong acidic and basic sites, with moderately basic or acidic sites dominating the distribution. Interestingly for Li-Al 500 and Mg-Al 500 strong acidic sites were slightly higher than the medium strength sites. Among mixed metal oxides prepared Li-Al 500 had highest number of total acid sites (177 $\mu\text{mol/g}$) and basic sites (274 $\mu\text{mol/g}$); with strong acid sites (73 $\mu\text{mol/g}$) and medium strength basic sites (133 $\mu\text{mol/g}$) being highest.

2B.7. Transesterification of EC/PC with methanol using single and binary

MMOs

Screening of single and binary MMOs was carried out for transesterification of cyclic carbonate (EC/PC) with methanol using standard reaction conditions as discussed in section 2B.4. and the results obtained are presented in Table 2A.3.

Table 2A.3: Transesterification of cyclic carbonate (EC/PC) with methanol using single and mixed metal oxide catalysts

Entry	Catalyst	EC + methanol system		PC + methanol system	
		EC conversion (%)	DMC selectivity (%)	PC conversion (%)	DMC selectivity (%)
1	Without catalyst	-	-	-	-
2	MgO	24	94	16	93
3	Al ₂ O ₃	12	91	4	88
4	NiO	8	85	-	-
5	Co ₃ O ₄	11	89	3	85
6	ZnO	17	88	7	84
7	Zn-Al 500	21	91	13	89
8	Ni-Al 500	11	86	6	86
9	Co-Al 500	18	91	9	89
10	Mg-Al 500	36	95	14	92
11 ^a	Li-Al 500	86	100	75	100

Reaction conditions: PC/EC: 23 mmol, methanol: 230mmol, PC/EC: MeOH: 1:10, catalyst: 2.5 wt% relative to PC/EC, reaction time: 3 h, temperature: 70 °C.

^aReaction time: 1 h

Catalyst was essential for the reaction and reaction did not proceed without any catalyst (Table 2A.3, Entry 1). Single metal oxides (MgO, Co₃O₄, ZnO, Al₂O₃ and NiO) showed very low activity for the synthesis of DMC from EC/PC and PC conversion was very low compared to that with EC (Table 2B.3, Entry 2-6). Reaction did not proceed with PC and methanol using NiO as the catalyst (Table 2B.3, Entry 4). EC/PC conversion increased (compared to single metal oxide catalyst) using MMOs and best results (86% EC and 75% PC conversion with 100% selectivity to DMC) were obtained with Li-Al 500 as the catalyst. The catalytic activity for binary MMOs increased in the order: Ni-Al 500 < Co-Al 500 < Zn-Al 500 < Mg-Al 500 < Li-Al 500. The Catalytic activity towards PC was found to be low as compared to that for EC in all cases. This difference in activity may be due to steric hindrance associated with the bulky methyl group in PC as compared with the symmetrical EC.¹⁶ Among several metal oxide catalysts screened in this work, Li-Al 500 showed the highest EC/PC conversion (75 and 86% respectively).

From the results it was clearly observed that, the EC or PC conversion and DMC selectivity strongly depended on the amount and type of basic and acidic sites present on the catalyst surface. Very low conversion of EC (11-18 %) and PC (6-13%) with DMC selectivity (86-91%) was observed with Ni-Al 500, Co-Al 500 and Zn-Al 500 as catalysts (Table 2B.3, Entry 5-7) having low acid and base sites. Moderate activity with Mg-Al 500 was observed for EC (36% EC conv. with 95 % DMC selectivity) and PC (14% PC conv., with 92 % DMC selectivity), having 192 μmol/g basic sites (weak: 47 μmol/g, medium: 76 μmol/g and strong 69 μmol/g) and 121 μmol/g acidic sites (weak: 16μmol/g, medium: 48μmol/g and strong 57μmol/g). Best results (86% EC conversion in 1 h and 75% PC conversion in 3 h with 100% DMC selectivity) were obtained with Li-Al 500 catalyst having 274 μmol/g basic sites (weak: 59 μmol/g , Medium: 133 μmol/g and strong: 82 μmol/g) and 177 μmol/g acidic sites (weak: 43 μmol/g, medium: 61

$\mu\text{mol/g}$ and strong: $73 \mu\text{mol/g}$). Mixed metal oxide derived from LiAl-HT is known to possess weak, medium and strong basic sites, corresponding to OH-groups, Li-O/Al-O ion pairs and surface O^{2-} ions respectively. The hydroxyl groups present on the surface of the catalyst can function as Brønsted base sites, while the remaining sites (medium and strong basic sites) can be expected to possess significant Lewis base character.⁷⁸ It is well known that the role of acid as well as base sites is important in transesterification reaction.^{73,74,79} Kumar et al.¹⁵ have investigated transesterification of PC and methanol to DMC using Cu-Zn-Al MMO as catalyst. They reported that the DMC yield was significantly affected by calcination temperature used (300, 500 and 800°C) and high activity (70.6% PC conversion and 92.4% DMC selectivity at 160°C and reaction time of 4 h) was observed with the catalyst calcined at 300°C . TPD results of the catalyst showed that acid and base site distribution changed with calcination temperature and catalyst calcined at 300°C showed the higher amount of acid and base sites (6.658 and 4.615 mmol/g respectively). Results obtained in the present work also can be attributed to the presence of higher amount of moderate and strong base and also acid sites on Li-Al 500 used as the catalyst (Table 2B.3, Entry 5) compared to other MMOs.

From the above studies, the variation of constituent elements in the mixed-metal oxides was found to significantly alter the acid-base properties of mixed metal oxides prepared and consequently influenced the DMC yield. Fine tuning of acid-base properties and a balanced proportion of surface acidic and basic sites was found to be critical for achieving high EC/PC conversion with high DMC selectivity. Best results were obtained with Li-Al 500 and hence detailed investigations were carried using the same catalyst. At first detailed characterization of the catalyst was carried out and the details are presented below.

2B.8. Effect of calcination temperature in Li-Al MMO

The effect of calcination temperature on the activity was investigated by calcining as synthesized LiAl-HT at 300, 500, 700 and 800°C. The mixed metal oxides obtained were labelled as Li-Al 300, Li-Al 500, Li-Al 700 and Li-Al 800 respectively. All the catalyst samples were characterized in detail by XRD, BET, TEM and CO₂-TPD.

2B.8.1. XRD Analysis

Powder XRD analysis of parent Li-Al HT as prepared and calcined samples at different temperatures in a range of 300-800°C was carried out and the results are presented in Fig. 2B.7.

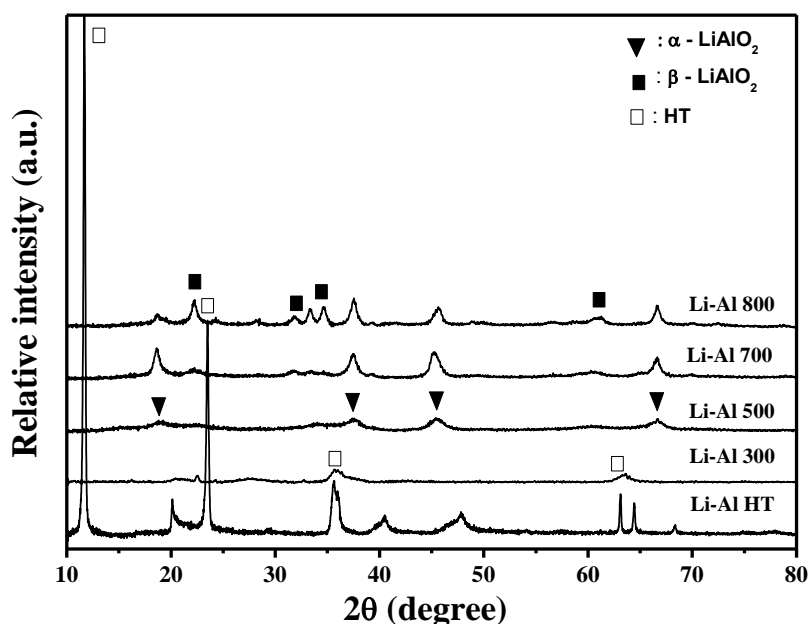


Figure 2B.7: XRD patterns of calcined LiAl-HT at different temperatures 300,500,700 and 800°C

At lower calcinations temperature of 300°C, the layered structure of HT was not completely broken and very weak *00l* plane peaks were observed (at $2\theta=20.2^\circ$, 22.9° , 35.7° , 63.2° and 64.1°) in the XRD analysis. XRD analysis of LiAl-HT calcined at 500°C revealed that LiAl-HT

gradually lost its layered structure and turned in to amorphous α -LiAlO₂ phase $2\theta=18.75, 45.6, 37.57, 45.6$ and 66.5°C (JCPDS file No. 42-0729). The lithium oxide (Li₂O) phase was not detected by XRD analysis of Li-Al500, suggesting well dispersion of Li₂O within the Al framework. With further increase in the calcination temperature to 700-800°C, peaks corresponds to α -LiAlO₂ phase becoming narrower and more intense and a new crystal phase of β -LiAlO₂ (PDF 33-0785) was also observed.^{79a}

2B.8.2. Surface area

Table 2B.4: Surface properties of Li-Al MMOs calcined at different temperature (300-800°C).

Entry	Catalyst	Calcination temperature (°C)	Surface area (m ² /gm)	Pore volume (cm ³ /gm)	CO ₂ uptake*	
					(μmol /g)	
1	LiAl-HT	Not calcined	62	0.47	-	-
2	Li-Al300	300	102	0.75	168	Weak: 43 Medium:82 Strong: 43
3	Li-Al500	500	156	0.86	274	Weak: 59 Medium:133 Strong: 82
4	Li-Al700	700	122	0.6	75	Weak: 17 Medium:58 Strong: 0
5	Li-Al800	800	96	0.51	44	Weak: 15 Medium:29 Strong: 0

*Weak 100-250°C, Medium250-450°C and Strong>450°C

The surface area of Li-Al HT was 62 m²/g and pore volume was 0.43 cm³/g. Surface area as well as pore volume increased with calcination of the catalyst till 500°C. Thus at 500°C surface area

of 156 m²/g and pore volume of 0.86 cm³/g was observed. Surface area as well as pore volume decreased with further increase in calcination temperature (700-800°C) and surface area of 122-96 m²/g with pore volume of 0.6-0.51 cm³/g respectively was observed.

According to reported thermogravimetric data^{73,79,80} decomposition of [Al₂Li(OH)₆](CO₃)_{0.5}-nH₂O (LiAl-HT) commences at 50°C and extends up to 450°C, with a DTG maximum at 204°C. Initial weight loss corresponds to elimination of the interlayer water; however, it was clear that this process overlaps with carbonate decomposition and the elimination of hydroxyl groups. Below 450°C the removal of carbonate and hydroxyl species will be incomplete; hence the surface area and pore volume observed at 300°C are expected to be low. At 500°C hydrotalcite structure was totally decomposed with the formation of amorphous α-LiAlO₂, leading to higher surface area and pore volume. Calcination of the Li-Al HT beyond 500°C led to the conversion of amorphous α-LiAlO₂ phase converted to spinal oxide phase (β- LiAlO₂) having lower surface area. Thus drop in the surface area as well as pore volume for catalysts calcined at 700°C and 800°C can be attributed to the formation of β- LiAlO₂. Formation of α-LiAlO₂ and β- LiAlO₂ was clearly observed from XRD (Fig. 2B.7). The results obtained in the present work are consistent with the literature reports.⁸⁰

2B.8.3. TEM Analysis

TEM analysis of Li-Al calcined at different temperatures was carried out and the results are presented in Fig. 2B.8. Fig. 2B.8a showed that the LiAl-HT (uncalcined sample) was composed of crystallites with the typical plate like morphology and often hexagonal shape which was in good agreement with the XRD study (Section 2B.5.1. / XRD Fig. 2B.3). Layered structure of HT was destroyed completely on calcining the LiAl-HT sample at 500°C (Li-Al 500) leading to the

formation of particles with numerous microholes. Thus the increase in porosity and surface area (Table 2B.4) can be attributed to the formation of craters through the layers due to the evolution of CO₂ and H₂O during the calcination of Li-Al HT at 500°C.

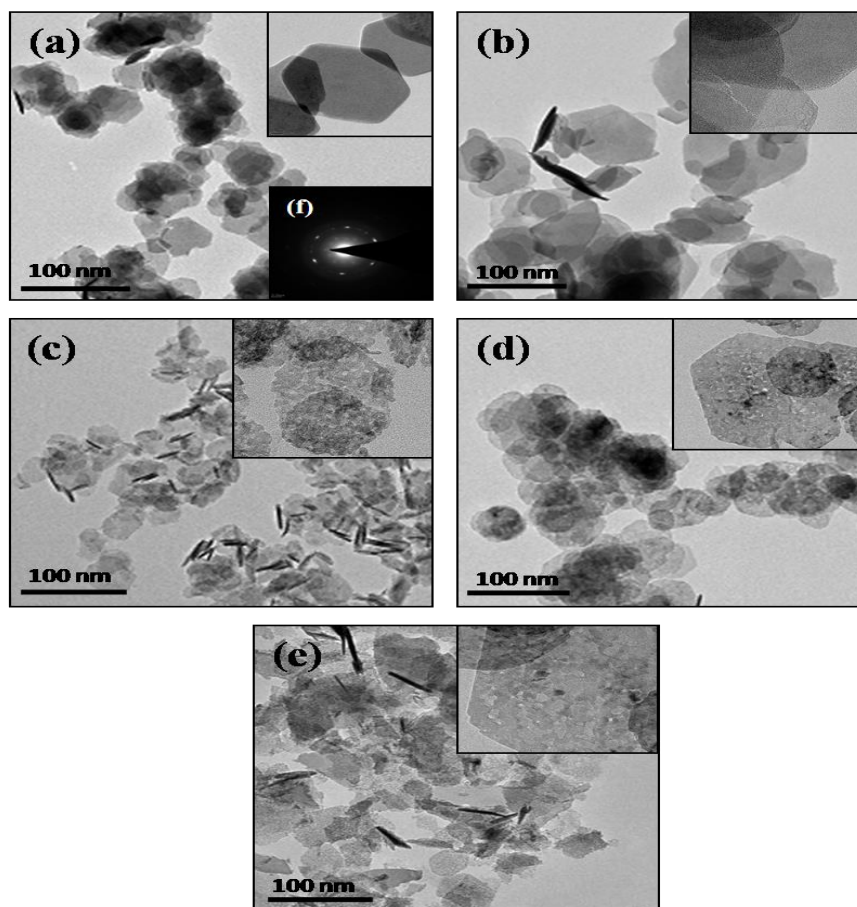


Figure 2B.8: TEM image of LiAl-HT calcined at different temperature (a) uncalcined LiAl-HT (f) SEAD image of LiAl-HT (b) Li-Al 300 (c) Li-Al 500 (d) Li-Al 700 (e) Li-Al 800

2B.8.4. CO₂ TPD analysis

The effect of calcination temperature (300-800°C) on the basic properties (CO₂-TPD) of LiAl-HT was also studied and the results are presented (Fig. 2B.9 and 10).

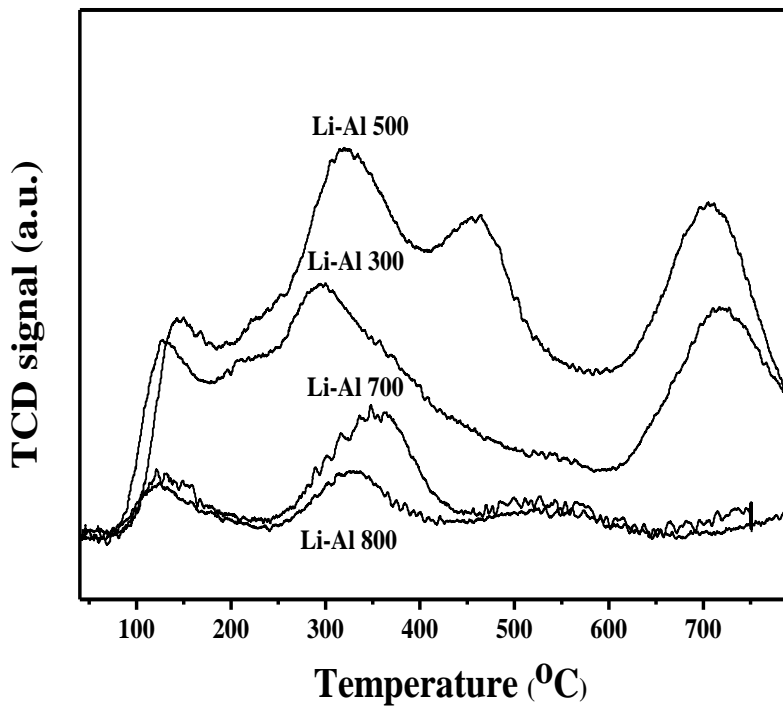


Figure 2B.9: CO₂-TPD of Li-Al HT calcined at different temperatures (300, 500, 700 and 800°C respectively)

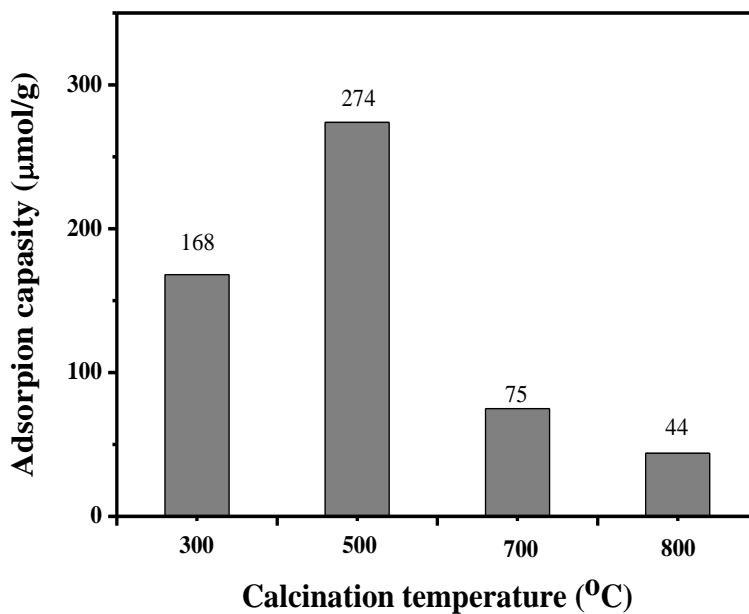
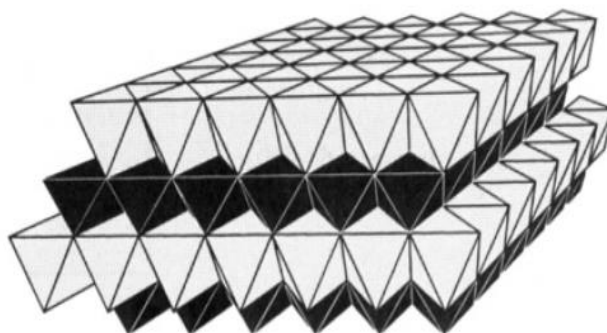


Figure 2B.10: The influence of calcination temperature on the CO₂ capture capacity

Li-Al calcined at 300°C showed 215 $\mu\text{mol/g}$ of basic sites. Basicity increased with the increase in calcination temperature up to 500°C (274 $\mu\text{mol/g}$), and then started to decrease with further increase in the calcination temperature from 700 to 800°C (75 and 44 $\mu\text{mol/g}$ respectively). According to literature reports the basicity of MMO is dependent on the calcination temperature.⁸¹ Constantino and Pinnavaia⁸² also observed that Mg_3Al_2 HT calcined at 500°C possessed higher amount of basic sites and basicity decreased significantly with increase in calcination temperature (>500°C) due to the formation of lower surface area spinel oxide phase.

A: (α - LiAlO_2) Octahedral structure



B: (β - LiAlO_2) Tetrahedral structure

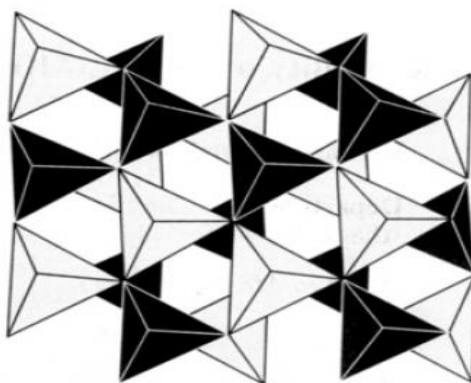


Figure 2B.11: A: Structure of Li-Al HT calcined at 500°C [Octahedral structure (α - LiAlO_2)] and B: calcined at 800°C [Tetrahedral structure (β - LiAlO_2)]^{79a}

According to literature report⁸⁰ Li-Al calcined at low temperature (500°C) forms α -LiAlO₂ phase, with a hexagonal structure. Calcination at a temperature in a range of 700-800°C results in the formation of β -LiAlO₂, with a orthorhombic structure, which is further converted to γ -LiAlO₂ phase having tetragonal structure at temperatures beyond 900°C.^{79a,80} For the α -LiAlO₂ (hexagonal structure) phase; all cations reside in octahedral 'O' environment and hence active centers (O²⁻) are available more at the edges and corners of the octahedra.^{79a} However in the case of β -LiAlO₂ with orthorhombic structure; all cations are present in the 'O' tetrahedra, which results in the lowest possibility of the availability of active sites on surface. The difference between both the structures is depicted in Fig. 2B.11. Thus 500°C was found to be the optimum temperature for decomposition of Li-Al HT to the crystalline α -LiAlO₂ (without formation of spinal phase) with high surface area, pore volume and presence of high amount of basic sites.

2B.8.5. Effect of calcination temperature on the activity

All the mixed metal oxides obtained by calcination of Li-Al HT were screened for transesterification of EC/PC and methanol to DMC and the results are presented in Table 2B.5. From the Table 2B.5 it was observed that catalyst activity was strongly influenced by a change in the calcination temperature. Thus EC/PC conversion increased with increase in calcination temperature up to 500°C and decreased with further increase in temperature (700-800°C). Among all calcined catalysts Li-Al 500 showed maximum EC (86%), PC (75%) conversion with very high DMC selectivity (for both systems 100% selectivity). The observed activity trend was found to be in good agreement with physicochemical properties of calcined catalysts presented earlier.

Table 2B.5: Effect of calcination temperature on the activity

Entry	Catalyst	Calcination temperature (°C)	PC + methanol system		EC + methanol system	
			PC conversion (%)	DMC selectivity (%)	EC conversion (%)	DMC selectivity (%)
1	LiAl-HT	-	30	92	41	95
2	Li-Al 300	300	57	100	72	100
3	Li-Al 500	500	75	100	86	100
4	Li-Al 700	700	49	97	63	99
5	Li-Al 800	800	28	95.2	52	98

Reaction conditions: PC/EC: 23 mmol, methanol: 230 mmol, PC/EC: MeOH: 1:10, catalyst: 2.5 wt% relative to PC/EC, reaction time: 1 h, temperature: 70 °C.

Based on the XRD, surface area, CO₂ TPD and TEM analysis Li-Al MMO calcined at 500°C was found to possess highest surface area, pore volume, high basic sites and α -LiAlO₂ phase. Also, thermogravimetric data reported in the literature^{73,79} indicate that elimination of CO₂ and H₂O is incomplete below 450°C. At higher calcination temperatures (700-800°C) formation of β -LiAlO₂ phase having very low surface area was observed. Li-Al calcined at 500°C was found to have highest surface area, pore volume, and basic sites compared to catalyst calcined at other temperatures (300, 700 and 800°C). Also, Li-Al 500 was present in the α -LiAlO₂ phase having maximum basic sites present on the surface. Best results were obtained with the Li-Al calcined at 500°C and hence further optimization work was carried out using this catalyst.

2B.9. Effect of reaction conditions

The effect of EC:MeOH molar ratio, reaction temperature and catalyst loading on the EC/PC conversion and DMC selectivity was investigated in detail using Li-Al 500 catalyst. All experiments in this study were carried out in a time range of 1-5h and DMC selectivity of 99-100% was observed in all experiments. Since selectivity was >99% for all the experiments; the results are presented in the form of conversion Vs time profiles under various reaction conditions.

2B.9.1. Effect of reaction temperature

The effect of reaction temperature on EC/PC conversion and selectivity was investigated by keeping other reaction conditions constant (Fig.2B.12 A and B).

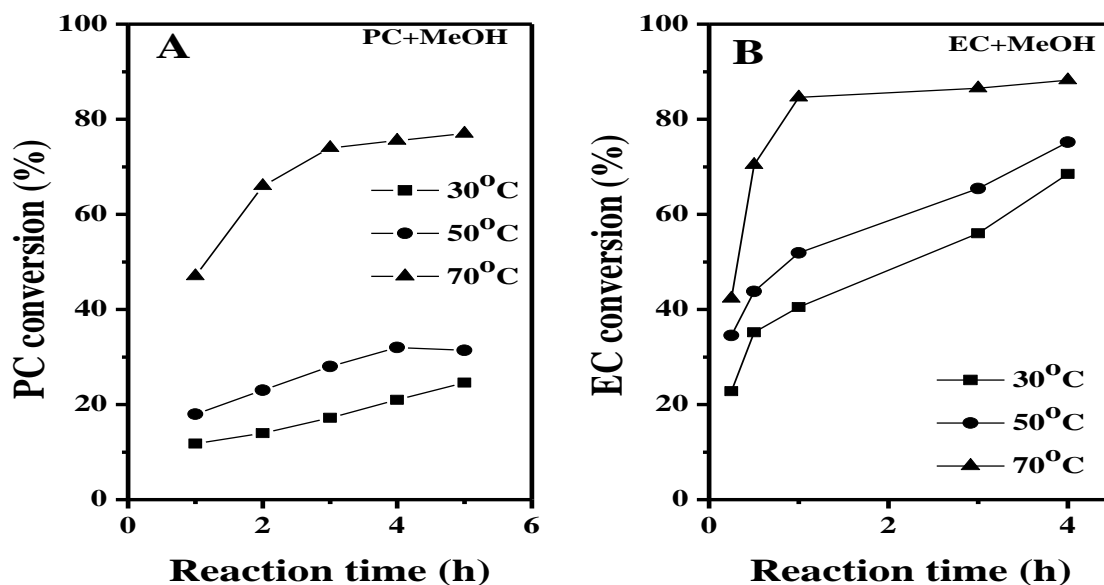


Figure 2B.12: Effect of reaction temperature on DMC yield (A) PC + MeOH system (B) EC+ MeOH system. DMC selectivity: 99-100%

Reaction conditions: EC: 23 mmol, PC: 23 mmol, MeOH: 230 mmol, EC/PC: MeOH: 1:10,

2B.9.2. Effect of EC/PC: MeOH molar ratio

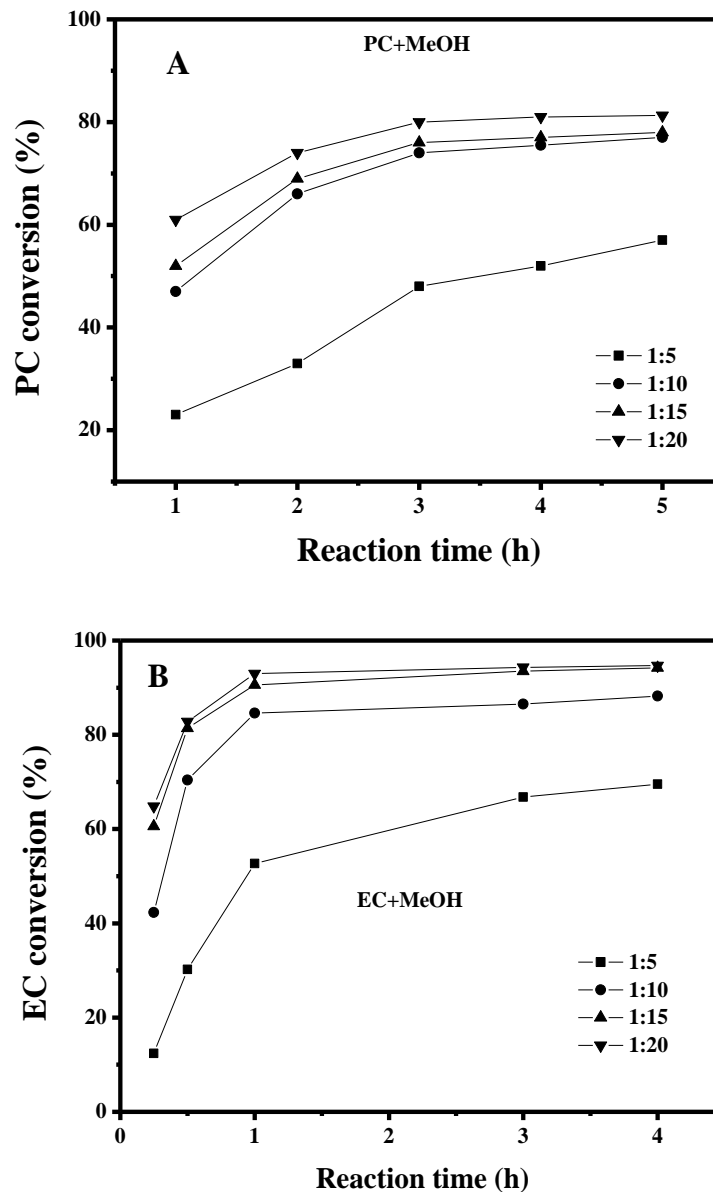


Figure 2B.13: Effect of Cyclic carbonate: MeOH molar ratio on DMC yield (A) PC + MeOH system (B) EC+ MeOH system

Reaction conditions: EC/PC: 23 mmol, PC/EC: MeOH: 1:5–1:20, catalyst: 2.5 wt% relative to PC/EC, reaction time: 0.25–5 h, temperature: 70 °C. DMC selectivity: 99–100%

From Fig.2B.13 it was observed that the PC/CH₃OH and EC/CH₃OH molar ratio had a significant impact on the transesterification reaction. Transesterification of PC/EC with methanol ($EC + MeOH \rightleftharpoons DMC + EG$) is an equilibrium controlled reaction and hence excess methanol is required to shift the equilibrium towards right and achieve high EC/PC conversion.^{16,22} PC conversion (48–75%) and EC conversion (67-88%) increased gradually with increase in the molar ratio of PC or EC /CH₃OH from 1:5 to 1:10 in 3h reaction time. Further increase in EC/PC:CH₃OH ratio from 1:15 to 1:20 had marginal effect on EC or PC conversion.

Thus optimum results (81% conversion of PC with 100% selectivity to DMC and 93% conversion of EC with 100% selectivity to DMC) were obtained at a EC/PC: methanol molar ratio of 1:10 at 70°C in 3 h reaction time.

2B.9.3. Effect of catalyst concentration

The effect of catalyst loading on EC or PC conversion is presented in Fig.2B.14. The activity was low at low catalyst loading and EC conversion of 71% and PC conversion of 17% was observed in 1 h. EC or PC conversion increased with reaction time and EC conversion of 82% and PC conversion of 64% was observed in 3 h. Activity increase with increase in catalyst loading and PC conversion increased from 64 to 75% and EC conversion increased from 82 to 86% in 3 h with increase in catalyst loading from 1.25-2.5 wt%. Further increase in catalyst loading to 5 wt% had marginal effect on EC or PC conversion in 3 h. DMC selectivity was very high (>99%) in all the experiments. The performance observed is mainly because of the higher availability of active catalytic sites with increasing the catalyst loading.

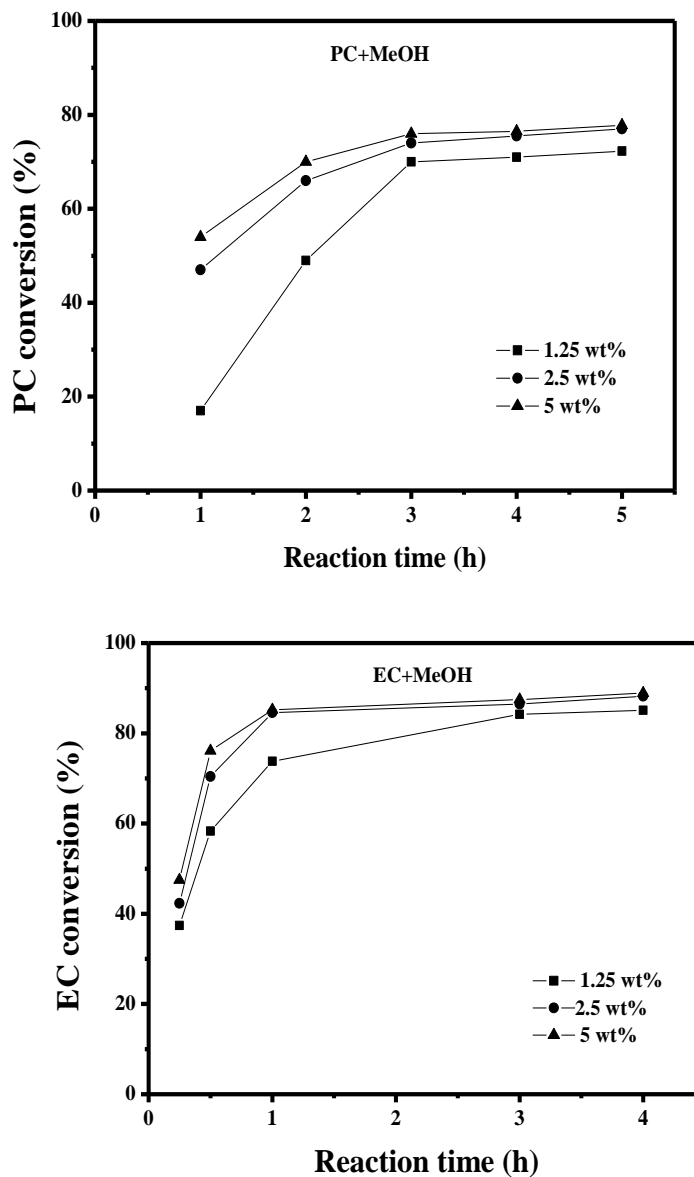


Figure 2B.14 Effect of catalyst concentration on conversion (A) PC + MeOH system (B) EC+ MeOH system

Reaction conditions: EC: 23mmol, PC: 23mmol, PC/EC: MeOH: 1:10, catalyst: 1.25-5 wt% relative to PC/EC, reaction time: 0.25-5 h, temperature: 70 °C.

DMC selectivity = 99-100%

2B.9.4. Effect of reaction time

From the optimization of reaction conditions it was observed that the best results were obtained with catalyst loading of 2.5 wt%, reaction temperature of 70 °C and PC/EC: CH₃OH molar ratio of 1:10. Finally effect of reaction time on PC/EC conversion under optimized reaction conditions using Li-Al500 catalyst is presented in Figure 2B.15. EC/PC conversion increased with increasing reaction time reaching a maximum of 78.6-90 % at 70°C in 4h reaction time for PC and EC respectively.

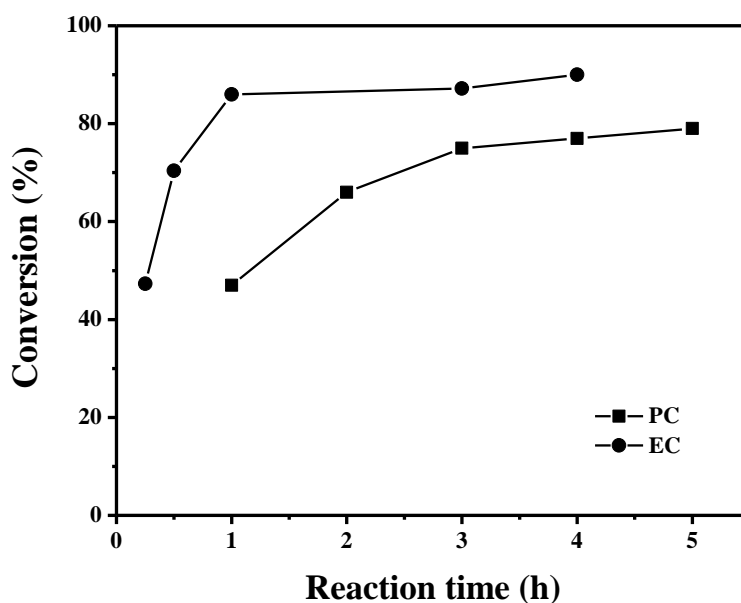


Figure 2B.15: Effect of reaction time on PC and EC conversion

Reaction conditions: PC/EC: 23 mmol, PC/EC: MeOH: 1:10, catalyst: 2.5wt% relative to PC/EC, reaction time: 0.25-5 h, temperature: 70 °C.

*DMC selectivity remains 99-100%

After the optimization of reaction conditions for PC and EC reaction system catalyst recycle study was carried out to know the stability of the catalyst. Based on the literature reports and results obtained possible reaction mechanism has been proposed with EC and methanol as

reactants. Various alcohols were screened with EC and Li-Al 500 catalyst and the results are presented below.

2B.10. Catalyst recycle study

After effect of reaction time on activity under optimization of reaction conditions, stability of the catalyst was tested by carrying out recycle study. For this purpose transesterification of EC with methanol was carried out as usual. Reaction mixture was cooled to room temperature and catalyst from reaction mixture was separated by filtration. Filtered catalyst was washed two times with methanol and dried at 100°C for 12h. The dried catalyst was activated at 500°C for 2h. Recycle experiment was carried out by using activated catalyst, EC to DMC in usual way. Five recycle experiments were carried out using the same procedure. EC: methanol molar ratio of 1:10 was maintained in the recycle experiments.

Table 2B.6 Recycle study using Li-Al 500 as catalyst.

Recycle number	EC conversion (%)	DMC selectivity (%)
1(fresh)	86	100
2	82	99.8
3	82.2	100
4	81	99.7
5	81.6	99.8
6	81	99.6

Reaction conditions: EC: 23 mmol, MeOH: 230 mmol EC: MeOH: 1:10, Li-Al 500: 2.5wt% relative to EC, reaction time: 1 h, temperature: 70 °C.

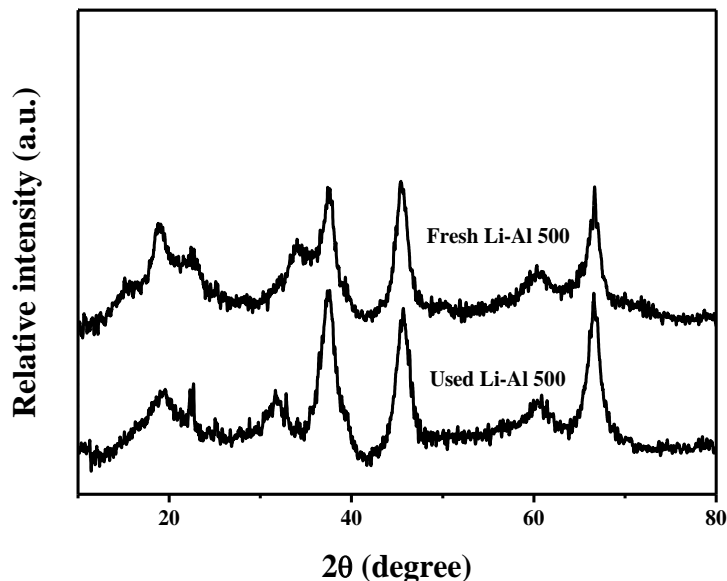


Figure 2B.16: XRD patterns of used and fresh Li-Al 500 catalyst

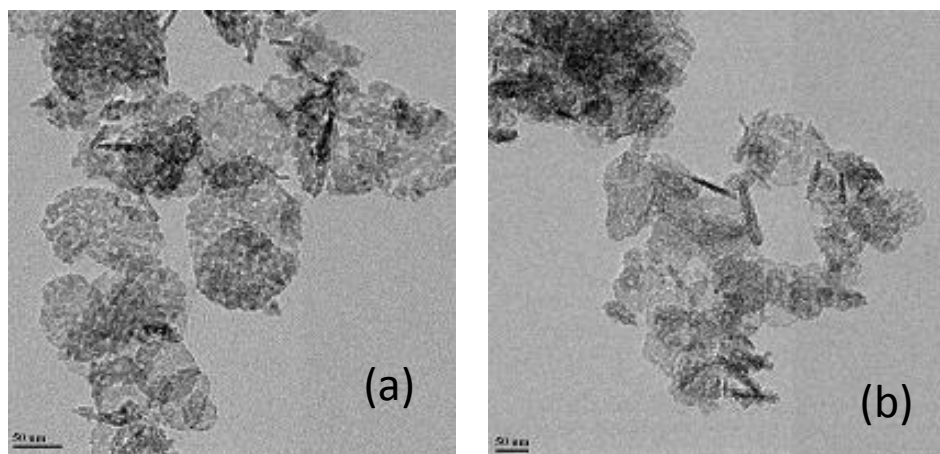


Figure 2B.17: TEM images of (a) fresh (b) used Li-Al 500 catalyst

From the results it was observed that the catalyst activity was good during 5 recycle experiments giving 86 % DMC yield in first recycle experiments with slight drop in DMC yield to 82 % in second recycle, which remained constant till 5th recycle (Table 2B.6). Results clearly show high stability of the catalyst in the recycle experiments. At the end of the 5 recycle experiments the XRD (Fig.2B.16) and TEM (Fig.2B.17) analysis of the used catalyst was carried out. No change

in the XRD pattern and morphology in TEM image were observed for used catalyst indicating high stability during recycle.

2B.11. Screening of different alcohols for transesterification of EC

Li-Al 500 was also active for the synthesis of other dialkyl carbonates by reaction of EC with different alcohols (Table 2B.7). The yield of dialkyl carbonates decreased with increasing chain length of the alkyl group in the alcohol. This difference in reactivity was due to difference in the pKa value of different alcohols.¹⁶ The pKa values for different alcohols increase with increasing chain length of the alkyl group.¹ Methanol being more acidic (low pKa), forms alkoxide species more readily than the other alcohols and leads to higher yield of dialkyl carbonate (DMC).

Table 2B.7: Dialkyl carbonate synthesis by transesterification of ethylene carbonate (EC) with different alcohols using Li-Al 500 catalyst^a

Entry	Alcohol	Dialkyl carbonate yield (%)	TOF (h ⁻¹)
1	Methanol	87	33.99
2	Ethanol	84	33.74
3	n-Propanol	82.3	33
4	n-Butanol	82.5	33.1
5	n-Pentanol	81.6	32.7
6	n-Hexanol	81	32.5

^aReaction conditions: EC = 23 mmol, alcohol: 230 mmol EC: alcohol = 1:10, catalyst = Li-Al500 (2.5wt% of EC), reaction temperature: reflux temperature of alcohol, and reaction time: 1h.

Dialkyl carbonate selectivity: 99.5-100%

2B.12. Proposed reaction mechanism

On the basis of the catalyst characterization and activity results discussed above and literature reports,^{22,72} a possible mechanistic pathway for the reaction of EC and methanol to DMC is depicted in Fig. 2B.18.

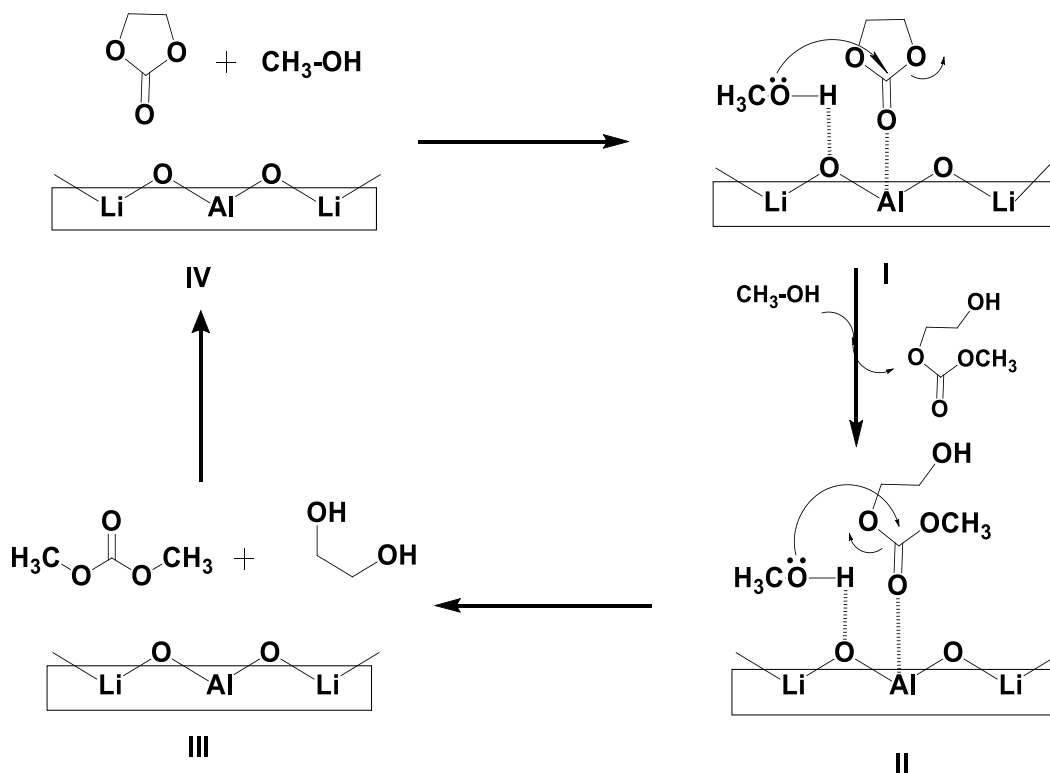


Figure 2B.18: A possible mechanism for the transesterification of ethylene carbonate with methanol catalyzed by Li-Al 500.

It is proposed that the reaction is initiated by adsorption of methanol on the Lewis basic sites to form a methoxide species, and independently, an EC is coordinated on the neighbouring acid site on the surface to generate relatively charge carbonyl carbon (Fig. 2B.18, Step I). Ring opening of coordinated EC by nucleophilic attack of methoxide species, leads to the formation of 2-HEMC intermediate (Fig. 2B.18, Step II). In next step (Fig. 2B.18, Step III) another methanol molecule

attacks in similar fashion to form DMC and EG as the final products and the catalyst is regenerated back (Fig. 2B.18, Step IV). Li-Al 500 has good catalytic activity compared to other metal oxides and mixed metal oxides. Probably the cooperative effect of both acidic and basic sites present on the catalyst surface (in vicinity) is responsible for the high activity observed with Li-Al 500 catalyst.

2B.13. DMC synthesis from PC/EC and methanol: Comparison with the literature reports

Activity of Li-Al 500 as catalyst was very good under reflux conditions with EC/PC as the reactants. From the literature it was observed that for most of the catalysts higher temperature was required to achieve good EC/PC conversion and DMC selectivity. Table 2B.8 presents comparison of the activity obtained with Li-Al 500 with other MMOs used as catalyst in the literature. Since the temperature and reaction time used are different the reaction conditions are also mentioned in the Table.2B.8. Catalytic activity of Li-Al 500 was found to be superior compared to the most of the reported solid catalysts (Table 2B.8) under mild reaction conditions. Recently Li et al.²⁰ studied Graphitic carbon nitride (g-C₃N₄) supported MgO for EC to DMC reaction and 81% EC conversion with 87% DMC selectivity was achieved at high reaction temperature (140°C) under 0.6 MPa CO₂ pressure. Reaction was carried out in the presence of CO₂ to avoid decomposition of DMC / PC at higher temperature. Binary and ternary MMOs showed 55-72% PC conversion with 92-96 % DMC selectivity (Table 2B.8, Entry 2-5),^{15, 68-70} however, high temperature (117-170°C) was necessary to achieve the result.

Table 2B.8: DMC synthesis from PC/EC and methanol: Comparison with the literature reports

Entry	Catalyst	PC conversion (%)	DMC selectivity (%)	Reaction time (h)	Reaction temperature (°C)	TOF (h ⁻¹)	Ref.
1 ^{a,b}	MgO/g-C ₃ N ₄ (5 wt%)	81	87	4	140	4.45	20
2	CaO-ZrO ₂	55	95	4	117	-	68
3	Cu-Zn-Al (3 wt %)	70.6	92.4	4	160	5.99	15
4	Ce-Cu (5 wt%)	65.4	93	4	160	3.4	69
5	Ce-La (5 wt%)	72	96	6	170	-	70
6	Mg-Al-La (10 w%)	35	89	4	100	33	16
		89 ^b	98	4	80	1.19	
7	Mesoporous CeO ₂ (5 wt%)	18	91	2	140	2.3	71
		76 ^b	92	2	140	8.36	
8	Hydrotalcite Mg-Al=1:5 (2.5 wt%)	72	97	4	130	7.4	22
		82 ^b	98.6	4	80	7.2	
9	Na ₂ WO ₄ .2H ₂ O (20 wt%)	54 ^a	90	4	150 ^a	0.7	72
		83 ^b	100	5	50	0.6	
10	Li-Al cal (2.5 wt%)	74	100	3	70	9.99	This work
11	Li-Al cal (2.5 wt%)	85 ^b	100	1	70	33.99	This work

^aCO₂ pressure: 0.6 MPa^b EC

From the Table 2B.8, Entry 6-9 it was observed that the activity of catalyst was lower with PC as reactant under similar reaction conditions. Thus PC conversion of 18-72% with 89-97% selectivity to DMC was obtained compared to 76-89% EC conversion with 92-100% DMC selectivity under similar reaction conditions.^{16,21,71,72} It may be noted that in some examples high EC conversion was observed at lower temperatures compared to that used for PC as reactant (Table 2B.8, Entry 6,8,9). Thus results obtained with Li-Al 500 catalyst are better than literature reports with PC and EC as reactants.

2B.14. Conclusion

A series of single- and mixed-metal oxides, derived from hydrotalcite precursors, consisting of metal cations (Mg, Li, Zn, Ni, Co and Al) were synthesized with the aim of modifying the acid-base properties. These materials were tested for transesterification of EC/PC with methanol. The binary MMOs were found to be active than single metal oxides and the activity increased in the order: Ni-Al 500 < Co-Al 500 < Zn-Al 500 < Mg-Al 500 < Li-Al 500. The Catalytic activity towards PC was found to be low as compared to that for EC in all cases. This difference in activity may be due to steric hindrance associated with the bulky methyl group in PC as compared with the symmetrical EC. Among several metal oxide catalysts screened in this work, Li-Al 500 showed the highest EC/PC conversion (86 and 75% respectively with 100% selectivity to DMC). Results obtained in the present work with Li-AL 500 catalyst can also be attributed to the presence of higher amount of moderate and strong basic sites and high surface area of Li-Al 500. Calcination temperature had significant influence on the activity and best results were obtained with Li-Al 500 catalyst. Activity decreased with increase in temperature beyond 500°C. The trend of activity was: Li-Al 300 < Li-Al 500 > Li-Al 700 > Li-Al 800. Li-Al 500 was active

towards transesterification of EC and various aliphatic alcohols to corresponding dialkylcarbonates. The Li-Al 500 was highly stable and gave good performance for 5 recycle experiments with slight drop in activity.

2B.15. Overall Conclusion

Transesterification of EC/PC was investigated using MgFeCe ternary hydrotalcite and Li-Al 500 mixed metal oxide as catalysts. Catalysts were prepared based on the literature known methods and characterized in detail by various spectroscopic and other techniques. The activity of catalysts was found to be very high with very high selectivity to DMC. Stability of the catalyst was very good as found from the recycle study. Highlights of the work are as follows:

2A. Synthesis of dimethyl carbonate by transesterification of EC with methanol using MgFeCe ternary Layered double hydroxide (LDH) catalyst

- ❖ MgFeCe ternary LDHs were prepared based on literature method and characterized in detail by various spectroscopic techniques.
- ❖ Molar ratio of Fe:Ce (Keeping molar ratio of Mg:Fe+Ce constant at 3:1) had significant influence on catalytic activity as well as surface and base properties of the LDH.
- ❖ Best catalytic performance (87% EC conversion with 100% DMC selectivity) was obtained with $Mg_3Fe_{0.85}Ce_{0.15}$ as the catalyst.

- ❖ Both the end members of this series Mg_3Fe_1 (LDH-1) and Mg_3Ce_1 (LDH-6) showed lower catalytic activity and selectivity to DMC.
- ❖ Various trivalent metals were also used to modify the LDH with composition $\text{Mg}_3\text{Fe}_{0.85}\text{M}_{0.15}$ [where $\text{M}^{3+} = \text{La}, \text{Sm}, \text{Y}$ and Cr] and the activity trend followed in order of $\text{La} \approx \text{Ce} > \text{Sm} > \text{Y} > \text{Cr}$. The results were found to be in good agreement with the electronegativities of incorporated third metal cations [M^{3+}].
- ❖ $\text{Mg}_3\text{Fe}_{0.85}\text{Ce}_{0.15}$ was recycled seven times showing high activity and maintaining high selectivity to DMC. XRD analysis after seven recycles indicated that the structure was intact after reuse.
- ❖ To the best of our knowledge this is the first report on the use of ternary LDH ($\text{Mg}_3\text{Fe}_{0.85}\text{Ce}_{0.15}$) as a catalyst with high activity, selectivity and stability at milder reaction conditions for this reaction.

2B. Synthesis of dimethyl carbonate by transesterification of cyclic carbonate (EC/PC) with methanol using Li-Al mixed metal oxide catalyst

- ❖ A series of metal oxides and mixed metal oxides were prepared from hydrotalcite like precursors consisting of Mg, Li, Zn, Co, Ni and Al.
- ❖ Very good results were obtained with Li-Al mixed metal oxide. Effect of calcinations temperature on the activity and selectivity was investigated and best results (86% conversion of EC with 100% selectivity to DMC at 70°C in 1 h) were obtained with mixed metal oxide calcined at 500°C (Li-Al 500) as catalyst.

- ❖ Li-Al 500 gave 75% conversion of PC with 100% selectivity to DMC at 70°C in 3 h. This is one of the best results for synthesis of DMC from PC and methanol under mild reaction conditions.
- ❖ Li-Al 500 was characterized in detail by various spectroscopic techniques. XRD analysis indicated the formation of α -LiAlO₂ phase on calcinations at 500°C. High activity observed with Li-Al 500 was attributed to the presence of higher amount of moderate and strong basic sites and high surface area of Li-Al 500.
- ❖ Li-Al 500 was highly stable and gave good performance for 5 recycle experiments with slight drop in activity.

2B.15. References

1. Huang, S., et al., *Recent advances in dialkyl carbonates synthesis and applications*. Chemical Society Reviews. **44**(10): p. 3079-3116. (1a). Fiorani, G., A. Perosa, and M. Selva, *Dimethyl carbonate: a versatile reagent for a sustainable valorization of renewables*. Green Chemistry. 2018.**20**:p. 288-322.
2. Tundo, P. and M. Selva, *The chemistry of dimethyl carbonate*. Accounts of chemical research, 2002. **35**(9): p. 706-716.
3. Shaikh, A.-A.G. and S. Sivaram, *Organic carbonates*. Chemical reviews, 1996. **96**(3): p. 951-976.
4. Pacheco, M.A. and C.L. Marshall, *Review of dimethyl carbonate (DMC) manufacture and its characteristics as a fuel additive*. Energy & Fuels, 1997.**11**(1): p. 2-29.
5. Babad, H. and A.G. Zeiler, *Chemistry of phosgene*. Chemical reviews, 1973. **73**(1): p. 75-91.
6. Drake, I.J., et al., *Dimethyl carbonate production via the oxidative carbonylation of methanol over Cu/SiO₂ catalysts prepared via molecular precursor grafting and chemical vapor deposition approaches*. Journal of Catalysis, 2005.**230**(1): p. 14-27.
7. Fukuoka, S., et al., *Green and sustainable chemistry in practice: development and industrialization of a novel process for polycarbonate production from CO₂ without using phosgene*. Polymer journal, 2007.**39**(2): p. 91.
8. Fakhnasova, D., et al., *Rational and statistical approaches in enhancing the yield of ethylene carbonate in urea transesterification with ethylene glycol over metal oxides*. ACS Catalysis. **5**(11): p. 6284-6295.

9. Yang, Z.-Z., et al., *Dimethyl carbonate synthesis catalyzed by DABCO-derived basic ionic liquids via transesterification of ethylene carbonate with methanol*. *Tetrahedron Letters*. **51**(21): p. 2931-2934.
10. Wang, J.-Q., et al., *Synthesis of dimethyl carbonate catalyzed by carboxylic functionalized imidazolium salt via transesterification reaction*. *Catalysis Science & Technology*. **2**(3): p. 600-605.
11. Xu, J., et al., *Ionic liquid immobilized on mesocellular silica foam as an efficient heterogeneous catalyst for the synthesis of dimethyl carbonate via transesterification*. *Applied Catalysis A: General*. **464**: p. 357-363.
12. Kim, D.-W., et al., *Production of dimethyl carbonate from ethylene carbonate and methanol using immobilized ionic liquids on MCM-41*. *Catalysis today*. **164**(1): p. 556-560.
13. Bhanage, B.M., et al., *Synthesis of dimethyl carbonate and glycols from carbon dioxide, epoxides, and methanol using heterogeneous basic metal oxide catalysts with high activity and selectivity*. *Applied Catalysis A: General*, 2001. **219**(1-2): p. 259-266.
14. Murugan, C. and H.C. Bajaj, *Mg/La mixed oxide as catalyst for the synthesis of dimethyl carbonate from cyclic carbonates and methanol*.
15. Kumar, P., V.C. Srivastava, and I.M. Mishra, *Dimethyl carbonate synthesis from propylene carbonate with methanol using CuZnAl catalyst*. *Energy & Fuels*. **29**(4): p. 2664-2675.
16. Unnikrishnan, P. and D. Srinivas, *Highly active and reusable ternary oxide catalyst for dialkyl carbonates synthesis*. *Journal of Molecular Catalysis A: Chemical*, 2015. **398**: p. 42-49.

17. Sankar, M., S. Satav, and P. Manikandan, *Transesterification of cyclic carbonates to dimethyl carbonate using solid oxide catalyst at ambient conditions: environmentally benign synthesis*. *ChemSusChem*.**3**(5): p. 575-578.
18. Bhanage, B.M., et al., *Synthesis of dimethyl carbonate and glycols from carbon dioxide, epoxides and methanol using heterogeneous Mg containing smectite catalysts: effect of reaction variables on activity and selectivity performance*. *Green Chemistry*, 2003.**5**(1): p. 71-75.
19. Tatsumi, T., Y. Watanabe, and K.A. Koyano, *Synthesis of dimethyl carbonate from ethylene carbonate and methanol using TS-1 as solid base catalyst*. *Chemical Communications*, 1996(19): p. 2281-2282.
20. Xu, J., et al., *Simple preparation of MgO/g-C₃N₄ catalyst and its application for catalytic synthesis of dimethyl carbonate via transesterification*. *Catalysis Communications*.**95**: p. 72-76.
21. Cavani, F., F. Trifira and A. Vaccari, *Hydrotalcite-type anionic clays: Preparation, properties and applications*. *Catalysis today*, 1991.**11**(2): p. 173-301. (21a) Nishimura, S., A. Takagaki, and K. Ebitani, *Characterization, synthesis and catalysis of hydrotalcite-related materials for highly efficient materials transformations*. *Green Chemistry*.**15**(8): p. 2026-2042.
22. Murugan, C. and H.C. Bajaj, *Transesterification of propylene carbonate with methanol using Mg-Al-CO₃ hydrotalcite as solid base catalyst*. *Indian journal of chemistry*, 2010.**49**, p:1182-1188. (22a) Watanabe, Y. and T. Tatsumi, *Hydrotalcite-type materials as catalysts for the synthesis of dimethyl carbonate from ethylene carbonate and methanol*. *Microporous and mesoporous materials*, 1998.**22**(1-3): p. 399-407.

23. Cantrell, D.G., et al., *Structure-reactivity correlations in MgAl hydrotalcite catalysts for biodiesel synthesis*. Applied Catalysis A: General, 2005.**287**(2): p. 183-190.(23a)Jana, S.K., P. Wu, and T. Tatsumi, *NiAl hydrotalcite as an efficient and environmentally friendly solid catalyst for solvent-free liquid-phase selective oxidation of ethylbenzene to acetophenone with 1 atm of molecular oxygen*. Journal of Catalysis, 2006.**240**(2): p. 268-274.
24. Pavel, O.D., et al., *The activity of yttrium-modified Mg, Al hydrotalcites in the epoxidation of styrene with hydrogen peroxide*. Applied Catalysis A: General. **403**(1-2): p. 83-90.
25. Kuang, Y., et al., *Morphologies, preparations and applications of layered double hydroxide micro-/nanostructures*. Materials. **3**(12): p. 5220-5235.
26. Stanjek, H. and W. Husler, *Basics of X-ray Diffraction*. Hyperfine Interactions, 2004.**154**(1-4): p. 107-119.
27. Phillips, D., *William Lawrence Bragg, 31 March 1890-1 July 1971*. 1979, The Royal Society.
28. Pistorius, A.M.A., *Biochemical applications of FT-IR spectroscopy*. 1996: [SI: sn].
29. Trombetta, M., et al., *FT-IR Studies on Light Olefin Skeletal Isomerization Catalysis: III. Surface Acidity and Activity of Amorphous and Crystalline Catalysts Belonging to the $\text{SiO}_2\text{Al}_2\text{O}_3$ System*. Journal of Catalysis, 1998.**179**(2): p. 581-596.
30. Ferraro, J.R. and L.J. Basile, *Fourier transform infrared spectra: applications to chemical systems*: Academic Press.
31. Brunauer, S., P.H. Emmett, and E. Teller, *Adsorption of gases in multimolecular layers*. Journal of the American chemical society, 1938.**60**(2): p. 309-319.

32. Brunauer, S., et al., *On a theory of the van der Waals adsorption of gases*. Journal of the American chemical society, 1940.**62**(7): p. 1723-1732.
33. Anderson, R.B. and W.K. Hall, *Modifications of the Brunauer, Emmett and Teller Equation III*. Journal of the American chemical society, 1948.**70**(5): p. 1727-1734.
34. Tanabe, K., et al., *New solid acids and bases: their catalytic properties*. Vol. 51. 1990: Elsevier.
35. Benesi, H.A., *Acidity of catalyst surfaces. II. Amine titration using Hammett indicators*. The Journal of Physical Chemistry, 1957.**61**(7): p. 970-973.
36. Yamanaka, T. and K. Tanabe, *New determination of acid-base strength distribution of a common scale on solid surfaces*. The Journal of Physical Chemistry, 1975.**79**(22): p. 2409-2411.
37. Fraile, J.M., et al., *The influence of alkaline metals on the strong basicity of MgAl mixed oxides: the case of transesterification reactions*. Applied Catalysis A: General, 2009.**364**(1-2): p. 87-94.
38. Williams, D.B. and C.B. Carter, *The transmission electron microscope*, in *Transmission electron microscopy*. 1996, Springer. p. 3-17.
39. Stefanaki, E.-C., *Electron microscopy: the basics*. Physics of advanced materials winter school, 2008: p. 1-11.
40. Winge, R.K., V.J. Peterson, and V.A. Fassel, *Inductively coupled plasma-atomic emission spectroscopy: prominent lines*. Applied Spectroscopy, 1979.**33**(3): p. 206-219.
41. Boumans, P., *Inductively coupled plasma-atomic emission spectroscopy: Its present and future position in analytical chemistry ICP-AES: Gegenwärtige und zukünftige Stellung in*

- der Analytischen Chemie*. Fresenius' Zeitschrift Analytische Chemie, 1979.**299**(5): p. 337-361.
42. Andrade, J.D., *X-ray photoelectron spectroscopy (XPS)*, in *Surface and interfacial aspects of biomedical polymers*. 1985, Springer. p. 105-195.
43. Shirley, D.A., *High-resolution X-ray photoemission spectrum of the valence bands of gold*. Physical Review B, 1972.**5**(12): p. 4709.
44. Bookin, A.S. and V.A. Drits, *Polytype diversity of the hydrotalcite-like minerals. I. Possible polytypes and their diffraction features*. Clays and Clay Minerals, 1993.**41**(5): p. 551-557.
45. Bellotto, M., et al., *A reexamination of hydrotalcite crystal chemistry*. The Journal of Physical Chemistry, 1996.**100**(20): p. 8527-8534.
46. Forano, C., et al., *Layered double hydroxides (LDH)*, in *Developments in clay science*, Elsevier. p. 745-782.
47. Triantafyllidis, K.S., et al., *Iron-modified hydrotalcite-like materials as highly efficient phosphate sorbents*. Journal of colloid and interface science. **342**(2): p. 427-436.
48. Peng, F., T. Luo, and Y. Yuan, *Controllable synthesis of MgFe layered double hydroxide nanoplates with specific Mg/Fe ratios and their effect on adsorption of As (V) from water*. New Journal of Chemistry.**38**(9): p. 4427-4433.
49. Wang, D., et al., *La-modified mesoporous MgAl mixed oxides: effective and stable base catalysts for the synthesis of dimethyl carbonate from methyl carbamate and methanol*. Catalysis Science & Technology. **6**(5): p. 1530-1545.
50. Tang, K., et al., *Construction of Ce (OH) 4 nanostructures from 1D to 3D by a mechanical force-driven method*. CrystEngComm.**17**(13): p. 2690-2697.

51. Ansari, A.A., *Optical and structural properties of solgel derived nanostructured CeO₂ film*. Journal of semiconductors. **31**(5): p. 053001.
52. Wang, Z., et al., *Reconstructed La-, Y-, Ce-modified MgAl-hydrotalcite as a solid base catalyst for aldol condensation: Investigation of water tolerance*. Journal of Catalysis.**318**: p. 108-118.
53. Pavel, O.D., et al., *The activity of yttrium-modified Mg, Al hydrotalcites in the epoxidation of styrene with hydrogen peroxide*. Applied Catalysis A: General.**403**(1-2): p. 83-90.
54. Zhao, Y., et al., *Structure and luminescence behaviour of as-synthesized, calcined, and restored MgAlEu-LDH with high crystallinity*. Dalton Transactions.**41**(39): p. 12175-12184.
55. Caravaggio, G.A., C. Detellier, and Z. Wronski, *Synthesis, stability and electrochemical properties of NiAl and NiV layered double hydroxides*. Journal of Materials Chemistry, 2001.**11**(3): p. 912-921.
56. Jun, H., et al., *Effect of metal composition in lanthanum-doped ferric-based layered double hydroxides and their calcined products on adsorption of arsenate*. RSC Advances.**4**(10): p. 5156-5164.
57. Perez, M.R., et al., *Influence of divalent metal on the decomposition products of hydrotalcite-like ternary systems Mg-Al-Cr (MII= Zn, Cd)*. Materials Chemistry and Physics.**132**(2-3): p. 375-386.
58. Baliarsingh, N., L. Mohapatra, and K. Parida, *Design and development of a visible light harvesting Ni-Zn-Cr CO₃² LDH system for hydrogen evolution*. Journal of Materials Chemistry A. **1**(13): p. 4236-4243.

59. Zhang, W.H., et al., *Preparation of Ni (II)/Ti (IV) layered double hydroxide at high supersaturation*. Journal of the European Ceramic Society, 2008.**28**(8): p. 1623-1629.
60. Navajas, A., et al., *Synthesis of biodiesel from the methanolysis of sunflower oil using PURALMgAlhydrotalcites as catalyst precursors*. Applied Catalysis B: Environmental. **100**(1-2): p. 299-309.
61. Xi, Y. and R.J. Davis, *Influence of water on the activity and stability of activated MgAlhydrotalcites for the transesterification of tributyrin with methanol*. Journal of Catalysis, 2008.**254**(2): p. 190-197.
62. Hu, Z., et al., *Effect of ceria crystal plane on the physicochemical and catalytic properties of Pd/ceria for CO and propane oxidation*. ACS Catalysis. **6**(4): p. 2265-2279.
63. Parida, K., M. Satpathy, and L. Mohapatra, *Incorporation of Fe³⁺ into Mg/Al layered double hydroxide framework: effects on textural properties and photocatalytic activity for H₂ generation*. Journal of Materials Chemistry.**22**(15): p. 7350-7357.
64. Rives, V., et al., *Synergistic effect in the hydroxylation of phenol over CoNiAl ternary hydrotalcites*. Journal of Catalysis, 2003.**220**(1): p. 161-171.
65. Roeffaers, M.B.J., et al., *Spatially resolved observation of crystal-face-dependent catalysis by single turnover counting*. Nature, 2006.**439**(7076): p. 572.
66. Greenwell, H.C., et al., *A density functional theory study of catalytic trans-esterification by tert-butoxide MgAl anionic clays*. The Journal of Physical Chemistry B, 2003.**107**(15): p. 3476-3485.
67. Vadrine, J.C., *Heterogeneous Catalysis on Metal Oxides*. Catalysts, 2017.**7**(11): p. 341

68. Wang, H., et al., *Influence of preparation methods on the structure and performance of CaOZrO₂ catalyst for the synthesis of dimethyl carbonate via transesterification*. Journal of Molecular Catalysis A: Chemical, 2006. **258**(1-2): p. 308-312.
69. Kumar, P., V.C. Srivastava, and I.M. Mishra, *Dimethyl carbonate synthesis by transesterification of propylene carbonate with methanol: Comparative assessment of Ce-M (M= Co, Fe, Cu and Zn) catalysts*. Renewable Energy, 2016. **88**: p. 457-464.
70. Kumar, P., V.C. Srivastava, and I.M. Mishra, *Synthesis and characterization of CeLa oxides for the formation of dimethyl carbonate by transesterification of propylene carbonate*. Catalysis Communications, 2015. **60**: p. 27-31.
71. Xu, J., et al., *Efficient synthesis of dimethyl carbonate via transesterification of ethylene carbonate over a new mesoporous ceria catalyst*. Applied Catalysis A: General, 2014. **484**: p. 1-7.
72. Sankar, M., et al., *Transesterification of cyclic carbonates with methanol at ambient conditions over tungstate-based solid catalysts*. Applied Catalysis A: General, 2006. **312**: p. 108-118.
73. Shumaker, J. L. et al. *Biodiesel synthesis using calcined layered double hydroxide catalysts* Applied Catalysis B: Environmental, 2008. **82**: p. 120–130.
74. Jiang P. et al, *Transesterification of Soybean Oil with Ethylene Glycol Catalyzed by Modified Li-Al Layered Double Hydroxides*. Chem. Eng. Technol. 2013, **36**,8:p. 1371–1377.
75. Rosseinsky J. et.al, *Selective conversion of 5-hydroxymethylfurfural to cyclopentanone derivatives over Cu–Al₂O₃ and Co–Al₂O₃ catalysts in water*, Green Chem., 2017, 19,1701.

76. Urakawa A et al. *Rational and Statistical Approaches in Enhancing the Yield of Ethylene Carbonate in Urea Transesterification with Ethylene Glycol over Metal Oxides*, *ACS Catal.* 2015, **5**, 6284–6295.
77. Xiao G. et al. High-efficiency and low-cost Li/ZnO catalysts for synthesis of glycerol carbonate from glycerol transesterification: The role of Li and ZnO interaction *Applied Catalysis A: General*, 2017. 532 : p. 77–85.
78. Li F. et al. *Structure and Catalytic Property of Li-Al Metal Oxides from Layered Double Hydroxide Precursors Prepared via a Facile Solution Route*, *Ind. Eng. Chem. Res.*, 2011. 50, 7120–7128.
79. Corma A. et al. *Lewis and Brønsted basic active sites on solid catalysts and their role in the synthesis of monoglycerides*, *Journal of Catalysis*, 2005. 234 :p.340–347.79a)
Jhonskowski R. et al. *Reactivity and Acidity of Li in LiAlO₂ Phases*, *Inorganic Chemistry*. 1993, Vol. 32, p.1-5
80. Wang Q. et al. *Synthesis of LiAl₂-layered double hydroxides for CO₂ capture over a wide temperature range* *J. Mater. Chem. A*, 2014, 2, 18454.
81. J. I. Di Cosimo *Structure and Surface and Catalytic Properties of Mg-Al Basic Oxides* *Journal of catalysis*, 1998, 178, p: 499–510.
82. Constantino R. L. et al. *Basic Properties of Mg²⁺-Al³⁺, Layered Double Hydroxides Intercalated by Carbonate, Hydroxide, Chloride, and Sulfate Anions*, *Inorg. Chem.*, 1995.34, p: 883-892.

Chapter 3

*Synthesis of methyl phenyl carbamate by
methoxycarbonylation of aniline with DMC using
solid catalysts*

Introduction

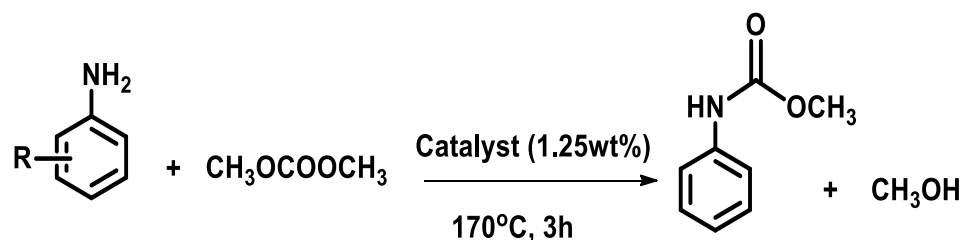
Organic carbamates are important intermediates in the synthesis of pesticides, insecticides, herbicides, pharmaceuticals, plastics and often used as protecting groups for amine functionality.¹⁻³ Methyl N-phenyl carbamate (MPC) is an important precursor for preparing methylene diphenyldiisocyanate (MDI) by condensation of MPC with formaldehyde, which is an important intermediate for the synthesis of polyurethanes (PUs).^{4,5} As presented in the literature chapter (Chapter 1, Section 1.5.), aromatic carbamates (stable form of isocyanates) and isocyanates are exclusively produced using phosgene as the reagent. Polyurethane industry accounts for 75% of phosgene usage worldwide and there is a need to the alternative and safer routes for these chemicals. Various routes have been developed for the synthesis of aromatic carbamates⁶ and methoxycarbonylation of aromatic amines with DMC has emerged as “The Green Route” for the synthesis of aromatic carbamates. One of the advantages of using DMC as a raw material is that only methanol is formed as the by-product. Methanol can be easily converted into DMC by Enichem process by oxidative carbonylation of methanol. Thus, the above two processes can be coupled to develop an atom efficient process for aromatic carbamate synthesis. Lot of work is being carried out on the development of efficient catalysts for this reaction.^{7,8} At present lead,^{8,9} zinc^{7,10-12} compounds and other catalysts¹³⁻¹⁵ are often applied for this reaction (see Chapter 1 Section 1.5.4. for details). Among these catalysts, lead and zinc compounds, especially $\text{Pb}(\text{OAc})_2$ and $\text{Zn}(\text{OAc})_2$, often give the best activity for aromatic carbamate synthesis. Thus Ono et al.⁸ observed 96% conversion of aniline with 98% selectivity to MPC with $\text{Pb}(\text{OAc})_2$ as catalyst at a temperature of 160°C in 1 h. Though results are very good with $\text{Pb}(\text{OAc})_2$ as catalyst; its toxicity has limited further developments. Zinc acetate was also good catalyst and 93% conversion of aniline with 97 % selectivity to MPC was observed at

160°C in 1 h. Similarly Li et al.¹⁶ found that sublimed zinc acetate ($Zn_4O(OAc)_6$) was good catalyst for the reaction and pretreatment of the catalyst with DMC significantly shortened induction period showing 99% aniline conversion with 99% MPC selectivity in 2 h reaction time at 130°C. However, catalyst/product separation is difficult because of the homogeneous nature of the zinc acetate catalyst. To overcome the afore mentioned shortcomings, various supported zinc acetate based catalysts ($Zn(OAc)_2/C/SBA-15$, $Zn(OAc)_2/AC$, $Zn(OAc)_2/\alpha-Al_2O_3$ and $Zn(OAc)_2/SiO_2$) have been developed showing good selectivity to MPC (78-98%).^{12,17,18} However it was observed that zinc acetate leached out from the support and also significant drop in activity was observed during recycle study. The drop in activity was attributed to the conversion of zinc acetate in to ZnO. Thus there is a need to develop active, selective and recyclable catalyst for this important reaction.

In this chapter we have investigated the synthesis of methyl phenyl carbamate by methoxycarbonylation of aniline with DMC using solid catalysts. All the catalysts were synthesized by reported procedures and characterized in detail by XRD, FT-IR, BET, TPD, TEM and XPS analysis. This chapter is divided in to two parts (A) synthesis of methyl phenyl carbamate by methoxycarbonylation of aniline with DMC using Zn (Proline)₂ as the catalyst (B) synthesis of methyl phenyl carbamate by methoxycarbonylation of aniline with DMC using CeZnZr mixed metal oxide catalyst.

Chapter 3A*Synthesis of methyl phenyl carbamate by methoxycarbonylation of aniline with DMC using Zn(Proline)₂ catalyst***3A.1. Introduction**

Zn (Proline)₂ is an efficient, stable, inexpensive, recyclable, water compatible, Lewis acid catalyst which is not dissociated under reaction conditions.¹⁹⁻²² This complex is soluble in water but insoluble in organic solvents, which allows simple and quantitative recovery of the catalyst. Zn(Proline)₂ is used as a powerful catalyst for a wide range of organic transformations including aldol, direct nitro aldol,^{22, 23} Hantzsch reaction,^{24, 25} and Knoevenagel condensation.²⁶ It has also been used for the synthesis of 1,5-benzodiazepines,^{27, 28} 1,2-disubstituted benzimidazoles,²⁸ quinoxaline,²⁹ pyrano[2,3-d]-pyrimidine,³⁰ and pyrazoles.³¹ In this part of the thesis methoxycarbonylation of aniline and DMC was investigated using metal amino acid complexes as catalysts (Scheme 3A.1). For this purpose various metal-amino acid complexes were prepared by varying cations such as (M²⁺) = Zn, Co, Cu, Ni, and Mg and different amino acids available (Valine, Asparagine, Alanine, Isolucine, Phenylalanine and Proline etc.) and used as catalysts for the synthesis of MPC.



Scheme 3A.1: Synthesis of aromatic carbamates by reaction of aromatic amine and DMC

3A.2. Materials

Zn(OAc)₂ (99.8%), Aniline (99%), N-N-dimethyl aniline (99.8%), N-methyl aniline (99.2%), DMC (99.5%), Mg(NO₃)₂·6H₂O (99.5%), Zn(NO₃)₂·6H₂O (99.5%), Co(NO₃)₂·6H₂O (99.8%), Ni(NO₃)₂·6H₂O (99%), were obtained from Loba Chemical Co., India. Ca(NO₃)₂ (99%) and Cu(NO₃)₂·4H₂O (99%) were purchased from Merck India. Glycine, Phenylalanine, Alanine, Valine, Leucine, Asparagine and proline were purchased from Spectrochem Pvt. Ltd.

3A.3. Catalyst preparation

Zn (Proline)₂ and other M(amino acid)₂ complexes were synthesized by reported method^{19,20} and detailed synthesis procedure is given below. Schematic diagram of Zn(Proline)₂ complex synthesis is given below Fig.3A.1.

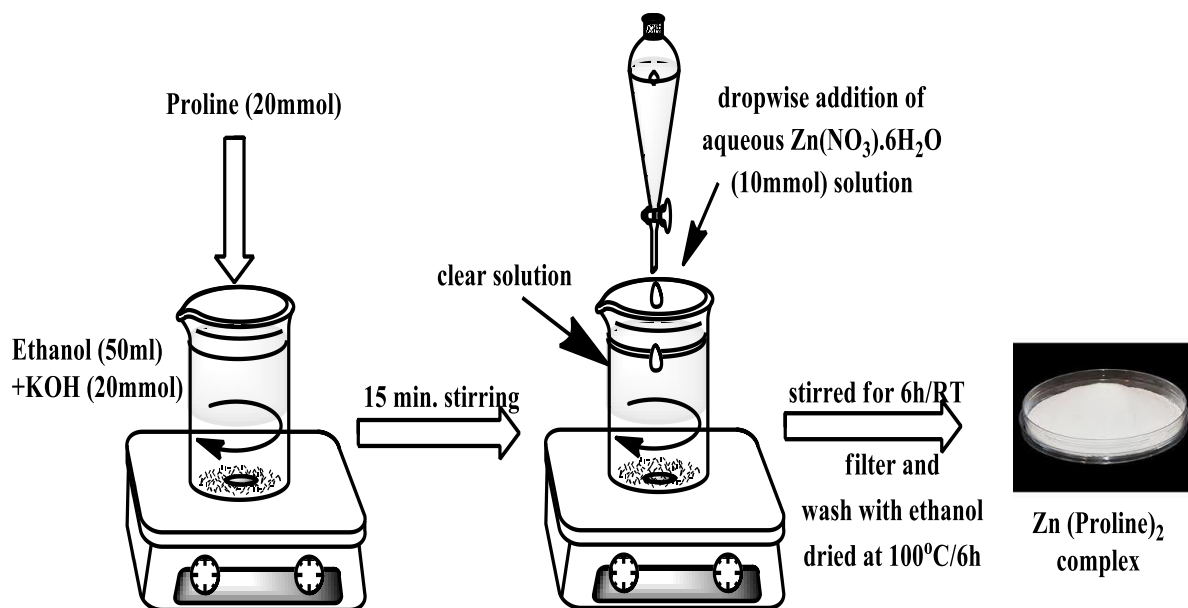


Figure 3A.1: Schematic diagram of Zn (Proline)₂ complex synthesis

3A.3.1. Synthesis of M (Proline)₂ complexes²¹

Proline (20 mmol) was dissolved in absolute ethanol (50 mL) containing potassium hydroxide (20 mmol) and magnetically stirred for 15 min in a round-bottomed flask at room temperature. In order to maintain the metal to ligand ratio of 1 : 2, 10 mmol of $M^{2+}(NO_3)_2 \cdot xH_2O$ was dissolved in a small quantity of double distilled water and added drop wise to the Proline solution. The contents were vigorously stirred at room temperature for 6 h by using a magnetic stirrer. The obtained solid was collected by filtration and dried at 70⁰C in vacuum for 6 h.

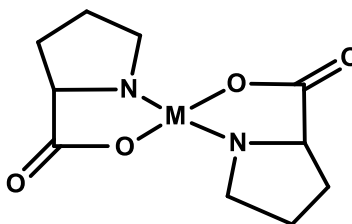


Figure 3A.2: M (Proline)₂ complexes³²

Fig. 3A.2 represents the M (Proline)₂ complex structure, where Metals (M^{2+}) used for the synthesis are: Zn, Co, Cu, Ni, Mg and Ca.

3A.3.2. Synthesis of Zn (amino acid)₂ complex²²

The amino acids (0.002 mol) were deprotonated by KOH (0.002 mol) in aqueous medium until the pH of the solution was 8-9. Then, aqueous solution of zinc acetate (0.001) was prepared which were added drop wise to prepared amino acid solution with vigorous stirring. The synthesized complexes were found to be insoluble in the commonly known organic solvents. The obtained solid was collected by filtration and dried at 70⁰C in vacuum for 6 h. All the metal complexes prepared are stable to air and moisture and decompose at very high temperatures (>300⁰C).²² Amino acids used for the synthesis are: Valine, Asparagine, Alanine, Isolucine,

Phenylalanine and proline List of the metal amino acid complexes prepared is given in Table 3A.1 and the structures obtained are given in Annexure 1a-f.

Table 3A.1: List of catalysts prepared

Metal	Amino acid
Zn	Valine, Asparagine, Alanine, Isolucine, Phenylalanine and Proline
Zn, Co, Cu, Ni and Mg	Proline

3A.3.3. FT-IR of $M(\text{Proline})_2$ and $\text{Zn}(\text{amino acid})_2$

All synthesized $M(\text{amino acid})_2$ complexes were characterized by FT-IR (Fig. 3A.3-4) which are in accordance with the literature reports.^{20,21}

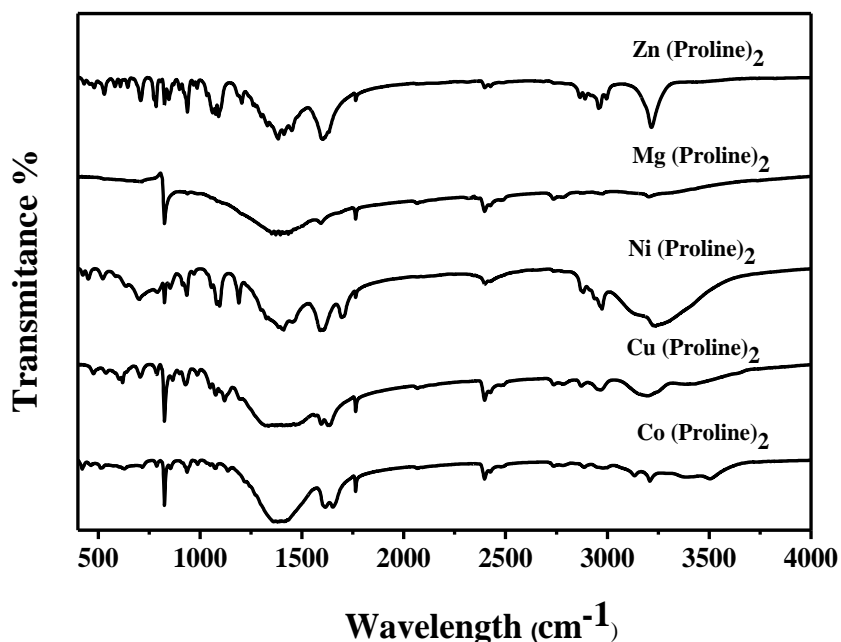


Figure 3A.3: FT-IR of $M(\text{Proline})_2$ complexes.

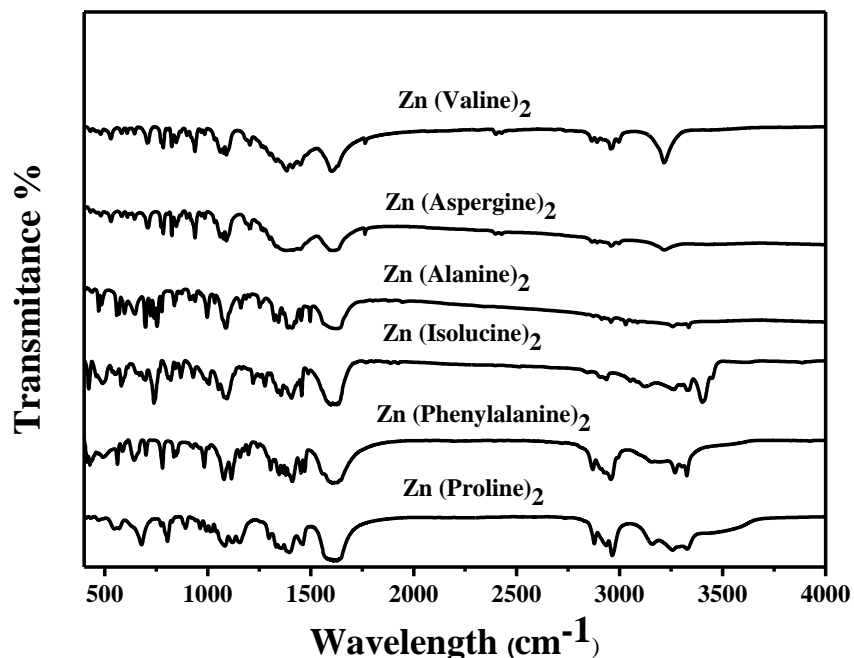


Figure 3A.4: FT-IR of Zn (Amino acid)₂ complexes.

The IR spectrum of the all synthesized compound (Fig. 3A 3-4) exhibited strong absorption bands at $\sim 3400\text{ cm}^{-1}$ assigned to the OH stretching of the coordinated water molecule. Absorption band in the region $3332\text{ to }3000\text{ cm}^{-1}$ follow the well-resolved NH stretching bands as expected from the zwitterionic RNH_3^+ group. All complexes have broad strong bands at about 1587^{-1} and 1400 cm^{-1} , which are assigned to COO asymmetric and symmetric stretching vibrations. The most important absorption bands of these complexes $500\text{-}200\text{ cm}^{-1}$ are assigned to the M-N and M-O stretching vibrations. Comparison of these spectra with those of reported metal complexes confirm the formation of M(Proline)_2 and Zn (Amino acid)_2 complexes.^{20,21}

3A.4. Experimental setup and procedure for the synthesis of MPC from aniline and DMC

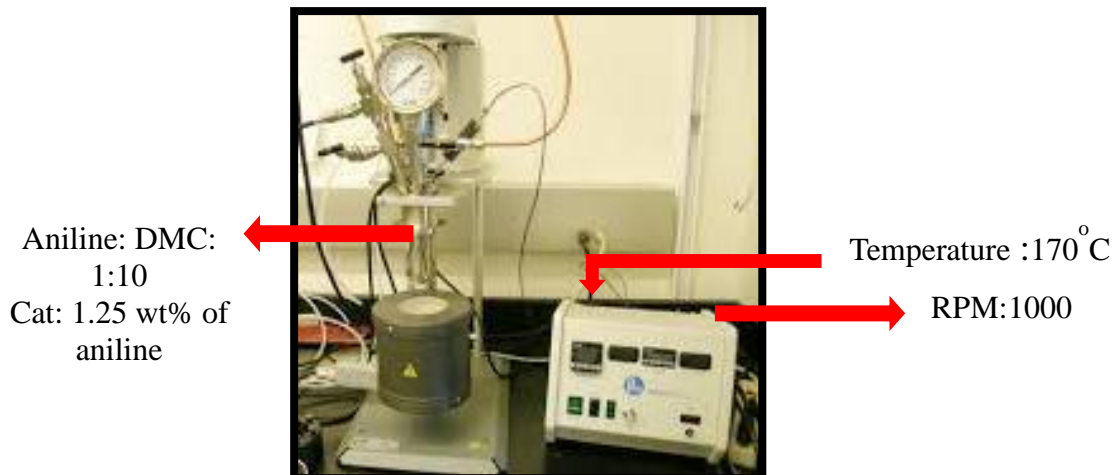


Figure 3A.5: Experimental set-up for synthesis of MPC from aniline and DMC.

The reaction of aniline and DMC was carried out in a 50 mL stainless Steel (SS-316) Parr autoclave as shown in Fig. 3A.5. In a typical experiment aniline 25 mmol, catalyst 1.25 wt% (w.r.t. aniline) and DMC 250 mmol were charged to the Parr reactor. The contents were heated to the desired temperature with slow stirring (~100 rpm). Once the temperature (170^oC) was reached the reaction was started by increasing stirring speed to 1000 rpm and the reaction was carried out for desired time duration (3 h). After completion of the reaction, the reactor was cooled to room temperature and the catalyst was recovered by centrifugation.

3A.5. Analytical methods

The quantitative analysis of the reaction mixture was carried out by using gas chromatograph (Agilent 6890N); equipped with an FID detector and an innowax capillary

column (30 m length × 0.53 mm ID × ~1 μm film thickness). The standard gas chromatograph operating conditions used for the analysis of reactants and products are given in Table 3A.2.

Table 3A.2: Conditions for gas chromatograph analysis

Oven	Temperature: 250°C		
	Pressure : 10 psi		
	Split ratio: 50:1		
	Ramp °C	Temp. °C	Hold time (min)
	40	2	
30	220	15	
Total Run time 17 min			
Flame ionization Detector	Temperature: 250°C		
	Hydrogen: 40 ml/min		
	Zero air: 400 ml/min		

Preliminary experiments were carried out using Zn (Proline)₂ as the catalyst. Reaction conditions used were: aniline: 25 mmol, DMC: 250 mmol, aniline: DMC mole ratio of 1:10, catalyst loading of 1.25wt% (w.r.t. aniline), and temperature: 170°C: and reaction time: 3 h. GC analysis (Fig. 3A.6) indicated the formation of MPC as the major product. Distinct separation of all reactants and products was observed using the analytical method developed. Conversion of aniline was very high (~98%) and small amount of N-methylaniline (NMA) and methyl-N-methyl-N-phenylcarbamate (MMPC), NN-dimethyl aniline (NNDMA) were formed as by-products. Formation of all products was confirmed by GC-MS (Agilent Technologies 6890N (GC) 5973 (MSD) equipped with an HP-5 capillary column) analysis (See Annexure 2-5).

Authentic sample of MPC and MMPC was not available commercially and hence the product obtained from the reaction mixture was separated by column chromatography. For this purpose (2.5%) Ethyl acetate in Pet ether solvent mixture was used for the separation of pure MPC and MMPC from the reaction mixture. ^1H NMR analysis of the MPC and NNPC separated and presented in Annexure 6 and 7 confirmed the formation of MPC and MMPC as the products. Pure MPC and MMPC thus obtained were used for the quantitative analysis of the reactions carried out in this work.

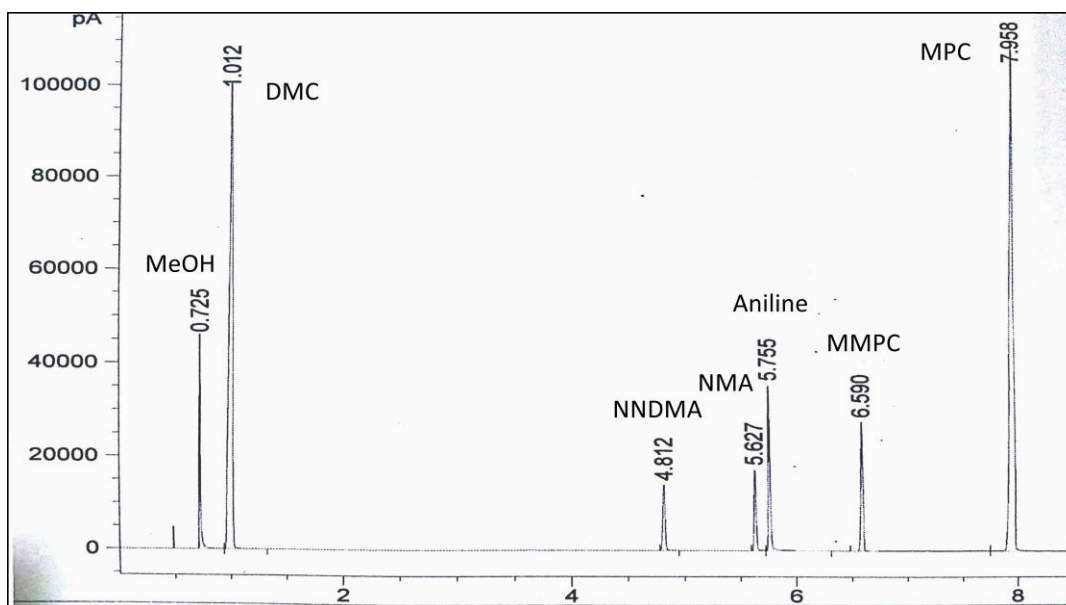


Figure 3A.6: A typical gas chromatogram for methoxycarbonylation of aniline and DMC using $\text{Zn}(\text{Proline})_2$ as catalyst.

3A.6. Quantitative analysis of reaction mixture

3A.6.1. External standard method

Quantitative analysis of the reaction mixture was carried out by using external standard method. In this method known quantities of reactants (aniline) and products (MPC, MMPC,

NMA and NNDMA) were dissolved in appropriate solvent (DMC) in 25 ml volumetric flask to make total volume 25 ml. Weight of each component was noted. Four such, samples with different concentration of reactants and products were prepared. The quantities were chosen such that they covered maximum and minimum amount for each component. Analysis of these samples was done on GC and calibration curve was generated and amount/area i.e. response factor was calculated. The response factor generated was used for quantitative analysis of reaction mixtures. In this analysis method the reaction sample to be analyzed and standard samples prepared are different and hence this method is called as external standard method.

$$\text{Aniline conversion (\%)} = \frac{\text{Initial moles of aniline} - \text{Final moles of aniline}}{\text{Initial moles of aniline}} \times 100$$

$$\text{MPC selectivity (\%)} = \frac{\text{Moles of MPC formed}}{\text{Initial moles of aniline}} \times 100$$

$$\text{MMPC selectivity (\%)} = \frac{\text{Moles of MPC formed}}{\text{Initial moles of aniline}} \times 100$$

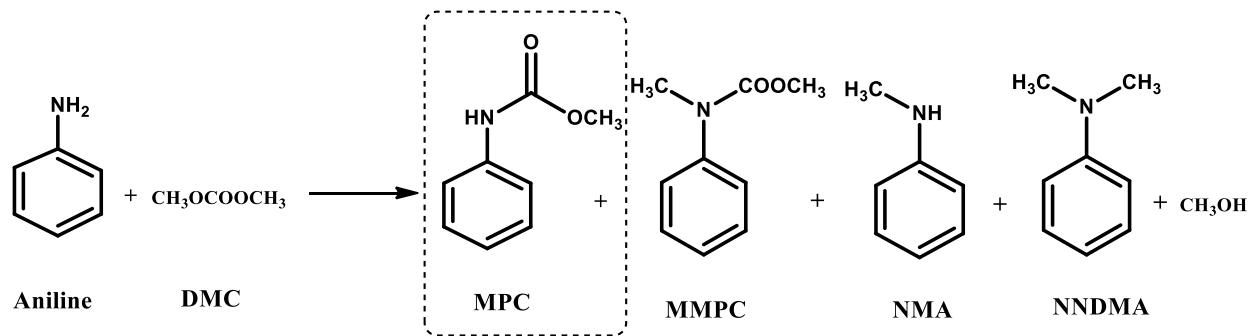
$$\text{NMA selectivity (\%)} = \frac{\text{Moles of NMA}}{\text{Initial moles of aniline}} \times 100$$

$$\text{NNDMA selectivity (\%)} = \frac{\text{Moles of NNDMA formed}}{\text{Initial moles of aniline}} \times 100$$

3A.7. Screening of catalysts for methoxycarbonylation reaction of aniline with

DMC

Methoxycarbonylation of aniline and DMC involve parallel and consecutive reactions (Scheme 3A.2) and selectivity pattern significantly depends on the acid base properties of the catalyst used.^{13,14}



Scheme 3A.2. Schematic of methoxycarbonylation of aniline with DMC and the possible by-products form during reaction.

Recently Jain et al.³⁹ have reported efficient synthesis of aliphatic and aromatic carbamates at room temperature using L-proline/TBAB (tetrabutyl ammonium bromide) catalyst system. L-proline was insoluble in DMC and hence TBAB was used phase transfer catalyst to improve the solubility of L-proline and improve the yield of product carbamate. However authors have reported good activity of catalyst for the synthesis of aromatic carbamates at room temperature; it is quite contradictory to other reported literature reports. According to Margetić and co-workers⁴⁰ aromatic amines such as aniline did not react with dimethyl carbonate at room temperature. Few experiments on methoxycarbonylation of aniline and DMC were carried out using L-proline/TBAB catalyst system at room temperature as well as at 90°C (reflux temperature) for 6 h. However, no product was detected in all these experiments (Table 3A.3, Entry 2-3). However, when reaction was carried out using same (L-proline/TBAB) catalyst system at 170°C; aniline conversion of 98.8% was observed with 2.4% selectivity to MPC (Table 3A.3, Entry 4). In light of this, experiments were planned to investigate activity of L-proline alone as catalyst and zinc complex of L-proline at 170°C and the results are presented in Table 3A.3.

Table 3A.3: The effect of various catalysts on the synthesis of MPC from aniline and DMC

Entry	Catalyst	Reaction time (h)	Conversion (%)	Selectivity (%)			
				MPC	MMPC	NMA	NNDMA
1	Without catalyst	3	-	-	-	-	-
2 ^a	L-proline/TBAB	6	-	-	-	-	-
3 ^b	L-proline/TBAB	6	-	-	-	-	-
4	L-proline/TBAB	3	98.8	2.4	58.6	3.3	34.2
5	Proline	0.5	39	45	24	29.3	0.6
6	Proline	1	54	21.6	49	26	2.6
7	Proline	2	72	14	60.5	17	8.4
8	Proline	3	96.8	3.5	76	9	11.2
9	Zn (Proline) ₂	3	98.6	97.8	0.17	0.7	0.42
10	Zn (OAc) ₂	3	98	98.4	0.07	0.6	0.5

Reaction conditions: Aniline: 25 mmol, DMC: 250 mmol, catalyst: 1.25wt%, temperature: 170°C, MPC: methyl-N-phenyl carbamate, MMPC: methyl-N-methyl-N-phenylcarbamate, NMA: N-methyl aniline, NNDMA: NN-dimethyl aniline,

a: L-proline: 5 mmol, TBAB: 5 mmol, temperature: RT (by reported method)

b: L-proline: 5 mmol, TBAB: 5 mmol, temperature: 90°C

The activity of Zn(OAc)₂, Proline and synthesized Zn(Proline)₂ complex were studied and the results are presented in Table 3A.3. Reaction did not proceed in the absence of catalyst indicating catalyst is essential for the reaction. Zn(OAc)₂ is known to be active and selective

catalyst for the reaction and 98% conversion of aniline with 98.4% selectivity to MPC was observed in 3 h reaction time (Table 3A.3, Entry 10). The performance of Zn (Proline)₂ complex was comparable to Zn (OAc)₂, however with L-Proline alone as catalyst, the selectivity pattern was different. Thus 96.8% conversion of aniline with 3.5% selectivity to MPC, 76% selectivity to MMPC, 9% selectivity to NMA and 11.2% selectivity NNDMA was observed (Table 3A.3, Entry 8). Therefore few experiments were carried out with Proline as the catalyst at different time intervals. Proline exhibited poor selectivity towards MPC (45 %) showing 39 % aniline conversion in 0.5 h (30 min) reaction time. With further increase in reaction time (1-3 h) aniline conversion increased from 54 to 96.8%, with drop in MPC selectivity (21.6-3.5%) (Table 3A.3, Entry 5-8). Decrease in MPC selectivity was due to formation of alkylation by-products (NMA, MMPC and NNDMA). It is well known that DMC can act as alkylating or methoxycarbonylating agent depending on the nature of catalyst.⁴¹⁻⁴³ Proline is an unusual naturally occurring amino acid with a secondary α -amino group, which makes it more basic than many other α -amino acids.¹⁹ Probably these basic sites are responsible for increase in the formation of alkylation by-products and affect the selectivity to MPC.

In case of Zn (Proline)₂ complex aniline conversion was high (97.6%) with 98.7% selectivity to MPC (Table 3A.3, Entry 9); which is very close to that of the best homogeneous reported catalyst, i.e. zinc acetate (Table 3A.3, Entry 10). Proline is the most prominent amino acid for the coordination with Zn. Its secondary amino group and carboxylate function being ideally suited for Zn²⁺ in low coordination number, which makes Zn complex a moderately soft Lewis acid.¹⁹ The moderate Lewis acid site of Zn (Proline)₂ complex lead to the improved activity of catalyst towards methoxycarbonylation. Thus the improved performance observed with Zn (Proline)₂ may be because of the tuning of acid/base properties.

3A.8. Screening of M(Proline)₂ complexes for methoxy-carbonylation of aniline with DMC

In order to evaluate the performance of metal complexes as catalysts; various M (Proline)₂ complexes with different M²⁺ metals (Ni, Co, Cu, Mg and Ca) were synthesized and screened for this reaction and the results are presented below in Table 3A.4.

Table 3A.4: Screening of M (Proline)₂ complexes for methoxycarbonylation of aniline with DMC.

Entry	M (Proline) ₂ complex	Aniline Conversion (%)	MPC Selectivity (%)	Sum of the selectivity's of by-products (%)
1	Zn (Proline) ₂	98.6	97.8	2.1
2	Co (Proline) ₂	88.9	96	3.8
3	Cu (Proline) ₂	58	94.5	5.1
4	Ni (Proline) ₂	21	94.6	4.9
5	Mg (Proline) ₂	16.4	95.8	3.9
6	Ca (Proline) ₂	-	-	-

Reaction conditions: Aniline: 25 mmol, DMC: 250 mmol, catalyst: 1.25wt%, reaction time: 3h, temperature: 170°C

All synthesized M (Proline)₂ complexes were screened for methoxycarbonylation reaction and the results are presented in Table 3A.4. From the results it was clearly observed that the activity increased in the order: Mg (Proline)₂ < Ni (Proline)₂ < Cu (Proline)₂ < Co (Proline)₂ < Zn (Proline)₂ with aniline conversion in a range of 16.4 to 98.4% and selectivity to MPC >94% for

all the complexes screened. However Ca (Proline)₂ was found to be inactive for the methoxycarbonylation of aniline (Table 3A.4, Entry 6). From the literature reports it was observed that the amino acids are known to form very weak complexes with alkali metal ions Mg(II) and Ca(II), showing the lower stability due to the large ionic radii.^{34,35} It may be noted that alkali metals don't have outermost valence shell d orbital and hence they are not able to form stable metal complexes.³⁴ This might be possible reason behind inactivity of Ca(Proline)₂ for methoxycarbonylation reaction. It is well known that stability of complexes increases with decrease in atomic size. In transition metal complexes (Co, Ni, Cu and Zn) Zn²⁺ possesses small atomic size as compared to other transition metals (1.52, 1.49, 1.45 and 1.42 Å° respectively).³⁶ Zn²⁺ with filled d electronic shell forms very stable complex³⁶ and its moderate Lewis acid site lead to the improved activity of catalyst towards methoxycarbonylation reaction observed (98.6% aniline conversion and 97.8% MPC selectivity) under identical reaction conditions. Best results were obtained with Zn among various divalent M (Proline)₂ complexes investigated and hence Zn complexes of various amino acids were also screened for the reaction. The results are presented below.

3A.9. Screening of different Zn(amino acid)₂ complexes for methoxycarbonylation of aniline with DMC

Zn(amino acid)₂ complexes were screened as catalysts for the methoxycarbonylation of aniline with DMC and the results are summarized in Table 3A.5. Among various Zn (Amino acid)₂ complexes, Zn (Proline)₂ complex showed highest activity (Table 3A.5, Entry 1) with very high selectivity to MPC as the product and aniline conversion varied with the type of amino acid used. These results indicate that the nature of amino acid (chain length, secondary or primary

amine group and its affinities towards the Zn^{2+}) used plays an important role in the activity of the catalyst.^{22, 23}

Table 3A.5: Screening of various Zn (Amino acid)₂ complexes for methoxycarbonylation of aniline and DMC.

Sr.No.	Zn (Amino acid) ₂ complexes	Aniline Conversion (%)	MPC Selectivity (%)	Sum of the selectivity's of other byproducts (%)
1	Zn-(Proline) ₂	98.6	97.8	2.1
2	Zn-(Phenyl alanine) ₂	93.9	98.5	1.3
3	Zn(Isoleucine) ₂	91.30	97.1	2.7
4	Zn(Valine) ₂	49.82	82.3	17
5	Zn(Alanine) ₂	27.19	71	28
6	Zn(Asparagine) ₂	5.39	35	64.2

Reaction conditions: Aniline: 25 mmol, DMC: 250 mmol, catalyst: 1.25wt%, reaction time: 3h, temperature: 170°C

Proline is cyclic amino acid and contains secondary amine group; which has high affinity towards Zn^{2+} . In Zn (Proline)₂ complex the cyclic nitrogen atom of proline is directly attached to the Zn and forms stable complex and results in better activity towards methoxycarbonylation reactions. In case of other amino acids (aliphatic and aromatic) free amine functional (primary amine) group forms weak or non-covalent interactions with Zn^{2+} leading to lower ability to form a stable complex and results in lower activity compared to Zn (proline)₂. From the Table 3B.5 (Entry 3, 4 and 5) it was observed that the activity increases with increase in chain length of aliphatic amino acid. The activity increased in the order: alanine < valine < isoleucine. In case of

Asparagine (Table 3A.5, Entry 6) electron withdrawing (-NH₂) groups are present on side chain of amino acid, which lowers activity of metal complex. Among all Zn (amino acid)₂ complexes, Zn (Proline)₂ showed the best activity, hence the detailed parametric study was carried out using Zn(Proline)₂ complex.

3A.10. Effect of reaction conditions

The effect of Aniline:DMC molar ratio, reaction temperature and catalyst loading was investigated in detail for methoxycarbonylation of aniline with DMC using Zn (Proline)₂ catalyst. All the experiments in this study were carried out with sampling in a time range of 1-5 h. conversion/selectivity Vs time profiles were obtained under various reaction conditions and are presented below.

3A.10.1. Effect of catalyst loading

Effect of catalyst loading on the reaction was investigated using Zn (Proline)₂ catalyst (catalyst loading of 0.67-2.5 wt%) at 170°C temperature. Experiments were carried out at 1, 2, 3 and 4 h reaction time for each catalyst loading to understand the reaction profile at different time intervals. Results obtained are presented in Table 3A.6. From the results it was observed that the aniline conversion was low (56.4%) with catalyst loading of 0.67 wt% in 1 h reaction time. With increased in reaction time (2-4 h) aniline conversion increased (66.7-91.8%) with slight decrease in MPC selectivity (96-93.9%). Decrease in MPC selectivity was observed due to the formation of alkylated by-products during reaction. Similar trend in aniline conversion and MPC selectivity was observed for catalyst loadings 1.25 and 2.5 wt% in 1-4 h reaction time (Table 3A.6, Entry 6-14). Aniline conversion increased with increase in catalyst loading. Thus aniline conversion

increased from 81.5 % at catalyst loading of 0.67 wt% in 4 h to 99.2% in 4 h at a catalyst loading of 2.5 wt%, however, selectivity to MMPC increased to 6.7%.

Table 3A.6: Effect of catalyst loading on methoxycarbonylation of aniline with DMC

Entry	Catalyst loading (mg)	Reaction time (h)	Aniline conv. (%)	Selectivity (%)			
				MPC	MMPC	NMA	NNDMA
1	0.67	1	56.4	97.3	0.2	2.1	0.4
2		2	66.7	96	1.2	1.7	0.9
3		3	81.5	94.3	2.2	1.2	1.6
4		4	91.8	93.9	3.1	0.6	1.9
6	1.25	1	70.6	98.9	0	0.98	0.09
7		2	95.7	98.5	0.2	0.74	0.1
9		3	98.6	97.8	0.4	0.6	0.23
10		4	99	96.7	1.7	0.3	1.2
11	2.5	1	82.65	99.2	0.1	0.23	0.04
12		2	96.8	99.4	0.31	0.12	0.08
13		3	98.4	94.2	4.8	0.8	0.18
14		4	99.2	91.5	6.7	0.5	0.9

Reaction conditions: Aniline: 25 mmol, DMC: 250 mmol, catalyst [Zn (Proline)₂]: 0.67-2.5 wt%, reaction time: 1-4 h, temperature: 170°C

From the Fig. 3A.7 it was clearly observed that optimum results were obtained with catalyst loading of 1.25 wt% (98.6% conversion of aniline with 97.8% selectivity to MPC in 3 h reaction time) and hence further study was carried out with the same catalyst loading.

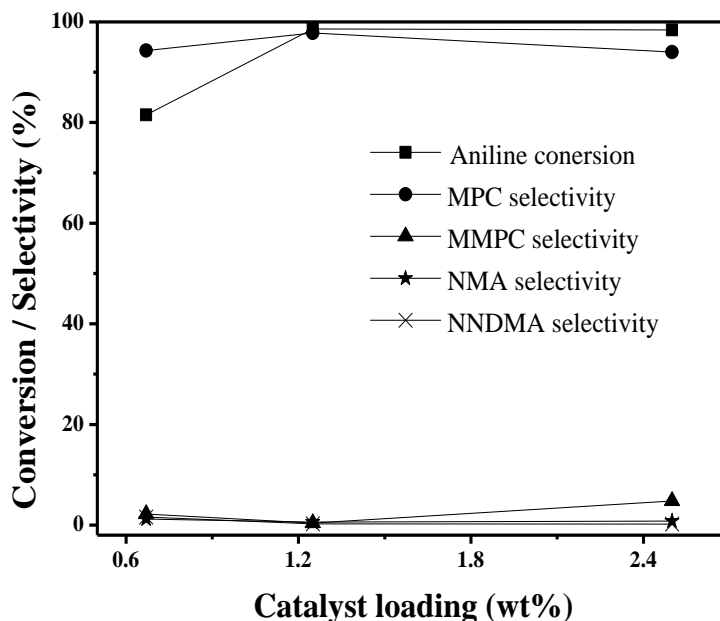


Figure 3A.7: Effect of catalyst loading on activity and selectivity of MPC

Reaction conditions: Aniline: 25 mmol, DMC: 250 mmol, catalyst $[\text{Zn}(\text{Proline})_2]$: 0.67-2.5wt%, reaction time: 3 h, temperature: 170°C.

3A.10. 2. Effect of Aniline:DMC molar ratio

The effect of Aniline:DMC molar ratio (1:5-1:20) on the methoxycarbonylation reaction was investigated at 170°C with 1.25 wt% catalyst loading and the results obtained are presented in Table 3A.7. At lower aniline:DMC ratio (1:5) selectivity to MPC was marginally lower and N-methylated by-product formation was observed (Table 3A.7, Entry 1-4). Also, selectivity to MPC decreased (94.1% to 85.6%) with increase in reaction time (1 to 4 h) at aniline:DMC ratio

of 1:5. In contrast MPC selectivity was in a range of 96-99% during 1 to 4 h reaction time at aniline:DMC ratio of 1:10 and 1:20.

Table 3A.7: Effect of aniline:DMC molar ratio on methoxycarbonylation of aniline with DMC

Entry	Aniline: DMC ratio	Reaction time (h)	Aniline conv. (%)	Selectivity (%)			
				MPC	MMPC	NMA	NNDMA
1	1:5	1	72.9	94	0.2	5.4	0.3
2		2	86	91.2	1.8	4.6	2
3		3	87.3	88	4.5	3.8	3
4		4	90.3	85.6	6.2	2.4	5.4
5	1:10	1	70.6	98.9	0	0.98	0.09
6		2	95.7	98.5	0.2	0.74	0.1
7		3	98.6	97.8	0.4	0.6	0.23
8		4	99	96.7	1.7	0.3	1.2
9	1:20	1	86.6	99.2	0	0.5	0
10		2	94.1	99	0.2	0.45	0.1
11		3	97.8	98.5	0.85	0.24	0.13
12		4	98.2	97.8	1.5	0.15	0.2

Reaction conditions: Aniline: 25 mmol, DMC: 250 mmol, Aniline/DMC: 1:5-1:20, catalyst [Zn (Proline)₂]: 1.25 wt%, reaction time: 3 h, temperature: 170°C

The results clearly indicate influence of aniline concentration and aniline:DMC ratio on the activity and selectivity. From Fig.3A.8 it was observed that aniline conversion (87.3-97.8%) and selectivity to MPC (88-98.5%) increased with increase in aniline:DMC molar ratio (1:5-1:20) in

3h reaction time (Table 3A.7, Entry 3, 7 and 11). The reason is that the excessive DMC increases the conversion of aniline and favor shifting of the reaction equilibrium to MPC synthesis. Good results were observed with aniline:DMC ratio of 1:10 (98.6% conversion with 97.8% selectivity to MPC in 3 h) and hence further work was carried out with this ratio.

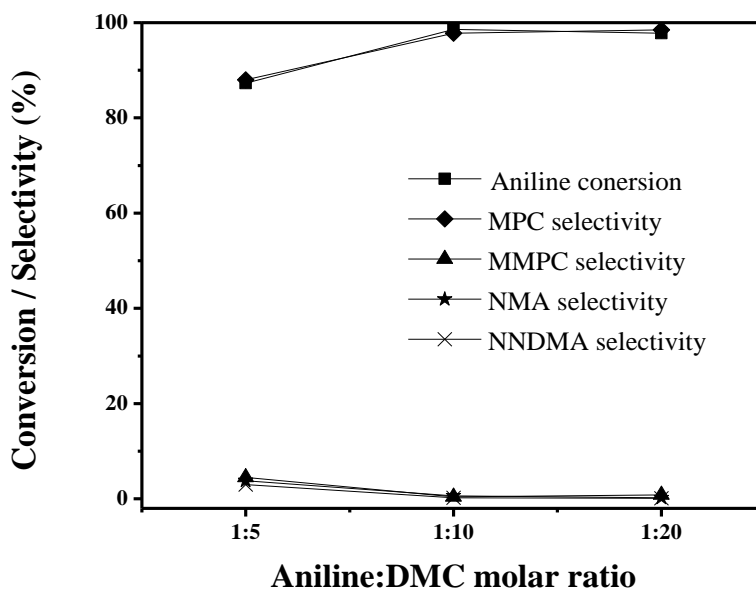


Figure 3A.8: Effect of aniline:DMC ratio on activity and selectivity of MPC

Reaction conditions: Aniline: 25 mmol, DMC: 250 mmol, Aniline/DMC: 1:5-1:20, catalyst [Zn (Proline)₂]: 1.25 wt%, reaction time: 3 h, temperature: 170°C.

3A.10. 3. Effect of Temperature

The effect of reaction temperature on methoxycarbonylation was investigated in a temperature range of 160-190°C by keeping other reaction conditions same (Table 3A.8). Aniline conversion was lower at 160°C (45.2 %) at 1 h reaction and increased to 93.5% in 4 h with high selectivity to MPC (98-99.3%). Formation of methylated products was observed with increase in reaction time. Aniline conversion increased with increase in temperature and selectivity to MPC

decreased from 96.7% in 4 h at 160°C to 88.5% in 4 h at 170°C. MMPC was observed as major methylated by-product (6.7 %) at 180°C.

Table 3A.8: Effect of temperature on Methoxycarbonylation reaction of Aniline with DMC

Sr. No.	Reaction Temperature (°C)	Reaction Time (h)	Conversion %	MPC selectivity (%)	MMPC selectivity (%)	NMA selectivity (%)	NNDMA selectivity (%)
1	160	1	45.2	99.3	0	0.64	0
2		2	88.5	99.0	0.04	0.5	0.02
3		3	92.2	98.6	0.2	0.35	0.18
4		4	93.5	98	0.7	0.23	0.3
5	170	1	70.6	98.9	0	0.98	0.09
6		2	95.7	98.5	0.2	0.74	0.1
7		3	98.6	97.8	0.4	0.6	0.23
8		4	99	96.7	1.7	0.3	1.2
9	180	1	94.5	97.3	0.7	1.8	0.3
10		2	98.2	95.2	2.3	1.2	1.4
11		3	98.9	91.4	4.2	2	2.3
12		4	99.2	88.5	6.7	1.5	3.1

Reaction conditions: Aniline: 25 mmol, DMC : 250 mmol, catalyst [Zn (Proline)₂] : 1.25wt%, reaction time: 1-4 h, temperature: 160-180°C

From the Fig.3A.9 it can be seen that aniline conversion increased (92.2-98.6%) with increase in temperature from 160-170°C with slight drop in selectivity to MPC (98.6-97.8%) in 3 h reaction

time. Aniline conversion increased marginally with further increase in reaction temperature 170 to 180°C (98.6-98.9%), however, selectivity to MPC decreased significantly (97.8-91.4%) with increase in N-methylated by-products (Table 3A.8, Entry 9-12). Presence of excess DMC results in the alkylation of MPC formed as main product at extended reaction times. Results clearly indicate influence of temperature on activity as well as selectivity pattern. From the literature reports it was clearly observed that with increase in a reaction temperature the formation of N-methylated products also increases. Li et al.³⁷ also observed that aniline conversion and MPC selectivity increased with the increase of reaction temperature from 120 to 170°C, and best results were observed at 170°C (85% aniline conversion with 93% MPC selectivity). With further increase of reaction temperature >190°C, aniline conversion 72% and MPC selectivity 63% decreased apparently with the formation of alkylated by-products in large quantity.³⁷

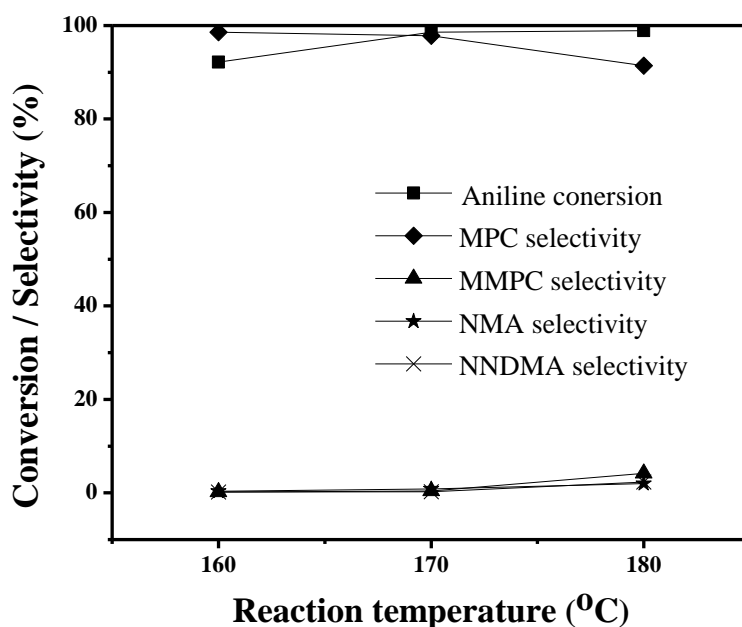


Figure 3A.9: Effect of reaction temperature on activity and selectivity of MPC

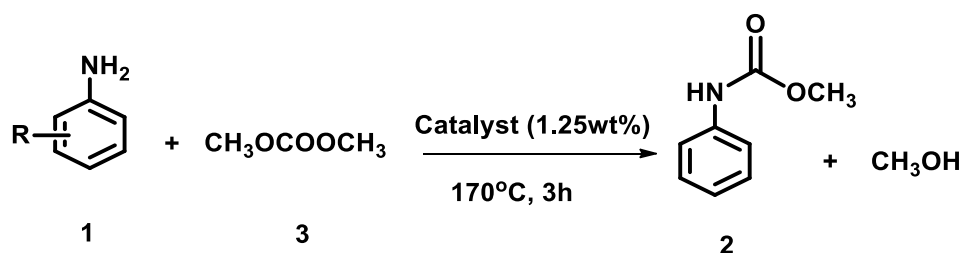
Reaction conditions: Aniline: 25 mmol, DMC: 250 mmol, catalyst [Zn (Proline)₂] :1.25 wt%, reaction time: 1-4 h, temperature: 160-180°C

Thus 98.6 % aniline conversion with 97.8 % selectivity to MPC was observed under optimized reaction conditions: aniline: DMC ratio: 1:10, temperature 170°C, catalyst loading: 1.25 wt% and reaction time: 3 h.

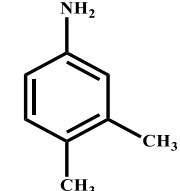
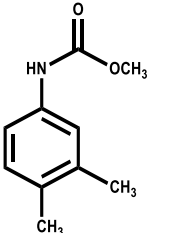
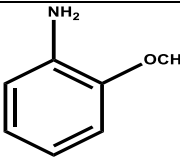
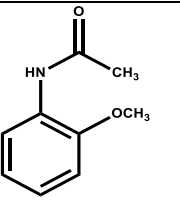
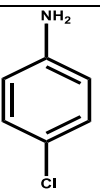
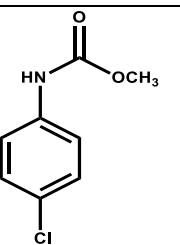
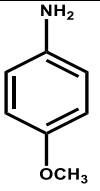
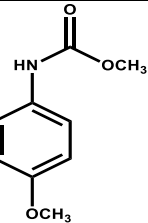
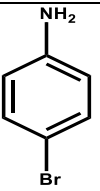
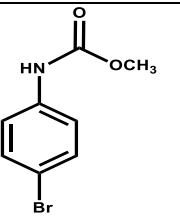
3A.11. Screening of aromatic amines for methoxycarbonylation reaction with DMC

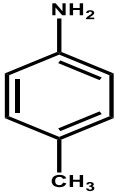
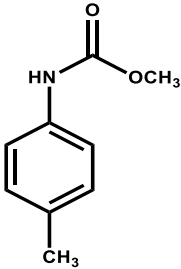
Substituted anilines (1a-g) were screened under optimized reaction conditions and the results are presented in Table 3A.9.

Table 3A.9: Screening of aromatic amines for methoxycarbonylation reaction with DMC



Entry	Substrate	Product	Conversion of amines (%)	Aromatic carbamates Selectivity (yield) (%)
1	 aniline 1a	 methyl N-phenylcarbamate 2a	98.6	97.8 (96.4)

2	 <p>3,4-dimethylaniline 1b</p>	 <p>methyl (3,4-dimethylphenyl)carbamate 2b</p>	78	96 (74.8)
3	 <p>2-methoxyaniline 1c</p>	 <p><i>N</i>-(2-methoxyphenyl)acetamide 2c</p>	64	89 (56.9)
4	 <p>4-chloroaniline 1d</p>	 <p>methyl (4-chlorophenyl)carbamate 2d</p>	99	97.3 (96.3)
5	 <p>4-methoxyaniline 1e</p>	 <p>methyl (4-methoxyphenyl)carbamate 2e</p>	98	94 (92.1)
6	 <p>4-bromoaniline 1f</p>	 <p>methyl (4-bromophenyl)carbamate 2f</p>	99	98 (97)

7	 <p><i>p</i>-toluidine 1g</p>	 <p>methyl <i>p</i>-tolylcarbamate 2g</p>	92	95.7 (88)
---	--	--	----	-----------

^a**Reaction conditions:** Substrate: 25 mmol, DMC: 250 mmol, catalyst [Zn (Proline)₂]: 1.25wt%, reaction time: 3h, temperature: 170°C

^b yield based on GC and confirmation of product done by GC-MS analysis (Annexure. 8-12)

Various substituted anilines bearing electron donating and withdrawing substituents on the phenyl ring were well tolerated under the present reaction conditions and provided the corresponding desired products (2a–g) in good to excellent yields (Table 3A.9, Entries 1–7). Lower yield of products observed with ortho substituted aniline (Table 3A.9, Entry 3) was due to steric hinderance of the methoxy group. With para-methoxy aniline 92.1% yield of product was observed compared to 56.9 % observed with *o*-methoxyaniline (Table 3A.9, compare Entries 3 and 5).

3A.12. Stability of the Zn (Proline)₂ (leaching test)

In order to check the leaching of the Zn (Proline)₂ complex into the reaction mixture during the course of the reaction, reaction was carried out at 170°C for 1 h under standard reaction conditions. The reaction was then stopped and catalyst was separated by filtration of hot reaction mixture (~70°C temperature). The reaction mixture was charged to the reactor and reaction was continued for one more hour at 170°C. The results are shown in the (Fig. 3A.10).

Reaction did not proceed further in the absence of Zn (Proline)_2 , indicating that Zn (Proline)_2 complex did not leach in the reaction mixture. In contrast standard reaction in the presence of the catalyst proceeded smoothly. The above study ensured that the methoxycarbonylation is catalyzed by purely by a heterogeneous Zn (Proline)_2 catalyst.

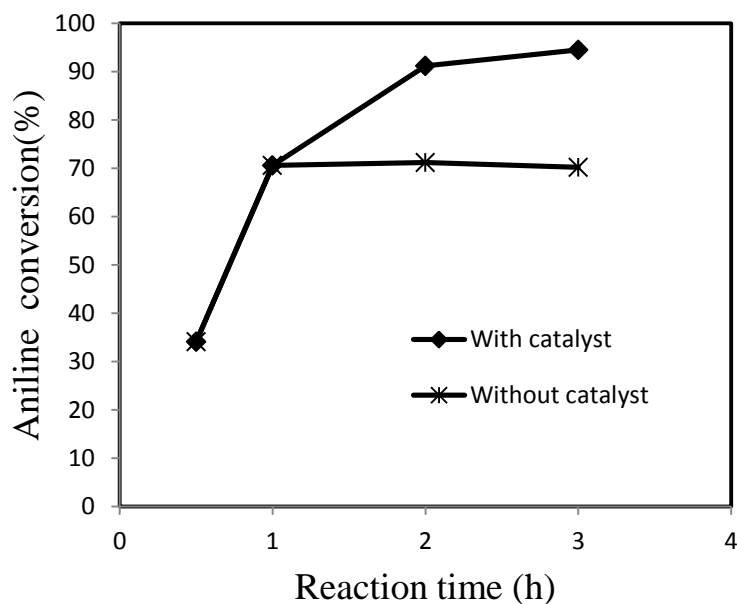


Figure 3A.10: Leaching of the catalyst

Reaction conditions: Aniline: 25 mmol, DMC: 250 mmol, catalyst $[\text{Zn (Proline)}_2]$: 1.25wt%, reaction time: 1- 2-3 h, temperature: 170°C .

3A.13. Recycle study of Zn (Proline)_2

Reaction of aniline and DMC was carried out as per the procedure described earlier. The catalyst from the reaction mixture was recovered by centrifugation, washed with DMC, and then dried overnight at 100°C for 12 h. The recovered catalyst was used to perform a new reaction by charging aniline and DMC to the reactor. Catalyst activities as well as selectivity to MPC decreased significantly during recycle experiments. The results obtained are presented in Table

3A.10. In order to understand the reason for drop in activity ICP analysis of reaction mixture was carried out and 1.6 ppm leaching of Zn from the catalyst was observed during recycle experiments. Probably part of the complex is decomposing during recycle experiment. XRD analysis of the spent catalyst was also carried out to find out the changes taking during recycle experiments.

Table 3A.10: Recycle study using Zn (Proline)₂ catalyst

	Aniline Conversion (%)	MPC Selectivity (%)
Fresh	98.6	97.8
Cycle 1	72.5	83
Cycle 2	48	62

Reaction conditions: Aniline: 25 mmol, DMC: 250 mmol, Zn (Proline)₂: 1.25wt%, reaction time: 3h, temperature: 170°C.

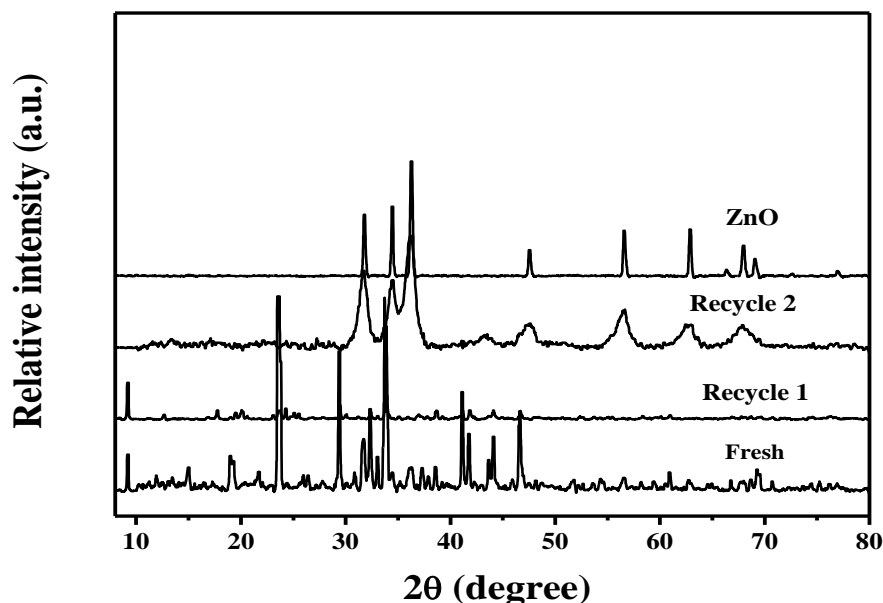


Figure 3A.11: XRD pattern of fresh, recycle Zn (Proline)₂ and * ZnO phase

XRD analysis of the fresh and recycled catalyst was carried out and the results are presented in Fig. 3A.11. For comparison XRD analysis of ZnO is also presented in the Fig. 3A.11. From the XRD pattern it was clearly observed that the peaks corresponding to Zn(Proline)₂ (47-1919 JCDPS) decreased for the recycled catalysts, while peaks corresponding to ZnO ($2\theta=31.7, 34.2,$ and 36.1°) appeared in the recycled catalysts and the intensity was prominent for catalyst recovered after second recycle. Thus probably formation of ZnO during recycle study is the reason for deactivation of Zn (Proline)₂ catalyst. Li et al.¹² also observed deactivation of Zn(OAc)₂ and supported Zn (OAc)₂ catalysts during reuse in their study. They attributed deactivation of the catalyst to the formation of ZnO because of the interaction of Zn (OAc)₂ with methanol.

3A.14. Proposed reaction mechanism

The reaction mechanism for carbamate (MPC) synthesis by reaction of amine with DMC over Lewis acid catalyst has been investigated widely.^{12,17,38} Based on the literature reports and results obtained in the present work a plausible mechanism has been proposed (Fig. 3A.12). Zn²⁺ from Zn (Proline)₂ complex represents Lewis acid sites suitable for the methoxycarbonylation reaction. Activation of DMC (generation of carbocation of DMC) takes place by interaction of DMC and Zn²⁺ (Fig. 3A.12, Step I). The lone pair on nitrogen of aniline attacks carbocation generated from activated DMC (Fig. 3A.12, Step II). Further internal rearrangement (Fig. 3A.12, Step III) leads to the formation of MPC as the product and methanol as the by-product. After dissociation of product from the catalyst surface active catalyst is regenerated back for the fresh reaction cycle (Fig. 3A.12, Step IV).

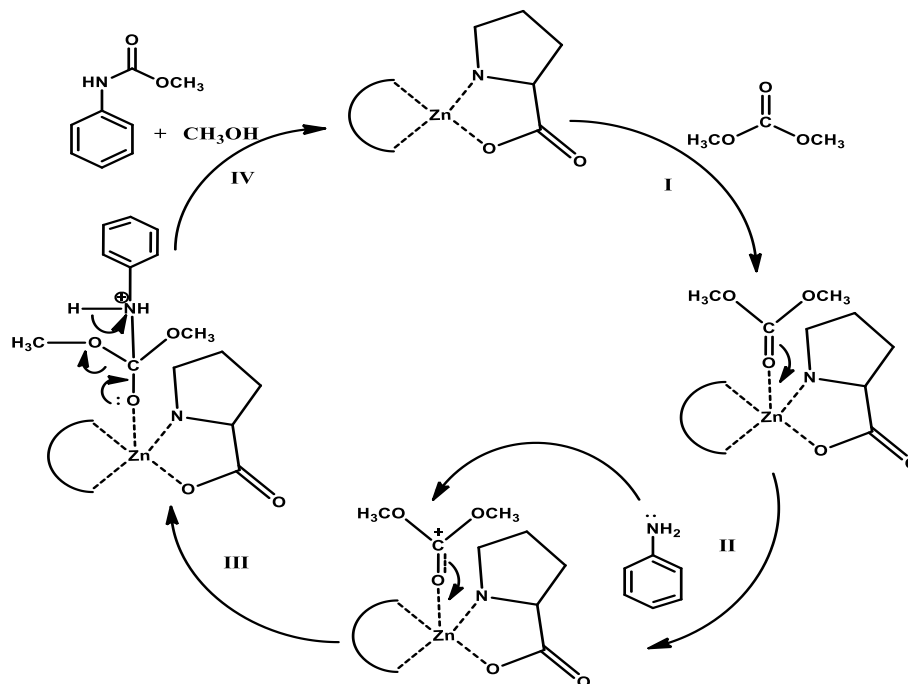


Figure 3A.12: Proposed mechanism for the Zn (Proline)₂ complex catalyzed synthesis of MPC.

3A.15. Conclusions

Methoxy carbonylation reaction of Aniline with DMC was investigated out using M(amino acid)₂ complexes as catalysts. Various Zn (amino acid)₂ complexes were prepared by precipitation method. From which Zn (Proline)₂ showed the best catalytic activity towards MPC synthesis, hence detailed parametric study of reaction was carried out using Zn (Proline)₂ catalyst. Good results were observed with aniline:DMC ratio of 1:10, reaction temperature of 170°C and reaction time of 3 h (98.6% conversion with 97.8% selectivity to MPC). The results clearly show that Zn (Proline)₂ is an efficient, Lewis acid catalyst for methoxycarbonylation reaction. However, activity decreased during recycles experiments. Comparison of XRD analysis of the fresh and recycled catalyst indicated the formation of ZnO during recycle, leading to drop in aniline conversion during recycle.

Chapter 3 B***Synthesis of methyl phenyl carbamate by methoxycarbonylation of aniline with DMC using Ce-Zn-Zr mixed metal oxide catalyst*****3B.1. Introduction**

From the literature report it was observed that there are few reports on mixed metal oxide catalysts for methoxycarbonylation of aniline with DMC (Chapter 1 section 1.5.4.). Kang et al.⁴⁴ used PbO as catalyst for the synthesis of MPC at 170°C for 4 h, the conversion of aniline was obtained 81%. Though PbO has an advantage over the other catalysts, its use should be limited because the lead compounds are toxic and not friendly to the environment. In addition, Li et al.⁴⁵ used In₂O₃/SiO₂ as catalyst, and the catalytic activity was low and 59.4% yield of MPC observed. Zhao et al.⁴⁶ studied ZrO₂/SiO₂ MMO catalyst for the reaction and 98.6% aniline conversion with 79.8% MPC yield was obtained at 170°C in 7h with DMC:aniline mole ratio of 20 and catalyst loading of 20 wt%. According to authors strong Lewis acid sites present on ZrO₂/SiO₂ surface results in higher selectivity towards MPC. However, catalyst activity decreased after 1st recycles experiment. Therefore, it is important to develop heterogeneous catalyst that is environment friendly, stable and exhibits better activity for the methoxycarbonylation reaction.

CeZr mixed metal oxide is a known Lewis acid catalyst and is used as stable and active catalyst in many organic transformations.⁴⁸⁻⁵⁰ In recent years there are many efforts on the enhancement of Lewis acid sites by incorporating third metal cation into CeZr MMO lattice to improve the catalytic activity.^{47-50,62} Methoxycarbonylation of aromatic amines are also catalyzed by Lewis acid catalysts^{46,51} Based on the above discussion, the aim of this work was to develop highly

active and selective catalyst with proper balance of acid base sites on the catalyst. In light of this various $Ce_3Zn_xZr_1$ catalysts were synthesized by co-precipitation method ($x = 0$ to 1) and calcined at $550^\circ\text{C}/6$ h. Catalysts were further characterized by XRD, BET, TEM, NH_3 TPD and XPS analysis in detail. Optimization of reactions was carried out and catalyst stability was also investigated.

3B.2. Materials

DMC (99.5%), $\text{Zn}(\text{OAc})_2$ (99.8%), Aniline (99%), N-N-dimethyl aniline (99.8%), N-methyl aniline (99.2%), DMC (99.5%), $\text{Mg}(\text{NO}_3)_2 \cdot 6\text{H}_2\text{O}$ (99.5%), $\text{Zn}(\text{NO}_3)_2 \cdot 6\text{H}_2\text{O}$ (99.5%), $\text{Co}(\text{NO}_3)_2 \cdot 6\text{H}_2\text{O}$ (99.8%), $\text{Ni}(\text{NO}_3)_2 \cdot 6\text{H}_2\text{O}$ (99%), NaOH (99.5%), Na_2CO_3 (99.5%), were obtained from Loba Chemical Co. $\text{ZrO}(\text{NO}_3)_2 \cdot \text{H}_2\text{O}$ (99.8%), $\text{Y}(\text{NO}_3)_3 \cdot 4\text{H}_2\text{O}$ IPA (99.5%), methanol (99.8%), $\text{Fe}(\text{NO}_3)_3 \cdot 9\text{H}_2\text{O}$ (98%), toluene (99.8%) were purchased from Merck India.

3B.3. Catalysts preparation (binary and ternary MMOs)

Syntheses of binary and ternary mixed metal oxides (MMOs) was carried out by co-precipitation method.⁵²⁻⁵⁴ The solution A contains mixture of binary/ternary metal precursors in appropriate molar ratios (as listed in Table 3B.1) dissolved in distilled water. Solution B contains NaOH (1.2 M) and Na_2CO_3 (0.1 M) dissolved in distilled water. The solutions A and B were simultaneously added drop wise in 100 ml de-ionized water with vigorous stirring at room temperature. During addition, pH of the solution was maintained at 10-11 by addition of appropriate amount of solution B. The formed suspension was continuously stirred for 30 min and aged at 70°C for 12 h. Finally the solid formed was separated by filtration and washed

thoroughly with deionized water until pH of the water wash became neutral. Resultant solid was then dried at 100°C for 12 h and calcined at 550°C for 6 hours in air.

Ce₃Zn_xZr₁ mixed metal oxides were synthesized by same (co-precipitation) method, where x= 0 to 1 mmol and the CeZr ratio was kept constant at 3:1. Catalysts synthesized were calcined at 550°C for 6 hours in air and labelled as named as Ce₃Zr₁, Ce₃Zn_{0.25}Zr₁, Ce₃Zn_{0.5}Zr₁, Ce₃Zn_{0.75}Zr₁, Ce₃Zn₁Zr₁ and Zn₃Zr₁ respectively.

Single-metal oxides (CeO, ZrO₂ and ZnO) were synthesized using the same protocol by using aqueous solution of the respective nitrate precursor.

3B.4. Experimental Procedure

The reaction of aniline and DMC was carried out in a 50 mL stainless autoclave (Parr reactor) with constant stirring. In a typical experiment aniline 25 mmol, DMC 500 mmol and (binary /ternary) mixed metal oxide catalyst 10 wt% relative to aniline, were charged to the reactor. The contents were heated to the desired temperature with slow stirring (~100 rpm). Once the temperature (180°C) was reached the reaction was started by increasing stirring speed to 1000 rpm and the reaction was carried out for desired time duration (2 h). The reactor was cooled to room temperature, the catalyst was recovered by centrifugation, and the quantitative analysis of the reaction mixture was carried out using Agilent 6890 GC (FTD detector, Innowax column). Confirmation of MPC was done by GC-MS analysis (Annexure 2).

3B.5. Analytical methods

Quantitative analysis by GC and confirmation of all products by GC-MS / NMR were carried out. All details are given in Chapter 3A .5 (Annexure 2-7).

3B.6. Screening of mixed metal oxides for methoxycarbonylation of aniline with DMC

MMOs act as Lewis acid catalysts for various organic transformations.⁵⁵⁻⁵⁸ Methoxycarbonylation of aromatic amines is also catalyzed by Lewis acid catalysts^{46,51} and hence selected MMOs synthesized were screened for MPC synthesis and the results obtained are presented in Table 3B.1.

Table 3B.1: Screening of binary /ternary MMOs for synthesis of MPC from aniline and DMC

Entry	Catalyst	Conversion Aniline (%)	Selectivity (%)	
			MPC	Sum of other by products
1	Ce ₃ :Zr ₁	54	72	27.6
2	Zn ₃ :Zr ₁	43	62	38.2
3	Y ₃ :Zr ₁	42	52	47
4	Ce ₃ :Al ₁	33	60	39.4
5	Zr ₃ :Y ₁	30.5	42	57
6	Zn ₃ :Al ₁	20.5	34.2	65
7	Ni ₃ :Al ₁	19.8	12.5	86.2
8	Co ₃ :Al ₁	26.3	58	41.6
9	Ce₃:Zn_{0.5}:Zr₁	98.4	98.6	1.3
10	Y ₃ :Zn _{0.5} : Zr ₁	64	78	21.3

Reaction conditions: Aniline: 25 mmol, DMC: 500mmol, Aniline/DMC:1/20, Catalyst: 10 wt % relative to aniline, Reaction Time: 2 h, Temperature: 180°C.

Various mixed metal oxides used as Lewis acid catalysts in other transformation were screened for methoxycarbonylation of aniline with DMC. From the results presented in Table 3B.1 it was

observed that all catalysts were active for methoxycarbonylation and aniline conversion was observed in a range of 19.8 to 54% with DMC selectivity in a range of 12.5 to 72% with alkylated compounds as by-products (Table 3B.1, Entries 1-7). In all the cases NMA and MMPC was found to be the major by-product. Among all binary MMOs $Ce_3:Zr_1$ showed good activity (54% aniline conversion with 72% MPC selectivity) with 27.6% alkylated by-products (MMPC as major byproduct 12% along with NMA 9.6%). Very Low activity was observed with $Ni_3:Al_1$ mixed metal oxide: 19.8% aniline conversion, 12.5% MPC selectivity with 86.2 % alkylated byproducts (NMA formed as a major byproduct with 52% selectivity). Thus aniline conversion and product selectivity pattern changed significantly with combinations of different metals used in the mixed metal oxides screened. Alkylation of aniline was the main side reaction with all catalysts investigated. The difference in activity and selectivity observed was due to the acid base properties of metal cations used. DMC is known to catalyze both methylation and methoxycarbonylation reactions and the activity is dependent upon the acid base properties of catalyst.⁴¹⁻⁴³ Since N-methylation by-products were dominating selectivity, it was thought to modify acid base properties of the binary MMO by incorporation of third metal. Good results were obtained with $Ce_3:Zr_1$ and $Y_3:Zr_1$ MMOs and hence Zn was used as third metal; since it is amphoteric with mild Lewis acid properties.

Aniline conversion as well as selectivity to MPC improved significantly with incorporation of Zn as third metal in $Ce_3:Zr_1$ and $Y_3:Zr_1$ MMOs (Table 3B.1, Entries 9 and 10). Best results (98.4% conversion of aniline with 98.6% selectivity to MPC) were obtained with $Ce_3:Zn_{0.5}:Zr_1$ as the catalyst (Table 3B.1, Entry 9). The results clearly indicated positive effect of incorporation of Zn as third metal on aniline conversion and selectivity to DMC. In order to understand the role of third metal in enhancing activity and selectivity to DMC; systematic study

on the effect of third metal loading (Zn) on the performance of the catalyst was investigated in detail and the results are presented below.

3B.7: Effect of Zn concentration

$Ce_3Zn_xZr_1$ MMOs were synthesized by co-precipitation method by varying Zn concentration (0-1 mole equivalent) and Ce:Zr molar ratio was kept constant at 3:1. All the MMOs were screened for methoxycarbonylation reaction and the results obtained are presented in Table 3B.2.

Table 3B.2: Effect of Zn loading on the activity and selectivity with Ce_3Zr_1 catalyst

Entry	Zn loading (mol)	Conversion (%)	Selectivity (%)			
			MPC	MMPC	NMA	NNDMA
1	Ce_3Zr_1 (0)	54	72	12	9.6	6
2	$Ce_3Zn_{0.25}Zr_1$ (0.25)	81	87.6	5.6	2.9	3.7
3	$Ce_3Zn_{0.5}Zr_1$ (0.5)	98.4	98.6	0.24	0.6	0.1
4	$Ce_3Zn_{0.75}Zr_1$ (0.75)	94	92.6	3.2	1.2	2.7
5	$Ce_3Zn_1Zr_1$	92	90.8	4.2	0.95	3.4
6	Zn_3Zr_1	43	62	3.5	27	7.2
7	CeO_2	10	75	-	24	-
8	ZnO	4	68	-	32	-
9	ZrO_2	-	-	-	-	-

Reaction conditions: Aniline: 25 mmol, DMC: 500 mmol, Aniline/DMC:1/20, Catalyst: 10 wt

% relative to aniline, Reaction Time: 2 h, Temperature: 180°C.

From the results it was observed that Ce_3Zr_1 showed 54% aniline conversion with 72, 12 and 9.6% selectivities to MPC, MMPC and NMA respectively. Aniline conversion as well as selectivity to MPC increased with incorporation of Zn in the MMO. Thus aniline conversion of 81% with 87.6% selectivity to MPC was observed with $Ce_3Zn_{0.25}Zr_1$ (Zn incorporation of 0.25 mol) also selectivity to MMPC (5.6) and NMA (2.9) decreased significantly. Aniline conversion (98.4%) as well as MPC selectivity (98.6%) increased with further increase in Zn incorporation of 0.5 molar equivalent ($Ce_3Zn_{0.5}Zr_1$) and decreased marginally with further increase in Zn content (Table 3B.2, Entries 4-6). Drop in MPC selectivity at higher Zn loading (0.75-1) was observed due to formation of alkylated by products (MMPC and NMA). Thus best results were obtained with $Ce_3Zn_{0.25}Zr_1$ as the catalyst.

In order to compare the activities of individual oxides, binary mixed metal oxides with best catalyst ($Ce_3Zn_{0.25}Zr_1$) few experiments were carried out and the results are presented in Table 3B.2 (Entries 6-9). It was observed that single metal oxide showed poor catalytic activity and selectivity for methoxycarbonylation. Thus aniline conversion was in a range of 4-10% with MPC selectivity in a range of 68-75%. ZrO_2 was inactive for the reaction. Reaction carried out with Zn_3Zr_1 showed 43% conversion of aniline with 62% selectivity to MPC. In contrast best results (98.4% conversion of aniline with 98.6% selectivity to MPC in 2 h) were observed with $Ce_3Zn_{0.5}Zr_1$ catalyst (Zn incorporation of 0.5). The observed variation in activity and selectivity observed may be due to the changes in structural and physiochemical properties of the catalyst with incorporation of Zn. Hence to understand the effect of Zn concentration in Ce_3Zr_1 MMO on the activity and selectivity pattern, all catalysts were characterized in detail and the results are discussed below.

3B.8. Result and discussion

3B.8.1. Characterization techniques of $Ce_3Zn_xZr_1$ MMOs

3B.8.1.1. XRD analysis

XRD analysis of all the Zn incorporated catalysts $Ce_3Zn_xZr_1$ was carried out and the results are presented in Fig.3B.1. XRD of ZnO and CeO_2 are also included for comparison. The lattice parameter (\AA) and average crystal size calculated from XRD analysis are also presented in Table 3B.3.

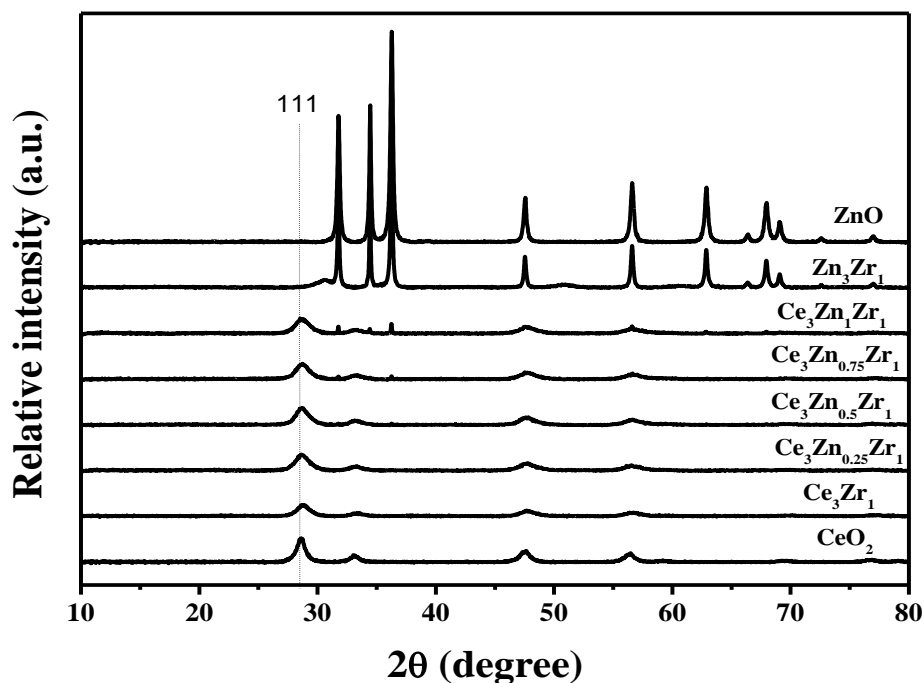


Figure 3B.1: XRD patterns of all synthesized single, binary and ternary MMOs.

XRD analysis of CeO_2 has four main diffraction peaks centered at $2\theta=28.9, 33.4, 47.9$ and 57.0° ; which can be assigned to the fluorite-type cubic CeO_2 structure. In XRD spectrum of Ce_3Zr_1 peaks corresponding to CeO_2 were observed. However, peaks corresponding to ZrO_2 diffraction were not observed; indicating incorporation of Zr^{4+} ions into the ceria lattice structure. This was

also confirmed by considerable shift of the 2θ (28.63 to 28.79°) values of Ce_3Zr_1 peak at higher diffraction position in comparison with pure CeO_2 (JCPDS 34394). It was assigned to the lattice shrinking after the replacement of Ce^{4+} (ionic radius: 0.097 nm) by smaller Zr^{4+} ions (0.083 nm), revealing the formation of uniform Ce–Zr–O solid solution.⁵⁹⁻⁶¹ Moreover, the lattice parameter A° of Ce_3Zr_1 was 5.355 A° and crystal size 10 nm which was less compared to that of pure CeO_2 (5.381 A° and 18 nm respectively). This was in good agreement with the result obtained by CaO et al.⁶²

Table 3B.3 : Lattice parameter (A°) and average crystal size of synthesized mixed metal oxides

Entry	Sample	Lattice parameter (A°)	Average crystallite size (nm)
1	CeO_2	5.381	18
2	Ce_3Zr_1	5.355	10
3	$Ce_3Zn_{0.25}Zr_1$	5.352	11
4	$Ce_3Zn_{0.5}Zr_1$	5.350	13
5	$Ce_3Zn_{0.75}Zr_1$	5.350	32
6	$Ce_3Zn_1Zr_1$	5.348	57
7	Zn_3Zr_1	-	75

Average crystal size: $\tau = K\lambda/\beta \cos \theta$

From the comparison of the XRD patterns of Zn substituted MMOs ($Ce_3Zn_{0.25}Zr_1$ and $Ce_3Zn_{0.5}Zr_1$) with that of Ce_3Zr_1 (Fig. 3B.1), it is observed that the 2θ value for peak corresponding to (111) plane is shifted from 28.79 to 28.83°. The shift in the position probably

indicates the incorporation of Zn in the Ce_3Zr_1 lattice. In addition, the lattice parameter of Zn incorporated MMOs also declined from 5.355 \AA to $5.352\text{-}5.350 \text{ \AA}$ implying the presence of ternary metal oxide solid $Ce\text{-}Zn\text{-}Zr\text{-}O$. Peaks of other crystalline phases, including ZnO ($2\theta = 31.8, 34.3, 36.2, 38.1$) were not observed in these two samples. This also indicates that Zn is homogeneously dispersed in the $Ce_3Zn_{0.25}Zr_1$ and $Ce_3Zn_{0.5}Zr_1$ MMOs. Decrease in lattice parameter (Table 3B.3) observed was due to the smaller ion radii of Zr^{4+} (0.086nm), Zn^{2+} (0.088 nm) as compared to Ce^{4+} (0.101 nm).⁵⁹ These results also indicate that there is strong interaction between Zinc and cerium for $Ce_3Zn_{0.25}Zr_1$ and $Ce_3Zn_{0.5}Zr_1$ which leads to the high dispersion of this Zn on Ce_3Zr_1 oxide. With further with increase in Zn concentration ($Ce_3Zn_{0.75}Zr_1$ and $Ce_3Zn_1Zr_1$); ZnO phase was clearly observed in these samples. This may be due to agglomeration of excess ZnO partials on Ce_3Zr_1 surface. XRD analysis indicates that ZnO is incorporated in the Ce_3Zr_1 phase till Zn concentration of 0.5 and peaks corresponding to ZnO were not observed. However, with further increase in Zn loading (0.75 to 1) peaks corresponding to ZnO were observed, indicating deposition of excess ZnO on Ce_3Zr_1 surface which lead to significant increase in crystal size 32-75nm.

3B.8.1.2. TEM analysis

TEM analysis of all $Ce_3Zn_xZr_1$ mixed metal oxide catalysts prepared was carried out and the results are presented in Fig. 3B.2.

The bulk surface of the Ce_3Zr_1 oxide was observed to be relatively uniform with spherical particles. Ce_3Zr_1 oxide was apparently nanocrystalline with an average particle size of 10-12 nm (Fig.3B.2A). In case of Zn incorporated MMOs $Ce_3Zn_{0.25}Zr_1$ and $Ce_3Zn_{0.5}Zr_1$ and $Ce_3Zn_{0.75}Zr_1$, it was difficult to distinguish the Zn species from the Ce_3Zr_1 support (Fig. 3B.2 B, C and D). With

increase in Zn concentration $\text{Ce}_3\text{Zn}_1\text{Zr}_1$ and Zn_3Zr_1 (Fig. 3B.2 E and F) agglomerated ZnO particles were clearly observed. Agglomeration of ZnO particles leads to increase in crystal size and lowering the uniformity on the surface.⁶⁰

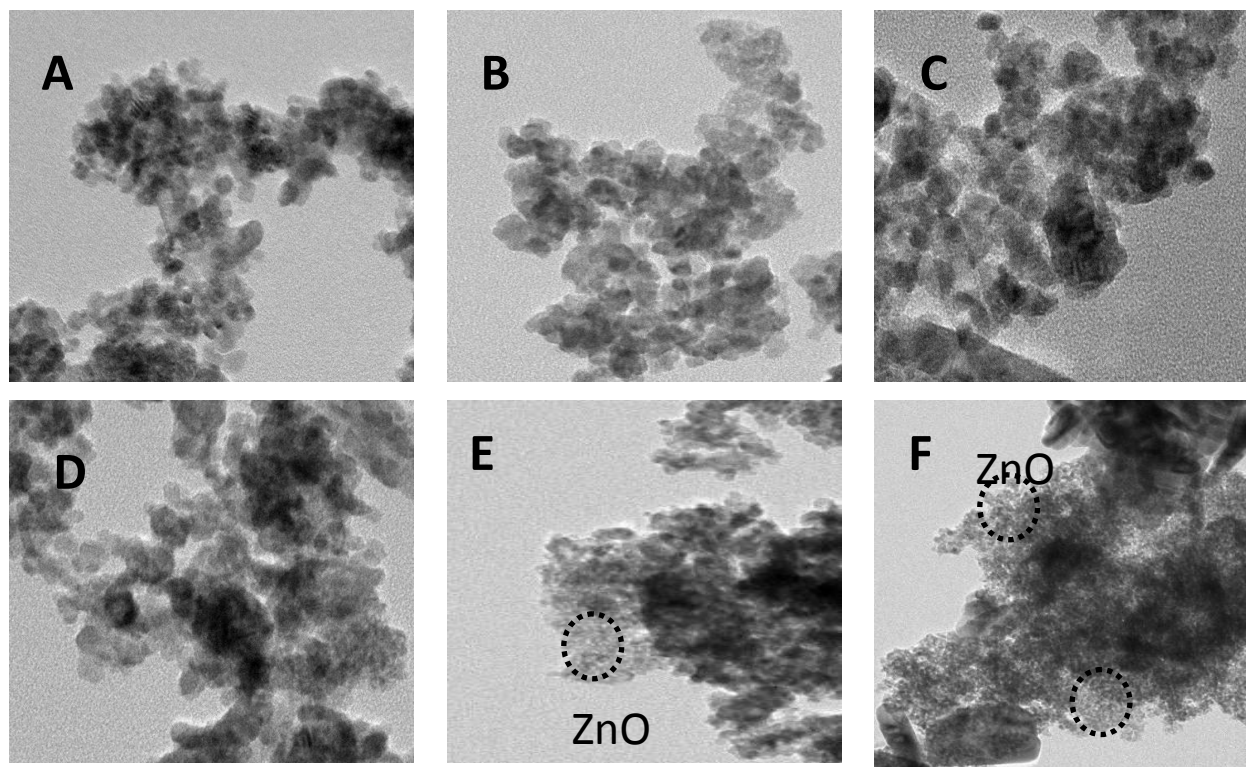


Figure 3B.2: TEM images of A) Ce_3Zr_1 B) $\text{Ce}_3\text{Zn}_{0.25}\text{Zr}_1$ C) $\text{Ce}_3\text{Zn}_{0.5}\text{Zr}_1$ D) $\text{Ce}_3\text{Zn}_{0.75}\text{Zr}_1$ E) $\text{Ce}_3\text{Zn}_1\text{Zr}_1$ F) Zn_3Zr_1

3B.8.1.3. Surface area and pore volume

The physicochemical properties of the catalysts prepared were estimated and the results are presented in Table 3B.4.

Table 3B.4: Surface area and pore volume of synthesized $Ce_3Zn_xZr_1$ MMOs.

Sample	Surface area m^2/g	Pore volume $C_{c/g}$
Ce_3Zr_1	84	0.08288
$Ce_3Zn_{0.25}Zr_1$	90	0.084
$Ce_3Zn_{0.5}Zr_1$	94	0.088
$Ce_3Zn_{0.75}Zr_1$	73	0.079
$Ce_3Zn_1Zr_1$	69	0.012
Zn_3Zr_1	58	0.068

The specific surface area of synthesized Ce_3Zr_1 after calcination at $550^\circ C$ was $84 m^2/g$. The surface area increased with the incorporation of Zn in Ce_3Zr_1 from $90 m^2/g$ for $Ce_3Zn_{0.25}Zr_1$ to $94 m^2/g$ for $Ce_3Zn_{0.5}Zr_1$. Surface area decreased significantly with further increase in Zn loading ($73 m^2/g$ at Zn loading of 0.75 and $58 m^2/g$ at Zn loading of 1), indicating that the ZnO particles are deposited on the external surface of Ce_3Zr_1 . The deposition of ZnO particles leads to decrease in pore size of samples with increase in Zn loading. The size of the Zn particles outside of the Ce_3Zr_1 pores was unrestricted, and these particles were free to grow with increase in Zn loading, resulting in the observed significant increase in crystallite size from 32 to 75 nm (Table 3B.3, Entry 5-7); resulting in decrease in surface area.

3B.8. 1.4. XPS analysis

The XPS analysis of all the catalysts was carried out and the presence of all components was confirmed based on the binding energies values. The XPS analysis of Ce, Zn, Zr and O was

carried out in detail for all the samples and the results are presented in Fig. 3B 3-5 and Table 3B.5. The XPS spectrum of Ce 3d was complex in nature and was fitted into ten peaks with the assignment defined in Fig.3B.3. These peaks are corresponding to five pairs of spin-orbit doublets, and were denoted as v_o (881.7 eV), v (882.9 eV), v' (885.7 eV), v'' (889.0 eV), v''' (897.6 eV), u_o (899.1 eV), u (901.2 eV), u' (903.0 eV), u'' (907.7 eV), and u''' (916.8 eV), The peaks denoted as “V” represent the Ce 3d 5/2 spin-orbit components and those labeled as “U” are attributed to the Ce 3d 3/2 spin-orbit components.^{61,62} The peaks labeled as V_o , V' , U_o and U' are assigned to Ce^{3+} species, while those labeled as V'' , V''' , U'' and U''' , are assigned Ce^{4+} species. XPS analysis indicated that both Ce^{3+} and Ce^{4+} species were present in all samples.

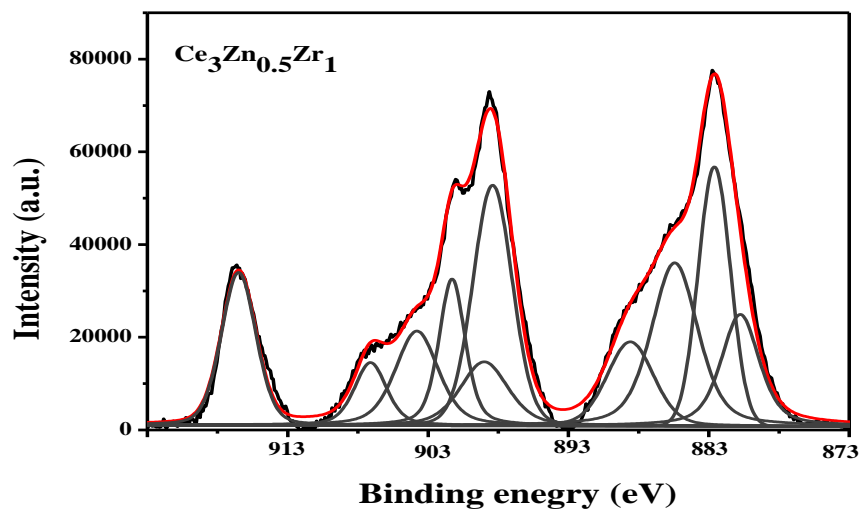
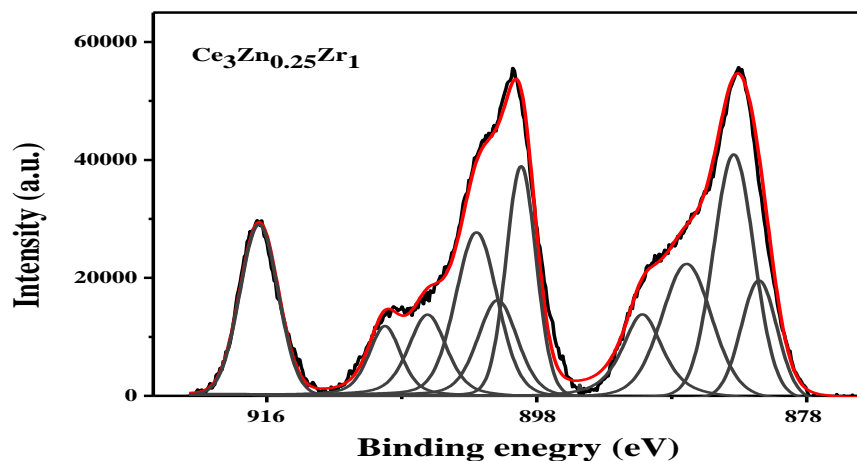
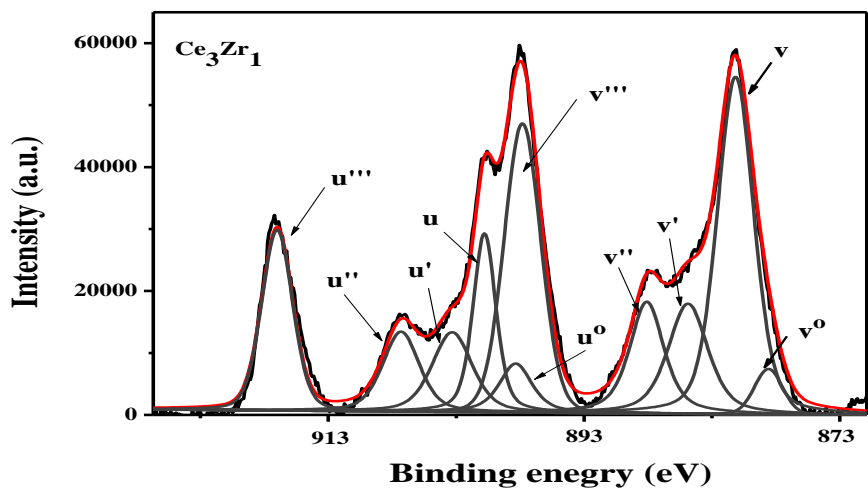
Table 3B.5. Surface composition and relative atomic ratio of Ce3d and O1s for the $Ce_3Zn_xZr_1$ MMOs determined from XPS measurements.

Entry	Sample	%				$Ce^{3+} : Ce^{4+}$	$O' : O''$
		Ce^{3+}	Ce^{4+}	O'	O''		
1	Ce_3Zr_1	32	68	82	18	0.47	0.21
2	$Ce_3Zn_{0.25}Zr_1$	39	61	67	33	0.64	0.49
3	$Ce_3Zn_{0.5}Zr_1$	46	54	52	48	0.85	0.92
4	$Ce_3Zn_{0.75}Zr_1$	41	59	73	27	0.69	0.36
5	$Ce_3Zn_1Zr_1$	35	65	76	24	0.53	0.31
6	Zn_3Zr_1	nd	nd	85	15	nd	0.17

Concentration of O 1s: $O' = O' / (O' + O'')$ and $O'' = O'' / (O' + O'')$

The relative percentages of Ce^{3+} and Ce^{4+} were calculated from the area ratio of $\text{Ce}^{3+}/(\text{Ce}^{4+} + \text{Ce}^{3+}) \times 100$, and $\text{Ce}^{4+}/(\text{Ce}^{4+} + \text{Ce}^{3+}) \times 100$. For this purpose deconvolution of peaks (Fig. 3B.3) was carried out for all the samples and the results are presented in Table 3B.5. For Ce_3Zr_1 the $\text{Ce}^{4+}/(\text{Ce}^{4+} + \text{Ce}^{3+})$ ratio was 68% and $\text{Ce}^{3+}/(\text{Ce}^{4+} + \text{Ce}^{3+})$ ratio was 32%. The percentage of Ce^{3+} increased with Zn loading (Ce^{3+} : 39 and 46%, Zn loading: 0.25 and 0.5 molar equivalent) till Zn loading of 0.5 with decrease in Ce^{4+} percentage (Ce^{4+} : 61-54%, Zn loading: 0.25 and 0.5 molar equivalent). With further increase in Zn loading (0.75-1 molar equivalent) decrease in $\text{Ce}^{3+}/(\text{Ce}^{4+} + \text{Ce}^{3+})$ ratio with increase in $\text{Ce}^{4+}/(\text{Ce}^{4+} + \text{Ce}^{3+})$ was observed (Table 3B.5, Entries 4 and 5).⁶² The observed result was probably due to the synergistic effect between Zn and Ce, which leads to some electronic interaction.⁶² The mixing of Zn and Ce together can cause a redox reaction such as $\text{Zn}^{2+} + \text{Ce}^{3+} \leftrightarrow \text{Zn}^+ + \text{Ce}^{4+}$. The transformation of Ce^{4+} to Ce^{3+} can create the charge imbalance and oxygen vacancy on the surface, which facilitates the adsorption of oxygen species or activates reactants in the reaction.^{62,63} Zn incorporated in the lattice is maximum at Zn loading of 0.5 according to XRD analysis (See Section 3B.8), thus mixing of Ce and Zn will be maximum at this Zn loading. At higher Zn loading ZnO is deposited on the Ce_3Zr_1 surface and does not interact with Ce and leads to decrease in Ce^{3+} concentration in these samples.

Zhu et al.⁶² Observed the same phenomenon in $\text{Cu}_x\text{-Ce}_{0.5-x}\text{Zr}_{0.5}$ catalyst used in the $\text{NH}_3\text{-SCR}$ of NO reaction. According to XPS studies, the synergistic effect between Cu and Ce leads to some electronic transfer, $\text{Cu}^{2+} + \text{Ce}^{3+} \leftrightarrow \text{Cu}^+ + \text{Ce}^{4+}$, increasing the amount of active oxygen species (oxygen vacancy). In addition, the synergistic effect also increased the acidity on the surface of catalyst, which is beneficial to the $\text{NH}_3\text{-SCR}$ reaction.



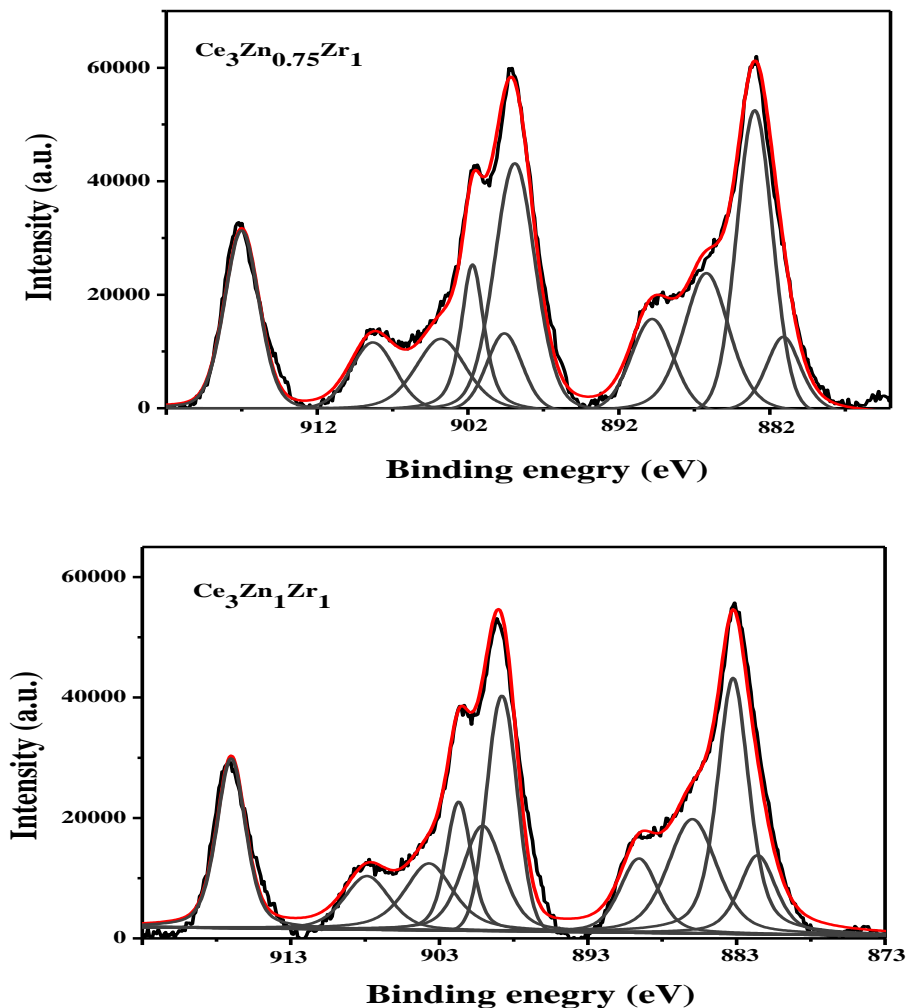
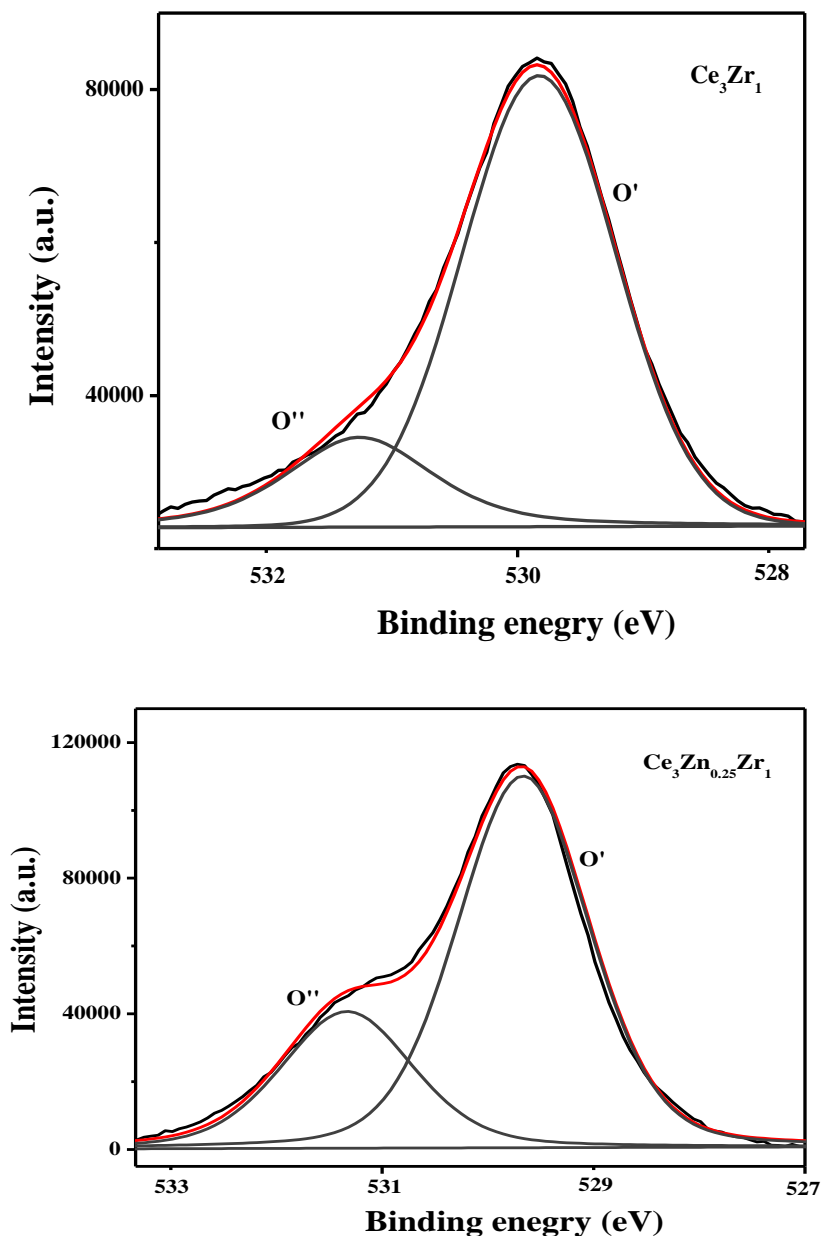
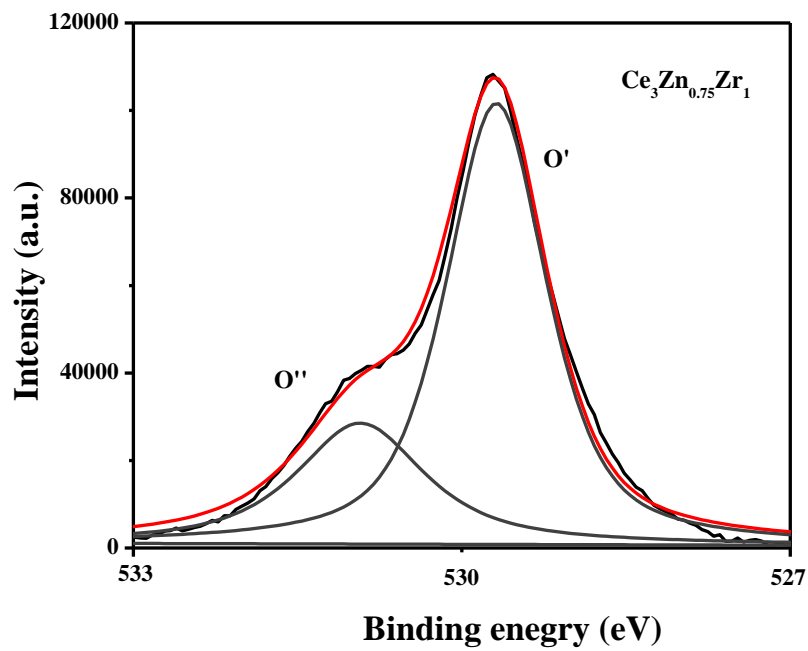
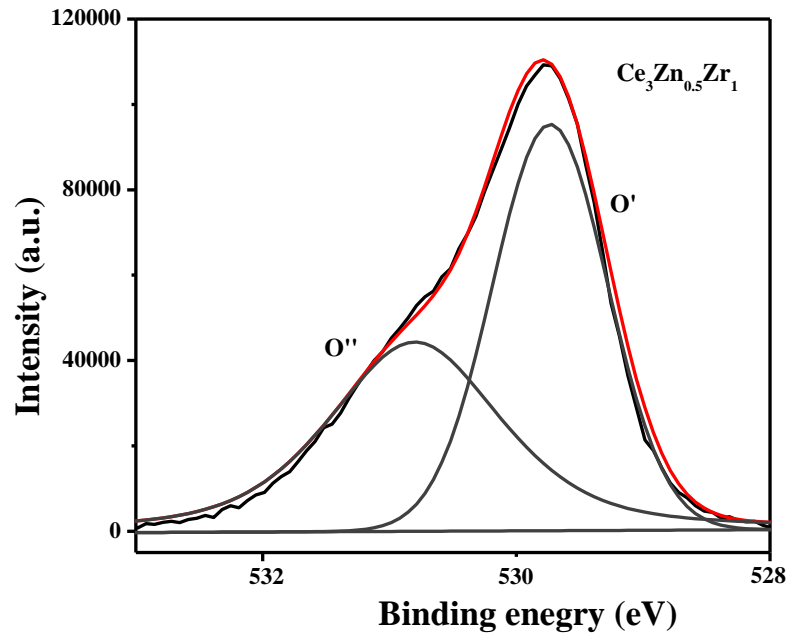


Figure 3B.3: Ce 3d 3/2, 5/2 XPS spectrum of synthesized $\text{Ce}_3\text{Zn}_x\text{Zr}_1$ MMOs

The high-resolution XPS spectrum for the O 1s ionization for all $\text{Ce}_3\text{Zn}_x\text{Zr}_1$ MMOs prepared is presented in Fig. 3B.4. The O 1s peaks for all MMOs are numerically fitted with two components (Fig.3B.4). The primary band O' (529.7eV) is attributed to the O 1s ionization for oxygen of the metal oxides (lattice oxygen), while the shoulder O'' (531.1 eV) at slightly higher binding energy is the result of chemisorbed oxygen (oxygen vacancy sites). We can notice that the O 1s ionization features for all of the catalysts are very similar (Fig. 3B.4). According to the literature, the chemisorbed oxygen species are more reactive than the lattice oxygen because of

its higher mobility.^{64,65} The relative concentration ratio of O' to O'' for all catalysts is summarized in Table 3B.5. The O' to O'' ratio for Ce₃Zr₁ is 0.21. The ratio increased with Zn loading (O' to O'' ratio: 0.49 and 0.92, Zn: 0.25 and 0.5 respectively). However, the ratio decreased significantly with further increase in Zn loading (O' to O'' ratio: 0.36 and 0.31, Zn: 0.75 and 1.0 respectively). The results indicate that Ce₃Zn_{0.5}Zr₁ contains more chemisorbed oxygen species than other mixed metal oxides prepared (Table 3B.5).





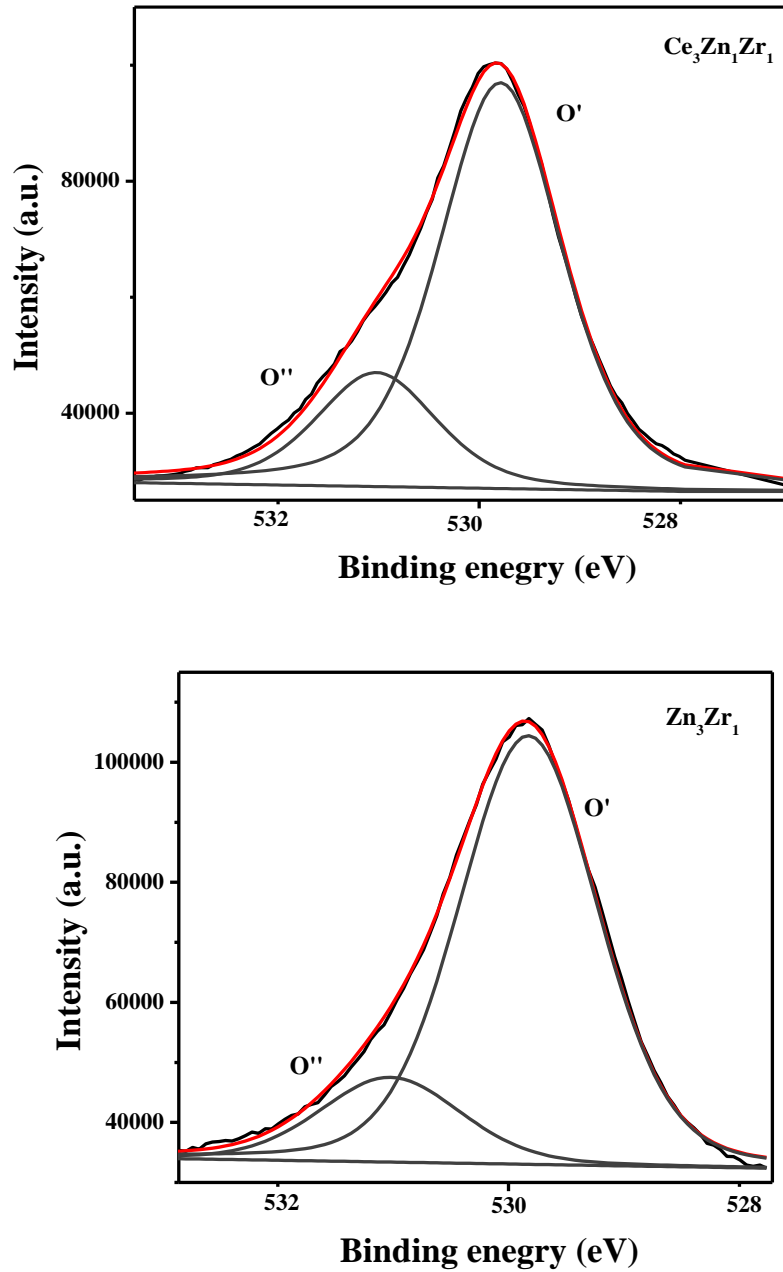


Figure 3B.4: O1s XPS spectrum of synthesized $\text{Ce}_3\text{Zn}_x\text{Zr}_1$ MMOs

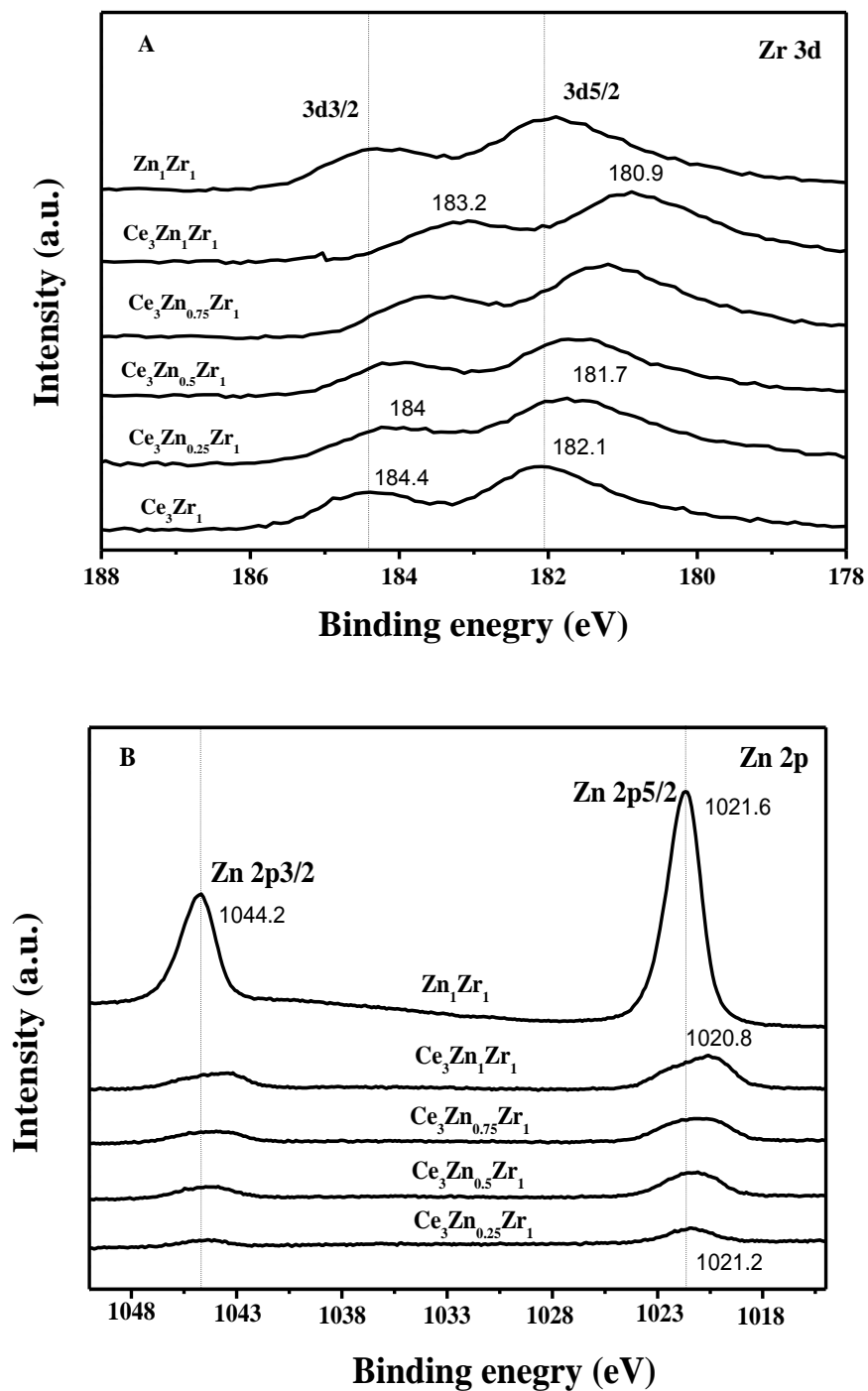


Figure 3B.5 : XPS spectra of (A) Zr3d and (B) Zn 2p of all synthesized $\text{Ce}_3\text{Zn}_x\text{Zr}_1$ MMOs.

XPS analysis of Zr 3d and Zn 2p carried out for all $\text{Ce}_3\text{Zn}_x\text{Zr}_1$ MMOs prepared are presented in Fig. 3B.5 A and B respectively. The binding energy of Zr in Ce_3Zr_1 and Zn_3Zr_1 observed at 182.1eV is consistent with the reported value for pure ZrO_2 (Zr^{4+} 182.1 eV). However, the

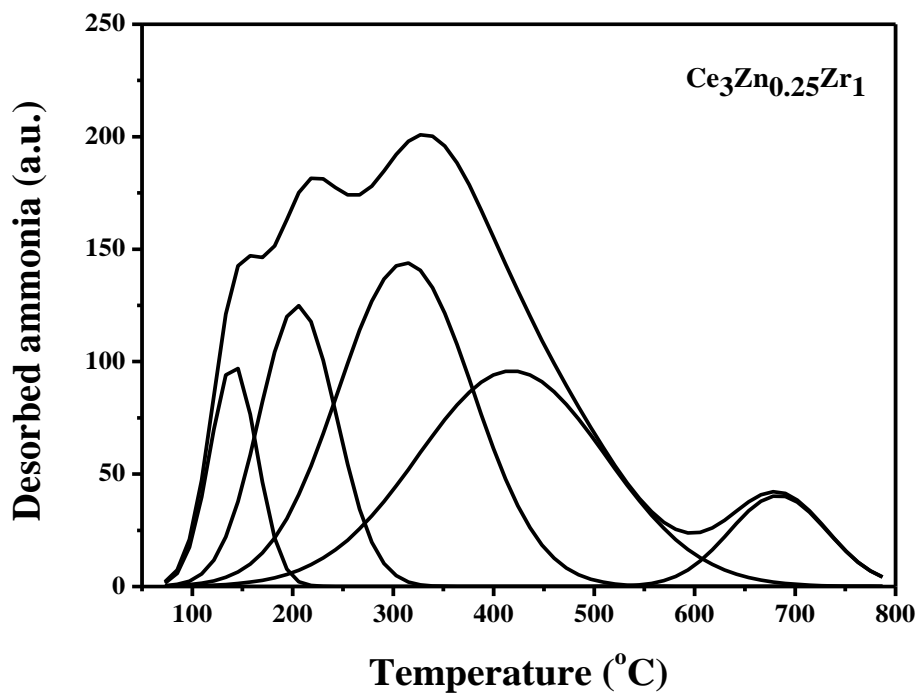
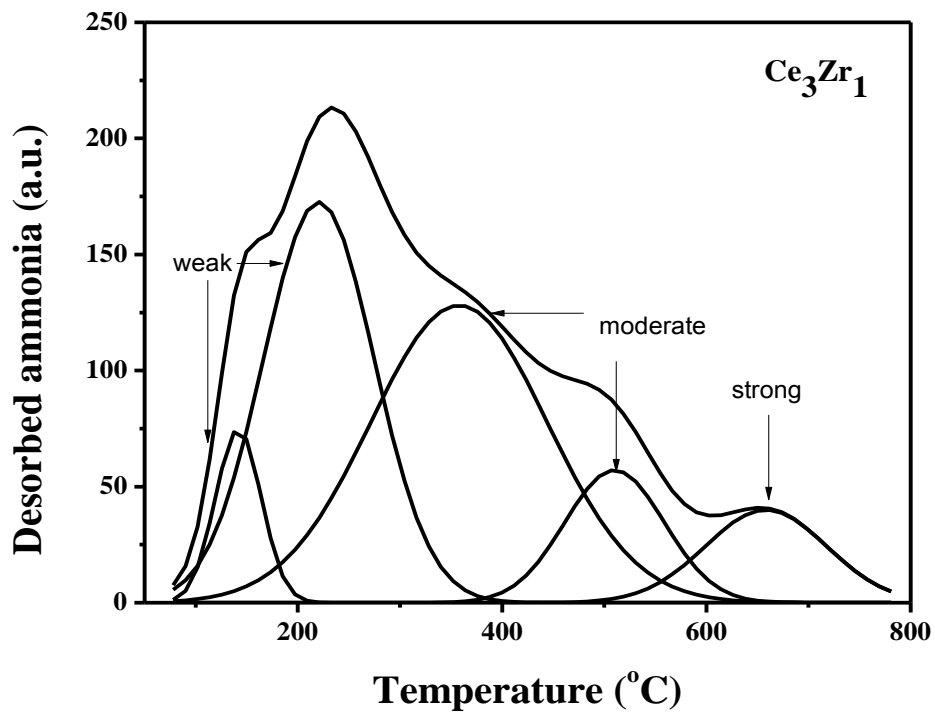
binding energy of Zr in Zn incorporated mixed metal oxide samples were observed to be slightly lower and in a range of 180.9-181.7 eV. Based on this the oxidation state of Zr in Zn incorporated samples is mainly 3^+ . Moreover, the peak positions of Zr 3d for Zn incorporated samples has shifted toward lower binding energy than that for Ce_3Zr_1 and Zn_3Zr_1 , suggesting that partial charge shift may occur from zinc and cerium species to zirconium species. According to the literature, it may be have according to the two possible reactions as follows: $Zn^+ + Zr^{4+} \leftrightarrow Zn^{2+} + Zr^{3+}$ and $Ce^{4+} + Zr^{3+} \leftrightarrow Ce^{3+} + Zr^{4+}$.⁶²

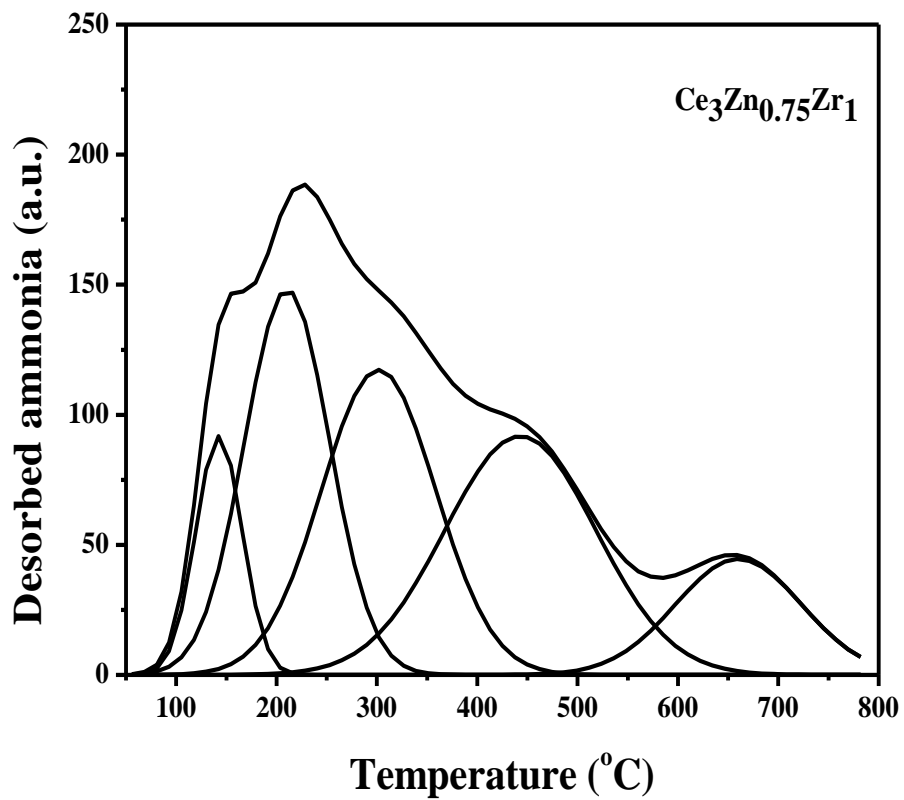
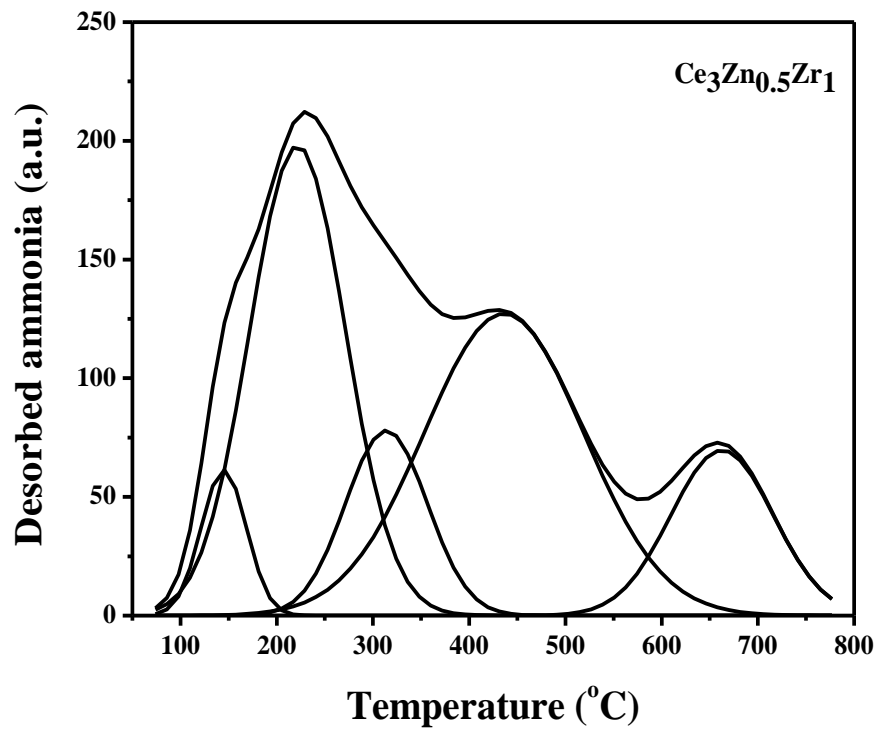
3B.8.1.5. NH_3 -TPD analysis

Acid properties of the synthesized $Ce_3Zn_xZr_1$ MMOs were studied using NH_3 -TPD analysis and the results are presented in Fig. 3B.6. Quantity of NH_3 desorbed from the weak (< 250°C), moderate (250-450°C) and strong (> 450°C) acidic sites are shown in Table 3B.6.

Table 3B.6: Acid properties of synthesized mixed metal oxides

Entry	Sample name	Desorbed NH_3 ($\mu\text{mol/g}$)			Total amount of acid sites ($\mu\text{mol/g}$)
		Weak < 250°C	Moderate 250-450°C	Strong > 450°C	
1	Ce_3Zr_1	122	137	38	297
2	$Ce_3Zn_{0.25}Zr_1$	130	156	41	327
3	$Ce_3Zn_{0.5}Zr_1$	144	163	59	366
4	$Ce_3Zn_{0.75}Zr_1$	135	143	46	324
5	$Ce_3Zn_1Zr_1$	132	129	42	303
6	Zn_3Zr_1	124	115	25	264





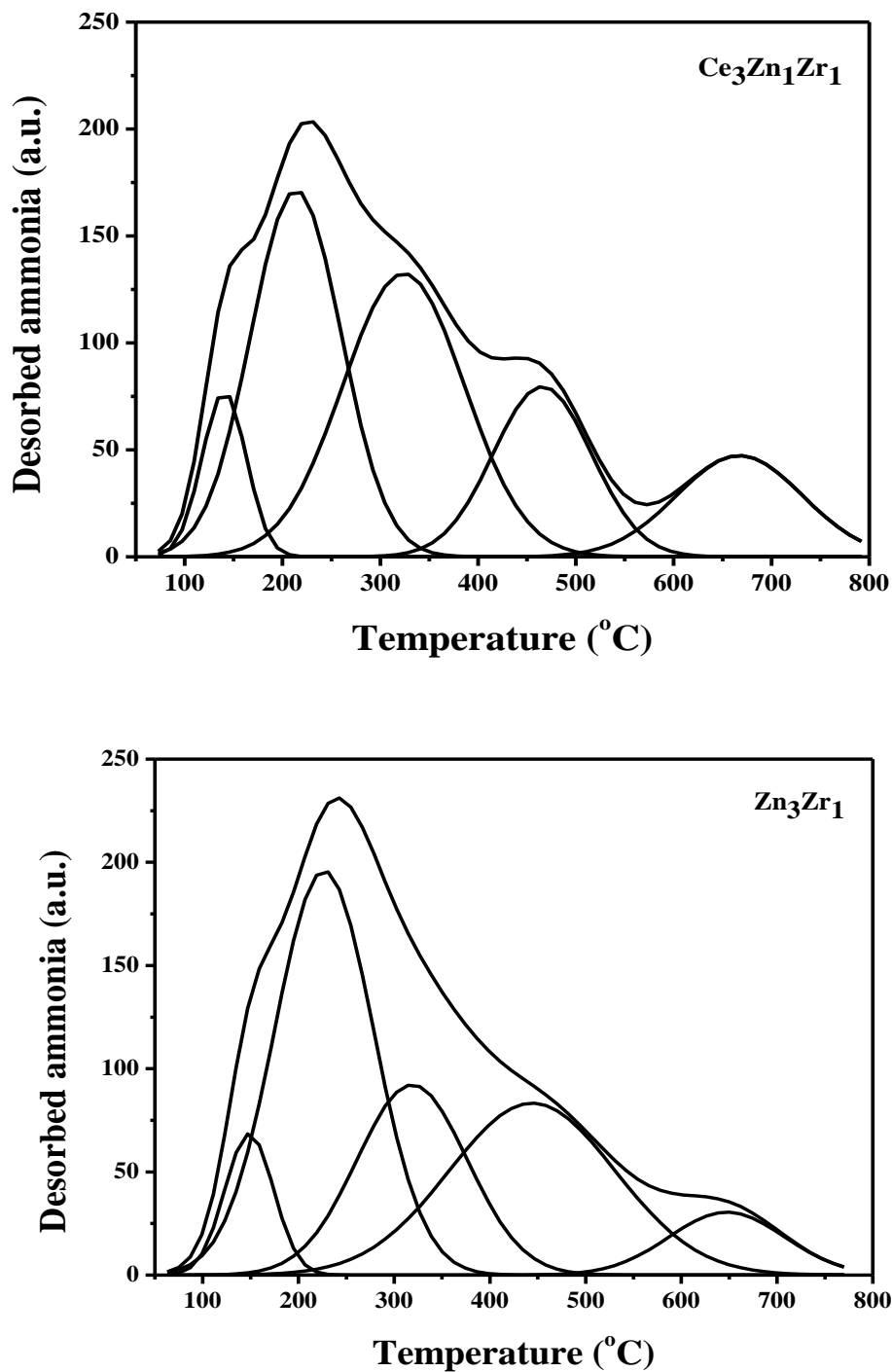


Figure 3B.6: NH_3 TPD of $Ce_3Zn_xZr_1$ MMOs.

As shown in Fig. 3B.6 and Table 3B.6; total acidity present in the binary metal oxides Ce_3Zr_1 and Zn_3Zr_1 was 297 and 264 $\mu\text{mol/g}$ respectively. Among these the contribution of weak and

medium strength acid sites was high for both the samples. Total acidity increased with Zn incorporation till 0.5 molar equivalents (Table 3B.6 Entries 2 and 3). With further increase in Zn loading total acid sites decreased (Table 3B.6, Entries 4 and 5). Thus total Acid sites varied in the order: $Ce_3Zr_1 < Ce_3Zn_{0.25}Zr_1 < Ce_3Zn_{0.5}Zr_1 > Ce_3Zn_{0.75}Zr_1 > Ce_3Zn_1Zr_1 > Zn_3Zr_1$. Among all synthesized MMOs $Ce_3Zn_{0.25}Zr_1$ showed the highest amount of weak (144 $\mu\text{mol/g}$) medium (163 $\mu\text{mol/g}$) and strong (59 $\mu\text{mol/g}$) acid sites based on the area of NH_3 desorption peak calculated by peak integral (Table 3B.6). Best result was observed with $Ce_3Zn_{0.25}Zr_1$ mixed metal oxide as the catalyst and may be attributed to the presence of highest amount of total acid sites.

Based on the characterization results and discussion above, it can be concluded that ZnO is incorporated in the Ce_3Zr_1 phase till Zn concentration of 0.5. However, with further increase in Zn loading (0.75 to 1) peaks corresponding to ZnO were observed (XRD Fig.3B.1.), indicating deposition of excess ZnO on Ce_3Zr_1 surface which lead to significant increase in crystal size 32-75nm. Agglomeration of ZnO particles leads to increase in crystal size and lowering the surface area and pore size, which was clearly observed from TEM analysis (Fig.3B.2). On the other hand the synergic effect between Zn and Ce oxides leads to the enhancement of electronic interaction through the redox reactions of $Zn^{2+} + Ce^{3+} \leftrightarrow Zn^+ + Ce^{4+}$ thus, increasing the amount of active oxygen species (oxygen vacancy) (see Table 3B.5). This synergic effect also increases the acidity on the surface of catalyst, which increases the activity towards methoxycarbonylation. Replacing cerium ions by cation having small ionic radii (Zn) increases the ion mobility inside the modified lattice, resulting in the formation of a defective fluorite-structured solid solution, Such modifications in the defect structure of ceria confer new properties to the catalyst such as better resistance to sintering at high temperatures and high catalytic activity for various reactions.⁶⁷ The mixing of two different oxides could result in the formation of new stable

compounds that may lead to totally different physico-chemical properties and catalytic behavior⁶¹⁻⁶³ as observed in the present work. Best results were obtained with $Ce_3Zn_{0.5}Zr_1$ MMO as the catalyst and hence detailed optimization study was carried out using this catalyst/

3B.9. Effect of reaction conditions

The effect of aniline:DMC molar ratio, reaction temperature and catalyst loading was investigated in detail for methoxycarbonylation of aniline with DMC using $Ce_3Zn_{0.5}Zr_1$ MMOs catalyst. All the experiments in this study were carried out with sampling in a time range of 1-5 h. conversion/selectivity Vs time profiles obtained under various reaction conditions are presented below.

3B.9.1. Effect of catalyst loading

Effect of catalyst loading on the reaction was investigated using $Ce_3Zn_{0.5}Zr_1$ MMO as the catalyst (catalyst loading of 5-15 wt%) at 180°C temperature (Table 3B.7). Experiments were carried out at 1, 2, 3 and 4 h reaction time for each catalyst loading to understand the reaction profile at different time intervals. Results obtained are presented in Table 3B.7 and aniline conversion profiles are presented in Fig. 3B.7. From the results it was observed that the activity was low with catalyst loading of 5 wt% in 1 h (60 % conversion with 92.7% MPC selectivity). Activity increased with reaction time and reached 98.2 % aniline conversion with 94.6 % selectivity to MPC in 4 h. MPC selectivity increased till reaction time of 3 h (97%) and decreased marginally at 4 h with increase in MMPC selectivity (Table 3B.7, Entry 4).

Table 3B.7: Effect of catalyst loading on methoxycarbonylation of aniline with DMC

Entry	Catalyst loading (wt%)	Time (h)	Aniline conversion (%)	Selectivity (%)			
				MPC	MMPC	NMA	NNDMA
1	5	1	60	92.7	0.9	5.2	0.2
2	5	2	87	95.8	1	2.3	0.39
3	5	3	92.5	97	1.2	0.9	0.7
4	5	4	98.2	94.8	2.6	0.5	1
5	10	1	73	97	0.08	1.9	-
6	10	2	98.4	98.6	0.1	1.2	0.09
7	10	3	98.6	96.6	1.4	1	0.6
8	10	4	98.5	95	2.6	0.6	0.9
9	15	1	84.8	97.6	-	2.3	-
10	15	2	96.3	96.6	1.6	1.5	0.2
11	15	3	98.2	95.7	2.3	1.2	0.3
12	15	4	97.9	90.5	7.9	0.9	0.6

Reaction conditions: Aniline: 25 mmol, DMC: 500 mmol, Aniline/DMC:1/20, Catalyst ($Ce_3Zn_{0.5}Zr_1$) : 5-15 wt % relative to aniline, Reaction Time: 1-4 h, Temperature: 180°C.

Aniline conversion increased with increase in catalyst loading with high selectivity to MPC. Drop in MPC selectivity because of the formation of methylated by-products was observed at longer reaction times and was prominent at higher catalyst loading. Thus 97.9% conversion of aniline with 90.9% selectivity to MPC, 7.9% selectivity to MMPC was observed with 15% catalyst loading at 4 h reaction time. Optimum results were obtained with catalyst loading of 10

wt% (98.4 % conversion of aniline with 98.6% selectivity to MPC in 2 h) and further work was carried out with the same catalyst loading.

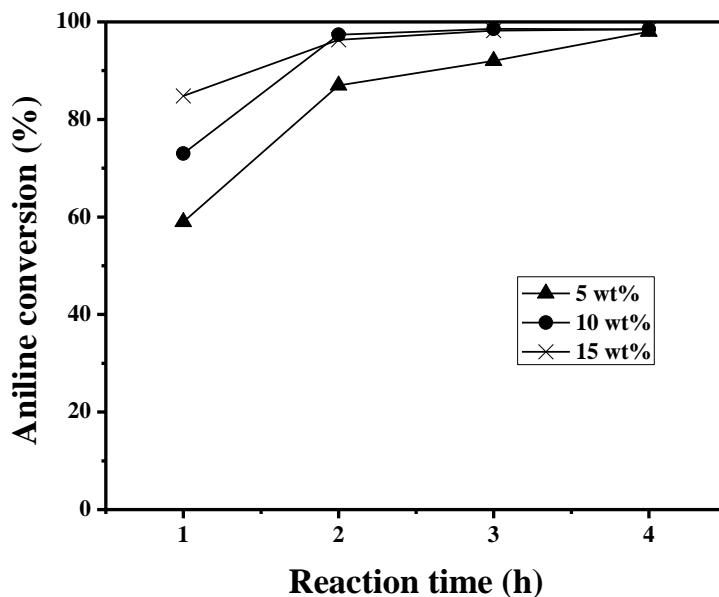


Figure 3B.7: Effect of catalyst loading on aniline conversion w.r.t reaction time

Reaction conditions: Aniline: 25 mmol, DMC: 500 mmol, Aniline/DMC:1/20, Catalyst ($Ce_3Zn_{0.5}Zr_1$) : 1.25-15 wt % relative to aniline, Reaction Time: 1-4 h, Temperature: 180°C.

3B.9.2. Effect of Aniline: DMC molar ratio

The effect of aniline:DMC molar ratio on the activity and selectivity was investigated at 180°C with 10 wt% catalyst loading. The results are presented in Table 3B.8 and Fig. 3B.8. Aniline conversion and selectivity to MPC increased with increase in aniline:DMC molar ratio. The reason is that the excessive DMC would ensure the high conversion of aniline and shifting the reaction equilibrium in favor of MPC synthesis.

Table 3B.8: Effect of aniline:DMC molar ratio on methoxycarbonylation reaction of aniline with DMC

Entry	Molar ratio Aniline:DMC	Time (h)	Aniline conversion (%)	Selectivity (%)			
				MPC sel.	MMPC	NMA	NNDMA
1	1:5	1	74	86	1.6	11	1.9
2	1:5	2	96.6	87	2.6	7	3.2
3	1:5	3	92.5	85	3.2	6.2	4
4	1:5	4	96	82	6	4.6	5.9
5	1:10	1	81.6	92	0.5	5.8	0.3
6	1:10	2	89	93.2	0.67	3.4	0.8
7	1:10	3	95.4	94	1.6	2.9	1.2
8	1:10	4	98.2	93.3	3.8	1.3	1.5
9	1:20	1	73	97	0.08	1.9	-
10	1:20	2	98.4	98.6	0.1	1.2	0.09
11	1:20	3	98.6	96.6	1.4	1	0.6
12	1:20	4	98.5	95	2.6	0.6	0.9

Reaction conditions: Aniline: 25 mmol, DMC: 500 mmol, Aniline: DMC molar ratio= 1:5 to 1:20, Catalyst ($Ce_3Zn_{0.5}Zr_1$) : 10 wt%, Reaction Time: 1-4 h, Temperature: 180°C.

At lower aniline:DMC ratio (1:5) selectivity to MPC was marginally lower and N-methylated by-product formation was observed. Selectivity to MPC decreased with increase in reaction time (86 % at 1 h versus 82% at 4 h) at a aniline:DMC ratio of 1:5. In contrast selectivity was in a

range of 92-93% and 95-98, 6% during 1 to 4 h reaction time at aniline:DMC ratio of 1:10 and 1:20 respectively. The results clearly indicate influence of aniline concentration and aniline:DMC ratio on the activity and selectivity. Good results were observed with aniline:DMC molar ratio of 1:20 (98.4% conversion with 98.6% selectivity to MPC in 2 h) and hence further work was carried out with this ratio.

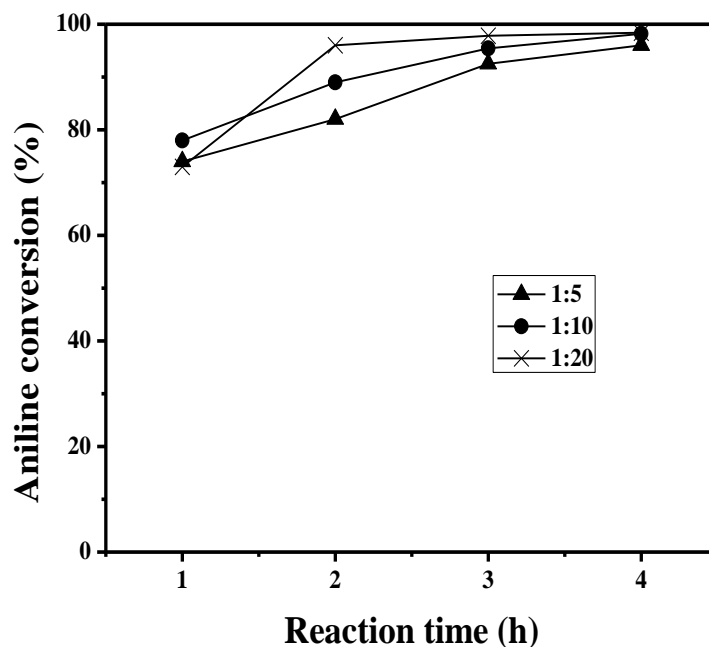


Figure 3B.8: Effect of Aniline: DMC molar ratio 1:5-1:20 on aniline conversion w.r.t reaction time.

Reaction conditions: Aniline: 25 mmol, DMC: 500 mmol, Aniline/DMC:1/5-1/20, Catalyst($\text{Ce}_3\text{Zn}_{0.5}\text{Zr}_1$) : 10 wt % relative to aniline, Reaction Time: 1-4 h, Temperature: 180°C.

3B.9.3. Effect of Temperature on activity and selectivity

The effect of temperature on methoxycarbonylation was investigated in a temperature range of 170-190°C by keeping other reaction conditions same. Results obtained are presented in Table 3B.9 and aniline conversion profiles in Fig. 3B.9.

Table 3B.9: Effect of temperature on methoxycarbonylation reaction of aniline with DMC

Entry	Reaction temperature	Time (h)	Aniline conv.(%)	Selectivity (%)			
				MPC	MMPC	NMA	NNDMA
1	170	1	53.8	95.4	0.2	3.4	-
2	170	2	80.5	97	0.6	2.2	0.2
3	170	3	91.5	97	1	1.6	0.5
4	170	4	98.3	96.2	1.5	1.3	0.9
5	180	1	73	97	0.08	1.9	-
6	180	2	98.4	98.6	0.1	1.2	0.09
7	180	3	98.6	96.6	1.4	1	0.6
8	180	4	98.5	95	2.6	0.6	0.9
9	190	1	91	93	1.5	3.8	0.9
10	190	2	97.5	96	1.6	1.9	1
11	190	3	98	93.4	4	1.3	1.2
12	190	4	98.5	86.7	7.8	0.8	2.3

Reaction conditions: Aniline: 25 mmol, DMC: 500 mmol, Aniline/DMC:1/20, Catalyst

(Ce₃Zn_{0.5}Zr₁) : 10 wt % relative to aniline, Reaction Time: 1-4 h, Temperature: 170-190°C.

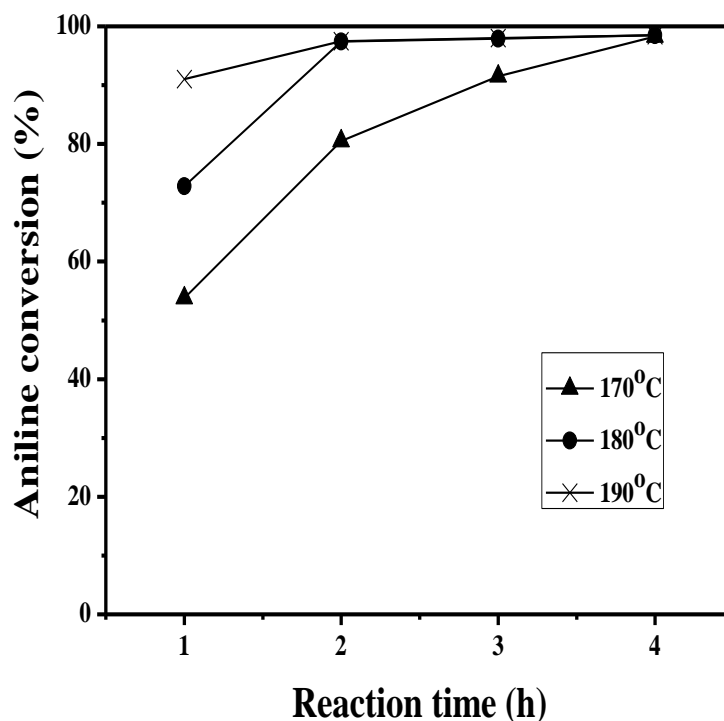


Figure 3B.9: Effect of reaction temperature on aniline conversion w.r.t reaction time

Reaction conditions: Aniline: 25 mmol, DMC: 500 mmol, Catalyst ($\text{Ce}_3\text{Zn}_{0.5}\text{Zr}_1$) : 10 wt%, Reaction Time: 1-4 h, Temperature: 170-190°C.

Aniline conversion increased (80.5-98.4% in 2 h) with increase in temperature from 170 to 180°C with high selectivity to MPC (97-98.6 %). Aniline conversion increased marginally with further increase in temperature to 190°C, however, selectivity to MPC decreased significantly with increase in N-methylated by products for 3 and 4 h reaction time (Table 3B.9, Entry 11-12). Results clearly indicate influence of temperature on the activity as well as selectivity pattern. Best results (98.4% conversion of aniline with 98.6% selectivity to MPC) were obtained at 180°C in 2 h reaction time.

3B.10. Stability of the $Ce_3Zn_{0.5}Zr_1$ MMO catalyst (recycle study)

In order to check the stability of the $Ce_3Zn_{0.5}Zr_1$ MMO catalyst for methoxycarbonylation reaction of aniline with DMC, reaction was carried out at 180°C for 2 h under optimized reaction conditions. The catalyst from the reaction mixture was recovered by centrifugation, washed with DMC, and then dried overnight at 100°C for 12 h and calcined at 550°C/6 h in air. The recovered catalyst was used to perform new reaction by charging aniline and DMC to the reactor. Catalyst was recycled five times using the same procedure.

Table 3B.10: Recycle study using $Ce_3Zn_{0.5}Zr_1$ ternary mixed metal oxide catalyst

	Aniline Conversion (%)	MPC Selectivity (%)
Fresh	98.4	98.65
Recycle 1	97.54	97.47
Recycle 2	94.17	97.20
Recycle 3	91.97	97.54
Recycle 4	91.93	96.61
Recycle 5	90.54	96.04
Recycle 6	89.2	96

Reaction conditions: Aniline: 25 mmol, DMC: 500 mmol, Aniline/DMC:1/20, Catalyst ($Ce_3Zn_{0.5}Zr_1$) : 10 wt % relative to aniline, Reaction Time: 2 h, Temperature: 180°C.

From the results presented in Table 3B.11 activity and selectivity was very high during recycle. Aniline conversion decreased from 98.4 to 89.2 with very high selectivity to MPC (96-98%). Slight drop in aniline conversion may be due to handling loss of the catalyst during recycle procedure. At the end of the 5 recycle experiments the XRD and TEM analysis of the used catalyst was carried out (Fig. 3B 10-11) and the results are compared with fresh catalyst sample. XRD analysis and TEM analysis of fresh catalyst and catalyst recovered after five recycle experiments showed similar pattern and did not show significant changes in the analysis. The results demonstrate good stability of the catalyst even after five recycle experiments. To the best of our knowledge this is the first catalyst with good activity and recyclability reported in the literature for methoxycarbonylation of aniline with DMC.

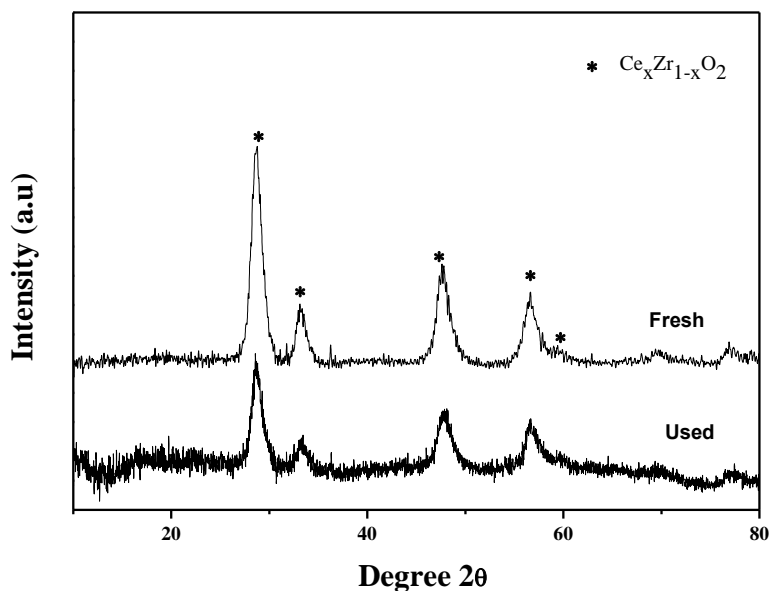


Figure 3B.10: XRD patterns of $Ce_3Zn_{0.5}Zr_1$ MMO fresh and used catalyst.

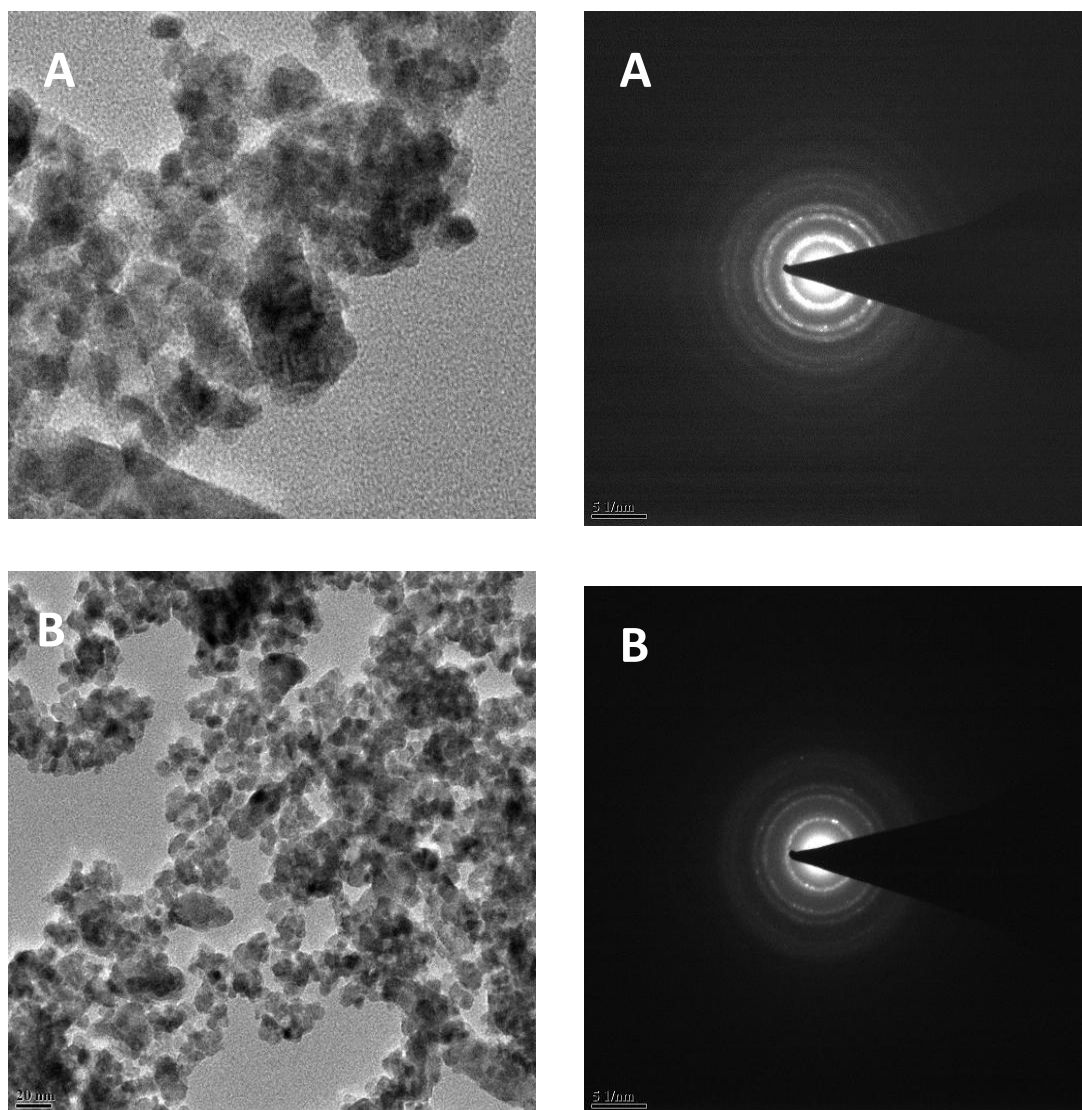


Figure 3B.11: (A) TEM and SAED image of fresh $\text{Ce}_3\text{Zn}_{0.5}\text{Zr}_1$ (B) TEM and SAED image of used $\text{Ce}_3\text{Zn}_{0.5}\text{Zr}_1$

3B.11. Screening of aromatic amines

Various aromatic amines were screened for methoxycarbonylation reaction using $\text{Ce}_3\text{Zn}_{0.5}\text{Zr}_1$ MMO catalyst under optimized reaction conditions and the results are presented in Table 3B.11.

Table 3B.11: Screening of aromatic amines for methoxycarbonylation reaction using $Ce_3Zn_{0.5}Zr_1$

Entry	Aromatic amines	Conversion of amines (%)	Aromatic carbamates Selectivity (%)
1	o-Toluidine	82.5	94.2
2	m-Toluidine	86.8	95
3	p-Toluidine	90	95.7
4	m-Anisidine	78	89
5	p-Anisidine	98	94
6	2,4 dimethyl aniline	64	96
7	4-Chloroaniline	99.09	97.3
8	4-Bromo aniline	99.40	98

Reaction conditions: Amine: 25 mmol, DMC: 500 mmol, Aniline/DMC:1/20, $Ce_3Zn_{0.5}Zr_1$: 10 wt % relative to aniline, Reaction Time: 2 h, Temperature: 180°C.

Various substituted aniline moieties bearing electron donating and withdrawing substituents on the phenyl ring were well tolerated under the present reaction conditions and provided corresponding carbamate derivatives in good to excellent yields (Table 3B.11, Entries 1-8). Different reactivity's of *O*- and *P*- substituted methoxy aniline was observed due to steric hindrance of the substituted group (-OCH₃). Ortho substituted methoxy aniline showed lower activity (82.5%) compared to para substituted methoxy aniline (90%) (Table 3B.11, Entry 1 and 3) with comparable selectivity to corresponding carbamate derivative.

3B.12. Preliminary investigations to understand reaction pathways

Methoxycarbonylation of aniline with DMC as methoxycarbonylating agent produces methyl *N*-phenyl carbamate (MPC) and alkylated products (MMPC, NMA and NNDMA) depending on the reaction conditions (temperature, aniline, NMA and DMC concentrations etc.). Different reactions possible under reaction conditions and products formed are presented in Fig. 3B.12.

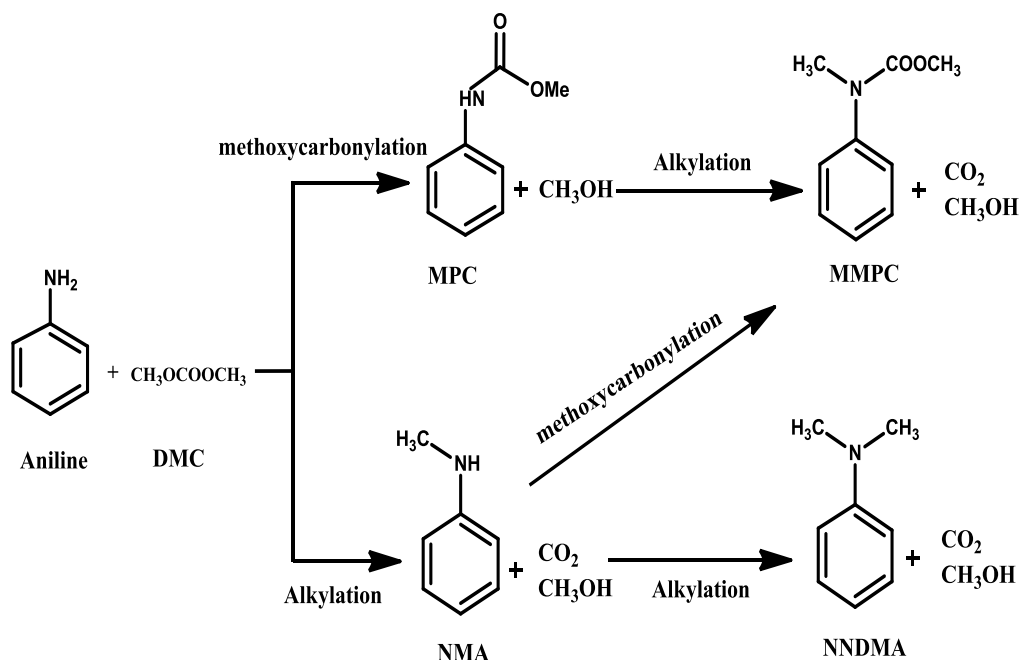


Figure 3B.12.: Schematic of methoxycarbonylation of aniline with DMC and the possible by-products form during reaction.

Methoxycarbonylation of aniline with DMC is a complex reaction with the possibility of various products as presented in Fig. 3B.12. Aniline is a hard base and leads to the formation of MPC as the product via methoxycarbonylation (Fig. 3B.12). *N*-methylation of aniline can lead to the formation of *N*-methyl aniline (NMA) as the product. Methyl *N*-methyl phenylcarbamate (MMPC) can be formed as product via two routes: 1) *N*-methylation of MPC formed as the

product or methoxycarbonylation of NMA as shown in the Fig. 3B.12. It is known that DMC can act as methoxycarbonylation as well as methylating agent depending on the reaction conditions and catalyst used.¹⁴ Tundo et al. observed that MPC obtained as the product undergoes methylation reaction preferably instead of methoxycarbonylation, favouring MMPC as the product.¹⁴ Finally N-methylation of NMA will lead to the formation of N,N-dimethylamine (NNDMA) as the product. In order to gain insight in to the product distribution and possible reaction path involved; few experiments were carried out using aniline, NMA and MPC as reactants and Zn(Proline)₂ and Ce₃Zn_{0.5}Zr₁ mixed metal oxide as catalysts and the results are presented in Table 3B.12 and 3B.13 respectively.

Table 3B.12: Interaction of reactants/products under methoxycarbonylation conditions using Zn (Proline)₂ catalyst

Entry	Substrate	Conversion (%)	Selectivity (%)			
			MPC	MMPC	NMA	NNDMA
1	Aniline+DMC*	-	-	-	-	-
2	Aniline+DMC	98.6	97.8	0.4	0.5	0.2
3	NMA+DMC	20	0.1	41.3	-	58.3
4	MPC+DMC	5	-	99.4	-	-

Reaction conditions: Substrate: 25 mmol, DMC: 250 mmol , Substrate/ DMC: 1:10, Catalyst Zn(Proline)₂: 1.25 wt% relative to substrate, Reaction Time: 3 h, Temperature: 170°C.

*Without catalyst

Table 3B.13: Interaction of reactants/products under methoxycarbonylation conditions using $Ce_3Zn_{0.5}Zr_1$ catalyst

Entry	Substrate	Conversion (%)	Selectivity (%)			
			MPC	MMPC	NMA	NNDMA
1	Aniline+DMC*	-	-	-	-	-
2	Aniline+DMC	97.4	98.7	0.24	0.49	0.1
3	NMA+DMC	24.69	0.4	62	-	36
4	MPC+DMC	4	-	99.3	-	-

Reaction condition: Substrate: 25 mmol, DMC: 500 mmol Substrate: DMC= 1:20, Catalyst ($Ce_3Zn_{0.5}Zr_1$): 10 wt % relative to substrate, Reaction Time: 2 h, Temperature: 180°C.

*Without catalyst

From the results presented in Tables 3B.12 ($Zn(Proline)_2$ catalyst) and 3B.13 ($Ce_3Zn_{0.5}Zr_1$ catalyst) it was observed that catalyst is necessary for the reaction. Reaction proceeded smoothly with aniline as reactant and $Zn(Proline)_2/Ce_3Zn_{0.5}Zr_1$ catalysts giving 98.6 and 97.4 % aniline conversion with 97.8 and 98.7% selectivity to MPC respectively. The selectivity to methylated by-products was very low with both the catalysts (Tables 3B.12- 3B.12). With N-methylaniline (NMA) as the reactant the activity was low with both the catalysts. Thus 20 and 24.7% aniline conversion was observed with $Zn(Proline)_2$ and $Ce_3Zn_{0.5}Zr_1$ catalysts respectively with MMPC (41.3% and 62%) and NNMDA (58.3% and 36%) as the products. Formation of NNDMA was favored with $Zn(Proline)_2$ as catalyst, while formation of MMPC was favored with $Ce_3Zn_{0.5}Zr_1$ as the catalyst. Interestingly MPC was stable under reaction conditions for both the catalysts and only 4-5% conversion was observed with selective formation of MMPC as the product. The

results indicate that aniline is reactive and both the catalysts are selective for the formation of MPC as the product with low selectivity to methylation by-products. NMA as reactant is less reactive still 20-25% conversion is observed and depending on the catalyst used mettoxycarbonylation or N-methylation of aniline is preferred. Interestingly MPC is stable under reaction conditions for longer reaction time. Depending on the reaction conditions used if N-methylation takes in the initial phase of the reaction, then product distribution can vary significantly. In the present study high selectivity to MPC is observed at higher aniline:DMC molar ratio for both the catalysts (aniline:DMC 1:10 Zn (Proline)₂ for and 1:20 for Ce₃Zn_{0.5}Zr₁). Selectivity to MPC is significantly affected by a change in aniline:DMC molar ratio and temperature of the reaction. As per the industry requirement there is a need to reduce aniline:DMC ratio as low as possible. Experiments carried out in this section will be useful in understanding reaction pathways and good stability of MPC under reaction conditions is important observation. Further work is necessary to optimize MPC selectivity at lower aniline:DMC molar ratio.

3B.13. Conclusion

Various binary and ternary mixed metal oxides were prepared by co-precipitation method and screened for the reaction. Best results 98.4% conversion of aniline with 98.6% selectivity to MPC was observed with Ce₃Zn_{0.5}Zr₁ MMO as the catalyst. The catalyst was characterized in detail by various characterization techniques. Characterization results elucidated the strong synergic interaction between active Zn and Ce₃Zr₁ support showing the high acid sites and oxygen vacancies on solid surface. Optimization of reaction conditions was carried out using Ce₃Zn_{0.5}Zr₁MMO as the catalyst. Good results were observed with aniline: DMC ratio of 1:20

reaction temperature 180°C/2h (98.4% conversion with 98.6% selectivity to MPC in 2 h). $Ce_3Zn_{0.5}Zr_1$ can be recycle up to 6 recycle experiments with slight drop in activity. $Ce_3Zn_{0.5}Zr_1$ catalyst is an efficient, stable, inexpensive and recyclable heterogeneous catalyst for methoxycarbonylation of aniline and DMC.

3B.14. Overall Conclusions

Methoxycarbonylation of aniline with DMC was investigated in details using $Zn(Proline)_2$ and $Ce_3Zn_{0.5}Zr_1$ as catalysts. Various metal-amino acid complexes and mixed metal oxides were prepared and screened for methoxycarbonylation reaction. Optimization of reaction conditions and recycle study was carried out for both the catalysts. Important highlights of the work are as follows:

3A. Methoxycarbonylation of aniline with $Zn(Proline)_2$ as the catalyst

- ❖ Various metal-amino acid complexes were screened for methoxycarbonylation of aniline with DMC, where $Zn(Proline)_2$ was found to be the best catalyst.
- ❖ Optimization of reaction conditions was carried out with $Zn(Proline)_2$ as the catalyst and good results were observed with aniline:DMC ratio of 1:10, reaction temperature of 170°C and reaction time of 3 h (98.6% conversion with 97.8% selectivity to MPC).
- ❖ Activity decreased during recycle study and XRD analysis of the fresh and recycled catalyst indicated the formation of ZnO during recycle, leading to drop in aniline conversion during recycle.

3B. Methoxycarbonylation of aniline with $Ce_3Zn_{0.5}Zr_1$ as the catalyst

- ❖ Various binary and ternary mixed metal oxides were screened for the methoxycarbonylation of aniline and $\text{Ce}_3\text{Zn}_{0.5}\text{Zr}_1$ MMO was found to be the best catalyst.
- ❖ Effect of Zn incorporation on the activity was investigated and 0.5 mole incorporation of Zn was found to be optimum for the reaction.
- ❖ The catalyst was characterized in detail by various characterization techniques.
 - Strong synergistic interaction between active Zn and Ce_3Zr_1 support showing the higher acid sites and oxygen vacancies on solid surface.
 - Oxygen vacancies present on the catalyst surface aid activation of reactants and leading to high activity and selectivity.
 - Methoxycarbonylation activity was very poor with individual metal oxides (ZnO , CeO_2 and ZrO_2). Very high activity with $\text{Ce}_3\text{Zn}_{0.5}\text{Zr}_1$ MMO clearly demonstrated the importance of ternary mixed metal oxide and distribution of acid sites in achieving good results.
- ❖ Optimization of reaction conditions was carried out using $\text{Ce}_3\text{Zn}_{0.5}\text{Zr}_1$ MMO as the catalyst. Good results were observed with aniline: DMC ratio of 1:20 reaction temperature $180^\circ\text{C}/2\text{h}$ (98.4% conversion with 98.6% selectivity to MPC in 2 h).
- ❖ Catalyst was recycled Six times with marginal drop in aniline conversion maintaining high selectivity to MPC (96-99%).
- ❖ Interaction of aniline, MPC and NMA with both the catalysts under reaction conditions revealed that NMA gave NNDMA and MMPC as products.
 - With NMA as reaction $\text{Zn}(\text{proline})_2$ favoured formation of NNDMA as the product, while $\text{Ce}_3\text{Zn}_{0.5}\text{Zr}_1$ favoured MMPC as the product.
 - Interestingly with both the catalyst MPC was stable under reaction conditions.

3B.15. References

1. Wu, T.T., et al., *Synthesis and herbicidal activity of alpha.-heterocyclic carbinol carbamates*. Journal of agricultural and food chemistry, 1987. **35**(5): p. 817-823.
2. Piccardi, P., *The role of synthetic chemicals in insect pest control: present and future*. ChemInform, 1987. **18**(17).
3. Greene, T.W., *PGM Wuts Protective Groups in Organic Chemistry*. 1991, Wiley, New York 1991.
4. Li, F., et al., *Condensation Reaction of Methyl N-Phenylcarbamate with Formaldehyde over HI Catalyst*. Industrial & Engineering Chemistry Research. **53**(13): p. 5406-5412.
5. Lee, C.W., et al., *Acid catalysed condensation of methyl N-phenylcarbamate*. Applied catalysis, 1990. **66**(1): p. 11-23.
6. Kreye, O., H. Mutlu, and M.A.R. Meier, *Sustainable routes to polyurethane precursors*. Green Chemistry. **15**(6): p. 1431-1455.
7. Baba, T., et al., *Characteristics of methoxycarbonylation of aromatic diamine with dimethyl carbonate to dicarbamate using a zinc acetate catalyst*. Green Chemistry, 2005. **7**(3): p. 159-165.
8. Fu, Z.-H. and Y. Ono, *Synthesis of methyl N-phenyl carbamate by methoxycarbonylation of aniline with dimethyl carbonate using Pb compounds as catalysts*. Journal of molecular catalysis, 1994. **91**(3): p. 399-405.
9. Wang, S., et al., *Investigations of catalytic activity, deactivation, and regeneration of Pb (OAc)₂ for methoxycarbonylation of 2, 4-toluene diamine with dimethyl carbonate*. Industrial & Engineering Chemistry Research, 2007. **46**(21): p. 6858-6864.

10. Reixach, E., et al., *Alkoxy carbonylation of Industrially Relevant Anilines Using Zn(OAc)₂·6H₂O as Catalyst*. Industrial & Engineering Chemistry Research. **51**(50): p. 16165-16170.
11. Qiu, Z., et al., *Formation of Intermediate and By-products in Synthesis of 4,4'-Methylenedimethyldiphenylcarbamate*. Catalysis letters, 2008. **124**(3-4): p. 243-249.
12. Li, F., et al., *Investigation of supported Zn(OAc)₂ catalyst and its stability in N-phenyl carbamate synthesis*. Applied Catalysis A: General. **475**: p. 355-362.
13. Zhang, L., et al., *Experimental and theoretical investigation of reaction of aniline with dimethyl carbonate catalyzed by acid-base bifunctional ionic liquids*. Catalysis Today. **158**(3-4): p. 279-285.
14. Grego, S., F. Aric, and P. Tundo, *Phosgene-free carbamoylation of aniline via dimethyl carbonate*. Pure and Applied Chemistry. **84**(3): p. 695-705.
15. Shen, Z.L. and X.Z. Jiang, *A novel synthesis of N-methyl-N-aryl carbamates from aromatic amines and dimethyl carbonate catalyzed by K₂CO₃/Bu₄NBr*. Chinese Chemical Letters, 2004. **15**(8): p. 889-891.
16. Li, F., et al., *The Induction Period and Novel Active Species in Zn(OAc)₂ Catalyzed Synthesis of Aromatic Carbamates*. Catalysis letters. **147**(6): p. 1478-1484.
17. Guo, X., et al., *Zinc carboxylate functionalized mesoporous SBA-15 catalyst for selective synthesis of methyl-4,4'-di (phenylcarbamate)*. Catalysis letters, 2009. **128**(3-4): p. 405-412.
18. Zhao, X., et al., *Synthesis of MDI from dimethyl carbonate over solid catalysts*. Industrial & Engineering Chemistry Research, 2002. **41**(21): p. 5139-5144.

19. Siddiqui, Z.N. and T.N.M. Musthafa, *An efficient and novel synthesis of chromonyl chalcones using recyclable Zn (l-proline) ₂ catalyst in water*. Tetrahedron letters. **52**(31): p. 4008-4013.
20. Kofoed, J., T. Darbre, and J.-L. Reymond, *Dual mechanism of zinc-proline catalyzed aldol reactions in water*. Chemical communications, 2006(14): p. 1482-1484.
21. Kidwai, M., A. Jain, and R. Poddar, *Zn [(L) proline] ₂ in water: a new easily accessible and recyclable catalytic system for the synthesis of pyrazoles*. Journal of Organometallic Chemistry. **696**(10): p. 1939-1944.
22. Darbre, T. and M. Machuqueiro, *Zn-proline catalyzed direct aldol reaction in aqueous media*. Chemical communications, 2003(9): p. 1090-1091.
23. Reddy, K.R., C.V. RajaSekhar, and G.G. Krishna, *Zinc "Proline Complex: An Efficient, Reusable Catalyst for Direct Nitroaldol Reaction in Aqueous Media*. Synthetic communications, 2007. **37**(12): p. 1971-1976.
24. Sivamurugan, V., et al., *Synthesis of hantzsch 1, 4-dihydropyridines under solvent-free condition using zn [(L) proline] ₂ as lewis acid catalyst*. Journal of heterocyclic chemistry, 2005. **42**(5): p. 969-974.
25. Siddiqui, Z.N. and F. Farooq, *Zn (Proline) ₂: a novel catalyst for the synthesis of dicoumarols*. Catalysis Science & Technology. **1**(5): p. 810-816.
26. Siddiqui, Z.N., et al., *Zn (Proline) ₂-catalyzed Knoevenagel condensation under solvent-free/aqueous conditions and biological evaluation of products*. Medicinal Chemistry Research. **20**(9): p. 1438-1444.

27. Sivamurugan, V., et al., *[(L) Proline] ₂Zn Catalysed Synthesis of 1, 5-Benzodiazepine Derivatives Under Solvent-Free Condition*. *Synthetic communications*, 2004. **34**(21): p. 3833-3846.
28. Ravi, V., et al., *Zn-proline catalyzed selective synthesis of 1, 2-disubstituted benzimidazoles in water*. *Chemical and Pharmaceutical Bulletin*, 2007. **55**(8): p. 1254-1257.
29. Montazeri, N., et al., *Highly Efficient, Fast, Room Temperature Synthesis of Tetrahydrobenzo [b] pyrans Catalyzed by Zn [(L)-proline] ₂ as Green and Reusable Heterogeneous Catalyst Under Dry Grinding*. *Asian Journal of Chemistry*. **24**(10): p. 4791.
30. Heravi, M.M., et al., *Zn [(L) proline] ₂: an efficient catalyst for the synthesis of biologically active pyrano [2, 3-d] pyrimidine derivatives*. *Synthetic Communications*. **40**(13): p. 1927-1931.
31. Blevins, J.E., *Zn (L-proline) ₂: A Highly efficient catalyst for the multicomponent synthesis dihydropyrano [2, 3-c] pyrazole derivatives*.
32. Goel, O.P., *Zinc complexes of natural amino acids for treating elevated copper caused toxicities*, Google Patents.
33. Trzaskowski, B., L. Adamowicz, and P.A. Deymier, *A theoretical study of zinc (II) interactions with amino acid models and peptide fragments*. *JBIC Journal of Biological Inorganic Chemistry*, 2008. **13**(1): p. 133-137.
34. Schmidbaur, H., H.G. Classen, and J. Helbig, *Aspartic and Glutamic Acid as Ligands to Alkali and Alkaline-Earth Metals: Structural Chemistry as Related to Magnesium*

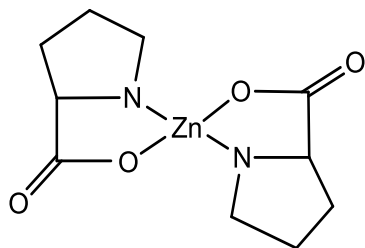
- Therapy*. Angewandte Chemie International Edition in English, 1990. **29**(10): p. 1090-1103.
35. Daniele, P.G., et al., *Weak alkali and alkaline earth metal complexes of low molecular weight ligands in aqueous solution*. Coordination chemistry reviews, 2008. **252**(10-11): p. 1093-1107.
36. Polfer, N.C., et al., *Infrared spectroscopy of phenylalanine Ag (I) and Zn (II) complexes in the gas phase*. Journal of the American Chemical Society, 2006. **128**(2): p. 517-525.
37. Li, Q.-F., et al., *A phosgene-free process for the synthesis of methyl N-phenyl carbamate by the reaction of aniline with methyl carbamate*. Journal of Molecular Catalysis A: Chemical, 2004. **212**(1-2): p. 99-105.
38. Zhao, X., et al., *Synthesis of methyl N-phenyl carbamate catalyzed by ionic liquid-promoted zinc acetate*. Industrial & Engineering Chemistry Research. **51**(35): p. 11335-11340.
39. Kumar, S. and S.L. Jain, *L-prolin TBAB-catalyzed phosgene free synthesis of methyl carbamates from amines and dimethyl carbonate*. New Journal of Chemistry, 2013. **37**(9): p. 2935-2938.
40. Margetić, Davor, et al. *Reactions of dimethyl carbonate with aliphatic amines under high pressure*. Synthetic communications, 2011. **41.15** : p. 2283-2289.
41. Aric, F. and P. Tundo, *Dimethyl carbonate: a modern green reagent and solvent*. Russian Chemical Reviews, 2010. **79**(6): p. 479-489.
42. Tundo, P., M. Selva, and S. Memoli, *Dimethylcarbonate as a green reagent*. 2000, 87-89 ACS Publications.

43. Fiorani, G., A. Perosa, and M. Selva, *Dimethyl carbonate: a versatile reagent for a sustainable valorization of renewables*. *Green Chemistry*. 2018.**20**:p. 288-322.
44. Li, Q.-F., et al., *Studies on synthesis of methyl N-phenylcarbamate by reaction of aniline and methyl carbamate*. *CHEMICAL JOURNAL OF CHINESE UNIVERSITIES-CHINESE EDITION-*, 2003. **24**(7): p. 1280-1283.
45. Li, Q., et al., *Synthesis of methyl N-phenyl carbamate by methoxycarbonylation of aniline with dimethyl carbonate*. *Chinese Journal of Catalysis*, 2003. **24**(8): p. 639-642.
46. Li, F., et al., *Synthesis of methyl N-phenyl carbamate from aniline and dimethyl carbonate over supported zirconia catalyst*. *Industrial & Engineering Chemistry Research*, 2006. **45**(14): p. 4892-4897.
47. Sadykov, V.A., et al., *Ceria-based fluorite-like oxide solid solutions as catalysts of methane selective oxidation into syngas by the lattice oxygen: synthesis, characterization and performance*. *Catalysis Today*, 2004. **93**: p. 45-53.
48. Si, Z., et al., *Modifications of CeO₂ZrO₂ solid solutions by nickel and sulfate as catalysts for NO reduction with ammonia in excess O₂*. *Catalysis Communications*. **11**(13): p. 1045-1048.
49. Cutrufello, M.G., et al., *Acid base properties and catalytic activity of nanophase ceria zirconia catalysts for 4-methylpentan-2-ol dehydration*. *Physical Chemistry Chemical Physics*, 1999. **1**(14): p. 3369-3375.
50. Vivier, L. and D. Duprez, *Ceria-Based Solid Catalysts for Organic Chemistry*. *ChemSusChem*. **3**(6): p. 654-678.
51. Li, F., et al., *Investigation of supported Zn (OAc)₂ catalyst and its stability in N-phenyl carbamate synthesis*. *Applied Catalysis A: General*. **475**: p. 355-362.

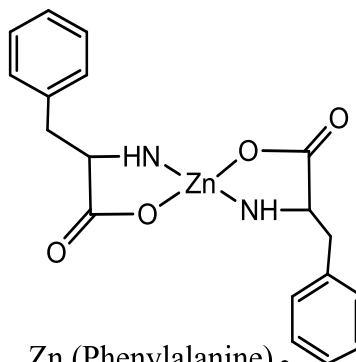
52. Kim, J.-R., W.-J. Myeong, and S.-K. Ihm, *Characteristics in oxygen storage capacity of ceria-zirconia mixed oxides prepared by continuous hydrothermal synthesis in supercritical water*. Applied Catalysis B: Environmental, 2007. **71**(1-2): p. 57-63.
53. Rossignol, S., F.o. Grard, and D. Duprez, *Effect of the preparation method on the properties of zirconia-ceria materials*. Journal of Materials Chemistry, 1999. **9**(7): p. 1615-1620.
54. Lan, L., et al., *Preparation of ceria-zirconia by modified coprecipitation method and its supported Pd-only three-way catalyst*. Journal of colloid and interface science. **450**: p. 404-416.
55. Ramalingam, S. and P. Kumar, *Multi-component carbon-carbon bond forming Mannich reaction catalyzed by yttria zirconia based Lewis acid*. Catalysis Communications, 2008. **9**(14): p. 2445-2448.
56. Vuurman, M.A., et al., *Combined Raman and IR study of MO V_2O_5/Al_2O_3 (MO x= MoO₃, WO₃, NiO, CoO) catalysts under dehydrated conditions*. Journal of the Chemical Society, Faraday Transactions, 1996. **92**(17): p. 3259-3265.
57. Sun, J., et al., *Direct conversion of bio-ethanol to isobutene on nanosized Zn_xZr_yO_z mixed oxides with balanced acid base sites*. Journal of the American Chemical Society. **133**(29): p. 11096-11099.
58. Martinez-Arias, A., et al., *Structural and redox properties of ceria in alumina-supported ceria catalyst supports*. The Journal of Physical Chemistry B, 2000. **104**(17): p. 4038-4046.
59. Neto, R.C.R. and M. Schmal, *Synthesis of CeO₂ and CeZrO₂ mixed oxide nanostructured catalysts for the iso-syntheses reaction*. Applied Catalysis A: General. **450**: p. 131-142.

60. Suhonen, S., et al., *Effect of Ce–Zr mixed oxides on the chemical state of Rh in alumina supported automotive exhaust catalysts studied by XPS and XRD*. Applied Catalysis A: General, 2001. **218**(1-2): p. 151-160.
61. Shin, H., et al., *Improvement of sulfur resistance of Pd/Ce–Zr–Al–O catalysts for CO oxidation*. Applied Surface Science. **429**: p. 102-107.
62. Cao, D., et al., *Syngas Production from Ethanol Dry Reforming over Cu/Ce_{0.8}Zr_{0.2}O₂ Catalyst*. Catalysis letters. **147**(12): p. 2929-2939.
63. Chen, X., A.R. Tadd, and J.W. Schwank, *Carbon deposited on Ni/CeZrO isooctane autothermal reforming catalysts*. Journal of Catalysis, 2007. **251**(2): p. 374-387.
64. Ali, S., et al., *Synergistic effect between copper and cerium on the performance of Cu_x-Ce_{0.5-x}Zr_{0.5} (x= 0.1–0.5) oxides catalysts for selective catalytic reduction of NO with ammonia*. Applied Catalysis B: Environmental. **210**: p. 223-234.
65. Li, W., et al., *Surface Lewis acid-promoted copper-based nanocatalysts for highly efficient and chemoselective hydrogenation of citral to unsaturated allylic alcohols*. Catalysis Science & Technology. **6**(7): p. 2337-2348.
66. Yao, X., et al., *A comparative study of different doped metal cations on the reduction, adsorption and activity of CuO/Ce_{0.67}M_{0.33}O₂ (M= Zr⁴⁺, Sn⁴⁺, Ti⁴⁺) catalysts for NO+ CO reaction*. Applied Catalysis B: Environmental. **130**: p. 293-304.
67. Grisdanurak, N., P. Phatai, and A. Neramittagapong, *Characteristics and performance of M-doped cerium zirconium mixed oxide nanosized catalysts (M= Zn, Sn) in CO oxidation*. Reaction Kinetics and Catalysis Letters, 2007. **92**(2): p. 213-221.

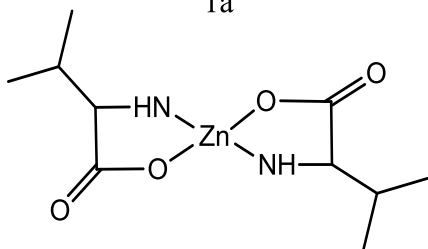
Annexure

1. Structures of Zn (amino acid)₂ complexesZn (Proline)₂

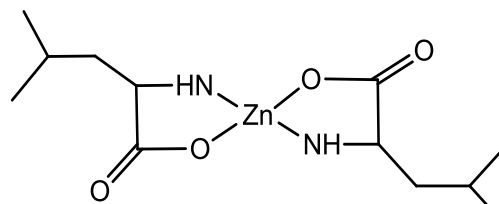
1a

Zn (Phenylalanine)₂

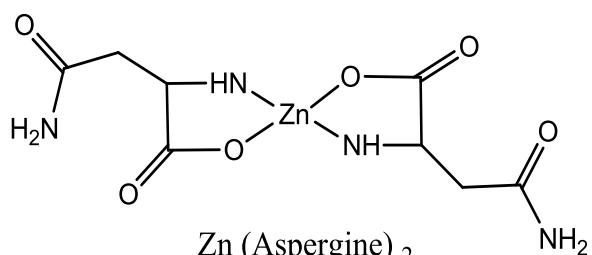
1b

Zn (Valine)₂

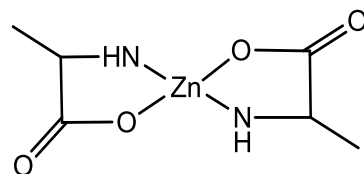
1c

Zn (Isolucine)₂

1d

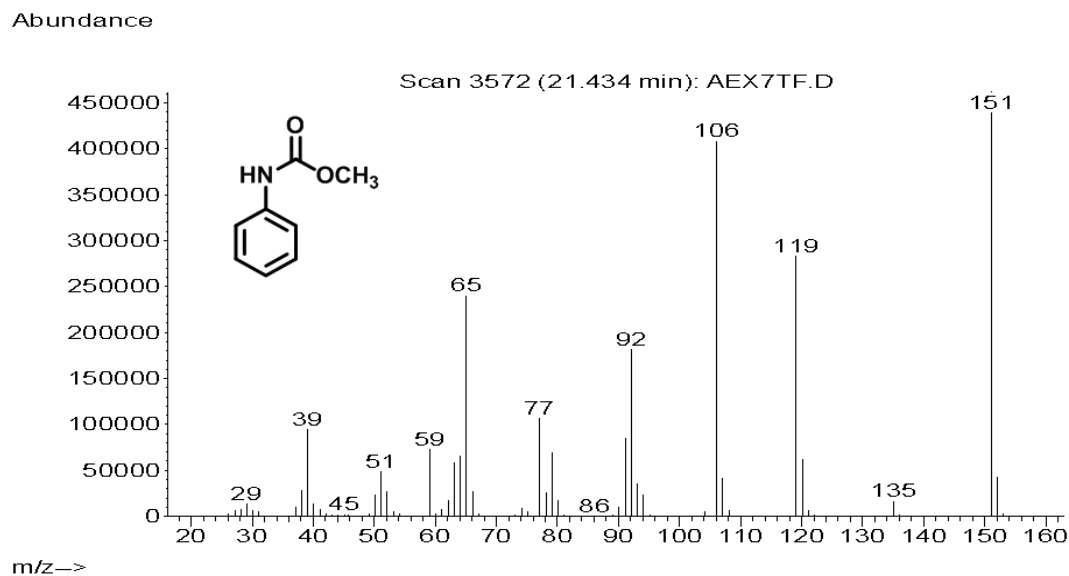
Zn (Aspergine)₂

1e

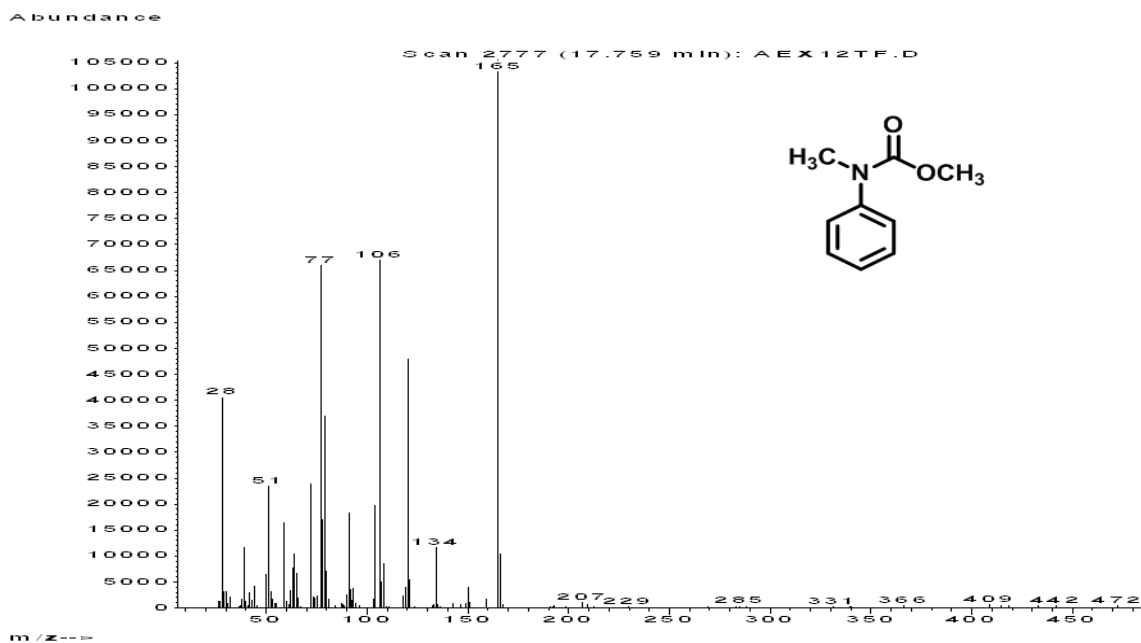
Zn (Alanine)₂

1f

2. GC-MS spectra of MPC (70 eV, EI)

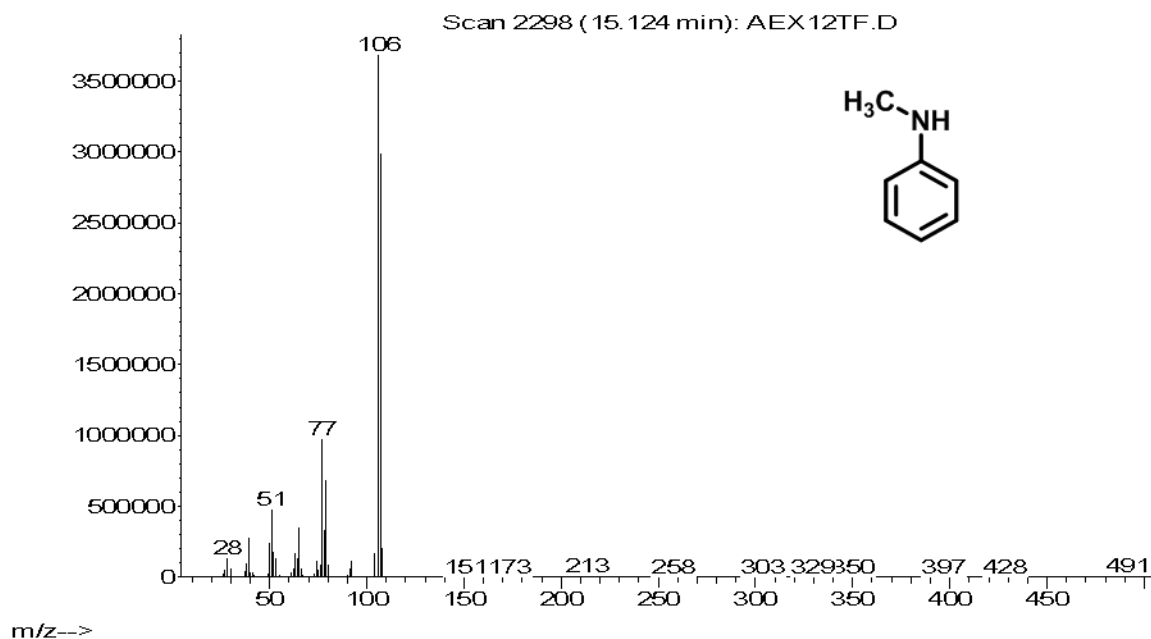


3. GC-MS spectra of MMPC (70 eV, EI)



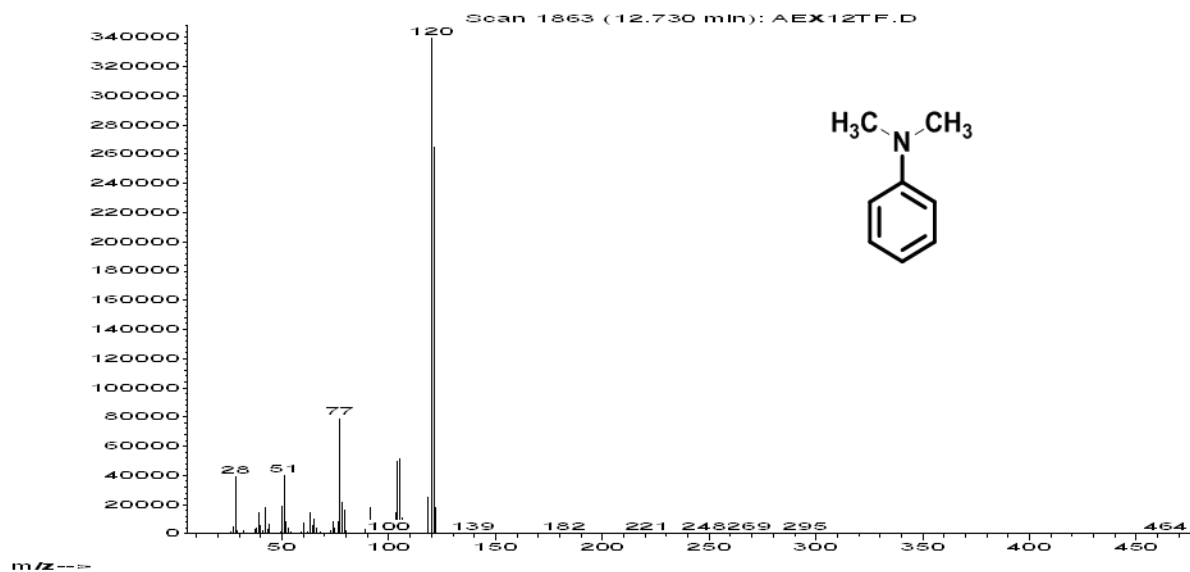
4. GC-MS spectra of NMA (70 eV, EI)

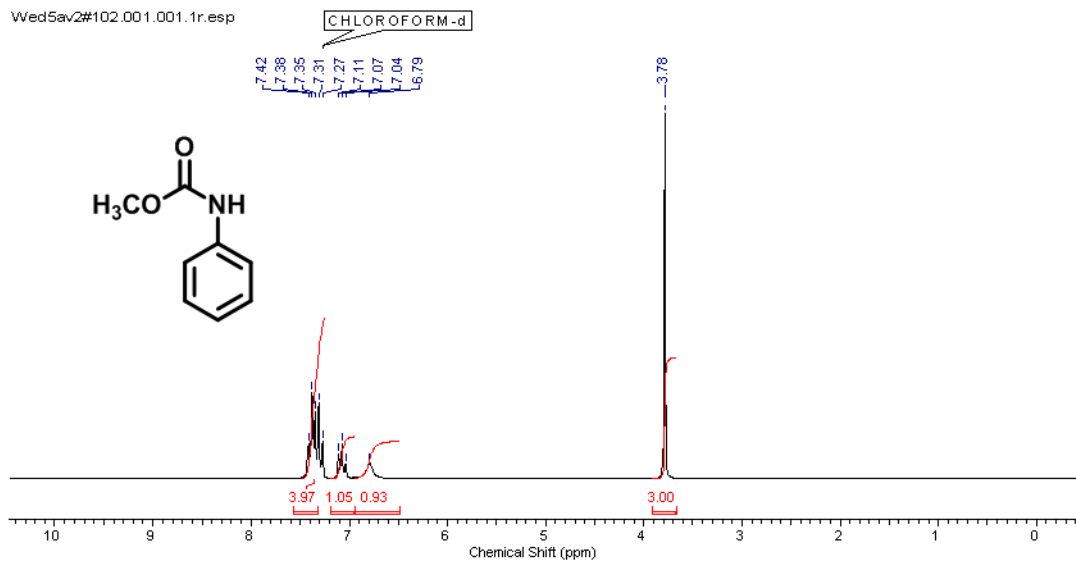
Abundance



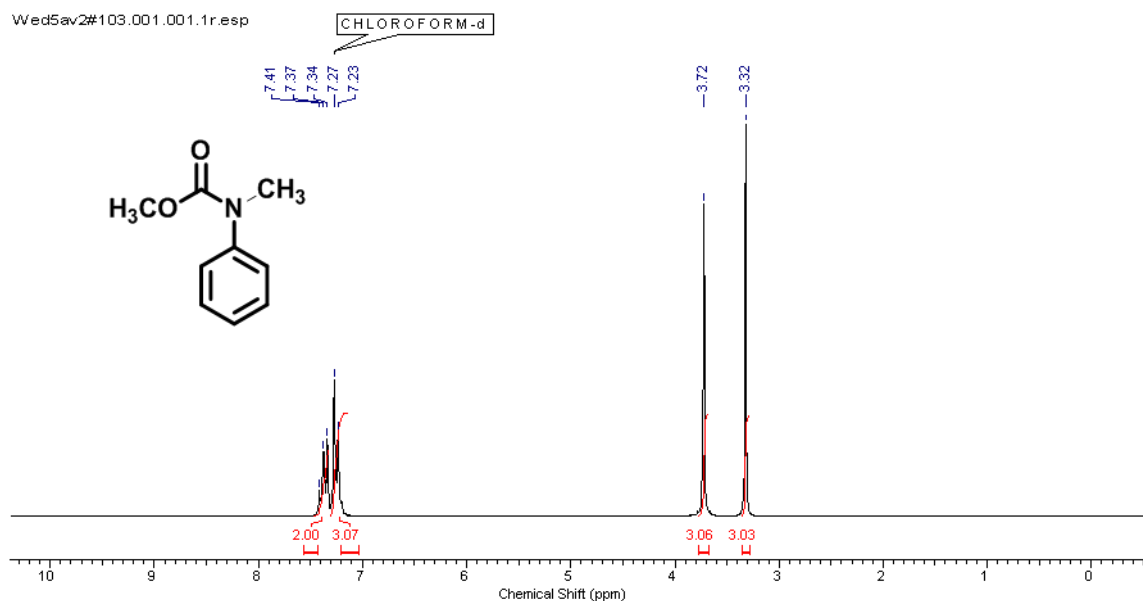
5. GC-MS spectra of NNDMA (70 eV, EI)

Abundance



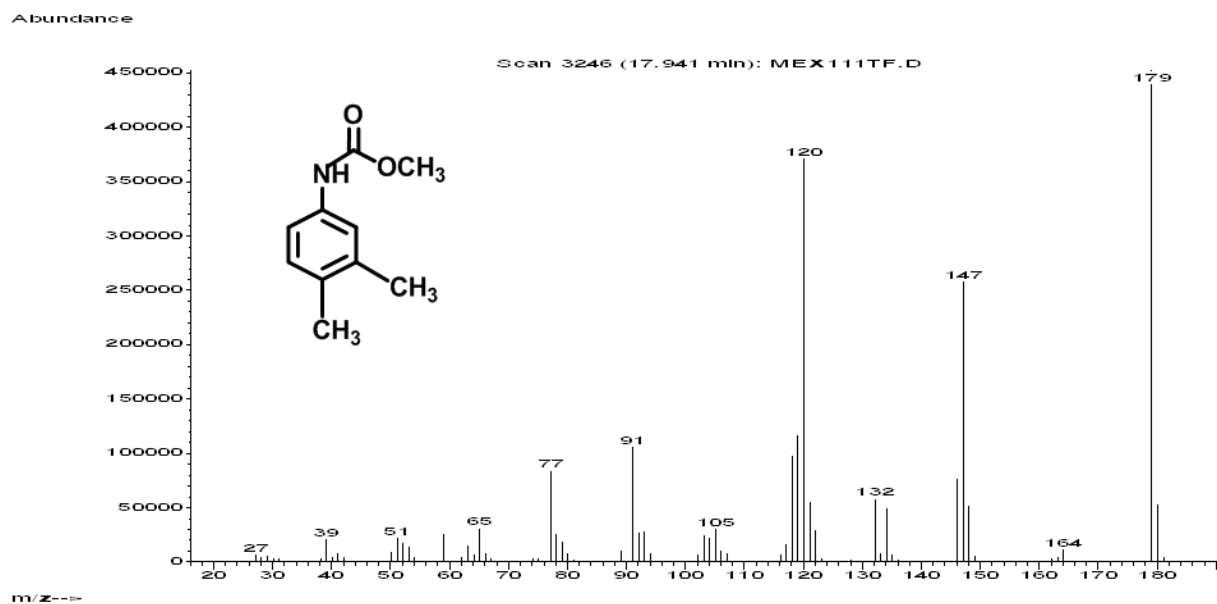
6. ^1H NMR of MPC

^1H NMR (200 MHz, CDCl_3) δ ppm 7.23 - 7.48 (m, 4 H) 6.95 - 7.19 (m, 1 H) 6.79 (br. s., 1 H)
3.78 (s, 3 H)

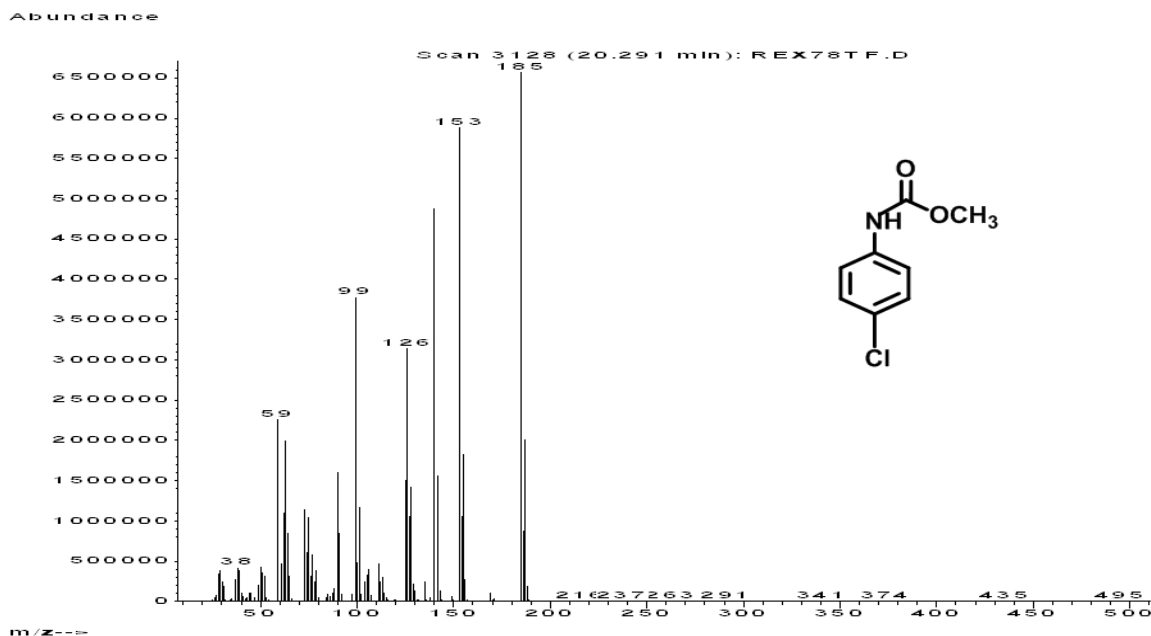
7. ^1H NMR of MMPC

^1H NMR (200 MHz, CDCl_3) δ ppm 7.33 - 7.46 (m, 2 H) 7.23 (s, 3 H) 3.72 (s, 3 H) 3.32 (s, 3 H)

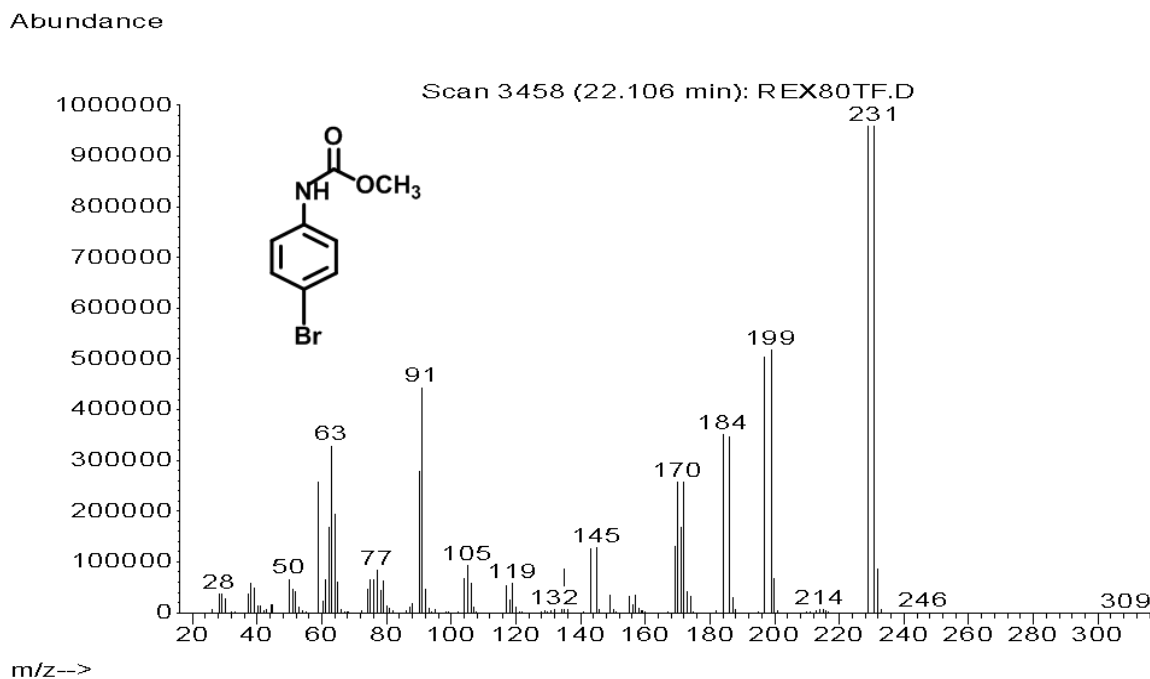
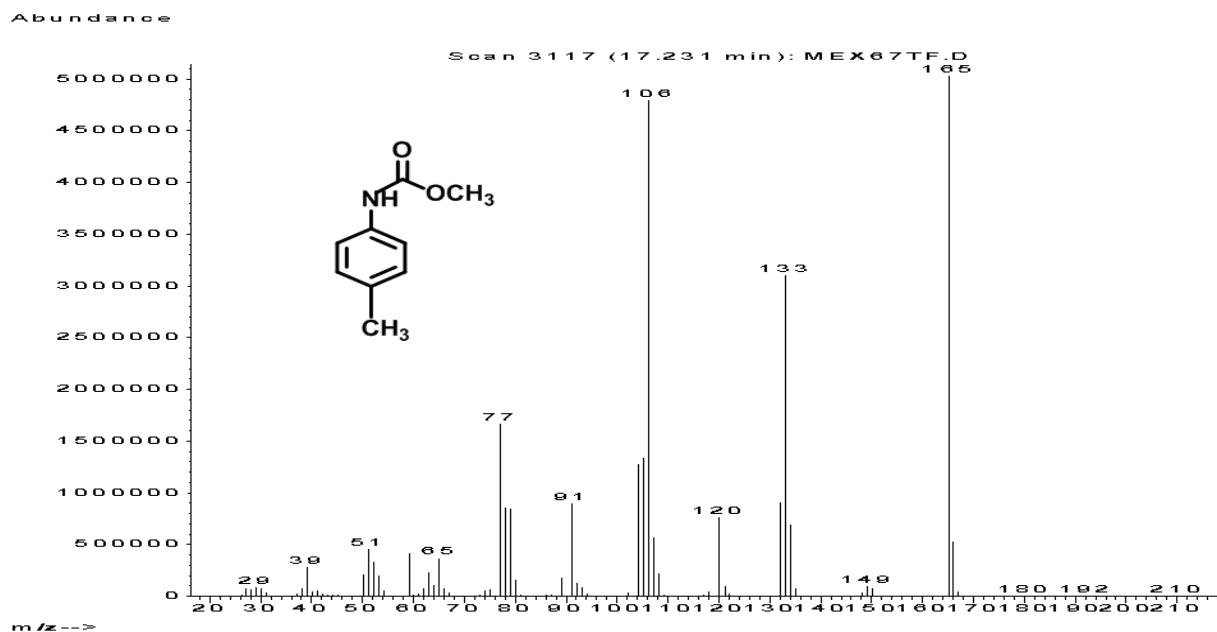
8. GC-MS spectra of methyl (3,4-dimethyl phenyl)carbamate (70 eV, EI)



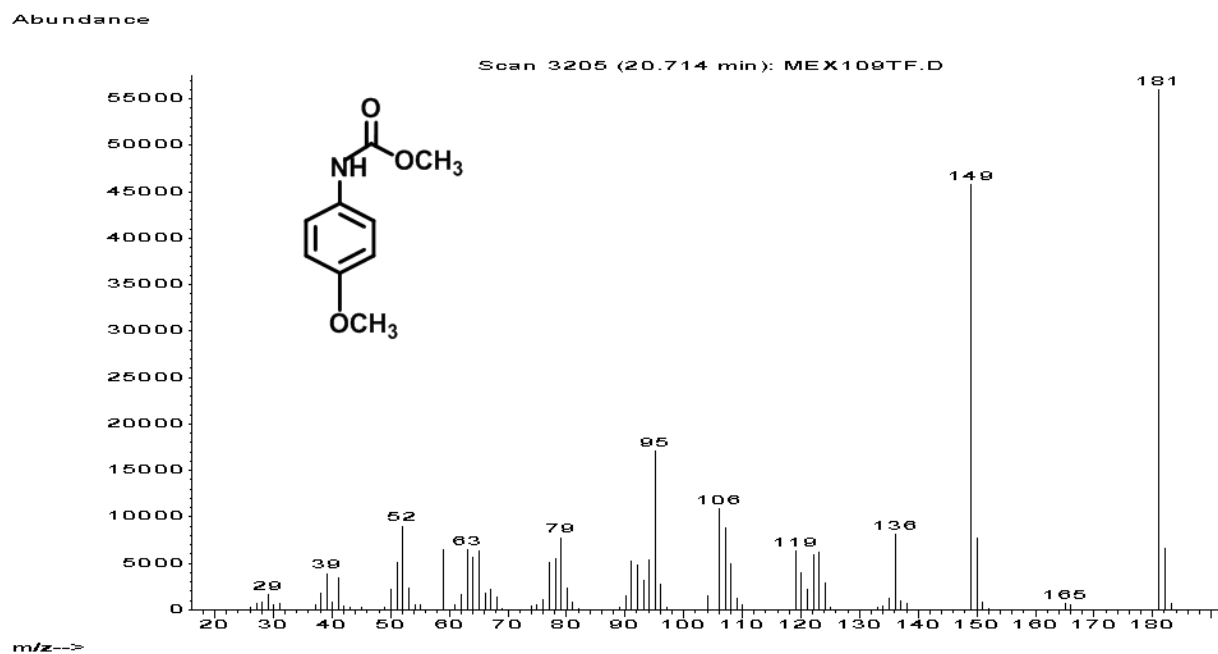
9. GC-MS spectra of methyl(4-chlorophenyl)carbamate (70 eV, EI)



10. GC-MS spectra of methyl(4-bromophenyl)carbamate (70 eV, EI)

11. GC-MS spectra of methyl *p*-tolylcarbamate (70 eV, EI)

12. GC-MS spectra of methyl (4-methoxyphenyl)carbamate (70 eV, EI)



Publications

1. N.T. Nivangune, A. A. Kelkar; “Synthesis of alkyl carbonate via transesterification of aromatic carbonate with methanol using mixed metal oxide catalyst” **Communicated...**
2. N.T. Nivangune, A. A. Kelkar; V. V. Ranade; “MgFeCe ternary layered double hydroxide as highly efficient and recyclable heterogeneous base catalyst for synthesis of dimethyl carbonate by transesterification” **Catalysis Letters** 147.10 (2017): 2558-2569.
3. A.A. Kulkarni, N. T. Nivangune, R. R. Joshi, and R. A. Joshi; “Continuous Flow Multipoint Dosing Approach for Selectivity Engineering in Sulfoxidation” **Org. Process Res. Dev.**(2013), 17 (10), pp 1293–1299.
4. A.A. Kulkarni, N.T. Nivangune, R. A. Joshi “Continuous flow synthesis of β -amino α , β -unsaturated esters in aqueous medium” **Green Process Synthesis** (2012), 1, 205-210.
5. A.A. Kulkarni, N.T. Nivangune, R.A. Joshi “Continuous flow nitration of salicylic acid” **Organic Process Research and Development** (2008), 12, 995-1000.

Patents

1. A. Kelkar; N.T. Nivangune, V.H. Rane “Synthesis of N-Methyl phenyl carbamate from aniline and dimethyl carbonate using CeZnZr ternary mixed metal oxide as a catalyst” **Patent under processing at IMPD: CSIR no. 2017-NF-0050.**

2. A. A. Kelkar; V. V. Ranade; N.T. Nivangune ; “Synthesis of N-methyl phenyl carbamate from aniline and dimethyl carbonate using Zn-proline as a heterogeneous catalyst” **Patent: Provisional filing no.201611018497, Filing date 30-5-2016.**
3. A. A. Kelkar; V. V. Ranade; N.T. Nivangune “Synthesis of Dimethyl carbonate and methanol using Ternaryhydrotalcite as a catalyst” **Patent: Provisional filing no.201611030994, Filing date 9-12-2016.**
4. A.A. Kulkarni, R.A. Joshi, N.T. Nivangune “Continuous flow process for the preparation of sulphoxide compounds” **WO 2012/004802 A1.**

Poster Presentation

1. Poster presented at **Sustainable Catalytic Technologies chemistry conference 2017** at the National chemical laboratory, Pune India.
2. Presented posters at **National Science Day poster presentation at CSIR-NCL**, February 2016, 2015, 2014, 2013 and 2010.
3. Poster presentation in **International conference on sustainable chemistry and engineering (SuschemE)** held at the Hotel Lalit, Mumbai 2015.
4. Poster presentation during **CATSYM-19 conference** at the National chemical laboratory, Pune, India.
5. Poster presented in **Advance in Chemical Engineering and Process Technology conference (ACEPT 2009)** held at the National chemical laboratory, Pune, India

Achievements

1. 1st prize for best poster

Presentation in International conference on sustainable chemistry and engineering (SuschemE) held at the Hotel Lalit, Mumbai during 8-9 sept-2015. Poster titled

“ Transesterification of ethylene carbonate with methanol using solid base catalyst”

2. 1st prize, Hindustan platinum award for the best poster

Presentation during CATSYM-19 conference held at the national chemical laboratory, Pune, India. Poster titled “Continuous flow Nitration of salicylic acid in microreactor”

3. Best poster award

In Advance in chemical engineering and process technology conference (ACEPT 2009) held at the National chemical laboratory, Pune India. Poster titled “Continuous flow synthesis of β -amino α , β -unsaturated esters in microreactor system”